Total Synthesis of the Antiviral Natural Products Cleistocaltone A and B

Inaugural-Dissertation

to obtain the academic degree

Doctor rerum naturalium (Dr. rer. nat.)

Submitted to the Department of Biology, Chemistry, Pharmacy

of Freie Universität Berlin

By

LORENZ WIESE

2024

The present work has been carried out in the period from May 2020 to July 2024 under the direction of Prof. Dr. MATHIAS CHRISTMANN at the Institute of Chemistry and Biochemistry of the Freie Universität Berlin.

Parts of this dissertation have been published in:

Lorenz Wiese, Sophie M. Kolbe, Manuela Weber, Martin Ludlow, Mathias Christmann, *Chem. Sci.* **2024**, *15*, 10121–10125. **DOI: https://doi.org/10.1039/D4SC01897D**

1st reviewer: Prof. Dr. MATHIAS CHRISTMANN

2nd reviewer: Prof. Dr. CHRISTIAN HACKENBERGER

Date of Disputation: 31.10.2024

Acknowledgements

At this point, I would like to express my sincere gratitude to everyone who contributed to the success of this work.

First and foremost, I would like to thank my supervisor, Professor Dr. MATHIAS CHRISTMANN, for accepting me into his research group and giving me the opportunity to work on this exciting topic. His numerous suggestions were invaluable to me.

I would also like to thank Professor Dr. CHRISTIAN HACKENBERGER for kindly agreeing to be the second reviewer of this work.

I thank all former and current members of the Christmann research group. The collegial atmosphere in our group contributed significantly to my feeling of well-being and motivation.

Special thanks go to my lab partners, Dr. MERLIN KLEOFF and KAMAR SHAKERI, who always supported me professionally and in a friendly manner. I learned a lot from you and enjoyed the time with you very much.

I would like to express my sincere gratitude to Dr. REINHOLD ZIMMER, whose organizational skills and advice ensured that the work could proceed smoothly.

I would also like to thank LAYTH ALAMA, KATHARINA PFEIFER, HAI DO, BILLY-JOE BUHRMEISTER, and TIM HORNER, who supported me enthusiastically in the context of their bachelor's theses and research internships.

I am very grateful to Dr. MARTIN LUDLOW and SOPHIE KOLBE for the fruitful collaboration and the development and execution of biological tests.

I would like to thank Dr. MERLIN KLEOFF, Dr. REINHOLD ZIMMER, KAMAR SHAKERI, JAN-HENDRIK DICKOFF, MAYAR ELBENDARY, and ZHEN WANG for proofreading this work.

Last but not least, I would like to thank my wife LORA for her patience, support, and loving encouragement. I would also like to thank my friends and family. Without them, this work would not have been possible.

Declaration of Independence

I hereby declare that I have written this dissertation independently and without any unauthorized assistance. I have not used any sources or aids other than those indicated by me. This work has not been submitted, in the same or similar form, to any other institution. I have not previously applied for a doctoral degree at any other institution.

Lorenz Wiese Berlin, 31.07.2024

Kurzzusammenfassung

Diese Arbeit beschreibt die Synthese von den Phloroglucinolmeroterpenoiden Cleistocaltone A und B, die von YE, WANG und Mitarbeitern aus der Pflanze *Cleistocalyx operculatus* im Jahre 2019 isoliert wurden und exzellente antivirale Aktivität gegen das respiratorische Synzytial-Virus (RSV) gezeigt haben.

Es wurden ein konvergenter und ein linearer Syntheseweg für Cleistocalton A ausgehend von 2-Acetylphloroglucinol und Geranylacetat entwickelt. Beide Strategien beinhalten eine TSUJI-TROST Kupplung, bei der die Phloroglucinoleinheit an das Terpenfragment gekoppelt wird und eine intramolekulare DIELS-ALDER Cycloaddition (IMDA), die den zehngliedrigen Makrozyklus und die Cyclohexeneinheit aufbaut, als Schlüsselschritte. Der konvergente Weg wurde mit einer längsten linearen Sequenz von 6 Schritten und einer Gesamtausbeute von 1.7% durchgeführt. Der lineare Weg wurde in 8 Schritten mit einer Gesamtausbeute von 2.2% realisiert und auf einen Grammmaßstab hochskaliert. Bei dem letzten Schritt der Synthese wurde ein interessantes Nebenprodukt isoliert, was ein einzigartiges tetrazyklisches Ringsystem mit einem achtgliedrigen zyklischen Ether beinhaltet. Es wurde vermutet, dass dieses Nebenprodukt auch ein Naturstoff aus *C. operculatus* ist, allerdings waren alle Isolationsversuche vergeblich.

Die Synthese von Cleistocalton B wurde mit einer TSUJI-TROST Kupplung als Schlüsselschritt mit anschließender Eintopf-Aldol-Kondensation durchgeführt. Cleistocalton B wurde als untrennbares 1:6 (*Z*/*E*) Gemisch mit seinem ungewünschten *E*-Isomer isoliert.

Die antivirale Aktivität von dem synthetischen Cleistocalton A wurde in Kollaboration mit MARTIN LUDLOW und SOPHIE KOLBE gegen einen aktuellen rekombinanten RSV-A Stamm getestet. Das synthetische Cleistocalton A zeigte einen höheren IC_{50} als das isolierte Material von YE, WANG und Mitarbeitern.

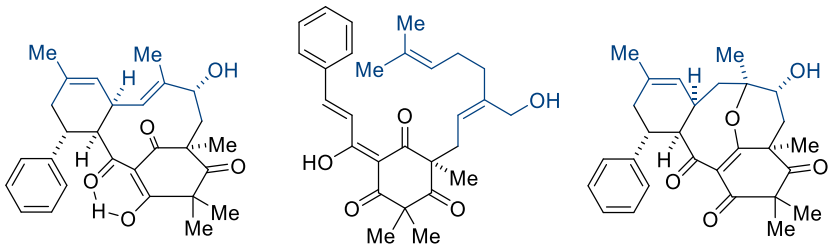

Cleistocalton A | Cleistocalton B | Nebenprodukt

Abstract

This work describes the synthesis of phloroglucinol meroterpenoids Cleistocaltones A and B which have been isolated from *Cleistocalyx operculatus* by YE, WANG, and coworkers in 2019 and displayed excellent antiviral activity against respiratory syncytial virus (RSV).

A convergent and a linear route have been developed for Cleistocaltone A starting from 2-acetyl phloroglucinol and geranyl acetate. Both routes include a TSUJI-TROST coupling, that tethers the phloroglucinol core to the terpene moiety and an intramolecular DIELS-ALDER cycloaddition (IMDA), that furnishes the 10-membered macrocycle and the cyclohexene moiety, as the key-steps. The convergent route was performed with a longest linear sequence of 6 steps with an overall yield of 1.7%. The linear route was performed in 8 steps with an overall yield of 2.2%. Additionally, the linear route was scaled up to a gram-scale. At the last step of the synthesis, an interesting side product was isolated that features a unique tetracyclic ring system with an eight-membered cyclic ether. It was suspected that this side product was a natural product from *C. operculatus* as well. However, all isolation attempts were unsuccessful.

The synthesis of Cleistocaltone B was performed with a TSUJI-TROST coupling as the key-step with a subsequent one-pot aldol condensation. Cleistocaltone B was isolated as an inseparable 1:6 (Z/E) mixture with its undesired E-isomer.

The antiviral activity of synthetic Cleistocaltone A was tested in a collaboration with MARTIN LUDLOW and SOPHIE KOLBE against a contemporary recombinant RSV-A strain. Synthetic Cleistocaltone A displayed a modestly higher IC_{50} than the isolated material from YE, WANG, and coworkers.

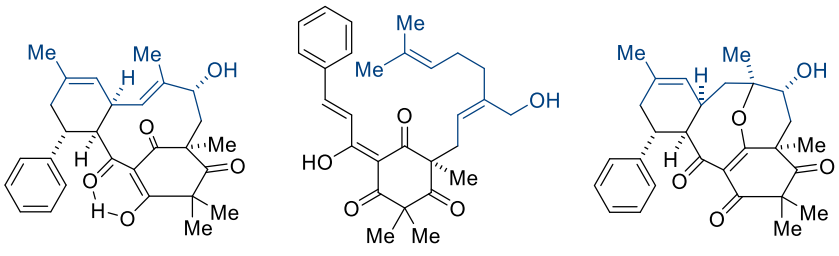

Table of Contents

1. Introduction

1.1 Natural Product Synthesis

Natural products (NPs) can be categorized into primary and secondary metabolites. Primary metabolites, consisting of carbohydrates, lipids, amino acids, and nucleic acids, are essential for fundamental cellular processes such as energy production, cell structure formation, and genetic information storage.[1,2]

Secondary metabolites, on the other hand, are not directly involved in growth, development, or reproduction. Instead, they serve diverse ecological functions, playing a role in chemical communication between organisms, defence against predators or pathogens, and competition with other species.[3] This ecological significance drives the high structural diversity of secondary metabolites, resulting in a wide range of interesting biological and pharmacological activities often optimized through millions of years of evolution.[4]

Accordingly, NPs have always been a rich and valuable source of therapeutics. Since the dawn of time humanity relied on NPs by utilizing plants, animals, microorganisms, and marine organisms for the treatment of various diseases and ailments.[5] The significance of NPs in modern drug discovery can also not be understated. Out of the 1211 approved drugs from 1981 to 2014, 33% were either NPs or NP-derivatives. Out of the 67% synthetic drugs, 27% mimic the mode of action of a NP.[6]

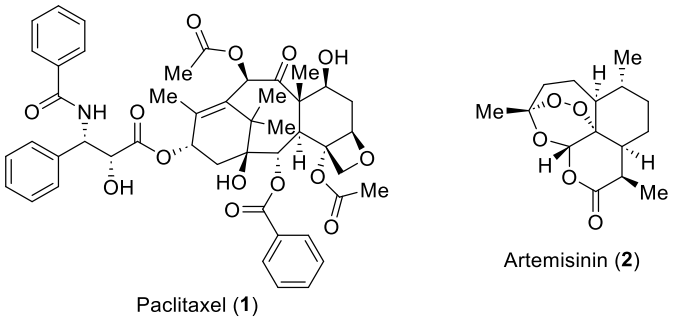

Figure 1: Structures of Paclitaxel (**1**) and Artemisinin (**2**).

Prominent examples of NPs that are approved to be used as therapeutics are the terpenoids Paclitaxel (**1**, Figure 1), a cancer drug that was isolated from the barks of *Taxus brevifolia* in 1971 by WANI, WALL, and coworkers[7] and Artemisinin (**2**, Figure 1), a drug against malaria that was discovered in 1972 from the plant *Artemisia annua* by TU and coworkers.[8] Since then, several total syntheses have been successfully executed for Paclitaxel (**1**)[9–20] and Artemisinin (**2**).[21–25]

Typically, the abundance of specific natural products within their natural sources is extremely low, requiring kilograms of the organism to extract only milligrams of the desired compound. Furthermore, the extraction and purification process is often highly complex due to the presence of thousands of different compounds in the crude extract.[26]

To enable further research, a synthetic access to the desired compound is essential, offering a more sustainable and scalable supply. Accordingly, NP synthesis has been an important field in organic chemistry for decades.[27]

NP synthesis also plays a crucial role in structure confirmation. When no crystal structure (XRD) of the NP is obtainable, the synthesis can confirm or contradict the proposed structure of the compound. In some cases, the proposed structure differs significantly from the actual structure of the NP. A notable example is Thiasporine A (**3**), where the NMR-spectra of the initially proposed structure **4** were inconsistent with the spectra of the isolated compound. This discrepancy led to a revision of the structure (Figure 2).[28]

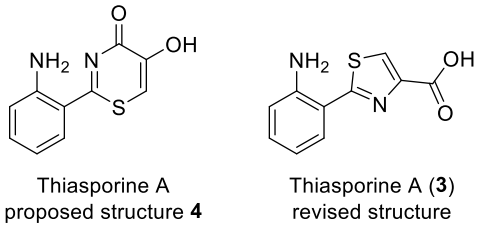

Figure 2: Proposed and revised structures for Thiasporine A.[28]

Lastly, NP synthesis is an important tool for drug discovery and development. When the synthetic route to the NP is established, it opens up the possibility to modify the structure of the NP at various stages of the synthesis. These derivatives and the intermediates of the synthesis that would otherwise not be available enable structure-activity relationship (SAR) studies to identify the mechanism of action and obtain even more active compounds.[29]

1.1.1 Biomimetic Natural Product Synthesis

An noteworthy approach to the synthesis of NPs are biomimetic strategies. The principle behind biomimetic NP synthesis is that in nature the syntheses of compounds are performed very efficiently as they have been optimized through the process of evolution. Consequently, by taking inspiration and imitating key steps from the biosynthetic pathway to certain NPs, one can synthesize complex structural motifs of the desired compounds in an elegant and step-efficient manner.[30] These strategies are supposed to exploit the innate reactivity of the molecule and therefore achieve the synthesis without the excessive use of protecting groups. As a result, biomimetic strategies have emerged in recent years as a powerful way to synthesize complex chemical structures.[31]

An exceptional example for this concept is the total synthesis of the meroterpenoid Peshawaraquinone (**5**) by GEORGE and coworkers from 2023.[32] It was proposed that **5** is produced in nature *via* an unsymmetrical dimerization of dehydro-α-lapachone (**6**). According to the proposed biosynthesis (Scheme 1), lapachol (**7**) is converted to **6** through an oxidative cyclization. **6** then isomerizes through a LEWIS acid catalyzed retro-6π-electrocyclization to **8** which dimerizes through an intermolecular MICHAEL addition by its deprotonated form **9** to produce dimer **10**. **10** then reacts in a 6π-electrocyclization to give the precursor **11** for the intramolecular (3+2) cycloaddition which ultimately results in Peshawaraquinone (**5**).[32]

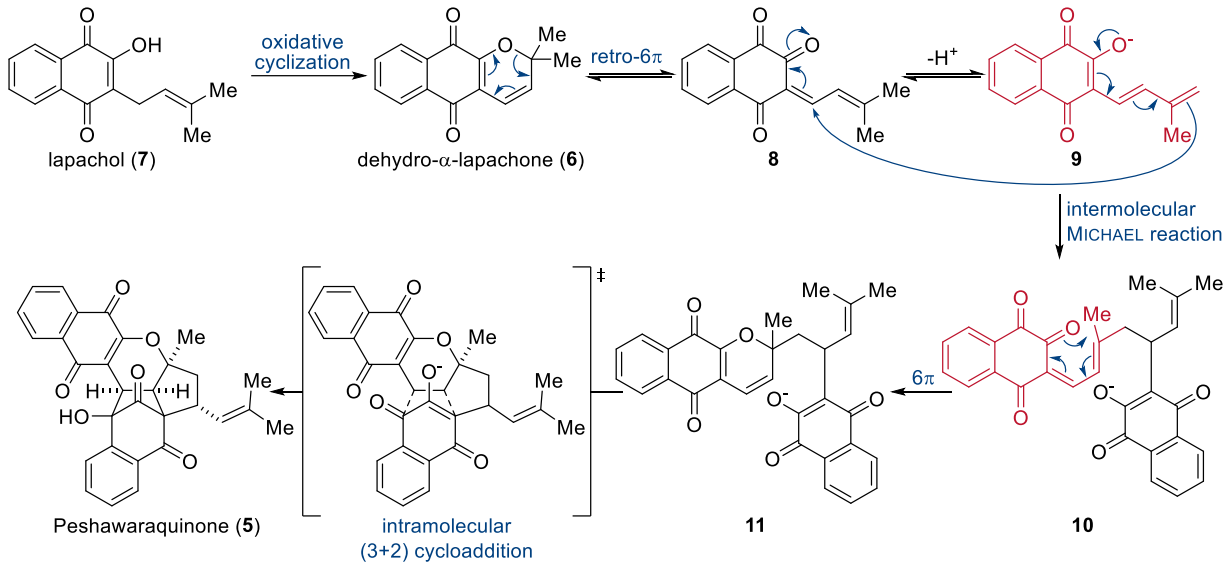

Scheme 1: Proposed biosynthesis of Peshawaraquinone (**5**).[32]

Synthetically, dehydro-α-lapachone (**6**) was obtained by reacting lawsone (**12**) in an KNOEVENAGEL condensation with prenal followed by a subsequent oxa-6π-electrocyclization. Afterwards, using DMAP as a base, **12** was converted to Peshawaraquinone (**5**) and its 11'-epimer with 46% yield and a d.r. of 2.2:1. Combining these two steps was successful and Peshawaraquinone (**5**) was formed in a single step with 8% isolated yield (Scheme 2).[32]

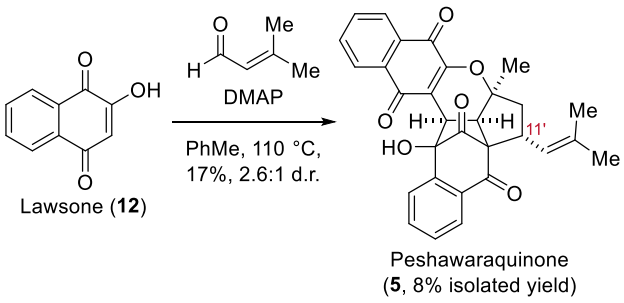

Scheme 2: One-step total synthesis of Peshawaraquinone (**5**) by GEORGE and coworkers.[32]

Two other NPs that has been efficiently synthesized utilizing a biomimetic strategy, also by GEORGE and coworkers[33] are Atrachinenins A (**13**, Scheme 3) and B (**14**, Scheme 3), two meroterpenoids

featuring a complex cage-like tetracyclic ring system with six contiguous stereocenters for **13** and a pentacyclic ring system with seven contiguous stereocenters and a peroxyhemiacetal bridge for **14**. The proposed biosynthesis commences with a DIELS-ALDER cycloaddition between geranyl-quinone **15** and the monoterpene *E*-β-ocimene (**16**) to give **17** which, after enolization to **18**, undergoes a (3+2) cycloaddition completing the tetracyclic structure in **19**. An oxidative cyclization completes the peroxyhemiacetal bridge and furnishes Atrachinenin B (**14**) which is transformed to Atrachinenin A (**13**) through reduction.[33]

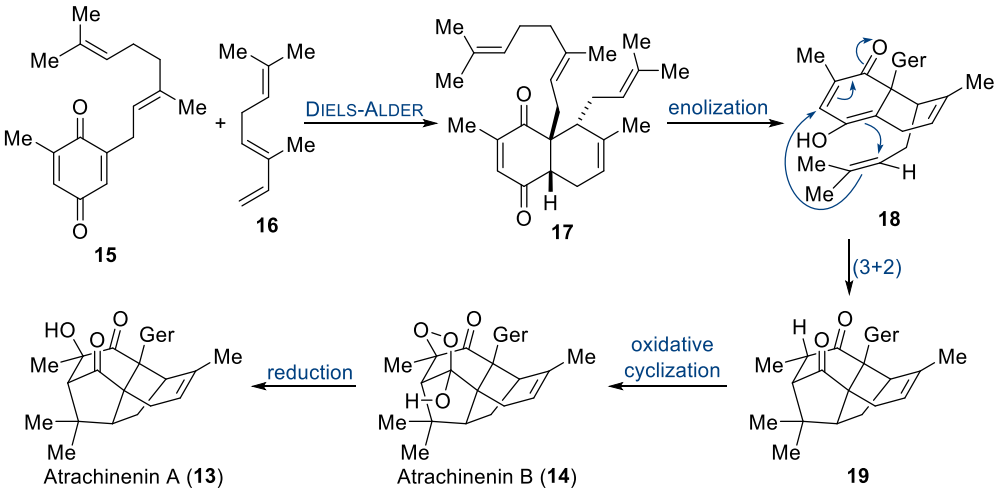

Scheme 3: Proposed biosynthesis of Atrachinenins A (**13**) and B (**14**) by GEORGE and coworkers.[33]

All these steps of the biosynthesis were successfully mimicked synthetically by GEORGE and coworkers (Scheme 4). Geranylation and oxidation of 4-methoxy-2-methylphenol gave **15** in two steps with 76% yield. The intermolecular DIELS-ALDER cycloadditon of **15** with **16** was promoted by $LiClO_4$ and gave all possible *endo*-diastereomers resulting in a 24% isolated yield of **17**. The (3+2) cycloaddition was successfully executed by using DABCO in PhMe at 95 °C yielding **19** with 32%. The oxidative cyclization was achieved by utilizing KO*t*-Bu under aerobic conditions in DMSO furnishing the cyclic peroxide in Atrachinenin B (**14**) with 57% yield which was then reduced with PPh_3 to yield Atrachinenin A (**13**) with 95%.[33]

Without requiring any protecting groups and furnishing complex natural products such as Peshawaraquinone (**5**) and Atrachinenins A (**13**) and B (**14**) in very few steps, these syntheses excellently showcase the power of biomimetic strategies.

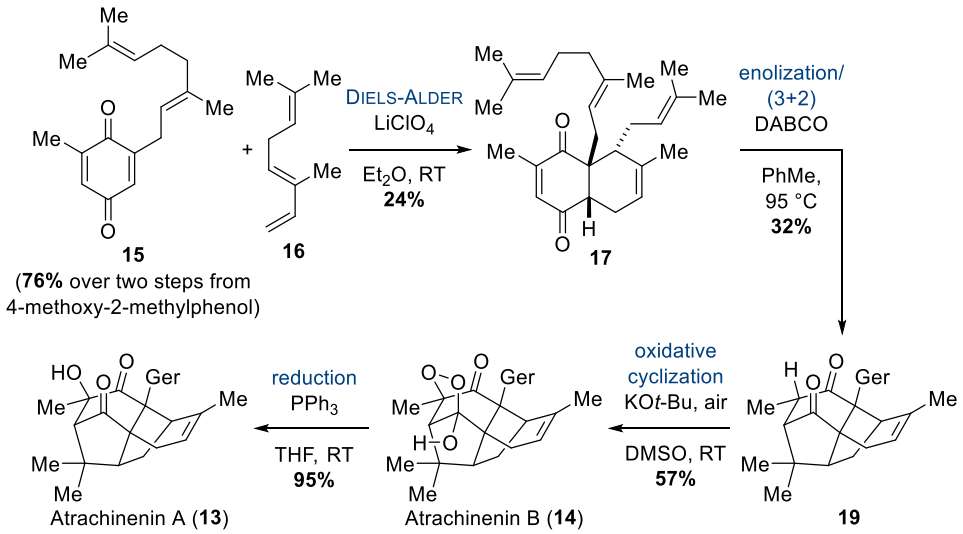

Scheme 4: Biomimetic total synthesis of Atrachinenins A (**13**) and B (**14**) by GEORGE and coworkers.[33]

1.2 Respiratory Syncytial Virus (RSV): Disease Burden and Treatment Challenges

Respiratory syncytial virus (RSV) is a single-stranded RNA-virus within the Paramyxoviridae family which possesses a non-segmented genome.[34] RSV was first discovered in 1956 in a colony of chimpanzees with coryza and was therefore labelled coryza agent. Later it was re-termed RSV due to causing a fusion of infected cells with neighbouring cells leading to a formation of large multinucleated syncytia.[35]

Since its discovery, RSV has emerged as a leading global cause of illness and death, particularly for infants in the first six months of life.[34] With 33.0 million RSV-associated acute lower respiratory infection episodes in children aged 0-60 months in 2019 resulting in 3.6 million hospital admissions, it is the most common cause of childhood acute respiratory infection (ARI) and thus, one of the biggest reason for infant hospitalization. In 2019, RSV was attributable for 26 300 in-hospital deaths and 101 400 overall deaths in this age group.[36] RSV's impact on vulnerable adults, including the frail elderly and immunocompromised individuals, can also not be understated. In 2019, RSV-ARI was attributed to 470 000 hospitalizations and 33 000 in-hospital deaths for ≥60-aged-adults in high-income countries.[37] In resource-limited settings, RSV is an even more significant cause of death due to lower respiratory tract infections, second only to pneumococcal pneumonia and Haemophilus influenzae type B. These regions experience more than double the rate of severe RSV disease compared to developed countries and account for 99% of global RSV-related deaths.[34] In recent years, the amount of RSV-specific antibodies in all age groups decreased significantly due to the social distancing measures against severe acute respiratory syndrome coronavirus 2 (SARS-CoV-2). Lifting of those measures caused an increase of RSV-related hospitalizations, exceeding the amount observed in regular seasons.[38]

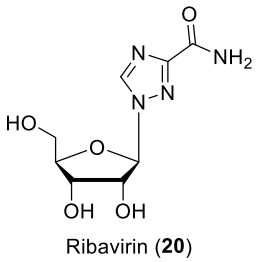

Ribavirin (**20**)

Figure 3: Structure of Ribavirin (**20**).

Due to the lack of specific therapies, treatment mostly relied on supportive care and passive immunization. Recently, four promising therapeutics against RSV have been approved. This includes RSVPreF3 and RSVPreF which are subunit vaccines and Palivizumab and Nirsevimab that are monoclonal antibodies. The only approved small-molecule drug against RSV is Ribavirin (**20**,

Figure 3) which, as a nucleoside analogue, targets the polymerase of RSV. However, its use is highly limited due to safety concerns and its high cost.[39] To diversify treatment options, the development of novel small-molecule antivirals against RSV is highly desirable.

1.3 Cleistocaltones A and B

1.3.1 Discovery and Biological Activity

Cleistocalyx operculatus (Roxb.) Merr. and Perry (alternative name: *Syzygium nervosum* A.Cunn. ex DC.) is a tree belonging to the Myrtaceae family and is native to tropical areas of South East Asia. Watery extracts of its leaves and flowers were used in traditional Vietnamese and Chinese medicine internally to treat digestive conditions and externally for various skin conditions. Additionally, in traditional Chinese medicine (TCM) the extraction of the plants flowers was used for the treatment of influenza.[40] These therapeutical capabilities can be attributed to various NPs, especially phloroglucinols, that are produced in the plant. The major constituent of the crude extract of *C. operculatus* is 2',4'-dihydroxy-6'-methoxy-3',5'-dimethylchalcone (DMC, **21**, Figure 4) ranging from 0.75% to 1.85%.[41,42] Different studies have shown that **21** possesses cytotoxic,[43–45] antidiabetic,[46] antioxidant,[47] and anti-inflammatory effects.[48,49] *C. operculatus* also contains antiviral compounds. A structurally interesting example is Cleistoperlone A (**22**, Figure 4) which displayed activity against herpes simplex virus type-1 (HSV-1).[50]

Intrigued by *C. operculatus*' application in TCM against respiratory illnesses such as influenza, YE, WANG, and coworkers investigated the activity of the compounds from the plant's extract against respiratory syncytial virus (RSV). In their studies, they isolated two novel phloroglucinol meroterpenoids Cleistocaltones A (**23**, Figure 4) and B (**24**, Figure 4).[51]

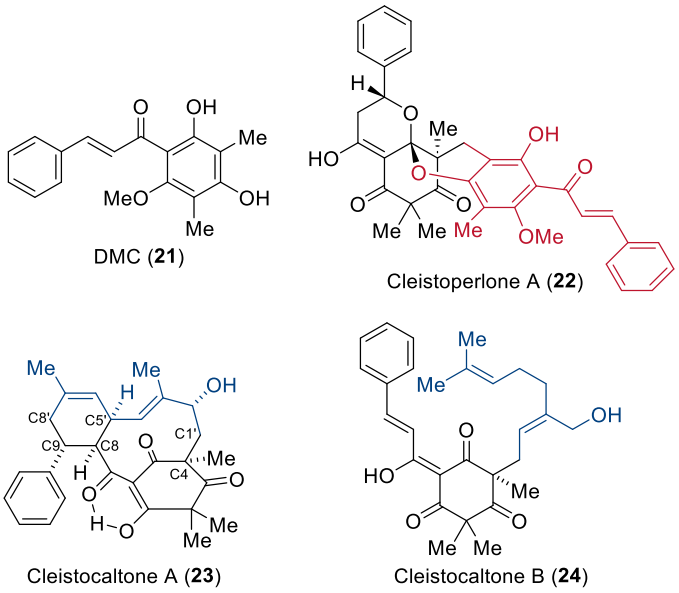

Figure 4: Structures of various phloroglucinols isolated from the extracts of *C. operculatus*.

As phloroglucinol meroterpenoids, **23** and **24** are both composed of a methylated phloroglucinol part containing a cinnamoyl moiety originating from Champanone B (**25**) and a monoterpene part

consisting of an oxidized geranyl chain. In **23** the terpene part is fused to the phloroglucinol part with 3 C–C bonds (C-4–C-1′, C-8–C-5′, and C-9–C- 8′) which is unique for this class of compounds. Both compounds were isolated as a racemic mixture. The structure of **23** was confirmed with XRD analysis. This was not possible for **24** since it was isolated as a viscous oil. Additionally, **24** was always present as a mixture of two interconverting diastereomers (**24a** and **24b**, Scheme 5) which gave two sets of signals in the ^{1}H and ^{13}C-NMR.[51]

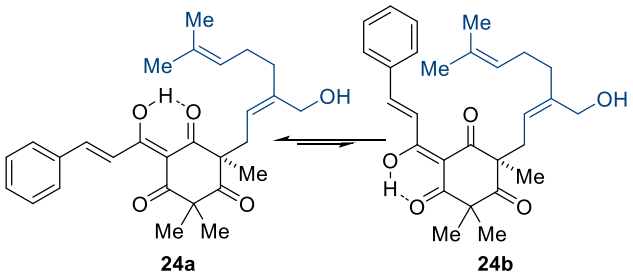

Scheme 5: Isomerization of Cleistocaltone B (**24**).

The antiviral activity of Cleistocaltones A (**23**) and B (**24**) against RSV was investigated through a cytopathic effect (CPE) reduction assay. Ribavirin (**20**) was used as the positive control. With an IC_{50} of 6.75 ± 0.75 µM for **23** and 2.81 ± 0.31 µM for **24,** they showed better inhibition against RSV than Ribavirin (**20**) with an IC_{50} of 15.00 ± 1.00 µM.[51]

1.3.2 Proposed Biosynthesis of Cleistocaltone A

There are many examples of phloroglucinol meroterpenoids in which the terpene part is supposed to originate from a geranyl side-chain. In these compounds, the biosynthesis commences with the geranylation of a phloroglucinol precursor with geranyl pyrophosphate (**26**) to form a geranylated phloroglucinol species. Then, the geranyl chain undergoes several oxidation and cyclization steps to form the NP. One example is the proposed biosynthesis of Elodeoidol G (**27**, Scheme 6): In geranyl phloroglucinol **28**, both carbon-carbon double bonds of the geranyl chain are epoxidized. Afterwards, **29** undergoes an epoxide opening cascade to produce **27**.[52] Here, the phloroglucinol part is bound to the terpene part with an additional C–O-bond.

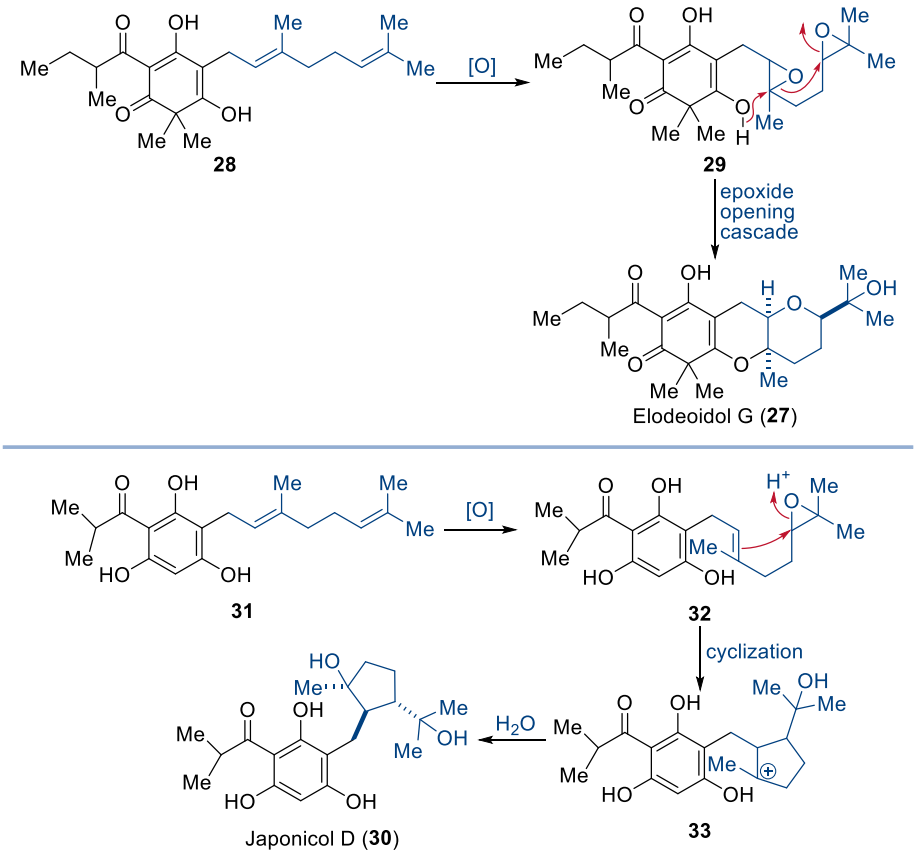

Scheme 6: Proposed biosyntheses of Elodeoidol G (**27**) and Japonicol D (**30**).[52,53]

The biosynthesis of Japonicol D (**30**, Scheme 6) begins with a similar geranyl phloroglucinol **31**, except that only one carbon-carbon double bond of the geranyl chain is epoxidized. Subsequently, in **32** the remaining double bond attacks the epoxide, generating cation **33** as an intermediate which is then hydrolyzed to produce Japonicol D (**30**).[53]

YE, WANG, and coworkers proposed a similar biosynthetic pathway to Cleistocaltone A (**23**) and B (**24**) which commences with Champanone B (**25**, Scheme 7) as the phloroglucinol fragment. **25** is first geranylated with geranyl pyrophosphate (**26**) generating geranyl Champanone B **34**. **34** could then be hydroxylated selectively at the C-9' methyl group of the geranyl chain to produce Cleistocaltone B (**24**). Alternatively, a dehydrogenation and olefin isomerization at the terminus of the geranyl chain in **34** could yield triene **35**. **35** is the precursor for an intramolecular DIELS-ALDER cycloaddition (IMDA). The electron-rich diene at the terminus of the terpene chain reacts with the electron-deficient dienophile of the cinnamoyl moiety in an *endo*-transition state (TS) which results in the formation of the 10-membered macrocycle and the cyclohexene in **36**. In the last step the α-position C-2' of the carbon-carbon double bond contained in the macrocycle is hydroxylated to furnish Cleistocaltone A (**23**).[51]

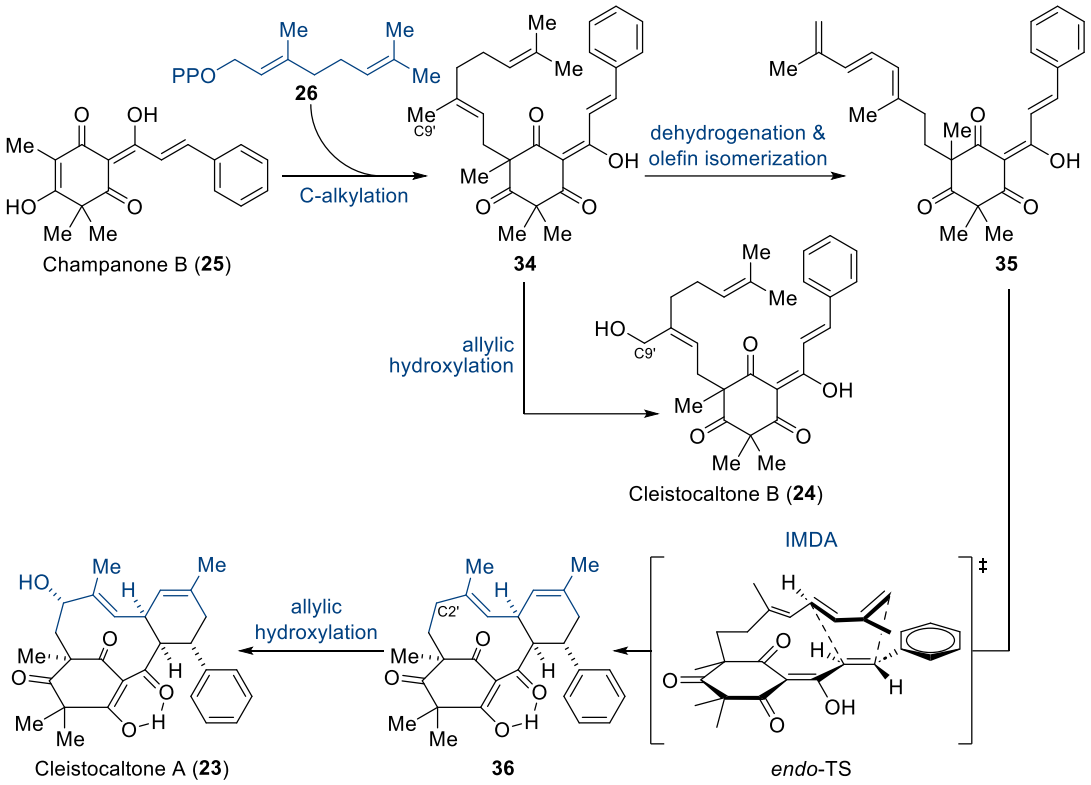

Scheme 7: Biosynthetic pathway to Cleistocaltones A (**23**) and B (**24**) as proposed by YE, WANG, and coworkers.[51]

1.4 Retrosynthetic Analysis of Cleistocaltone A

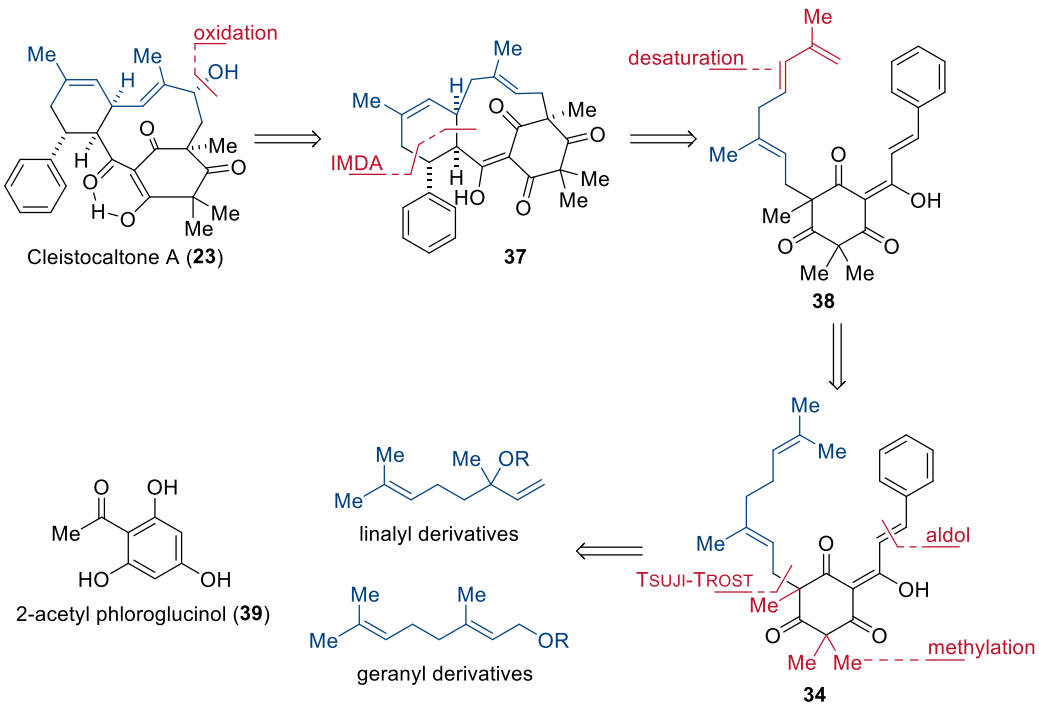

Scheme 8: Biosynthesis-inspired retrosynthetic analysis of Cleistocaltone A (**23**).

In line with the principle of biomimetic synthesis, the retrosynthetic analysis of Cleistocaltone A (**23**, Scheme 8) was inspired by the proposed biosynthesis of YE, WANG, and coworkers.[51] Accordingly, the first retrosynthetic step is the oxidation of the carbon backbone which leads to intermediate **37**. **37** features a cyclohexene moiety which, according to the proposed biosynthesis, could be formed in an IMDA. The key-intermediate **38** required for the IMDA features an electron-rich diene located at the terpene part and an electron-deficient dienophile located at the phloroglucinol part of the molecule. The diene is to be formed out of the terminus of the geranyl fragment in intermediate **34** via a desaturation sequence. The geranyl moiety could be installed through a TSUJI-TROST alkylation,[54] the cinnamoyl moiety through an aldol condensation and the methyl groups through nucleophilic substitution reactions. This ultimately leads to the commercially available 2-acetyl phloroglucinol (**39**) as the phloroglucinol part. For the terpene part, different options are imaginable such as linalyl and geranyl derivatives featuring various allylic leaving groups that are suitable for the TSUJI-TROST alkylation.

1.5 Synthesis of Key-Structural Motifs

1.5.1 TSUJI-TROST Reaction

One of the key steps in the synthesis of Cleistocaltones A (**23**) and B (**24**) is an allylic alkylation, coupling the terpene and phloroglucinol fragments. A powerful tool for this type of reaction is the TSUJI-TROST allylation.[54] This reaction has been discovered by TSUJI and coworkers in 1965 and further developed by TROST and coworkers.[54,55] In this palladium-catalyzed process, a substrate containing an allylic leaving group **40** reacts with a $Pd^{(0)}$ or $Pd^{(II)}$ source, typically a phosphine ligand, and a nucleophile (with an optional base) resulting in coupling product **41** (Scheme 9).

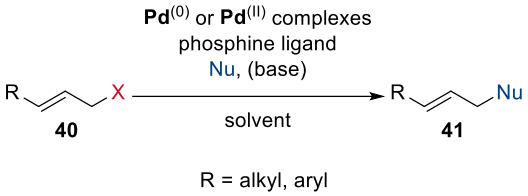

Scheme 9: General setup for the TSUJI-TROST reaction.[56]

Mechanistically (Scheme 10), the TSUJI-TROST reaction commences with the *in situ* formation of the active catalyst $L_nPd^{(0)}$ through reduction of the $Pd^{(II)}$ precursor and coordination of the phosphine ligand (L). The carbon-carbon double bond of the allylic substrate **40** then coordinates to the $L_nPd^{(0)}$ complex, facilitating an oxidative addition that generates a cationic Pd π-allyl complex **42**. The nucleophile attacks the π-allyl moiety in a substitution step. Finally, a reductive elimination releases the coupled product **41** and regenerates the $L_nPd^{(0)}$ catalyst, completing the catalytic cycle.[57]

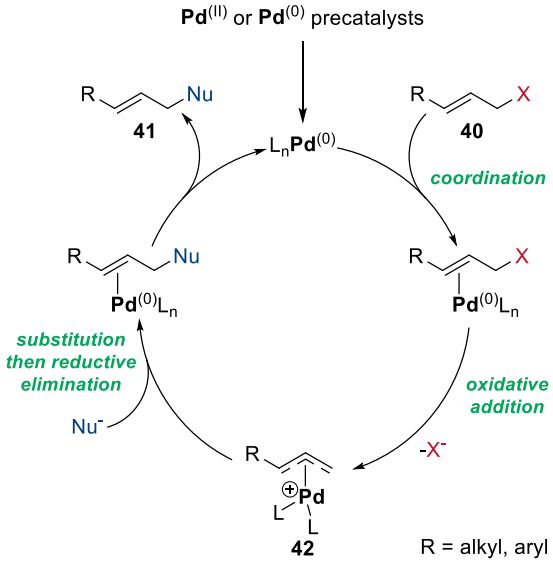

Scheme 10: Mechanistic cycle of the TSUJI-TROST reaction.[57]

Within the TSUJI-TROST mechanism, variations in the substitution step can occur depending on the nature of the nucleophile.[57]

- **Soft nucleophiles** (e.g., stabilized carbanions or certain heteroatom nucleophiles) tend to undergo an **outer sphere attack**, directly attacking the carbon of the π-allyl moiety (Scheme 11).[58]
- **Hard nucleophiles** (e.g., unstabilized enolates, primary amines, alcoholates), on the other hand, favour an **inner sphere attack**. In this case, the nucleophile initially attacks the Pd center in **42**, forming a new Pd complex **43** with the nucleophile coordinated to the metal. Subsequently, **reductive elimination** occurs, coupling the nucleophile and allyl fragment to form the final product **41** and regenerating the catalyst (Scheme 11).[58]

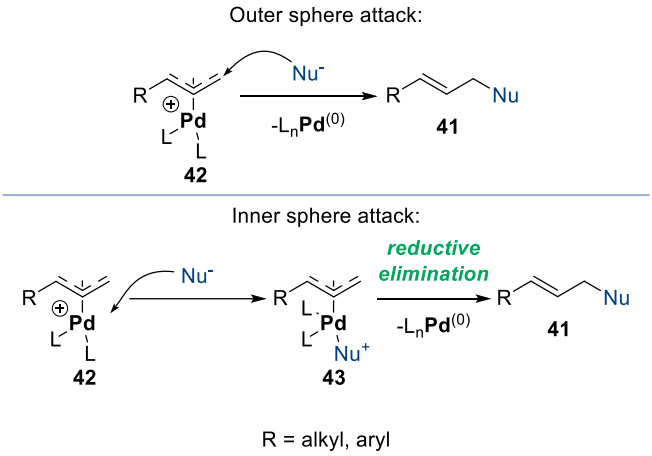

Scheme 11: Outer and inner sphere attack of nucleophiles.[57]

Furthermore, the TSUJI-TROST reaction can proceed via two distinct regiochemical pathways, depending on the site of nucleophilic attack on the π-allyl complex **44** (Scheme 12): Path a where the nucleophile attacks the less substituted terminal carbon of the π-allyl complex **44** and path b where the nucleophile attacks the more substituted internal carbon of the π-allyl complex **44**. The preference for one pathway over the other primarily depends on stereo-electronic factors, including the steric environment around the allyl carbons and the electronic properties of the nucleophile and the electrophile.[54] Consequently, two different constitutional isomers, **45** and **46**, could potentially be formed, raising regioselectivity challenges in the TSUJI-TROST reaction.

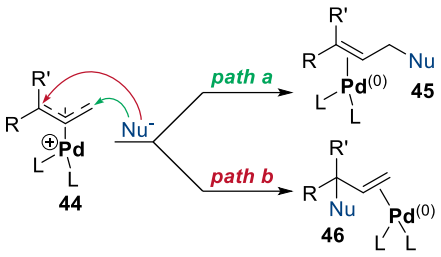

Scheme 12: Different pathways for the nucleophilic substitution in the TSUJI-TROST reaction.[54]

In the TSUJI-TROST reaction, a range of leaving groups (X) can be utilized. Common choices include acetates, halides, and carbonates such as OBoc, OTroc, and methyl carbonate. Acetates are readily available and widely used, but often require elevated temperatures or more reactive catalysts. Halides are typically more reactive than acetates, but can be prone to side reactions. Carbonates offer the distinct advantage of liberating CO_2 as a driving force during the oxidative addition step, facilitating the formation of the π-allyl complex and potentially leading to milder reaction conditions and improved efficiency.[56] The leaving group can be located terminally, as in substrate **47**, or internally (tertiary position), as in substrate **48** (Scheme 13). This will have an influence on the diastereo- and regioselectivity of the reaction.[59]

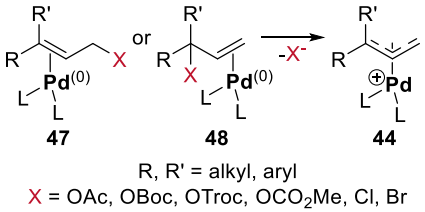

Scheme 13: Leaving group position in the TSUJI-TROST reaction.[56,59]

A unique case within the range of leaving groups for the TSUJI-TROST coupling involves allylic epoxides **49** (Scheme 14). Upon coordination of the palladium catalyst to the epoxide, an allylic complex **50** is generated. Subsequent substitution by the nucleophile and reductive elimination will predominantly yield an allylic alcohol product **51**.[60] This particular pathway is valuable in the synthesis of Cleistocaltone B (**24**), where this structural motif is required.

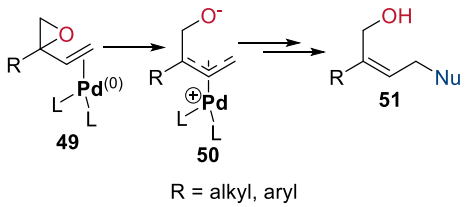

Scheme 14: Epoxides as a leaving group in the TSUJI-TROST reaction.[60]

A significant advantage of palladium-catalyzed coupling reactions is the ability to utilize chiral ligands and achieve enantioselective transformations. While this principle extends to the TSUJI-

TROST reaction, achieving enantioselectivity in this context presents a greater challenge. This difficulty arises because the nucleophilic attack typically occurs from the face opposite the palladium complex. Consequently, to induce chirality, the catalyst's "chiral pocket" must be sufficiently large to effectively differentiate between the enantiotopic faces of the π-allyl intermediate.[58]

To address this challenge, TROST and coworkers developed specialized ligands, such as **52** and **53**, incorporating a chiral (1,2)-diaminocyclohexane (DACH) core (Figure 5). These ligands create a large chiral environment around the palladium center, akin to an enzyme's active site. This expansive "chiral pocket" enhances the catalyst's ability to discriminate between the enantiotopic faces of the π-allyl intermediate, thereby promoting enantioselective nucleophilic attack and the formation of enantioenriched products.[54]

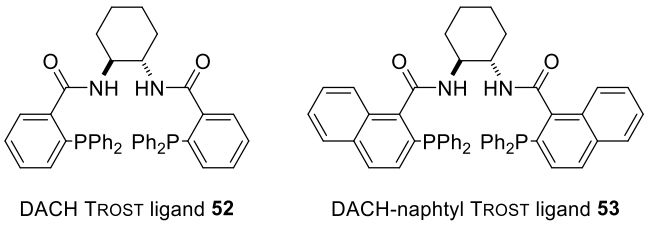

Figure 5: Structure of TROST ligands **52** and **53**.

These ligands have been used to great success in stereoselective allylic alkylation reactions. Notably, they have even facilitated the formation of quaternary stereocenters with high *ee*, such as in product **54**, resulting from the reaction of substrate **55** with allylic acetate **56** using TROST ligand **52**, $(allylPdCl)_2$, LDA, and Me_3SnCl (Scheme 15).[61]

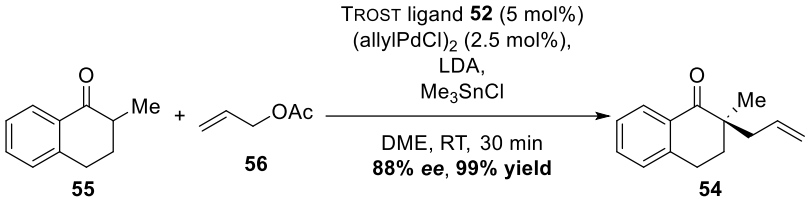

Scheme 15: Example for an enantioselective TSUJI-TROST reaction.[61]

1.5.2 Intramolecular DIELS-ALDER Cycloaddition

The DIELS-ALDER reaction is a pericyclic [4+2] cycloaddition between a diene and a dienophile discovered by DIELS and ALDER in 1927 (Scheme 16).[62] It is a powerful reaction with an optimal atom economy able to generate compounds with a tremendous amount of complexity out of relatively simple starting materials in a single step.

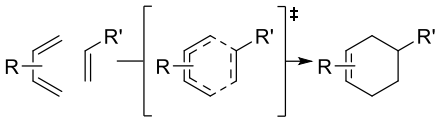

Scheme 16: General example for the DIELS-ALDER reaction.

Mechanistically, the DIELS-ALDER reaction proceeds through a concerted pericyclic process involving the interaction of the π-orbitals of the diene and dienophile, resulting in the formation of two new σ-bonds. The electronic properties of the reactants play a crucial role in determining the reaction pathway, leading to two distinct types of DIELS-ALDER reactions.[63]

In the *normal electron-demand DIELS-ALDER reaction*, the diene is electron-rich, typically bearing electron-donating groups (EDGs), while the dienophile is electron-poor, often possessing electron-withdrawing groups (EWGs). This electronic configuration lowers the energy of the dienophile's lowest unoccupied molecular orbital (LUMO), facilitating a favourable interaction with the highest occupied molecular orbital (HOMO) of the diene (Scheme 17).[63]

Conversely, the *reverse electron-demand DIELS-ALDER reaction* features an electron-poor diene, substituted with EWGs, and an electron-rich dienophile, bearing EDGs. In this scenario, the EWGs on the diene lower the energy of its LUMO, enabling a productive interaction with the HOMO of the dienophile (Scheme 17).[63]

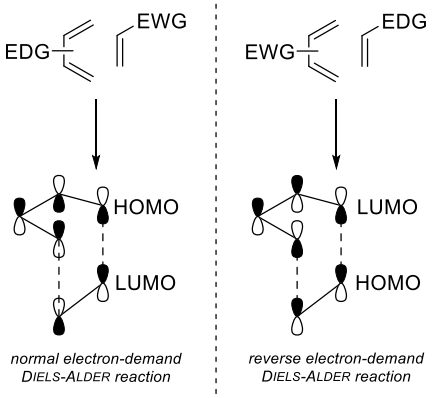

Scheme 17: Different types of DIELS-ALDER reactions according to frontier molecular orbital theory.[64]

Two distinct transition states are possible in the DIELS-ALDER reaction (Scheme 18). In the *endo*-transition state, the substituents R and R' are oriented on the same side of the developing cyclic system. This pathway leads to the formation of the product **57**, which is often favoured kinetically due to stabilizing secondary orbital interactions between the diene and dienophile substituents during the transition state.[65]

Alternatively, the *exo*-transition state involves the substituents R and R' positioned on opposite sides of the forming ring. This configuration results in the product **58**, which may be

thermodynamically more stable due to reduced steric interactions between the substituents in the final product.[65]

The selectivity between the *endo* and *exo* pathways primarily depends on the interplay of secondary orbital interactions and steric effects. Achieving the desired diastereoselectivity can be a challenge in DIELS-ALDER reactions, often requiring careful consideration of the substituents and reaction conditions to favour the formation of the desired product.[65]

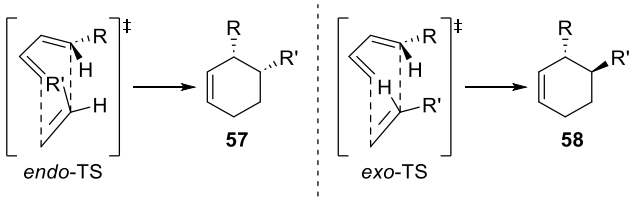

Scheme 18: *endo*- and *exo*-TS for the DIELS-ALDER reaction.

A unique variant of the DIELS-ALDER reaction is the intramolecular DIELS-ALDER cycloaddition (IMDA), where the diene and dienophile components are linked within the same molecule. This intramolecular tethering facilitates the reaction by pre-organizing the reactants into a favourable conformation for cycloaddition, often leading to enhanced rates and improved regio- and stereoselectivity compared to intermolecular reactions.[66]

IMDAs can be classified into two types (Figure 6). In the first type, the tether connects to one of the terminal carbons of the diene moiety. In the second type, the tether is attached to one of the internal carbons of the diene. The nature and length of the tether can significantly influence the regio- and stereochemical outcome of IMDA reactions.[67]

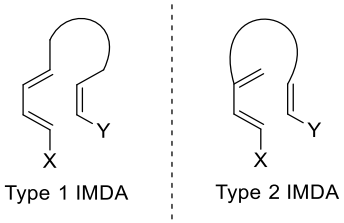

Figure 6: Different types of IMDA.[67]

Due to the large increase of complexity, IMDAs are highly desirable key-steps in total syntheses and have been used to great success in the past. One famous example is the synthesis of Norzoanthamine (**59**) by MIYASHITA and coworkers where a thermal IMDA of **60** was used to diastereoselectively furnish the B and C rings of the natural product yielding the *exo*-product **61** after deprotection of the silyl ether (Scheme 19).[68]

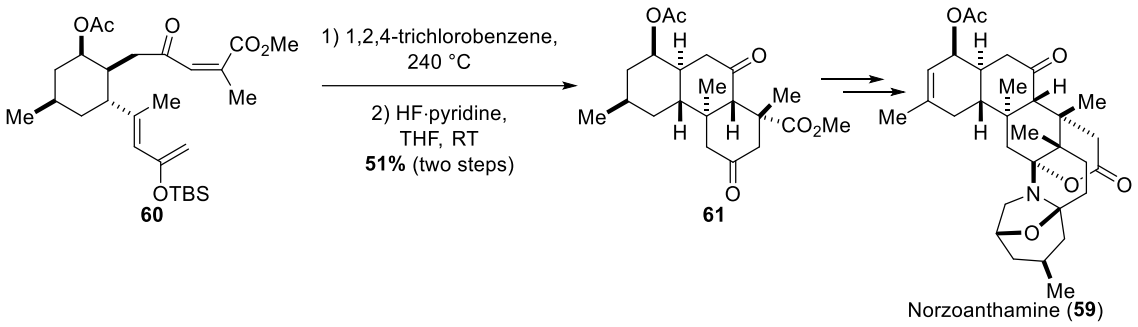

Scheme 19: Thermal type 1 IMDA of **60** yielding the *exo*-product **61** after silyl ether deprotection in the total synthesis of Norzoanthamine (**59**) by MIYASHITA and coworkers.[68]

In addition to thermal activation, LEWIS acids can also catalyze DIELS-ALDER reactions, particularly when the dienophile possesses a carbonyl group in the α-position. The LEWIS acid coordinates to the carbonyl oxygen, lowering the energy of the dienophile's LUMO and enhancing its reactivity towards the diene.[69]

A notable example of LEWIS acid-catalyzed IMDA is found in BARAN and coworkers' synthesis of Taxadiene (**62**), an important intermediate in the synthetic preparation of the anticancer drug Paclitaxel (**1**). The key IMDA step involved the substrate **63** containing a 1,3-diketone moiety adjacent to the dienophile. By employing $BF_3{\cdot}OEt_2$ as the LEWIS acid catalyst, the reaction proceeded efficiently, completing the carbon skeleton of Taxadiene (**62**) and affording the desired product (**64**) in 47% yield (Scheme 20).[70] This example demonstrates the high value of the IMDA for the construction of ring systems in polycyclic natural products.

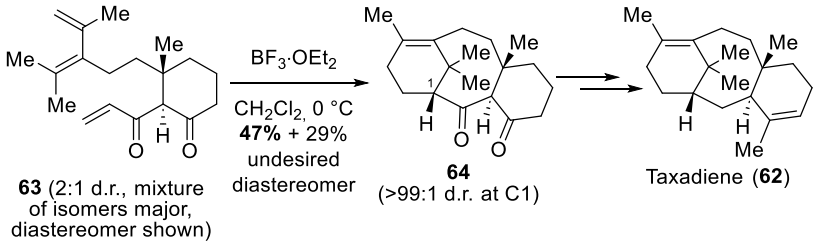

Scheme 20: LEWIS acid catalyzed type 2 IMDA in the synthesis of Taxadiene (**62**) by BARAN and coworkers.[70]

2. Research Objectives

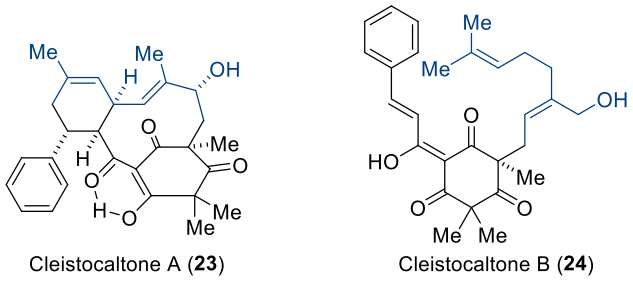

Figure 7: Structures of Cleistocaltones A (**23**) and B (**24**).

The excellent antiviral activity makes Cleistocaltones A (**23**, Figure 7) and B (**24**, Figure 7) valuable targets for a total synthesis. The development of a synthetic access could enable further research and contribute to the discovery of new antivirals which are urgently needed, as the recent COVID-19 pandemic caused by severe acute respiratory syndrome coronavirus 2 (SARS-CoV-2) has starkly demonstrated.

In this work, a biomimetic approach for the total syntheses of Cleistocaltone A (**23**) and B (**24**) based on the developed retrosynthesis (Scheme 8) should be investigated. For this purpose, an efficient synthesis of Champanone B (**25**) should be established. Then, different terpene fragments containing a diene and a suitable leaving group should be synthesized. Subsequently, as the first key-step of the total synthesis, an enantioselective TSUJI-TROST alkylation should be developed to tether the terpene side-chain to Champanone B (**25**). This should assemble the precursor for an IMDA **38**. The IMDA as the second key-step should diastereoselectively construct the carbon skeleton of Cleistocaltone A (**23**). An oxidation of the macrocycle in **37** should then lead to the desired NP. When a method for the allylic alkylation of **25** is developed, Cleistocaltone B (**24**) should be synthesized in a similar manner by installing the appropriate oxidized geranyl side-chain.

With a synthetic access to Cleistocaltones A (**23**) and B (**24**) established, the developed reactions should be optimized and scaled-up to a gram-scale to achieve a sustainable supply of the compounds. This should provide a sufficient amount of material for biological studies and the development of derivatives for SAR-studies to identify even more potent target molecules. Moreover, the total synthesis of Cleistocaltone B (**24**) should give a confirmation of the proposed structure as a structural elucidation by XRD is probably not possible due to its equilibrium with its diastereomer.

3. Results and Discussion

3.1 Synthesis of Champanone B

Biosynthetically, the phloroglucinol part of Cleistocaltone A (**23**) supposedly derives from Champanone B (**25**).[51] **25** is a natural product which was first isolated by DUQUE and coworkers in 2005 from the seeds of *Campomanesia lineatifolia* native to the Amazonas region.[71]

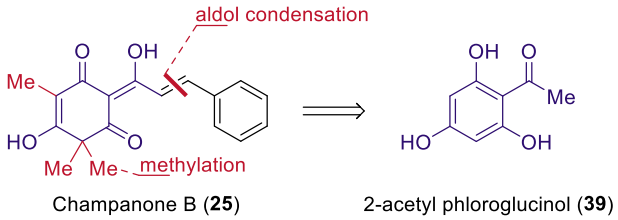

Scheme 21: Structural features of Champanone B (**25**).

Champanone B (**25**) structurally originates from 2-acetyl phloroglucinol (**39**) which, along with methylation of the aromatic ring, must undergo an aldol condensation to transform the acetyl group into a cinnamoyl moiety (Scheme 21). Champanone B (**25**) has been first synthesized by LEE and coworkers as an analogue of Desmosdumotin C (**65**) which was isolated 2002 from *Desmos dumosus* and synthesized 2005 also by LEE and coworkers.[72–74] The synthesis (Scheme 22) commences with 2-acetyl phloroglucinol (**39**) which is methylated under use of MeI and NaOMe as a base to give trimethylated acetyl phloroglucinol **66** with a yield of 56%. The methylation of the oxygen in **66** proved to be quite difficult due to the presence of a strongly acidic proton at the C-4 position. Therefore, typical methylation methods employing a base and MeI only gave the C-methylated product. Only under mild, base-free conditions using $TMSCN_2$ a selective O-methylation giving **67** with 88% yield was possible. After an aldol condensation of the acetyl group in **67** under typical conditions using PhCHO and KOH with 78% yield, Desmosdumotin C (**65**) was obtained.[72] The cleavage of the O–methyl-group was accomplished by refluxing Desmosdumotin C (**65**) in MeOH and acetone in the presence of HCl to give Champanone B (**25**) with a suboptimal yield of 40%. Additionally, a cyclized side product **68** was yielded with 13%.[73] The synthesis was published three months prior to the isolation of Champanone B (**25**). Therefore, it was presumably not known during this time that Champanone B (**25**) was, in fact, a natural product and optimization of the synthesis was likely not a primary goal of that work.

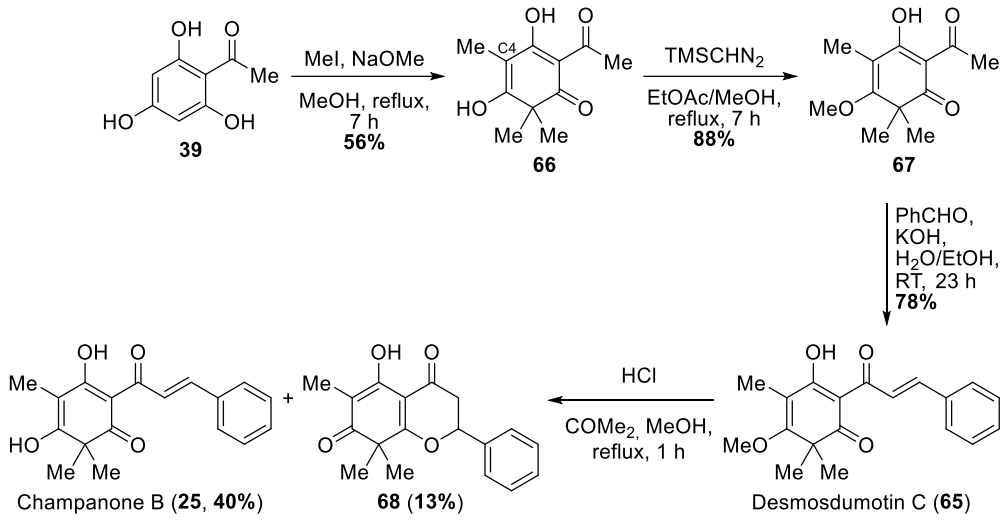

Scheme 22: First total synthesis of Champanone B (**25**) published 2005 by LEE and coworkers.[72,73]

Due to the unfavourable yield of the demethylation step and the employment of expensive and dangerous $TMSCHN_2$, the aim was to develop an optimized route to give access to Champanone B (**25**) in large quantities.

3.1.1 Synthesis *via* Methylation of 2',4',6'-Trihydroxychalcone

In the attempt to optimize the synthesis of Champanone B (**25**), the first route that was developed is shown in Scheme 23. The first step consists of the MOM-protection of two of the enols in 2-acetyl phloroglucinol (**39**). To avoid working with the highly carcinogenic MOMCl, a method developed by BERLINER and coworkers was utilized where MOMCl is generated *in situ* by the zinc-catalyzed reaction of dimethoxymethane with acetyl chloride.[75] Excess MOMCl was quenched before the opening of the reaction vessel. Therefore, the risk of exposure was minimized. Thus, MOM-protected acetyl phloroglucinol **69** was obtained with a yield of 38%. Although the yield of this reaction was below-par, it was determined that the higher safety standards outweighed the diminished yield. Moreover, all reactants and reagents utilized in this step were inexpensive and a scale-up was easily conceivable.

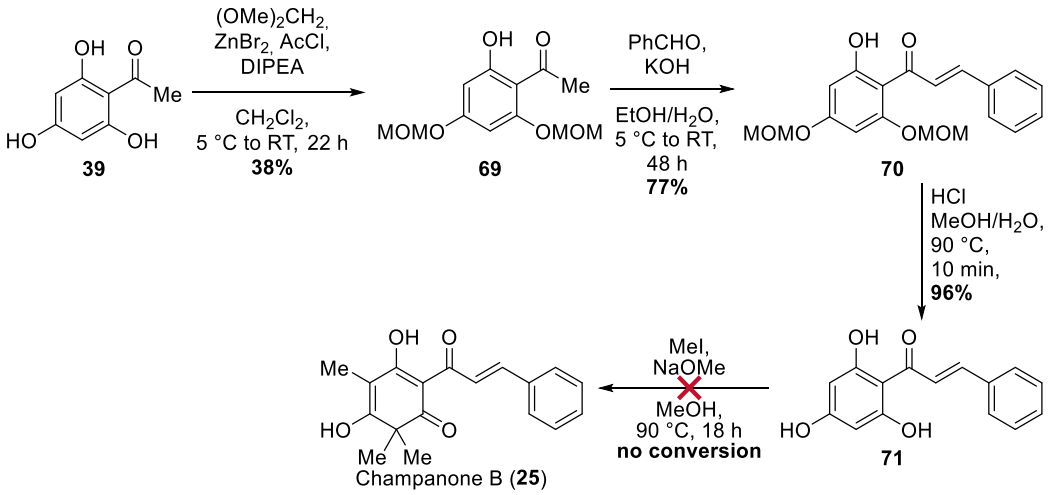

Scheme 23: Attempt to synthesize Champanone B (**25**) *via* cinnamoyl phloroglucinol **71**.

In the next step, MOM-protected acetyl phloroglucinol **69** was transformed to the corresponding cinnamoyl phloroglucinol **70** under classic aldol condensation conditions using PhCHO and KOH in ethanol/water with a yield of 77%. The deprotection of the MOM-protected enols was successfully achieved by boiling of **70** in methanol/water under the presence of HCl yielding 2-cinnamoyl phloroglucinol (**71**) with an excellent yield of 96%. For the methylation of **71** the same method as employed by LEE and coworkers was utilized.[72] However, even after boiling **71** for 18 h with excess MeI and NaOMe, no conversion at all could be observed. Presumably, the presence of the cinnamoyl moiety on the phloroglucinol ring creates a large conjugated system that causes a delocalization of the negative charge in the deprotonated phloroglucinol. This lowers its nucleophilicity to a significant extent so that no nucleophilic substitution can be achieved. Therefore, this route was not further pursued.

3.1.2 Synthesis *via* Protected Champanone B

In the next attempt to synthesize Champanone B (**25**), the methylation of 2-acetyl phloroglucinol (**39**) was performed before the aldol condensation to avoid the problems present in the first route (Scheme 24). Utilizing the conditions of LEE and coworkers,[72] 2-acetyl phloroglucinol (**39**) was boiled in methanol in the presence of 3.3 equiv. of MeI and 3.7 equiv. of NaOMe. After neutralization of the reaction mixture with HCl, LEE and coworkers performed an extraction followed by a column chromatography to obtain pure trimethyl acyl-phloroglucinol **66**.[72] However, this procedure was only feasible for small reaction scales. Because of the presence of acidic protons, the behaviour of **66** on the silica gel column was suboptimal. If attempted to purify large quantities of crude **66** by column chromatography, no amount of pure **66** could be obtained. Additionally, large amounts of solvent were wasted to attempt the purification. Recrystallization of the residue from the EtOAc extract was also unsuccessful. Luckily, it was observed that after the neutralization of the reaction mixture an off-white substance precipitated. This substance was

identified as the already pure trimethyl acetyl-phloroglucinol **66**. After filtration and washing of the substance with water, pure off-white powderous product could be obtained leaving all impurities, such as the dimethyl acetyl-phloroglucinol, in the filtrate. This optimized work-up procedure did not only improve the yield significantly from 56% (LEE and coworkers)[72] to 69%, but also massively simplified the purification process. Interestingly, this method of purification worked only when the reaction was stopped after 7 h, because in this case, the impurities consist mainly of the water-soluble mono- and dimethylated products. When the reaction mixture is refluxed overnight, the main impurity is composed of the tetramethylated product, which is also not soluble in water. However, due to the poor solubility of **66** in CH_2Cl_2, this impurity is easily removed by washing the crude product after filtration with CH_2Cl_2. Although in this case, the yield is significantly diminished.

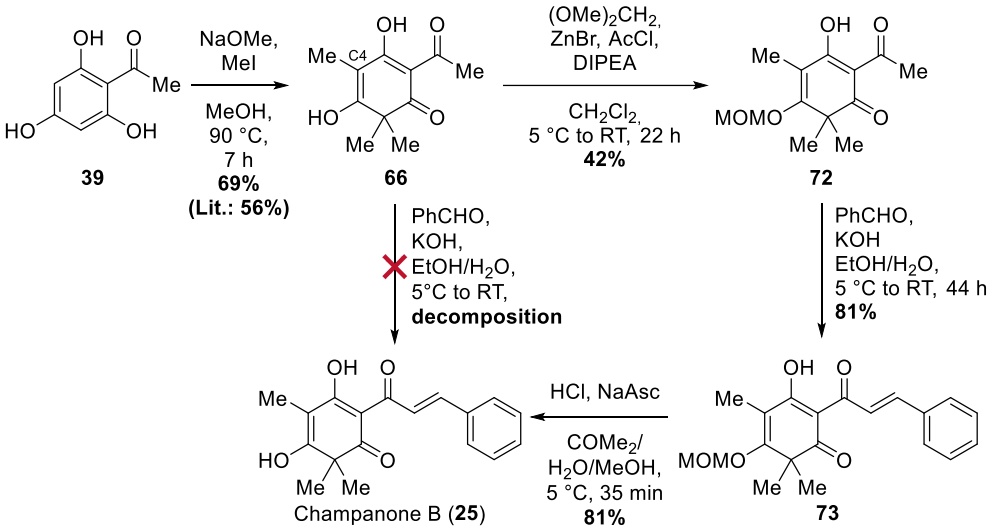

Scheme 24: Synthesis of Champanone B (**25**) *via* MOM-protected phloroglucinol **73**.

With large amounts of trimethyl acetyl-phloroglucinol **66** available, the direct aldol condensation was attempted to obtain Champanone B (**25**) in two steps. However, only a complex mixture was obtained suggesting that the compound decomposed. This occurred possibly due to the reactive C-4 position in **66** which could undergo many side reactions. Therefore, a protection of the reactive enol was in order. Using similar conditions according to BERLINER and coworkers, MOMCl was once again generated *in situ* to obtain MOM-protected enol **72** with a yield of 42%. The following aldol condensation proceeded smoothly and cinnamoyl phloroglucinol **73** was produced with a yield of 81%. To obtain Champanone B (**25**), the deprotection of the MOM-ether was attempted. This proved to be much more challenging than anticipated. Due to the formation of an electrophilic oxonium ion in the deprotection process many unwanted side products emerged which were not separable from the product. A method that would circumvent this issue was required. Several different conditions were examined (Table 1).

Table 1: Conditions for the deprotection of MOM-protected Champanone B (**73**).

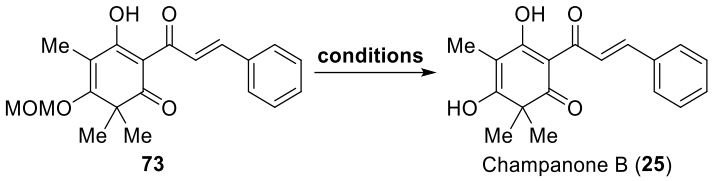

Entry	Conditions	Comment
1[a]	HCl, 1,4-dioxane/H_2O, RT, 60 min	decomposition
2[a]	HCl, MeOH/$COMe_2$/H_2O, 0 °C, 60 min	decomposition
3	*n*-PrSH, $ZnBr_2$, CH_2Cl_2, 0 °C, 35 min	decomposition
4[b]	HCl, MeOH/$COMe_2$/H_2O, –20 °C, 2 h	no reaction
5[b]	HCl, MeOH/$COMe_2$/H_2O, 0 °C, 35 min	decomposition
6[b]	HCl, NaAsc, MeOH/$COMe_2$/H_2O, 0 °C, 35 min	81% yield

a) The HCl-solution was added to a solution of MOM-protected Champanone B **73** dropwise. b) A solution of MOM-protected Champanone B **73** in acetone was added to the reaction mixture over 30 min using a syringe pump.

Since MOM-protected Champanone B **73** was insoluble in methanol or water, the deprotection was tested in 1,4-dioxane at RT (Table 1, entry 1). However, this lead to an inseparable complex mixture of products. Next, the deprotection should be examined at a lower temperature. However, due to the high melting point of 1,4-dioxane, the solvent was adjusted accordingly. It was observed that **73** was soluble in acetone. Therefore, in the next attempt a solution of HCl in methanol and water was added to the **73** solution in acetone at 0 °C (Table 1, entry 2). This, unfortunately, resulted in decomposition once more. As acid catalyzed deprotection methods did not lead to any success until this point, a different method using *n*-PrSH and $ZnBr_2$ was evaluated (Table 1, entry 3). This method was developed by RAWAL and coworkers and further investigated and optimized by SOHN, RYU, and coworkers.[76,77] Unfortunately, this method of using propyl thiol as a oxonium-ion scavenger was not successful in the case of MOM-protected Champanone B **73**. As the alternative method of the MOM-deprotection was unsuccessful, the acid catalyzed deprotection was investigated once more. To prevent the oxonium-ion from reacting with an excess of unreacted starting material, the solution of MOM-protected Champanone B **73** dissolved in acetone was added to the HCl-solution very slowly over a period of 30 min. The first attempt was made at –20 °C (Table 1, entry 4). However, no reaction was taking place at this temperature. Therefore, the temperature was elevated to 0 °C (Table 1, entry 5). As this also resulted in a complex mixture, in the next experiment, sodium ascorbate was added (Table 1, entry 6). The reasoning behind this was that sodium ascorbate, a mild reducing agent, could function as a scavenger of the reactive oxonium-ion. Luckily, this method was successful and afforded Champanone B (**25**) with a yield of 81%. However, it is to be noted that the mechanism of this reaction was not further investigated and is therefore unknown.

3.2 Synthesis of Terpene Fragments for Cleistocaltone A

With an efficient synthesis of Champanone B (**25**) established, several terpene fragments should be synthesized for the TSUJI-TROST coupling. Viable fragments could structurally derive from linalool (**74**) which possesses a tertiary hydroxy-group at the C-3 position and geraniol (**75**) where the hydroxy-group is situated at the terminal C-1 position (Scheme 25).

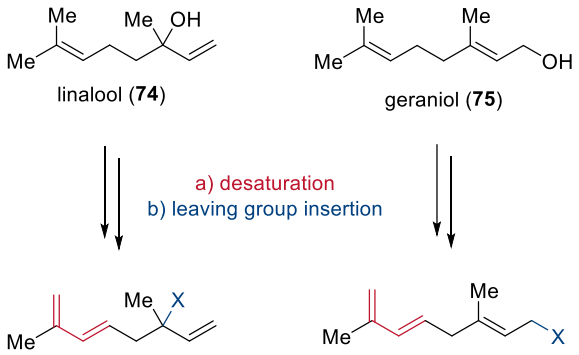

Scheme 25: Synthesis of terpene fragments featuring a diene and a leaving group **X**.

Being more electron-rich due to the absence of any electron-withdrawing functionalities in the near vicinity, the terminus should be transformed selectively into the diene via a desaturation sequence. The hydroxy-group could be transformed into a vast array of leaving groups such as acetates, carbonates or halogenates which are all feasible leaving groups for the TSUJI-TROST reaction.

3.2.1 Synthesis of Hotrienyl Derivatives

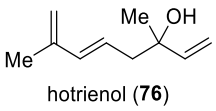

Figure 8: Structure of hotrienol (**76**).

The first target compound was hotrienol (**76**, Figure 8), a linalool derivative, which meets the desired structural requirements. It has first been isolated and identified in 1969 by YOSHIDA, MURAKI, KAWAMURA, and KOMATSU for Takasago Perfumery Co. from the leaves of the Japanese fragrant camphor tree *Cinnamomum camphora* as a fruity smelling compound.[78] A convenient synthesis without any C–C-bond formations was developed in 2003 also for Takasago Perfumery Co. by YUASA and coworkers.[79] Since this route was very step-efficient, had good yields, involved inexpensive reagents and was already scaled up to a kg-scale, it seemed to be the ideal starting point and was attempted first (Scheme 26).

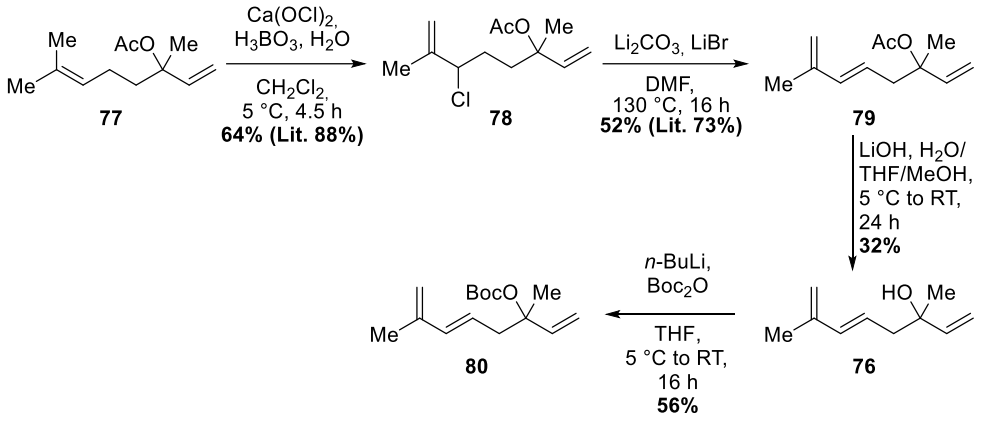

Scheme 26: Synthesis of hotrienol (**76**) according to YUASA and coworkers and derivatization to the corresponding *tert*-butyl carbonate **80**.[79]

The synthesis commenced with linalyl acetate (**77**) in which the terminus was chlorinated through an ene-type chlorination using $Ca(OCl)_2$ and boric acid. The authors developed an ingenious method where they exploited the poor solubility of the reagents in CH_2Cl_2. To start the reaction, water was added. This resulted in a triphasic reaction mixture where in the aqueous phase, boric acid and $Ca(OCl)_2$ reacted to form hypochlorous acid as the chlorinating agent in a controlled manner. These mild reaction conditions allowed for a selective chlorination of the more electron-rich double bond forming the allylic chloride **78** under release of water. For this reaction, vigorous stirring was crucial as even stopping for only a moment resulted in a coagulation of the salt and formation of one semi-solid piece of reagents. While the reaction was easily set up and carried out, the work-up process became very tedious due to the formation of poorly soluble salts consisting of the by-products from the reaction. Moreover, in literature, the product was purified by distillation which facilitated the scale-up immensely. Here, this method of purification was not reproducible, because at the given pressure and temperature, no product could be collected. Therefore, the temperature was required to be elevated which resulted in a pyrolysis of the product. In the end, column chromatography was employed. Therefore, the literature yield could not be replicated. However, a yield of 64% was still more than acceptable.

In the next step, the diene **79** was formed by a dehydrochlorination of allylic chloride **78** under basic conditions. Harsh reaction conditions were necessary to accomplish this feat. Using Li_2CO_3 as a base and LiBr as an additive in DMF, the reaction mixture was heated to 130 °C. Again, the literature procedure required adjustments. According to literature, heating for 2 h was sufficient to drive the reaction to completion. In this case, 16 h were required. Moreover, distillation was still unsuccessful at the given pressure and temperature. Purification by column chromatography was difficult due to the formation of many side products, probably accountable to the longer reaction time. Only after carefully degassing the solvent *via freeze-pump-thaw*, the reaction

proceeded smoothly without the formation of many by-products and purification *via* column chromatography was successful. Diene **79** was obtained with a yield of 52%.

For the saponification of the acetyl ester an entirely new method was required. The literature procedure using a 10% NaOH solution in MeOH and water produced hotrienol (**76**) with a yield of only 20% (Lit. 85%).[79] The presence of a by-product with an intense orange colour which rapidly decomposed when attempting purification by column chromatography suggested that the elimination of the acetyl group and formation of a compound with a conjugated π-system was a competing side-reaction. Using LiOH in a solvent system of water/MeOH/THF, the yield was slightly improved giving hotrienol (**76**) with 32%.

To transform the hydroxy-group in hotrienol (**76**) into a leaving group, it was substituted with the *tert*-butyl carbonate under usage of Boc_2O and *n*-BuLi as a base. This gave the corresponding hotrienyl *tert*-butyl carbonate (**80**) with 56% yield.

With this route concluded, two potential coupling partners for the TSUJI-TROST reaction were synthesized, hotrienyl acetate (**79**) and hotrienyl *tert*-butyl carbonate (**80**).

3.2.2 Synthesis of Terpene Fragments Containing a Terminal Leaving Group

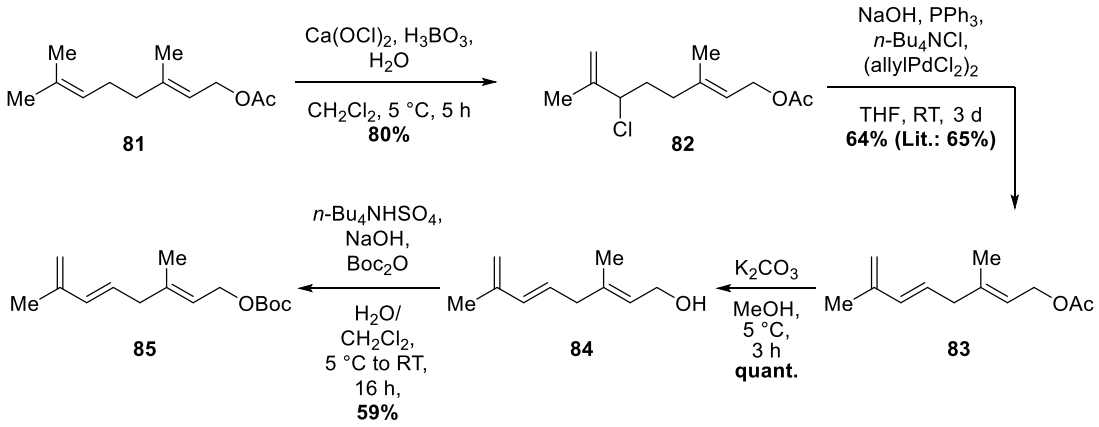

Scheme 27: Synthesis of terpene fragments containing a terminal leaving group.

To synthesize the terpene fragments that contain a terminal leaving group, the synthesis (Scheme 27) commenced with the chlorination of geranyl acetate (**81**). The same conditions according to the chlorination of linalyl acetate (**77**) by YUASA and coworkers were employed.[79] Geranyl acetate (**81**) was vigorously stirred in a suspension of boric acid and $Ca(OCl)_2$ in CH_2Cl_2 at 5 °C while water was added over 4.5 h using a syringe pump. This gave allylic chloride **82** with a yield of 80%. Compared to the chlorination of linalyl acetate, the yield is significantly improved. This is probably

owed to the fact that in this case the electron-deficient double bond is even more sterically hindered leading to even fewer unwanted side reactions.

Table 2: Conditions for the dehydrochlorination of allylic chloride **82**.

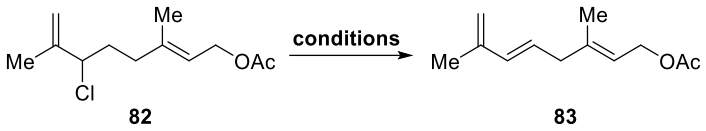

82 **83**

Entry	Conditions	Comment
1	Li_2CO_3, LiBr, DMF, 130 °C, 16 h	decomposition
2	KO*t*-Bu, THF, –60 °C, 3 h	deprotection (24% of **82** recovered)
3	NaOH, PPh_3, $(allylPdCl)_2$, *n*-Bu_4NCl, THF, RT, 3 d	64% yield (Lit.: 65%)[80]

The dehydrochlorination of allylic chloride **82** proved to be more challenging compared to the previous route. Using similar conditions as YUASA and coworkers only decomposition products could be observed (Table 2, entry 1). The terminal acetate appeared to be much more reactive than the tertiary acetate in **78**. Therefore, presumably, a deprotection and other unwanted side reactions could take place. Using a stronger base (KO*t*-Bu) at a lower temperature of –60 °C (Table 1, entry 2) only let to the deprotection of the acetate which seemed to be faster than the dehydrochlorination. Of course, at this point, non-nucleophilic bases like DBU could be investigated. However, a different approach using palladium-chemistry was chosen (Table 2, entry 3).[80] The proposed catalytic cycle for this reaction is shown in Scheme 28. First, the $Pd^{(II)}$-precatalyst allyl-palladium chloride dimer is transformed to the active $Pd^{(0)}(PPh_3)_2$-species. After an oxidative addition into the allylic C–Cl bond of **82** during which a $Pd^{(II)}$-complex is formed, a β-hydride elimination takes place releasing the diene **83** and the $(PPh_3)_2Pd^{(II)}$-complex with a hydrogen and a chlorine atom bound. This complex undergoes a reductive elimination regenerating the Pd(0) catalyst under release of HCl. To prevent HCl from causing any unwanted side reactions, NaOH is used. However, large amounts of NaOH could deprotect the acetate as well. Therefore solid NaOH, which is insoluble in THF, is used in combination with a phase-transfer catalyst *n*-Bu_4NCl. These mild conditions produced diene **83** successfully with a yield of 64%. Despite the tame conditions, moderate amounts of the deprotected alcohol **84** could be observed.

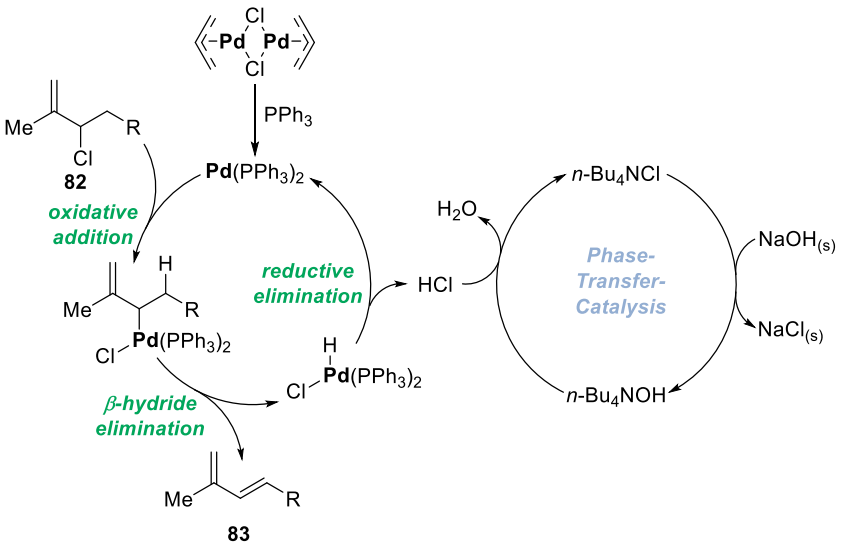

Scheme 28: Proposed catalytic cycle for the dehydrochlorination of allylic chloride **82** to form diene **83**.

To obtain the corresponding *tert*-butyl carbonate **85**, acetate **83** was first saponificated by treatment with K_2CO_3 in ice-cold methanol. This gave alcohol **84** in a quantitative yield. The product did not require any purification as all side-products were water soluble.

Table 3: Conditions for the Boc substitution of alcohol **84**.

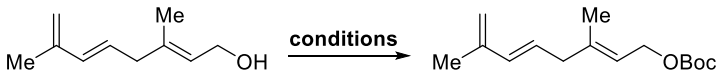

84 **85**

Entry	Conditions	Comment
1	*n*-BuLi, Boc_2O, THF, 0 °C to RT, 16 h	decomposition
2	NEt_3, DMAP, Boc_2O, CH_2Cl_2, RT, 3 h,	26% yield
3	*n*-Bu_4NHSO_4, NaOH, Boc_2O, H_2O/CH_2Cl_2, 0 °C to RT, 16 h	59% yield

Different conditions were examined to transform alcohol **84** into the *tert*-butyl carbonate **85** (Table 3). First, similar conditions as described above using *n*-BuLi and Boc_2O were utilized (Table 3, entry 1). However, this only lead to decomposition. It seemed that the primary hydroxyl-group was more sensitive than the tertiary one. Using milder conditions with triethylamine as a base, DMAP as a catalyst, and Boc_2O, the product was obtained with 26% yield. This was not satisfactory. Therefore, to accomplish even milder conditions, once more a biphasic reaction system was exploited (Table 3, entry 3). Here, alcohol **84** and Boc_2O were dissolved in CH_2Cl_2 and NaOH was present as the base in the aqueous phase. Tetrabutylammonium hydrogen sulphate acted as a phase transfer catalyst, improving the yield to 59%.

With this, four viable compounds for the TSUJI-TROST coupling **79**, **80**, **83**, and **85** were produced in an efficient manner (Figure 9).

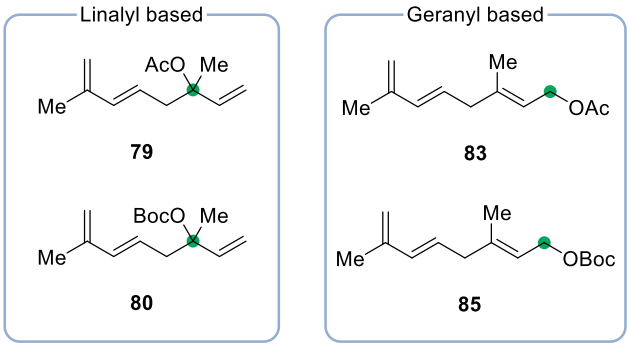

Figure 9: Terpene fragments for the TSUJI-TROST coupling.

3.3 Coupling Attempts

3.3.1 TSUJI-TROST Coupling Attempts

The first coupling attempts of Champanone B (**25**) with the terpene fragment consisted of a TSUJI-TROST coupling with the linalyl based acetate **79** and *tert*-butyl carbonate **80** (Table 4).

Table 4: Conditions for TSUJI-TROST coupling of Champanone B (**25**) with linalyl based terpene fragments.

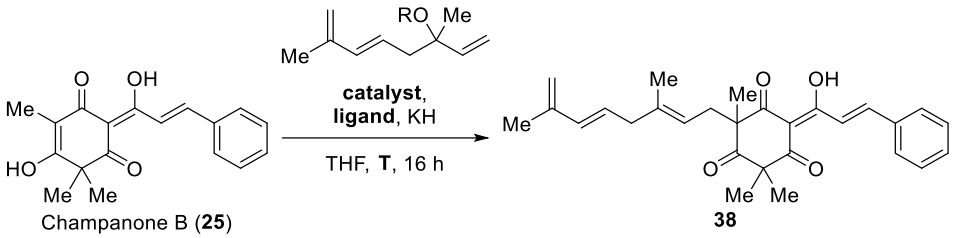

Entry	R	Catalyst	Ligand	T	Comment
1	Ac	Pd_2dba_3	-	–78 °C to 60 °C	no conversion
2	Ac	Pd_2dba_3	dppf	RT to 60 °C	no conversion
3	Ac	$Pd(PPh_3)_4$	PPh_3	RT to 60 °C	no conversion
4	Boc	$Pd(PPh_3)_4$	PPh_3	RT to 60 °C	no conversion

First, using the acetate **79**, Pd_2dba_3 as a catalyst, and KH in mineral oil as a base, the reagents were carefully combined at –78 °C (Table 4, entry 1). As no reaction took place the mixture was allowed to warm up to RT which also did not amount to any conversion. Even heating to 60 °C did not yield the desired results. The same was the case when dppf or PPh_3 were used as a ligand (Table 4, entry 2 and 3). Next, the *tert*-butyl carbonate **80** was used as it should be more reactive (Table 4, entry 4). However, again, no conversion could be observed.

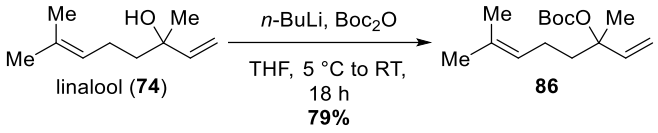

Scheme 29: Synthesis of linalyl *tert*-butyl carbonate **86** for model reactions.

To avoid wasting any more precious diene on test reactions, linalool (**74**) was substituted to the *tert*-butyl carbonate **86** (Scheme 29). Further screening was carried out with this compound. Now, Cs_2CO_3 was used as a base and PPh_3 as a ligand. Again, at RT and at 60 °C no conversion was observed (Scheme 30).

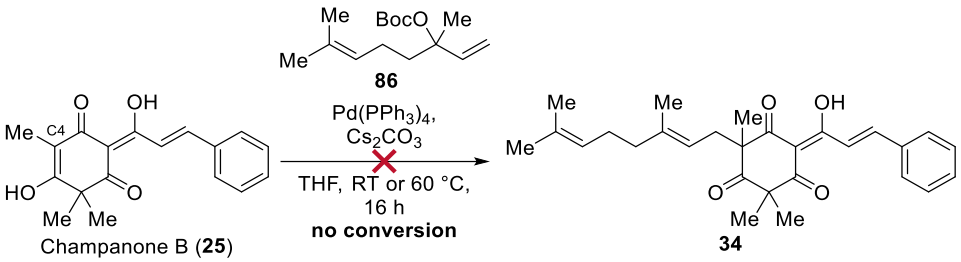

Scheme 30: Conditions for the TSUJI-TROST coupling of Champanone B (**25**) with linalyl *tert*-butyl carbonate **86**.

Since coupling with various ligands and various linalyl based terpene fragments was unsuccessful, it was questioned whether the problem originated from the lacking nucleophilicity of Champanone B (**25**). It was hypothesized that the nucleophilicity of the C-4 position was diminished due to the presence of a large conjugated system. After deprotonation, the negative charge was likely delocalized to such an extent that a nucleophilic substitution could not take place anymore. To test this hypothesis, the nucleophilic substitution was examined with geranyl bromide (**87**) and geranyl chloride (**88**), two very reactive electrophiles.

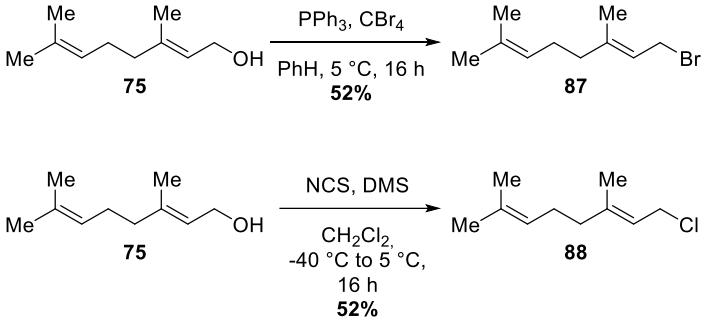

Scheme 31: Syntheses of geranyl bromide (**87**) via an APPEL reaction and geranyl chloride (**88**) via a COREY-KIM reaction from geraniol (**75**).

As demonstrated in Scheme 31, geranyl bromide (**87**) was synthesized out of geraniol (**75**) via an APPEL reaction using PPh_3 and CBr_4.[81] The product was obtained with a moderate yield of 52%, presumably due to its instability. Geranyl chloride (**88**) was also synthesized out of geraniol (**75**) via a COREY-KIM reaction with a yield of 52%.[82]

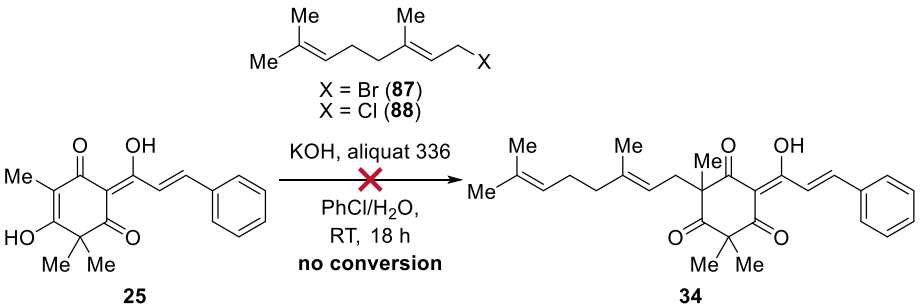

Scheme 32: Attempted nucleophilic substitutions with Champanone B (**25**).

With both electrophiles available, the nucleophilic substitution was examined (Scheme 32). The reaction was set up using a biphasic system with PhCl and H_2O as solvents. KOH was employed as a base and aliquat 336 as a phase transfer catalyst. This setup was chosen due to the good solubility of Champanone B (**25**) in PhCl and because biphasic systems proved to be very effective in previous syntheses. In both cases, no conversion at all was observed even after 18 h. Therefore, the hypothesis of a weakly nucleophilic C-4-position was assumed to be true.

To circumvent this issue, the TSUJI-TROST coupling was examined using the trimethylated acyl phloroglucinol **66** as the nucleophile. First test reactions were performed with linalyl *tert*-butyl carbonate (**86**) as a coupling partner. Pd_2dba_3 was used as the Pd-source and different ligands were tested (Table 5). The nucleophile **66** was deprotonated beforehand using LDA as a base producing the lithiated species **89** and the solution was added to the reaction mixture after all other reagents were dissolved in THF and allowed to stir for 10 min to allow for the formation of the allyl-Pd complex.

Table 5: Conditions for the TSUJI-TROST coupling of deprotonated trimethylated acetyl phloroglucinol **89** with linalyl *tert*-butyl carbonate (**86**).

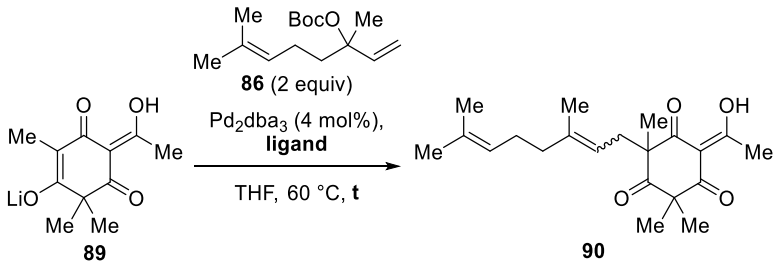

Entry	Ligand	t	Yield	d.r. (*E*:*Z*)[a]	Comment
1	PPh_3 (30 mol%)	20 h	18%	3:1	-
2	dppf (15 mol%)	20 h	44%	3:1	-
3	P(2-furyl)$_3$ (30 mol%)	20 h	35%	3:2	-
4	P(*o*-tolyl)$_3$ (30 mol%)	20 h	-	-	complex mixture
5	dppp (15 mol%)	20 h	37%	3:1	-
6	BINAP (15 mol%)	20 h	34%	5:1	-
7	XPhos (30 mol%)	3 h	77%	5:1	-

a) All d.r. were determined by ^{1}H-NMR after purification.

Fortunately, all ligands showed formation of product **90**. However, in the case of P(*o*-tolyl)$_3$ (Table 5, entry 4) it was not possible to purify the product due to the formation of many inseparable side products. Concerning the other ligands, one inseparable impurity was always present. Identification was difficult, because the desired product **90** and the impurity were always in an equilibrium of two tautomers and therefore gave two sets of signals leading to a total of 4 different

sets. However, on account of the similarity of the different sets it was assumed that the impurity consisted of the *Z*-isomer of **90**. The d.r. were determined by evaluating the integrals in the ^{1}H-NMR. The comparison of the d.r. showed that bulkier ligands such as BINAP and XPhos clearly favoured the formation of the *E*-isomer of **90** (Table 5, entries 6, and 7) with 5:1. In the case of PPh_3, dppf, and dppp (Table 5, entries 1,2, and 5) the preference was not as prominent with 3:1. P(2-furyl)$_3$, the least bulky ligand, gave a d.r. of 3:2 (Table 5, entry 3) showing that there was a small preference. All ligands except for XPhos did not lead to a complete conversion of the starting material. Therefore, the reaction was stopped after 20 h as no notable change was visible by TLC. Accordingly, the yields of **90** from these reactions were suboptimal and ranged from 18% in the case of PPh_3 (Table 5, entry 1) to 44% in the case of dppf (Table 5, entry 2). In contrast, regarding XPhos (Table 5, entry 7), the starting material was consumed completely after 3 h giving the product **90** with 77% yield and the least amount of the undesired *Z*-isomer. Consequently, XPhos was clearly the best performing ligand in this reaction.

Albeit the *E*-isomer of **90** being favoured, the amount of inseparable *Z*-isomer was still too high which could cause problems in later steps. Thus, a method was required where the d.r. was improved.

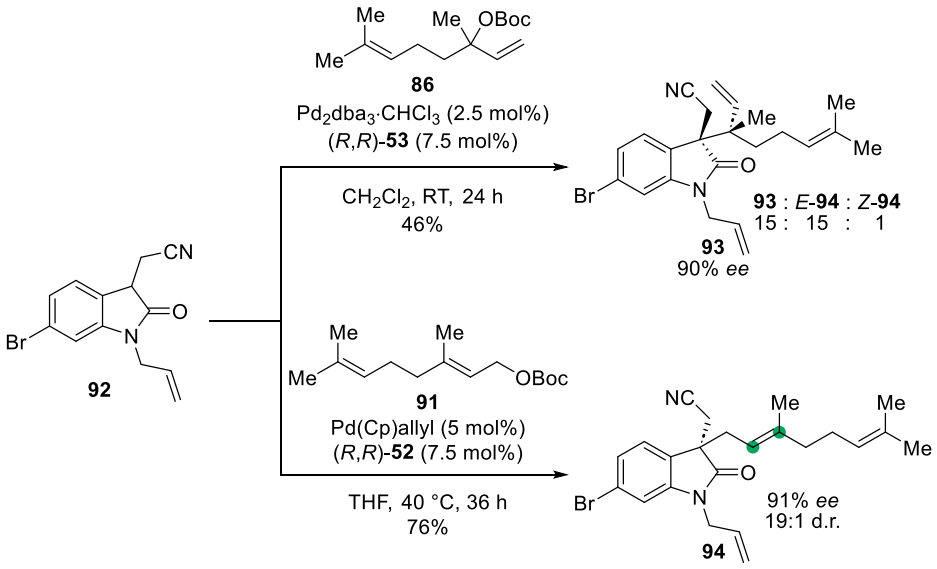

Scheme 33: Studies by TROST and coworkers about the TSUJI-TROST coupling of 3-alkyloxindole **92** with linalyl *tert*-butyl carbonate (**86**) and geranyl *tert*-butyl carbonate **91**.[59]

In a publication of TROST and coworkers, the coupling of different terpene fragments including linalyl *tert*-butyl carbonate (**86**) and geranyl *tert*-butyl carbonate (**91**) with 3-alkyloxindoles such as **92** was studied (Scheme 33).[59] In their studies, TROST and coworkers were able to control the regio- and stereoselectivity of the coupling reactions using the TROST ligands **52** and **53** (Figure 5). Moreover, it was found that in the case of linalyl *tert*-butyl carbonate (**86**) different products such as the tertiary substituted product **93** and the *E*- and *Z*-isomers (with regards to the internal

double bond of the terpene side chain) of the terminally substituted product **94** formed. In contrast, with geranyl *tert*-butyl carbonate (**91**), a very clean reaction with no tertiary substitution and a high 19:1 d.r. towards the *E*-isomer of **94** occurred.[59]

It was interesting to examine whether these findings could be replicated in the synthesis of Cleistocaltone A (**23**) utilizing the TROST ligand and geranyl based coupling partners. Therefore, the coupling of trimethylated acetyl-phloroglucinol **66** with geranyl derived *tert*-butyl carbonate **85** was examined (Table 6).

Table 6: Screening for the TSUJI-TROST coupling of trimethylated acetyl phloroglucinol **66** with geranyl based *tert*-butyl carbonate **85**.

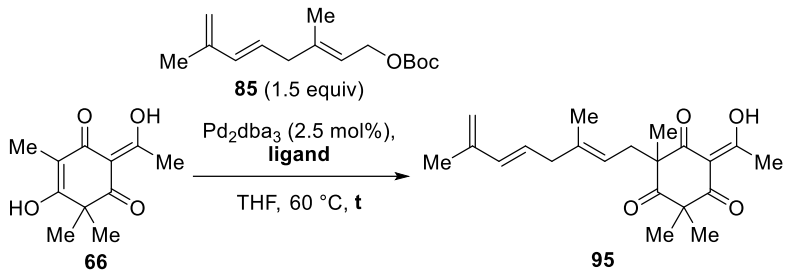

Entry	Ligand	Base	t	Yield	Comment
1[a]	(*R*,*R*)-TROST Ligand **52** (7.5 mol%)	LDA	24 h	-	no conversion
2[a]	(*R*,*R*)-TROST Ligand **52** (7.5 mol%)	*t*-BuOK	24 h	-	no conversion
3	(*R*,*R*)-TROST Ligand **52** (7.5 mol%)	Cs_2CO_3	24 h	-	no conversion
4	(*R*,*R*)-TROST Ligand **52** (7.5 mol%)	-	3 d	8%	impure product
5	XPhos (15 mol%)	-	3 d	10%	impure product
6	XPhos (7.5 mol%)	-	22 h	42%	-

a) **66** was combined with 1.00 equiv of base in a separate SCHLENK tube at 0 °C and added to the mixture of the other reagents in THF at RT.

The first reactions were investigated using this(*R*,*R*)-TROST ligand **52** . At first, different bases were explored. In the case of LDA, no conversion was observed (Table 6, entry 1). Therefore, a different cation utilizing *t*-BuOK, was assessed (Table 6, entries 2). Again, no conversion could be shown. Using a weaker base, Cs_2CO_3, yielded the same result (Table 6, entry 3). With no base, finally a small amount of product could be obtained after 3 d of stirring at 60 °C (Table 6, entry 4). However, a yield of 8% was not satisfactory and the product contained small amounts of inseparable impurities. Since the base seemed to have a negative impact on the reaction, the following couplings were performed without a base. Moreover, XPhos was used as a ligand since it was superior in prior test reactions. Unfortunately, only a slightly better yield of 10% was achieved (Table 6, entry 5). Since XPhos is a sterically demanding ligand, it was suspected that a high excess of this ligand could have a negative impact on the reaction. Accordingly, the amount

of XPhos was lowered to 7.5 mol% so that only a slight excess was present (Table 6, entry 6). Fortunately, this approach was successful and provided a 4-fold increase of the yield. The product was obtained with 42% yield after 22 h. Additionally, no amount of undesired *Z*-isomer emerged.

During every reaction a decomposition of the terpene-fragment could be observed. Therefore, it was assumed that a less reactive leaving group might yield better results. Thus, the coupling was also investigated with the acetate **83** (Table 7).

Table 7: Ligand screening for the TSUJI-TROST coupling of trimethylated acyl phloroglucinol **6** with geranyl based acetate **83**.

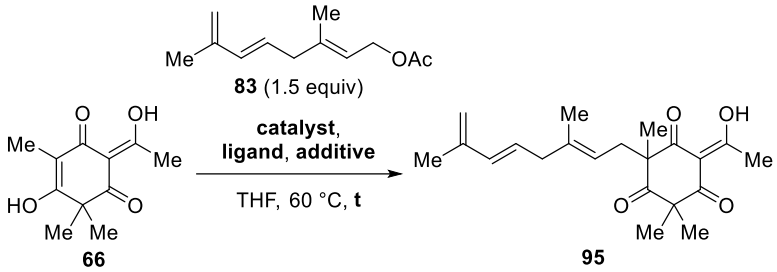

Entry	Catalyst	Ligand	Additive	t	Yield	Comment
1	Pd_2dba_3 (2.5 mol%)	(*R*,*R*)-TROST Ligand **52** (5 mol%)	-	36 h	-	No conversion
2	Pd_2dba_3 (2.5 mol%)	Xantphos (5 mol%)	-	20 h	-	Decomposition of **83**
3	Pd_2dba_3 (2.5 mol%)	XPhos (15 mol%)	-	30 h	2%	-
4	XPhos Pd G2 (5 mol%)	-	NaOAc (5 mol%)	22 h	44%	-
5	Pd_2dba_3 (2.5 mol%)	XPhos (7.5 mol%)	-	19 h	67%	-
6	Pd_2dba_3 (2.5 mol%)	dppf (5 mol%)	-	3 h	72%	-

With (*R*,*R*)-TROST ligand **52** no conversion was observed (Table 7, entry 1). Xantphos only lead to a decomposition of acetate **83**, but no formation of product (Table 7, entry 2). As expected with 15 mol% of XPhos, the yield was poor with 2% (Table 7, entry 3). Using XPhos Pd G2, a good yield of 44% could be obtained which was already better than the results from using the *tert*-butyl carbonate **85** (Table 6). At the appropriate amount of 7.5 mol%, XPhos gave an even better yield of 67% (Table 7, entry 5). However, the best performing ligand in this case was dppf which lead to full consumption of the nucleophile after 3 h and produced geranylated phloroglucinol **95** with an excellent yield of 72% (Table 7, entry 6).

With these optimized conditions, the coupling of trimethylated acetyl-phloroglucinol **66** with geranyl acetate (**81**) was also evaluated to open up the possibility for a linear route to key-intermediate **38** (Scheme 34).

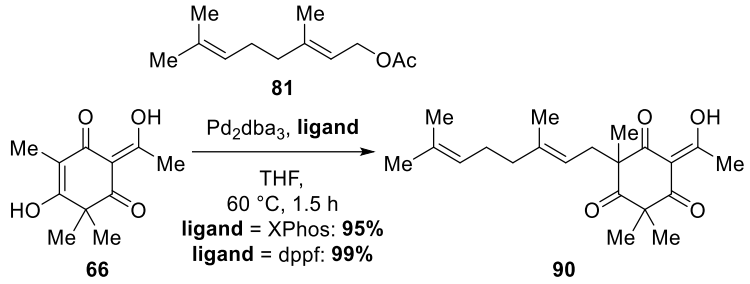

Scheme 34: Coupling of geranyl acetate (**81**) with trimethylated acetyl-phloroglucinol (**66**) using XPhos and dppf.

Luckily, this was achieved with no issues producing geranylated acetyl-phloroglucinol **90** with excellent yields of 95% in the case of XPhos and 99% with dppf as a ligand.

Achieving enantioselective control in this coupling would be highly beneficial. The stereocenter formed in this step ultimately dictates the synthesis of either (+)- or (–)-Cleistocaltone A (**23**), as all subsequent reactions are diastereoselective. Theoretically, a chiral ligand could provide the necessary stereo-control. To identify the optimal choice, a variety of chiral ligands were systematically evaluated with the optimized conditions (Table 8).

Table 8: Ligand screening for the enantioselective TSUJI-TROST coupling of geranyl acetate (**81**) and trimethylated phloroglucinol **66**. (Reproduced (adapted) from Ref.[83] with permission from the Royal Society of Chemistry.)

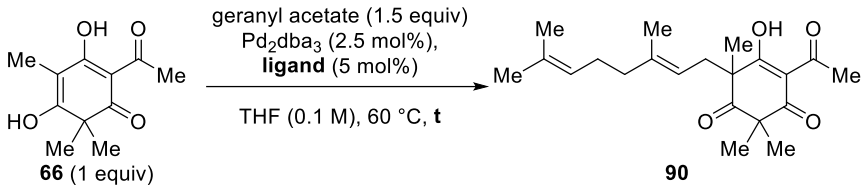

Entry	Ligand[a]	t	Yield	*ee*[b]	Comment
1	(*R*)-BINAP	48 h	-	-	no conversion
2	DuPhos	48 h	-	-	no conversion
3	(*R*,*R*)-TROST Ligand **52**	36 h	22%	0%	
4	Josiphos-SL-J001-1	16 h	-	-	no conversion
5	Josiphos-SL-J002-1	16 h	-	-	no conversion
6	Josiphos-SL-J003-1	16 h	-	-	no conversion
7	Josiphos-SL-J005-1	16 h	-	-	no conversion
8	Taniaphos-SL-T001-1	16 h	-	-	no conversion
9	Taniaphos-SL-T002-1	16 h	-	-	no conversion
10	Walphos-SL-W001-1	16 h	12%	0%	-
11	Walphos-SL-W002-1	16 h	55%	0%	-
12	Mandyphos-SL-M001-1	16 h	61%	0%	-
13	Mandyphos-SL-M004-1	16 h	44%	0%	-
14	Rophos-SL-P001-2	16 h	-	-	no conversion
15	MeOBIPHEP-SL-A-101-1	16 h	-	-	no conversion
16	MeOBIPHEP-SL-A-109-1	16 h	-	-	no conversion

a) All ligands except for (*R*)-BINAP, Duphos, and (*R*,*R*)-TROST Ligand **52** were used from Solvias Asymmetric Ligands Screening Kit (Figure 10).[84] b) All *ee* were determined by NP-HPLC using a Chiralpak IC column. The eluent consisted of 0.5% *iso*-propanol in *n*-hexane with a flow rate of 0.5 mL/min. The retention times for both enantiomers were 10.7 min and 11.5 min, respectively.

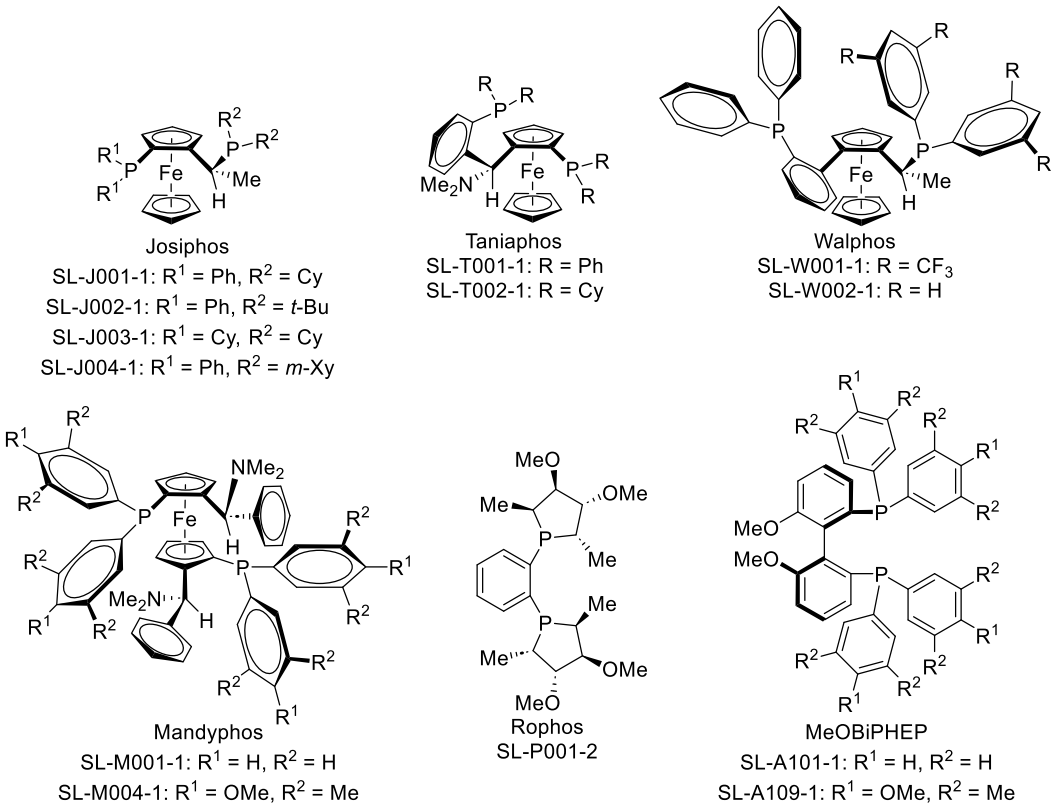

Figure 10: Structures of chiral ligands from Solvias Asymmetric Ligands Screening Kit.[84] (Reproduced from Ref.[83] with permission from the Royal Society of Chemistry.)

The majority of the chiral ligands tested were used from the Solvias Asymmetric Ligands Screening Kit (Figure 10). These consisted of ferrocene-based ligands such as Josiphos-, Taniaphos-, Walphos-, and Mandyphos-derivatives. Moreover, one Rophos ligand and two MeOBIPHEP-derivatives were utilized from the kit. Additionally, (*R*)-BINAP, Duphos, and the (*R*,*R*)-TROST Ligand **52** were tested. Out of all ligands, only few showed any conversion. The (*R*,*R*)-TROST Ligand **52** produced the geranylated product **90** with 22% yield (Table 8, entry 3). Walphos-SL-W001-1 and Walphos-SL-W002-1 gave the product with 12% yield and 55% yield, respectively (Table 8, entries 10 and 11). The Mandyphos-ligands were the overall best performing ligands. Mandyphos-SL-M001-1 yielded **90** with 61% and Mandyphos-SL-M004-1 with 44%. However, none of these ligands produced any *ee*. Since a large variety of chiral ligands were tested to no success, no further attempts were made to perform the coupling enantioselectively. Therefore, the synthesis was continued with the racemic mixture of the terpenyl phloroglucinols.

3.3.2 Miscellaneous Coupling Attempts

Other methods for the geranylation of phloroglucinol fragment (**66**) have also been tested. The first method was a FRIEDEL-CRAFTS-type alkylation where $BF_3{\cdot}OEt_2$ is used as a LEWIS acid and linalool (**74**) as the terpene fragment. The LEWIS-acid would presumably coordinate the hydroxy

group of linalool (**74**) and the nucleophile would attack at the terminal position of the double-bond causing a double-bond rearrangement and cleavage of the C–O-bond to give the geranylated product.

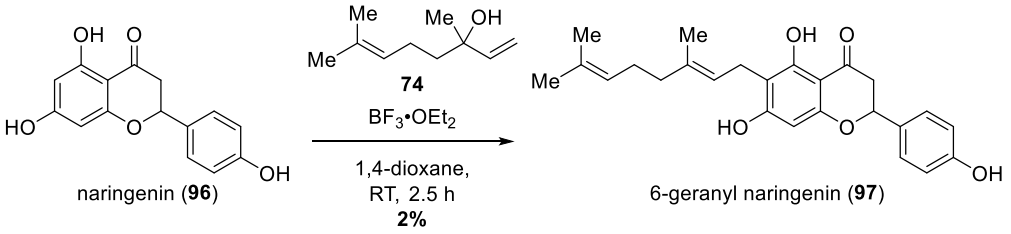

Scheme 35: Geranylation of naringenin (**96**) with linalool (**74**) and $BF_3{\cdot}OEt_2$ to obtain 6-geranyl naringenin (**97**) according to STEVENS and coworkers.[85]

This method has been employed by STEVENS and coworkers for the geranylation of naringenin (**96**) to obtain 6-geranyl naringenin (**97**), a flavonoid formed during the fermentation of hops in beer-production (Scheme 35). The yield of STEVENS and coworkers was quite poor with only 2%.[85] However, in naringenin (**96**) many possible nucleophilic positions are available such as different aromatic positions and free hydroxy groups. Therefore, the formation of side products is inevitable.

Additionally, this method has been employed with better success by KASSIOU and coworkers with a different terpene fragment **98** and 3-hexyl phenol (**99**) yielding the coupling product **100** with 42% (Scheme 36).[86]

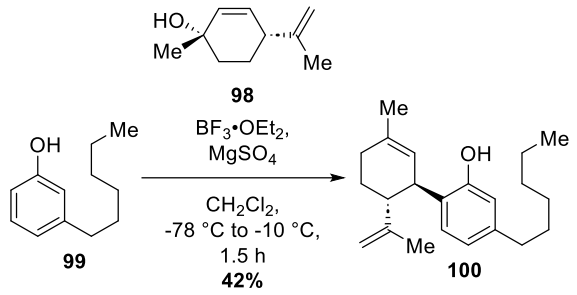

Scheme 36: LEWIS-acid mediated coupling of phenol **99** with terpene **98** according to KASSIOU and coworkers.[86]

In the methylated acetyl-phloroglucinol **66** the amount of nucleophilic positions and therefore the expanse of side reactions seemed to be manageable. Hence, this method was explored as an alternative geranylation protocol.

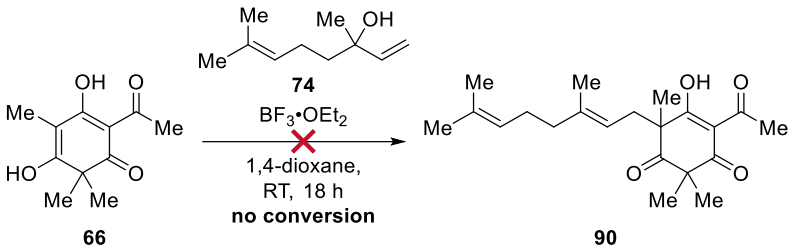

Scheme 37: Attempted LEWIS-acid catalyzed coupling of linalool (**74**) with trimethylated acetyl-phloroglucinol **66**.

Unfortunately, no conversion was observed when methylated acetyl-phloroglucinol **66** was combined with linalool (**74**) and $BF_3{\cdot}OEt_2$ (Scheme 37). Since even at RT no reaction was observed, this method was not further investigated. Moreover, all examples of this reaction featured only aromatic systems as nucleophiles. This suggests that the trimethylation of phloroglucinol, which disrupts aromaticity, prevents the compound from participating in FRIEDEL-CRAFTS-type alkylations.

Next, the geranylation of 2-acetyl phloroglucinol (**39**) in a simple nucleophilic substitution using potassium carbonate as a base and geranyl bromide (**87**) as an electrophile developed by LEE and coworkers was investigated (Scheme 38).[87] While formation of geranylated 2-acetyl phloroglucinol **101** was observable, significant side reactions, including O-alkylation and multiple alkylations, led to a complex, inseparable mixture.

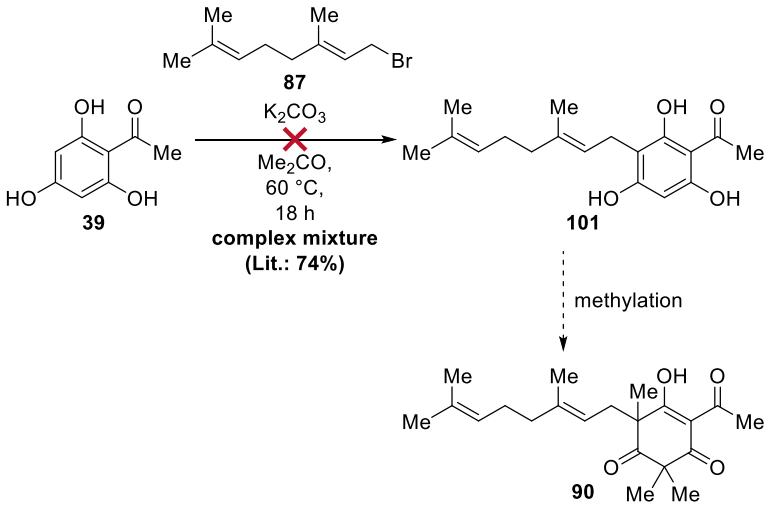

Scheme 38: Attempted route towards geranylated acetyl-phloroglucinol **39** according to LEE and coworkers.[88]

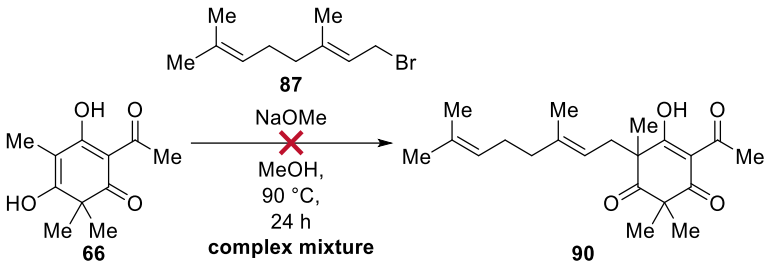

Scheme 39: Attempted geranylation of trimethylated acetyl-phloroglucinol **66** with geranyl bromide (**87**).

A reversal of the methylation and the geranylation steps was also not met with success (Scheme 39). The attempted nucleophilic substitution of methylated acetyl phloroglucinol **66** with geranyl bromide (**90**) gave a complex mixture containing the desired product as well. However, purification was once more not successful.

Since these alternative geranylation methods were unsatisfactory and the established method was already almost optimal, further improvement efforts were deemed unnecessary.

3.4 Convergent Route to Key-Intermediate 38

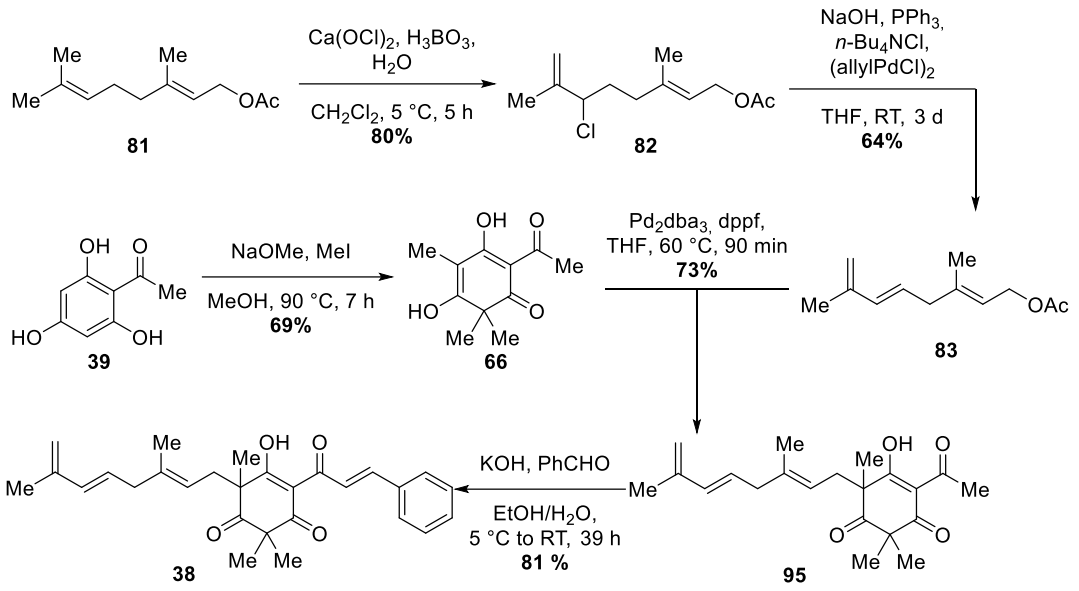

Scheme 40: Convergent route to key-intermediate **38**.

With the methylation and TSUJI-TROST coupling established, only the aldol condensation generating the cinnamoyl dienophile was missing to synthesize key-intermediate **38**. This reaction was attempted under classic conditions with KOH and benzaldehyde in a water-ethanol mixture. The reagents were combined at 0 °C and allowed to warm up to RT. During the reaction it was observed that at some point, no further conversion could be achieved although the starting material was not fully consumed. In order to push the equilibrium towards the product side, more benzaldehyde was added. In total, 6.00 equiv. of benzaldehyde were required to drive the reaction to completion. During purification, it was discovered that the main side product consisted of benzyl alcohol. This suggested that benzaldehyde was consumed in a competing CANNIZZARO-reaction forming benzyl alcohol and benzoic acid.[89] The workup procedure was modified accordingly. While the product is excellently soluble in cyclohexane, benzoic acid and benzyl alcohol both show a poor solubility in this solvent. Accordingly, when using cyclohexane for the extraction, these side products mostly remain in the aqueous phase. This massively simplified the purification process. When before, two column chromatographies were necessary (the first one for removing the bulk of the side products and the second one for purifying the product), now only one column chromatography achieved purification. Excess benzaldehyde was removed by drying the product overnight under SCHLENK line vacuum with stirring in a 40 °C water bath. Thus, key-intermediate **38** was obtained with a yield of 81% and the convergent route was established (Scheme 40). The longest linear sequence consisted of 4 steps with an overall yield of 30%.

3.5 Linear Route to Key-Intermediate 38

Like mentioned in Chapter 3.3.1, geranylated acetyl phloroglucinol **90** could be used to generate key-intermediate **38** in a linear route. By interchanging the TSUJI-TROST coupling and the desaturation sequence to generate the diene, the excellent yield from the TSUJI-TROST coupling with geranyl acetate (**81**) could be leveraged to improve the overall yield of the synthesis. Moreover, many issues caused by the instability of the allylic acetate and the diene in the terpene fragment could be avoided.

Firstly, the chlorination of the geranyl moiety in **90** was examined. It was anticipated that there might be selectivity issues, because the two double bonds in the terpene chain were now more electronically similar. Different conditions were explored (Table 9).

Table 9: Conditions for the chlorination of geranyl phloroglucinol **90**.

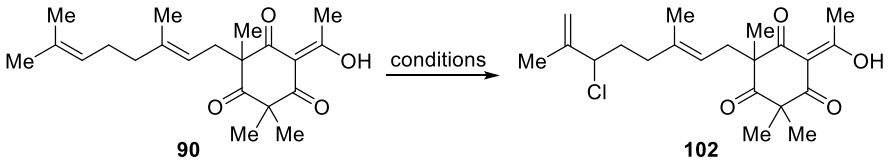

Entry	Conditions	Comment
1	$Ca(OCl)_2$, H_3BO_3, H_2O/CH_2Cl_2, 5 °C, 4.5 h	decomposition
2	TCCA, *n*-hexane, –10 °C, 6 h	45% yield (mixture of two isomers)
3	NCS, PhSeCl, CH_2Cl_2, RT, 1 h	78% yield (mixture of two isomers)

The conditions used in the previous route with calcium hypochlorite and boric acid were tested (Table 9, entry 1). However, with this substrate only decomposition could be observed. Then a biphasic system with TCCA, which is insoluble in *n*-hexane, was employed (Table 9, entry 2). This lead to a clean conversion. The product **102**, however, consisted of an inseparable mixture of two isomers indicated by the presence of four sets of signals in the ^{1}H- and ^{13}C-NMRs. At first, it was suspected that these isomers might be constitutional isomers formed by chlorination of the two different double bonds. Therefore, NCS in combination with phenyl selenyl bromide was utilized which is supposed to selectively chlorinate the terminal double bond. Although this led to a better yield of 78%, two isomers were still isolated (Table 9, entry 3).

Since no selectivity could be achieved, the route was continued in hopes that in the following steps the mixture might be separable.

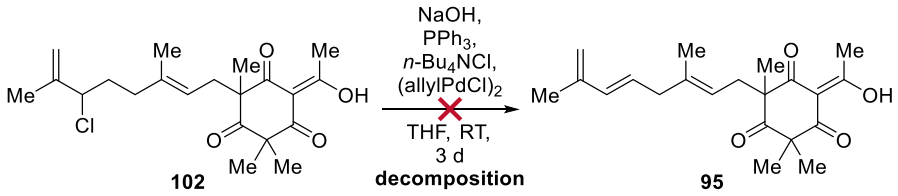

Scheme 41: Attempted dehydrochlorination of allylic chloride **102**.

The dehydrochlorination of allylic chloride **102** under the previously established conditions with the palladium-catalyzed β-hydride elimination was, unfortunately, unsuccessful leading to a decomposition of the starting material (Scheme 41). Supposedly, the nucleophilic acetyl group might cause problems.

Therefore the route was modified once more. This time the aldol condensation was performed prior to the chlorination in order to mask the acetyl group (Scheme 42).

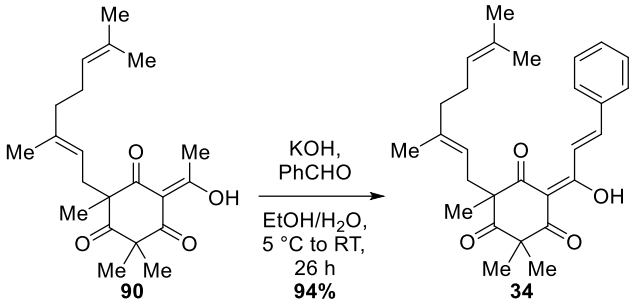

Scheme 42: Aldol condensation of geranyl acetyl phloroglucinol **90** to obtain geranyl Champanone B **34**.

According to the previously established conditions **90** was reacted with 6.00 equiv benzyl alcohol to obtain geranyl Champanone B **34** with 94%.

Geranyl Champanone B **34** was then attempted to be chlorinated under different conditions (Table 10).

Table 10: Conditions for the chlorination of geranyl Champanone B **34**.

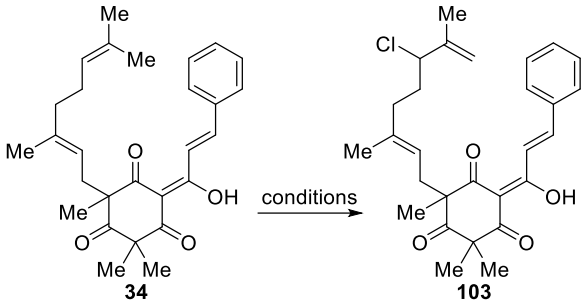

Entry	Conditions	Comment
1[a]	TCCA, *n*-hexane, –10 °C, 60 h	32% yield (mixture of two isomers)
2	NCS, PhSeCl, CH_2Cl_2, RT, 3 h	60% yield (mixture of two isomers)
3	TCCA, CH_2Cl_2, –40 °C to –10 °C, 90 min	85% yield (mixture of two isomers)
4	TCCA, CH_2Cl_2, –78 °C to 10 °C, 18 h	85% yield (mixture of two isomers)

a) 1.00 equiv. of TCCA was added in three portions with intervals of 20 h.

The first attempt was made using TCCA in *n*-hexane at –10 °C (Table 10, entry 1). Under these conditions it was difficult to drive the reaction to completion due to solubility issues. Even after addition of 1.00 equiv. TCCA in three portions with intervals of 20 h no complete conversion could be achieved. The reaction was terminated since no change was observable on the TLC. Therefore, the yield of **103** did amount to only 32%. Additionally, a mixture of inseparable isomers was obtained. Under similar conditions as before using NCS and phenyl selenyl chloride the yield was slightly improved to 60% of two isomers (Table 10, entry 2). To circumvent the solubility issues with TCCA in *n*-hexane, in further attempts CH_2Cl_2 was used as a solvent. However, to improve selectivity now the cooling was intensified. Both under controlled warming from –40 °C to –10 °C over 90 min and uncontrolled warming from –78 °C to 10 °C overnight 85% yields were achieved (Table 10, entries 3 and 4). However, still a mixture of two isomers was obtained.

At this point, it was still unclear whether these two isomers consisted of constitutional isomers **103** and **104** or diastereomers of **103** (Figure 11) which in both cases would both give four sets of signals in the ^{1}H- and ^{13}C-NMRs due to tautomerization.

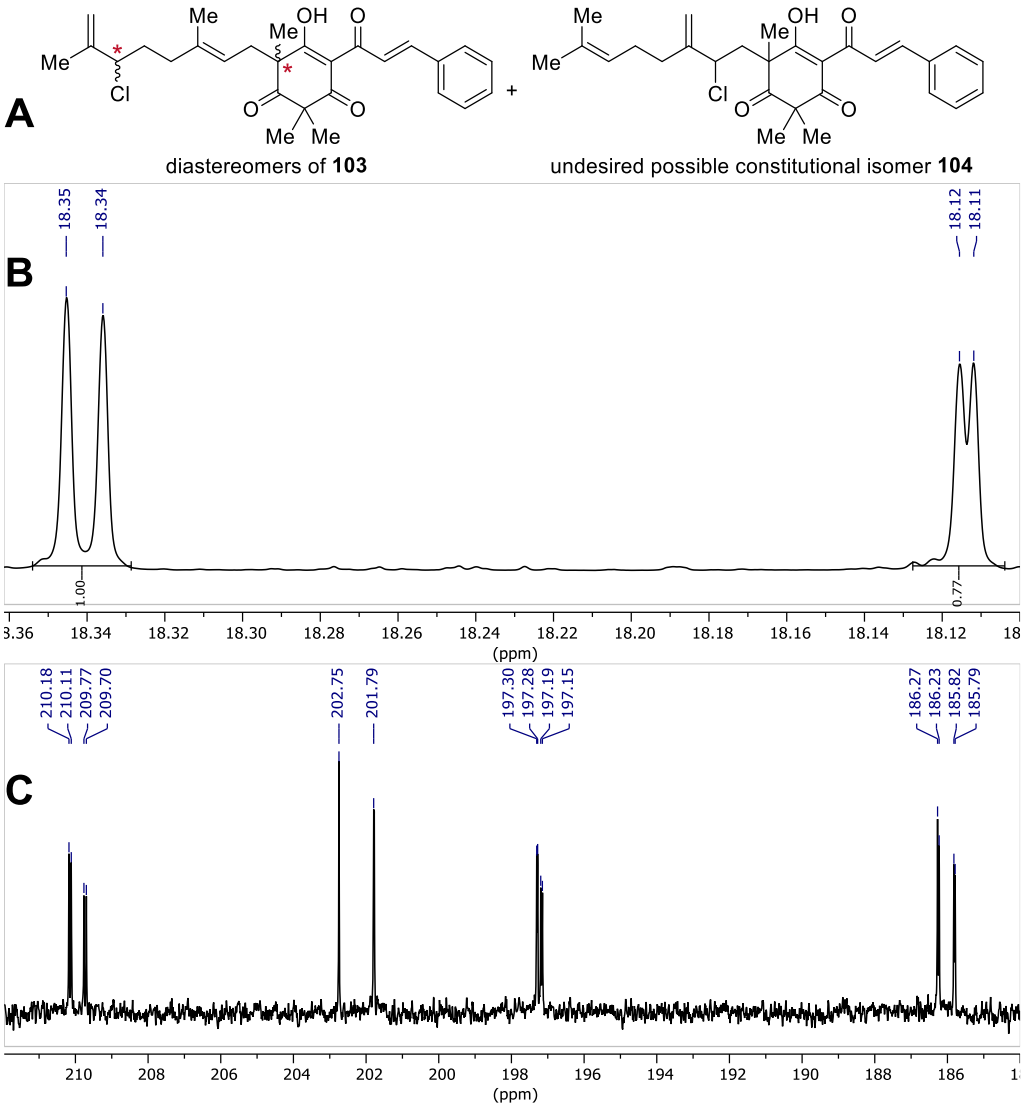

Figure 11: **A**: Possible isomers forming in the chlorination of geranyl Champanone B (**34**). **B**: Low-field section of the ^{1}H-NMR of **103**, **C**: Low-field section of the ^{13}C-NMR of **103**.

The simplest way to distinguish between diastereomers and constitutional isomers was to continue with the elimination step. If this yielded only one isomer, the different signal sets indicate diastereomers.

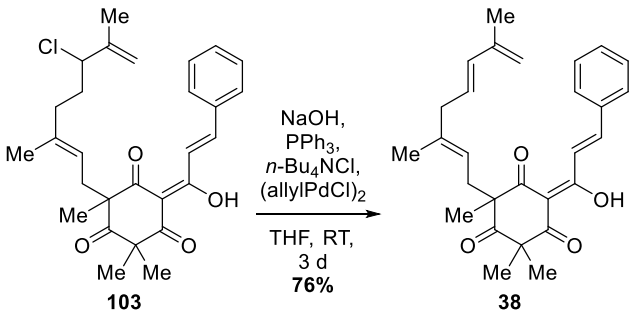

Scheme 43: Dehydrochlorination of allylic chloride **103** to obtain key-intermediate **38**.

The dehydrochlorination was performed in a similar fashion as before with the palladium-catalyzed β-hydride elimination (Scheme 43). Fortunately, the product was pure and showed only two sets of signals in the ^{1}H- and ^{13}C-NMRs. Thus, it was proven that the four sets of signals from the previous step belonged to diastereomers and not to constitutional isomers. The key-intermediate **38** was obtained from allylic chloride **103** with 76% yield.

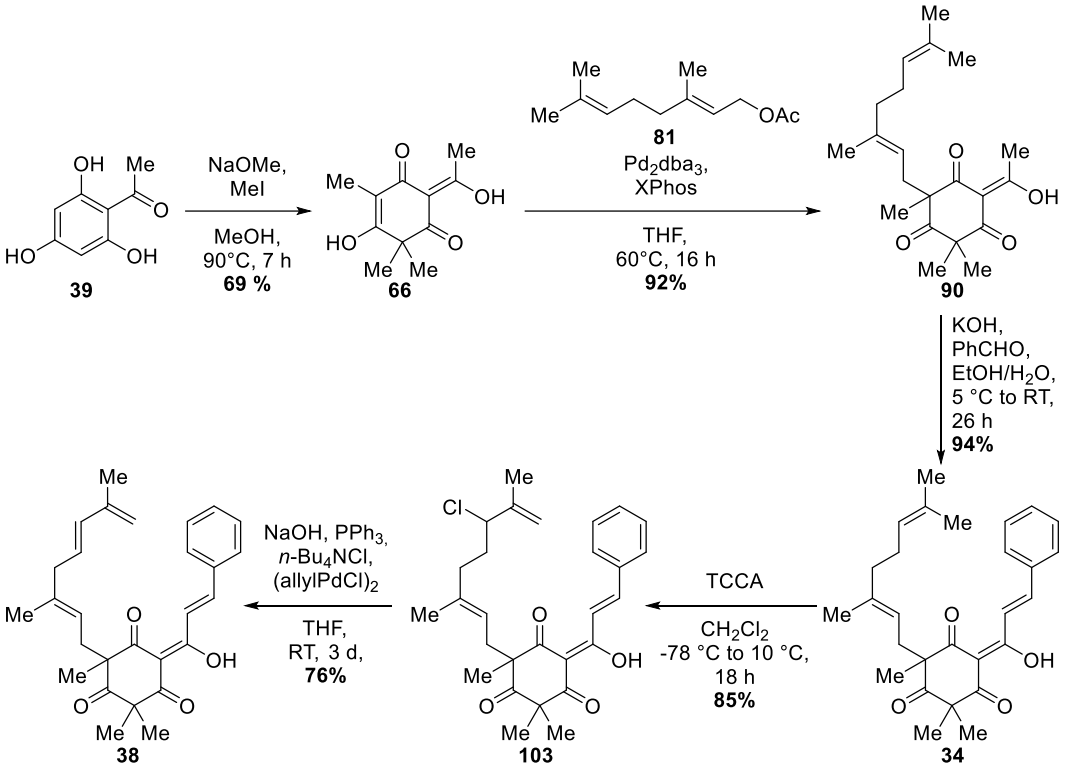

Scheme 44: Linear route to key-intermediate **38**.

This established a second, 5-step linear route to key-intermediate **38** (Scheme 44) with an impressive 39% overall yield. Compared to the convergent route (Scheme 40), this linear approach achieved a 9% yield-improvement despite the additional step.

3.6 Intramolecular DIELS-ALDER Cycloaddition

3.6.1 Thermal Intramolecular DIELS-ALDER Cycloaddition

The IMDA was first attempted under thermal conditions by heating **38** in toluene for 4 days. Luckily, this reaction showed conversion and two new products formed which showed a distinct turquoise and azure colour on the TLC-plate after staining with anisaldehyde (Scheme 45).

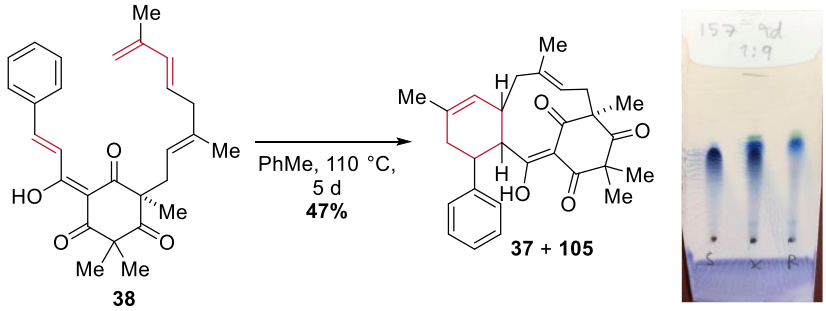

Scheme 45: First attempt of a thermal IMDA with key-intermediate **38** and TLC plate of the reaction stained with anisaldehyde after four days.

It was proposed that these two products consisted of two diastereomers **105** and **37** formed in the IMDA (Scheme 46). At this point, the absolute configuration of the products was still unknown. To determine the configuration, the separation of the two diastereomers was essential. However, this proved to be quite difficult at first due to the structural similarities of the compounds.

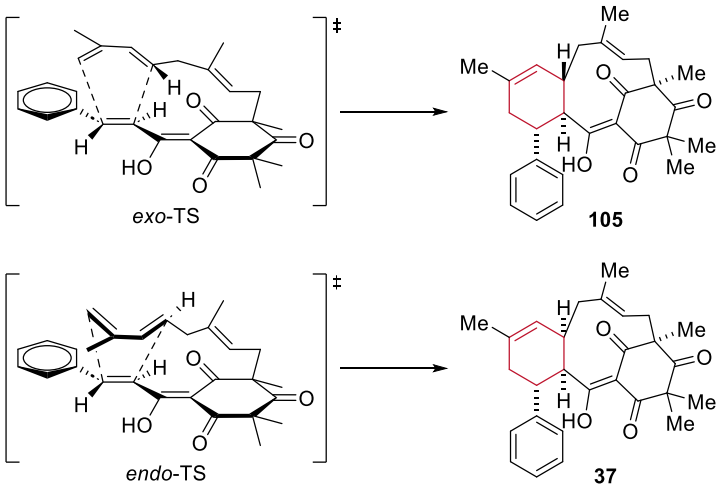

Scheme 46: Possible diastereomers with transition states resulting from the IMDA.

Many attempts have been made to purify the products **105** and **37** by column chromatography. At first, a solvent mixture of ethyl acetate and pentane was tested. Even at a ratio as low as 1% ethyl acetate no separation was achieved. Surprisingly, when switching to diethyl ether as the polar solvent, the separation improved significantly and purification with 2% diethyl ether in

pentane was somewhat successful. While small amounts of pure products could be obtained, a large portion remained as a mixture of the two products. Additionally, this separation only succeeded with very small sample amounts and usage of comparatively large columns. Nevertheless, the amount of pure **105** and **37** was sufficient for analytical purposes.

The analysis of the NOE-interactions of the two bridgehead-protons was inconclusive. Therefore, the relative configurations were determined *via* XRD. Single crystals were obtained by the vapor diffusion technique using a saturated solution of **105** or **37** in CH_2Cl_2 with pentane.

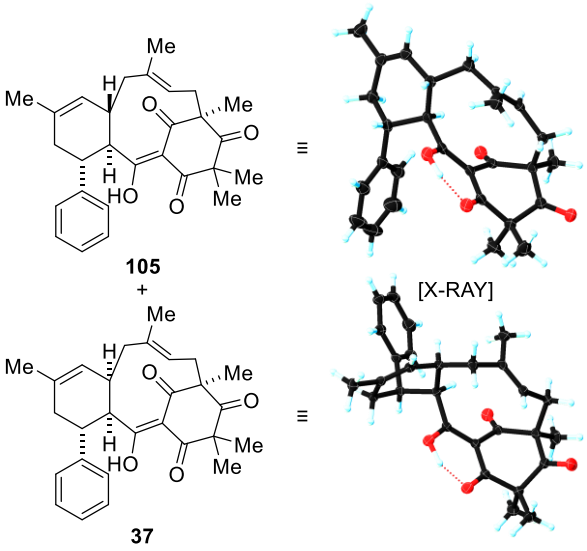

Figure 12: Absolute configurations of IMDA-diastereomers **105** and **37** determined by XDR-analysis with the crystal structures shown on the right.

Thus, it was revealed that **105** with the higher R_f-value consisted of the undesired *exo*-diastereomer and **37** with the lower R_f-value was the desired *endo*-diastereomer (Figure 12).

An analysis of the crude ^{1}H-NMR of the thermal IMDA in toluene showed that the products were obtained in a 10:7 (**105**:**37**) d.r. As the desired diastereomer **37** was in the minority and the established separation method was impractical, conditions in which **37** formed in an excess were required. First, different solvents were screened to examine whether the solvent played a significant role in this reaction (Table 11). As the thermal IMDA proceeded only at high temperatures, solvents with a high boiling point in which the starting material **38** was soluble were utilized.

Table 11: Solvent screening for the IMDA of key-intermediate **38**. (Reproduced (adapted) from Ref.[83] with permission from the Royal Society of Chemistry.)

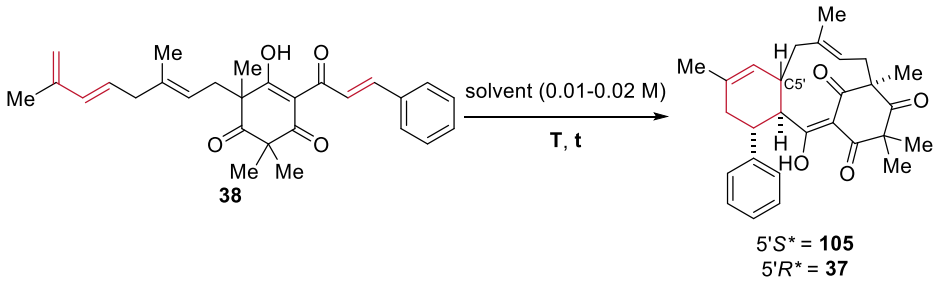

Entry	Solvent	t	T	d.r. (105:37)[a]	Comment
1[b]	ethanol/water	4 d	110 °C	5:2	-
2[b]	*n*-butanol	4 d	110 °C	3:1	-
3[b]	*tert*-butanol	4 d	110 °C	5:4	-
4[b]	pyridine	5 d	120 °C	3:1	significant decomposition
5[b]	tetrahydrofuran	1 d	110 °C	5:4	significant decomposition
6[b]	2-methyltetrahydrofuran	1 d	110 °C	4:3	significant decomposition
7[b]	1,4-dioxane	5 d	120 °C	5:4	-
8[b]	1,2-dimethoxyethane	1 d	110 °C	4:3	-
9[b]	diglyme	5 d	120 °C	4:3	-
10[b]	1,2-dichloroethane	1 d	110 °C	4:3	-
11[b]	benzotrifluoride	5 d	120 °C	10:7	-
12[b]	chlorobenzene	5 d	120 °C	5:3	-
13[b]	toluene	5 d	120 °C	10:7	-
14[b]	heptane	5 d	120 °C	10:7	-
15	toluene/water	5 d	90 °C	3:2	78% yield (mixture)

a) All d.r. were determined by crude ^{1}H-NMR using the integrals of the enol-O–H at 17.50 ppm for **105** and 17.96 ppm for **37**. b) Reaction was carried out in a capped vial.

Amongst the tested solvents were polar protic solvents such as ethanol/water, *n*-butanol, and *tert*-butanol (Table 11, entries 1-3), polar aprotic solvents such as pyridine, THF, 2-methyl-THF, 1,4-dioxane, 1,2-dimethoxyethane, diglyme, 1,2-dichloroethane, benzotrifluoride, chlorobenzene (Table 11, entries 4-12) and nonpolar solvents such as toluene and heptane (Table 11, entries 13 and 14). The d.r. was analysed by comparing the enol-O–H signal integrals at 17.50 ppm for **105** and at 17.96 ppm for **37**. This signal was chosen as it was very isolated in the low-field and could be properly analysed even in complex mixtures with many side products.

Unfortunately, in all cases the undesired diastereomer **105** was in excess. Nevertheless, this varied significantly amongst the different solvents. In protic solvents, except for *tert*-butanol, the excess of **105** was higher and came up to 3:1 in *n*-butanol. In pyridine which is strongly basic, unsurprisingly, significant decomposition occurred. Similar effects were observed with THF and 2-methyl-THF. These solvents may become unstable at the high reaction temperature, leading to unwanted side reactions with the starting material. In the remaining solvents only minor differences in d.r. were observed. Notably, the d.r. most in favour of the desired diastereomer **37** was detected in 1,4-dioxane with 5:4. Additionally, a biphasic solvent mixture of toluene and water was tested (Table 11, entry 15). Certain reactions, especially pericyclic reactions, that are performed "on water" have shown to proceed on a higher rate than the same reactions performed neat or in a non-protic solvent.[90] This was also applicable for the IMDA of **38**. With a toluene-water mixture the reaction proceeded at a much lower temperature of 90 °C compared to the 120 °C in pure toluene. This led to the formation of fewer side products which not only simplified the purification, but also improved the yield from 47% to 78% (yields of the mixture of **105** and **37**). Therefore, this solvent mixture proofed to be superior although the d.r. of 3:2 was not the most favourable. The lower amount of side products also allowed for a much more efficient purification method. Treatment of the crude product with pentane followed by cyclohexane preferentially dissolved the undesired IMDA diastereomer **105**, leaving the desired diastereomer **37** as a solid. However, some amount of **37** also dissolved, resulting in a reduced yield of only 26% (compared to a possible 32% as determined by ^{1}H-NMR). Pure **105** was obtained by treating the concentrated filtrate with pentane giving **105** with a yield of 20%. All attempts to retrieve the remaining amounts of either **105** or **37** from the mixture were unsuccessful.

3.6.2 LEWIS Acid Catalyzed Intramolecular DIELS-ALDER Cycloaddition

The presence of a carbonyl group in the cinnamoyl-dienophile in **38** opens up the possibility for a LEWIS acid catalyzed IMDA. This change in electron density could have an effect on the *exo*/*endo*-selectivity of the IMDA. Different LEWIS acids were tested to examine their influence on the d.r. of the reaction (Table 12).

Table 12: LEWIS acid screening for the IMDA of key-intermediate **38**.

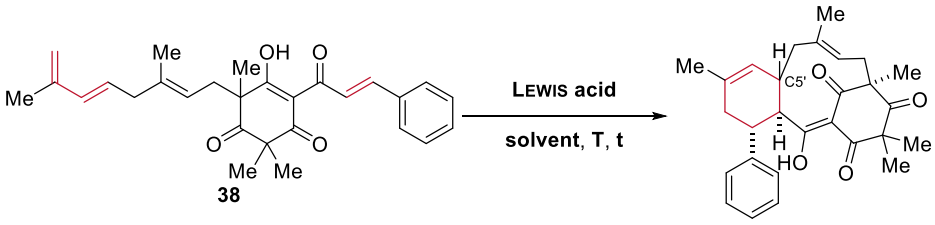

Entry	LEWIS acid (equiv.)	t	T	d.r. (105:37)[a]	Comment
1	$ZnCl_2$ (1.1)	15 h	RT	-	decomposition
2	$ZnBr_2$ (1.5)	2 h	0 °C	-	decomposition
3	ZnI_2 (1.5)	2 h	0 °C	-	decomposition
4	Me_3Al (2.0)	2 h	–78 °C to RT	-	decomposition
5	Me_2AlCl (0.4)	2 h	–78 °C to RT	-	decomposition
6	Et_2AlCl (0.2)	2 h	–78 °C to RT	-	decomposition
7	$TiCl_4$ (0.5)	72 h	–23 °C	4:1	-
8	$TiCl_4$ (0.5)	2 h	RT	-	decomposition
9	$SnCl_4$	3 h	–78 °C to –10 °C	-	decomposition
10	$BF_3{\cdot}OEt_2$ (2.0)	19 h	–10 °C to RT	1:0	-
11	$BF_3{\cdot}OEt_2$ (2.0)	2 h	RT	-	decomposition

a) All d.r. were determined by crude ^{1}H-NMR using the integrals of the enol-O–H at 17.50 ppm for **105** and 17.96 ppm for **37**.

With almost all LEWIS acids only decomposition took place indicating that some unwanted side reactions took place. One exception was $TiCl_4$ where at –23 °C product formation occurred although in a 4:1 excess for the undesired diastereomer (Table 12, entry 7). With $BF_3{\cdot}OEt_2$ at –10 °C to RT only formation of the undesired **105** was observed (Table 12, entry 10). As a result, the LEWIS acid catalyzed IMDA did not give any advantage over the thermal IMDA in this synthesis. Nevertheless, the ability to selectively obtain diastereomer **105** was still a valuable discovery.

Another advantage of the LEWIS-acid catalyzed IMDA is the possibility for the application of chiral ligands. LEI and coworkers used BH_3 in combination with chiral biaryl ligands such as BINOL and VAPOL (Figure 13) to influence the *exo*/*endo*- and the enantioselectivity of an intermolecular DIELS-ALDER cycloaddition of diene **106** and dienophile **107** in the synthesis of Kuwanon X (**108**).[91]

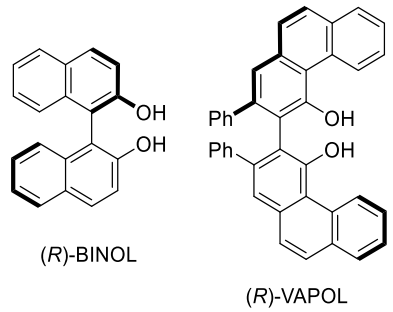

Figure 13: Structures of chiral biaryl ligands (*R*)-BINOL and (*R*)-VAPOL.

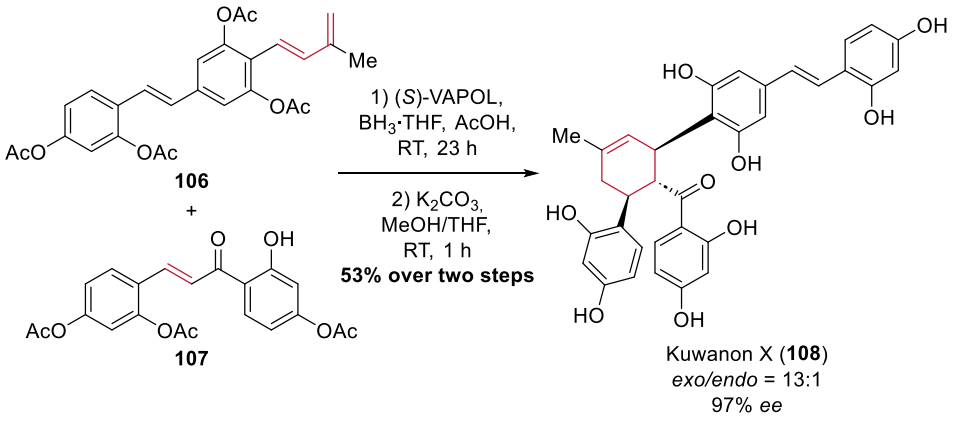

Scheme 47: Enantio- and *exo*-selective LEWIS acid catalyzed DIELS-ALDER cycloaddition in the synthesis of Kuwanon X (**108**) by LEI and coworkers.[91]

By employing (*S*)-VAPOL, LEI and coworkers were able to synthesize Kuwanon X (**108**) out of **106** and **107** with an *endo*/*exo*-ratio of 13:1 and 97% *ee* (Scheme 47).[91] Inspired by their findings, it was examined whether this could be transferred to the synthesis of Cleistocaltone A (**23**). The aim was to influence the d.r. of the IMDA of **38** by utilizing BINOL and VAPOL as ligands. Additionally, if one of the enantiomers of **38** was to react at a higher rate with the chiral LEWIS acid, it could open up the possibility for a kinetic resolution to obtain enantiopure **37** for the synthesis of either (+)- or (–)-Cleistocaltone A (**23**).

VAPOL was synthesized through a procedure developed by WULFF and coworkers wherein the racemic material was co-crystallized with the chiral counterion (–)-Cinchonidine to obtain enantiopure (*R*)-VAPOL.[92] (*R*)-BINOL was commercially available. The reactions for the IMDA were carried out according to the procedure of LEI and coworkers (Table 13).

Table 13: Chiral ligand screening for the LEWIS acid catalyzed IMDA of key-intermediate **38**.

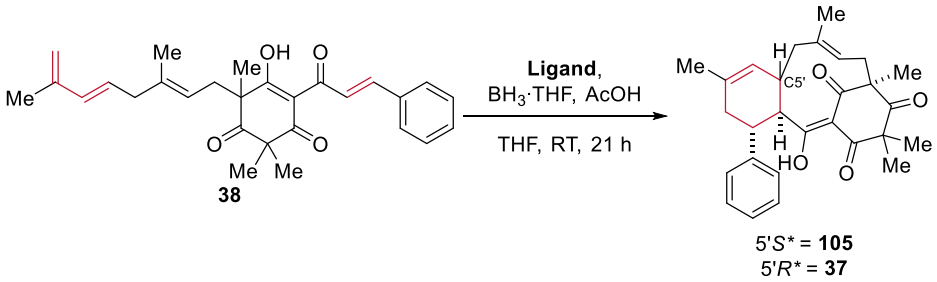

Entry	Ligand	Conversion	d.r. (105:37)[a]
1	(*R*)-BINOL	93%	4:1
2	(*S*)-BINOL	70%	5:3
3	(*R*)-VAPOL	0%	-

a) All d.r. were determined by crude ^{1}H-NMR using the integrals of the enol-O–H at 17.50 ppm for **105** and 17.96 ppm for **37**.

(*R*)-BINOL as a ligand gave the product with a d.r. of 4:1 in favour of the undesired diastereomer **105**. The conversion amounted to 93% indicating that in this case no kinetic resolution was possible (Table 13, entry 1). With (*S*)-BINOL the d.r. was improved to 5:3 in favour of **105**. However, the conversion was still above 50% (Table 13, entry 2). These results indicated that the steric control exerted by BINOL was too low to have any impact on the outcome of the reaction. On the other hand, with (*R*)-VAPOL no conversion was observed (Table 13, entry 3). In VAPOL the chiral pocket is much larger which should improve the influence on the reaction.[92] However, this also increases the ligand's sterical demand and thus lowers its reactivity. In the case of **38** the reactivity was probably lowered to such an extent that the IMDA could not occur anymore.

In further studies, less sterically demanding ligands such as VANOL could be tested. However, due to the unfavourable d.r. obtained in LEWIS acid catalyzed IMDA and the complex and time-consuming syntheses of additional chiral biaryl ligands, this endeavour was not further pursued at this point.

3.7 Backbone Oxidation

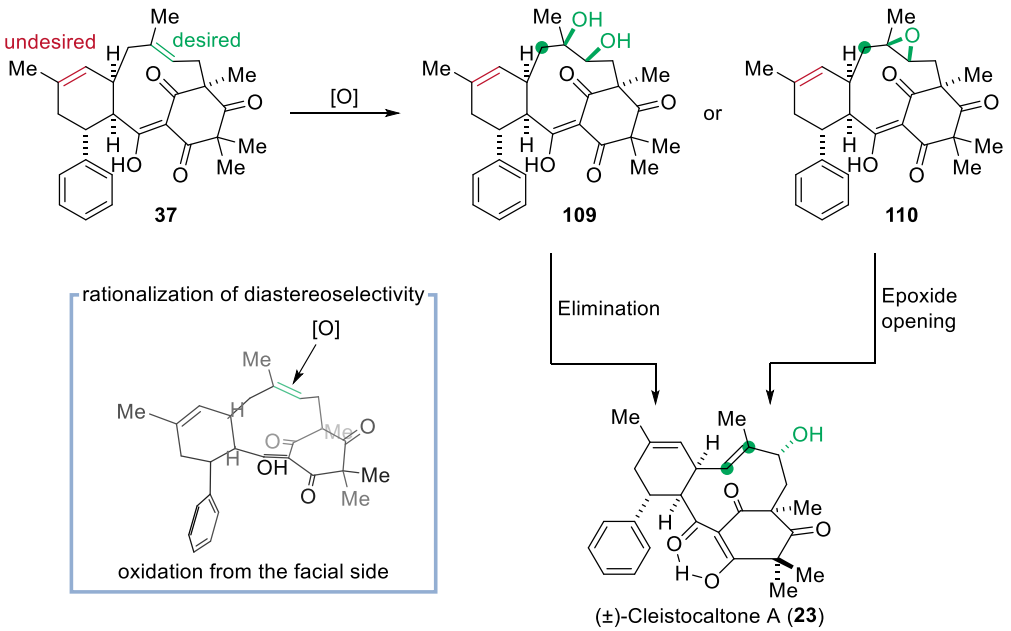

Scheme 48: Strategy for the backbone oxidation of **37**.

Multiple strategies for the backbone oxidation of **37** are imaginable. Two promising and step-efficient strategies are outlined in Scheme 48. The macrocyclic double bond could be oxidized to either diol **109** or epoxide **110**. According to the crystal structure, the oxidation should occur from the unshielded, facial side. Therefore, the oxidation was predicted to be diastereoselective. The tertiary hydroxyl-group in diol **109** could be eliminated under basic or acidic conditions. The epoxide in **110** could be opened under basic, LEWIS- or BRØNSTED-acidic conditions. This would give the allylic alcohol in Cleistocaltone A (**23**) in two steps starting from **37**. However, these strategies posed a challenge as the two trisubstituted double bonds in **37** appeared electronically similar. Nevertheless, due to the strain-release in the transition state, the macrocyclic double bond should be significantly more reactive.

For the dihydroxylation osmium and manganese based oxidating agents have been tested (Table 14).

Table 14: Screening of dihydroxylation conditions of **37** to produce diol **109**.

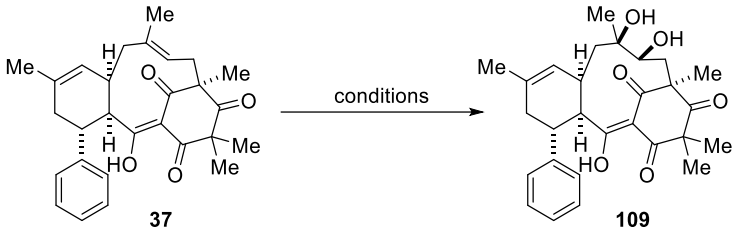

37 **109**

Entry	Conditions	Comment
1	OsO_4, NMO, THF/H_2O, RT, 2 h	partial decomposition
2	$KMnO_4$, Et_3BnNCl, CH_2Cl_2, 0 °C, 7 h	partial decomposition
3	K_2OsO_4, NMO, Me_2CO/THF/H_2O, 0 °C, 7 °C	partial decomposition

Firstly, UPJOHN-conditions with catalytic amounts of OsO_4 and NMO as an oxidizing agent were examined (Table 14, entry 1).[93] Unfortunately, only partial decomposition could be observed while most of the starting material did not react. The reaction with $KMnO_4$ in CH_2Cl_2 with Et_3BnNCl as a phase-transfer-catalyst yielded similar results (Table 14, entry 2). Conditions with K_2OsO_4 as the osmium source (Table 14, entry 3) did not improve the results. Since none of the screened conditions appeared to be working, this approach was not further pursued.

Next, epoxidation methods were screened to examine whether the second strategy was more promising (Table 15).

Table 15: Screening of epoxidation conditions of **37** to produce epoxide **110**.

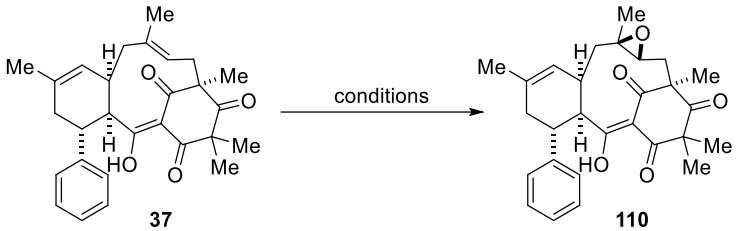

37 **110**

Entry	Conditions	Comment
1	*m*-CPBA, Na_2HPO_4, H_2O/CH_2Cl_2, 5 °C, 2 h	decomposition
2	*m*-CPBA, $NaHCO_3$, H_2O/CH_2Cl_2, –15 °C, 2 h	no conversion
3	*m*-CPBA, NaOAc, H_2O/CH_2Cl_2, RT, 2 h	decomposition
4	*m*-CPBA, CH_2Cl_2, RT, 1.5 h	decomposition
5	AcO_2H, NaOAc, H_2O/CH_2Cl_2, 5 °C to RT, 2 h	45%
6	AcO_2H, NaOAc, H_2O/CH_2Cl_2, RT, 1 h	66%

With *m*-CPBA as the oxidizing agent, different bases and temperatures were tested. While at RT and 5 °C using Na_2HPO_4 and NaOAc as bases (Table 15, entries 1 and 3) decomposition took place,

a lower temperature of –15 °C with $NaHCO_3$ showed no conversion at all (Table 15, entry 2). When no base was employed at RT, once more decomposition was observed (Table 15, entry 4). As *m*-CPBA appeared unviable for this reaction, the focus was shifted to a different oxidizing agent, peroxyacetic acid. Since peroxyacetic acid is more water soluble than *m*-CPBA, a mild, biphasic reaction setup could be exploited. With NaOAc as a base at 0 °C small amounts of product were observed. To drive the reaction to completion, the temperature was elevated to RT and more peroxyacetic acid was added. Thus, epoxide **110** was yielded with 45% (Table 15, entry 5). Since at RT no decomposition took place, the reaction was examined without cooling as well. Expectedly, this improved the yield to 66% (Table 15, entry 6).

With epoxide **110** successfully synthesized, different opening conditions including base, LEWIS and BRØNSTED acids were explored (Table 16).

Table 16: Screening of epoxide opening conditions of **110**.

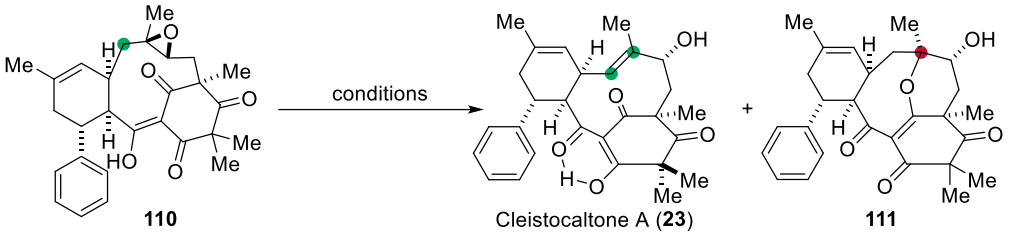

Entry	Conditions	Comment
1	*n*-BuLi (2.20 equiv.), THF, –78 °C to 0 °C, 7 h	partial decomposition
2	Al(O*i*-Pr)$_4$, PhMe, 120 °C, 18 h	decomposition
3	Ti(O*i*-Pr)$_4$, CH_2Cl_2, 90 °C, 2 h	partial decomposition
4	$ZnBr_2$, CH_2Cl_2, RT, 18 h	traces of **111**
5	Al_2O_3, PhH, RT, 18 h	traces of **111**
6	PTSA, THF/H_2O, 80 °C, 5 d	traces of **23**
7[a]	HCl (1% in MeOH), $CHCl_3$, 50 °C, 30 min	34% (55% brsm)
8[b]	HCl (1% in MeOH), $CHCl_3$, 50 °C, 30 min	24% (47% brsm) of **23**, 12% (24% brsm) of **111**
9[c]	HCl (1% in MeOH), $CHCl_3$, 50 °C, 2 h	33% of **23**, 9% of **111**

a) Reaction was carried out with 70.0 mg of starting material **110**. b) Reaction was carried out with 710 mg of starting material **110**. c) Reaction was carried out with 1.74 g of starting material **110** and brought to full conversion.

Base mediated opening reactions were unsuccessful. Even with a very strong base such as *n*-BuLi at 0 °C almost no conversion took place. Only small amounts of decomposition products were observable (Table 16, entry 1). LEWIS-acidic conditions seemed to be more promising. With Al(O*i*-Pr)$_4$ at 120 °C and Ti(O*i*-Pr)$_4$ only decomposition was observed (Table 16, entries 2 and 3).

However, with $ZnBr_2$ and Al_2O_3 traces of a new product **111** were visible (Table 16, entries 4 and 5). It is to be noted, that at this point **111** could not be structurally identified due to the lack of sufficient amounts of material. Finally, with the BRØNSTED acid PTSA after 5 d of refluxing in THF/H_2O traces of Cleistocaltone A (**23**) were visible (Table 16, entry 6). With this promising result, HCl was tested as a stronger BRØNSTED acid. A solution of HCl in MeOH was added to a solution of epoxide **110** in $CHCl_3$ at 50 °C (Table 16, entry 7). During the reaction it was observed that decomposition products were forming with their amount increasing over time. Therefore, the reaction was stopped after 30 min although conversion was not completed. This yielded Cleistocaltone A (**23**) with 34% (55% brsm). This first successful attempt was performed on a 70 mg-scale. When attempting the same procedure on a 710 mg-scale, the yield dropped down to 24% (47% brsm). Nevertheless, on this scale sufficient amounts of **111** with a yield of 12% (24% brsm) could be obtained (Table 16, entry 8). The crystallization of **111** was successful in Et_2O and the absolute configuration was confirmed through XRD (Scheme 49). The product features a unique tetracyclic system with an eight-membered cyclic ether. Since only one diastereomer formed during the reaction, it was proposed that the formation of **111** proceeded through a concerted mechanism *via* an S_N2 attack on the tertiary carbon centre of the BRØNSTED or LEWIS acid activated epoxide (Scheme 49). In order to maximize the yield, the reaction was allowed to proceed to complete conversion on a 1.74 g scale. However, this proved to be suboptimal with the amount of decomposition increasing. While the yield of **23** amounted to a respectable 33%, no starting material could be reisolated and the yield of **111** dropped down to 9% (Table 16, entry 8). Consequently, the optimal reaction time appeared to be between 30 min to 1 h for larger reaction scales.

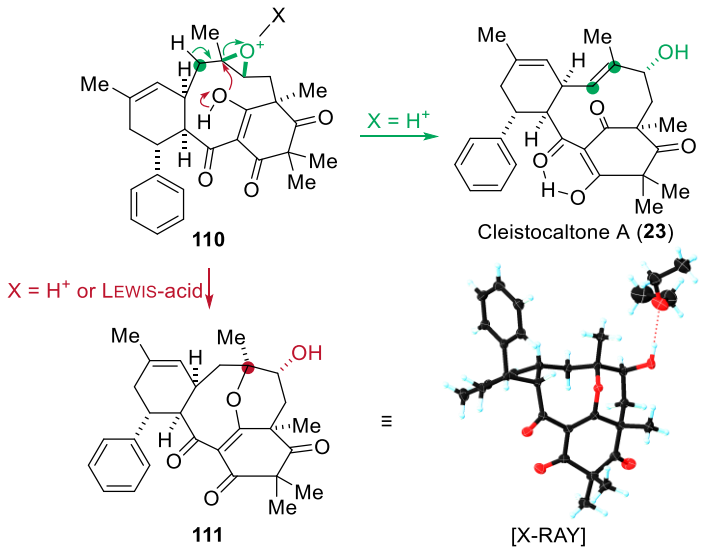

Scheme 49: Proposed mechanism for the formation of Cleistocaltone A (**23**) through BRØNSTED acid catalysis and cyclic ether **111** through LEWIS or BRØNSTED acid catalysis. Racemic **111** crystallizes as a conglomerate. The configuration of the enantiomer present in the obtained crystal

was opposite to that shown for (±)-**111**. (Reproduced (adapted) from Ref.[83] with permission from the Royal Society of Chemistry.)

Thus, the total synthesis of Cleistocaltone A (**23**) was successfully completed with a longest linear sequence of 7 steps with an overall yield of 1.7% for the convergent route and in 8 steps with an overall yield of 2.2% for the linear route.

Since the linear route was more efficient, it was attempted to be scaled up to a gram-scale (Scheme 50). This was successfully achieved with minimal complications. The only step that posed a challenge was the chlorination of the terminus of the geranyl moiety in **34** with TCCA to obtain allylic chloride **103**. In this reaction, diligent cooling was crucial. However, this was problematic on larger reaction scales. Consequently, on a 20.9 g-scale the yield dropped from 85% (98.0 mg-scale) to 50%. Additionally, a more complicated column chromatography was necessary due to the increased formation of side products. In most other steps the yield was even improved on a larger reaction scale. Starting from 15.0 g 2-acetyl phloroglucinol (**39**), 587 mg of Cleistocaltone A (**23**) have been produced and thus the gram-scale synthesis was successful.

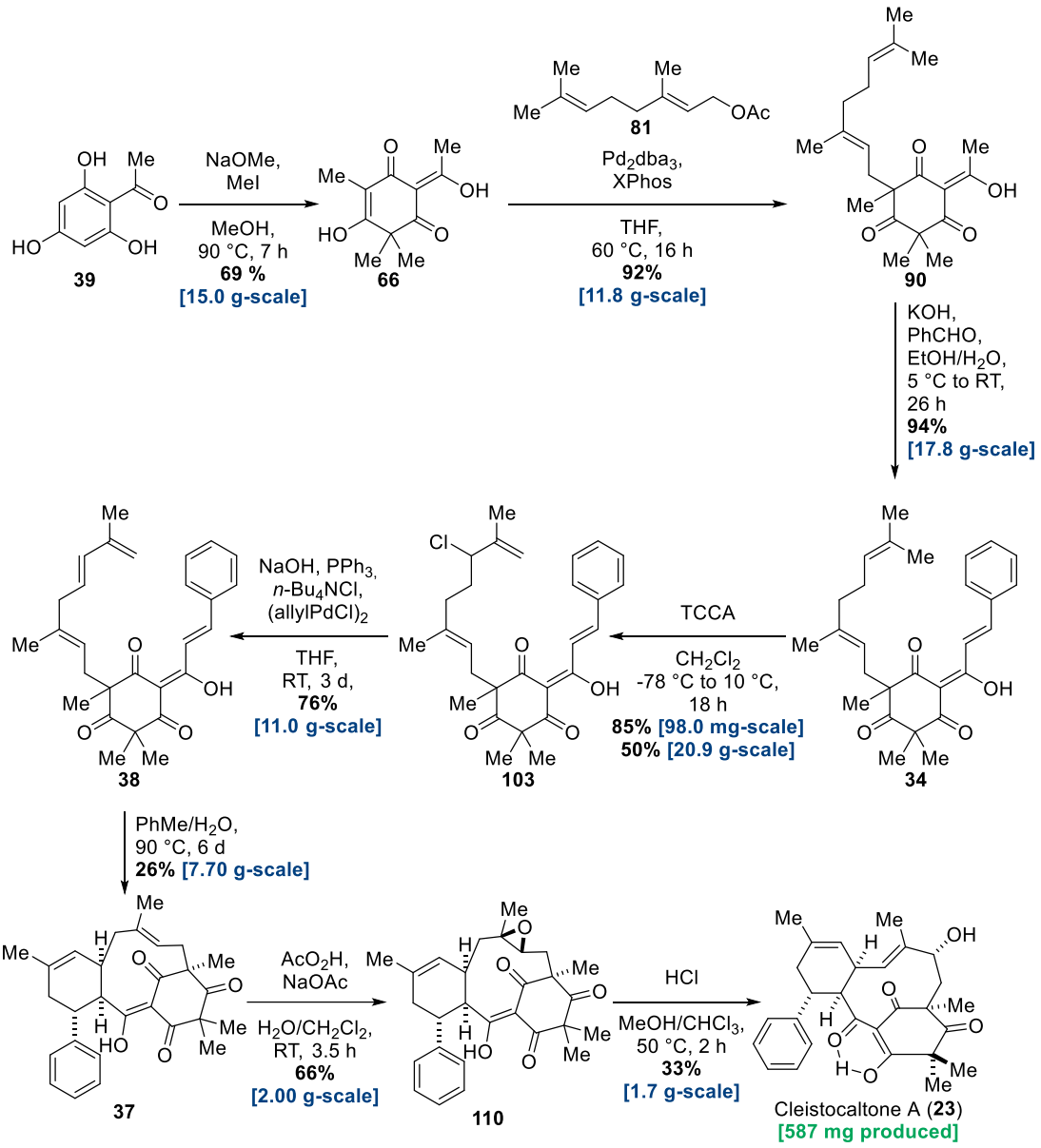

Scheme 50: Linear synthesis of Cleistocaltone A (**23**) on a gram-scale.

3.8 Biological Evaluation of Cleistocaltone A

With sufficient amounts of Cleistocaltone A (**23**) available, a biological evaluation of the synthetic material was performed in cooperation with MARTIN LUDLOW and SOPHIE M. KOLBE (Figure 14).[83] The antiviral efficacy of Cleistocaltone A (**23**) against a recombinant contemporary strain of RSV-A (0594, genotype ON1)[94] was evaluated in an *in vitro* model system. Presatovir which has been previously shown to be a selective and highly effective inhibitor of RSV induced virus-to-cell and cell-to-cell fusion,[95] was used a positive control in these experiments. The IC_{50} of Presatovir was determined to be 0.0056 µM, confirming the high antiviral efficacy of this compound. Cleistocaltone A (**23**) also inhibited RSV infection, with an IC_{50} of 54.55 µM. Although the IC_{50} of synthetic (±)-Cleistocaltone A (**23**) is about tenfold higher than that reported for the isolated racemic compound (IC_{50} = 6.75 ± 0.75 µM),[51] it remains within a relevant range.[83]

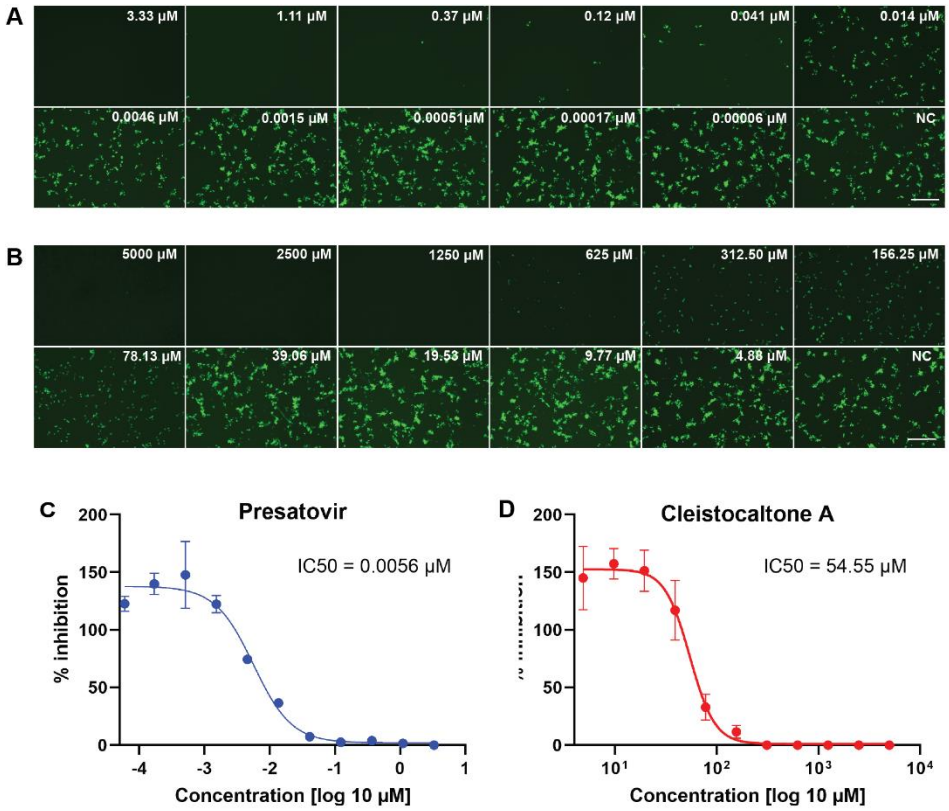

Figure 14: Assessment of the antiviral efficacy of Cleistocaltone A against RSV. (A-B) Vero cells were pretreated with three-fold serial dilutions of the fusion inhibitor Presatovir or two-fold serial dilutions of Cleistocaltone A (**23**) and infected with rRSV-A-0594-EGFP (2000 $TCID_{50}$/well) in the presence of each compound. Fluorescence photomicrographs showing EGFP fluorescence were obtained by UV microscopy at 48 hours post-infection. Scale bars, 500 µm. (C-D) Quantification of EGFP fluorescence in drug treated Vero cells was performed in 4% PFA fixed cells at 48 h.p.i. using a Tecan Infinite 2000 plate reader and normalized to untreated controls wells containing 0.1% DMSO. IC_{50} values were determined by nonlinear regression analysis using GraphPad Prism 10. Error bars represent the standard deviations from two independent experiments (*n* = 8). (Reproduced from Ref.[83] with permission from the Royal Society of Chemistry.)

3.9 Attempted Isolation of Side Product 111

There are various examples of natural products that have been synthesized "by accident" before their isolation and characterization from natural sources.[96] Champanone B (**25**) is such an example. Like mentioned in Chapter 3.1 its first synthesis by LEE and coworkers was published three months prior to its isolation by DUQUE and coworkers in 2005.[71,73] An earlier example is the synthesis of proline in 1900 by WILLSTÄTTER which was accomplished three years before its isolation by FISCHER and coworkers.[97,98] A more recent and vastly more complex natural product was Isoepicolactone (**112**, Figure 15) which has been isolated as a by-product in the synthesis of Epicolactone (**113**, Figure 15) by TRAUNER and coworkers in 2015.[99] At this time it was suspected that Isoepicolactone (**112**) may be a natural product as well. Five years later it was isolated by LONG and coworkers from the fungus *Epicoccum nigrum* SCNU-F0002.[100]

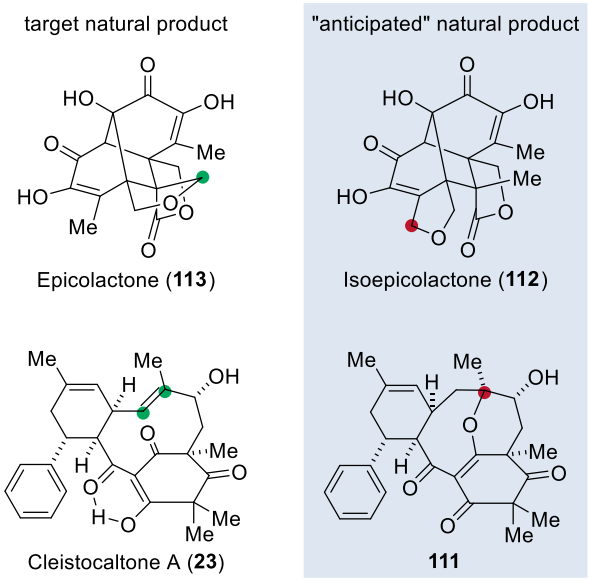

Figure 15: Structures of Epicolactone (**113**), Isoepicolactone (**112**), Cleistocaltone A (**23**) and side product **111**.

Based on this concept of "natural product anticipation",[96] it was hypothesized that side product **111** might also be a natural product awaiting its isolation (Figure 15). It was proposed that **111** might be a by-product in the biosynthesis of Cleistocaltone A (**23**). Consequently, an effort was made to isolate **111** from the plant material. Luckily, the dried buds of *Cleistocalyx operculatus*, from which Cleistocaltone A (**23**) was isolated,[51] are commonly used as a herbal tea in Vietnam known as "nước vối"[101] and were commercially available in sufficient amounts.

3.9.1 Analysis of Plant Material

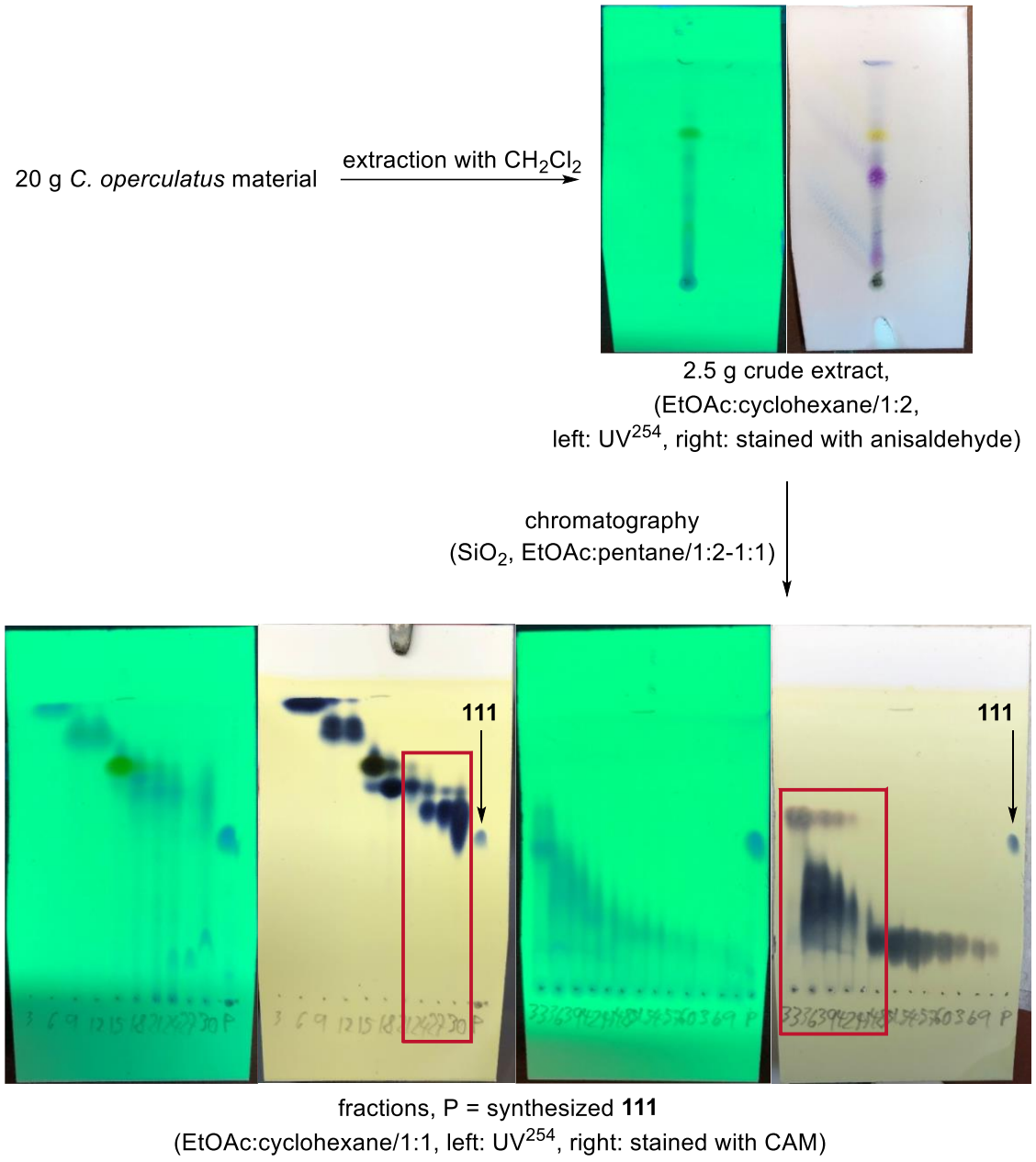

Scheme 51: Extraction, fractionation, and analysis of the "nước vối"-tea via TLC. The fractions marked in red were the chosen fractions which were further analyzed via HPLC/MS.

20.0 g of the purchased "nước vối"-tea were ground, suspended in CH_2Cl_2 (100 mL) and sonicated for 1 h. During this time, the sonication bath warmed up to 40 °C. This extract was filtered through a patch of silica which was thoroughly rinsed with EtOAc. The filtrate was concentrated under reduced pressure. The obtained residue of the crude extract amounted to 2.5 g. The TLC analysis of this crude extract revealed that a multitude of substances were present (Scheme 51). The crude extract was further fractioned via column chromatography with EtOAc:cyclohexane/1:2 to 1:1. The TLCs of the fractions showed that no notable amount of compounds with the same R_f-value

as **111** were visible (Scheme 51). Nevertheless, all fractions with compounds that possessed an R_f-value in a similar range were combined and concentrated under reduced pressure giving 582 mg of substance (Scheme 51). These fractions were then further analysed with HPLC/MS as a more sensitive analysis method.

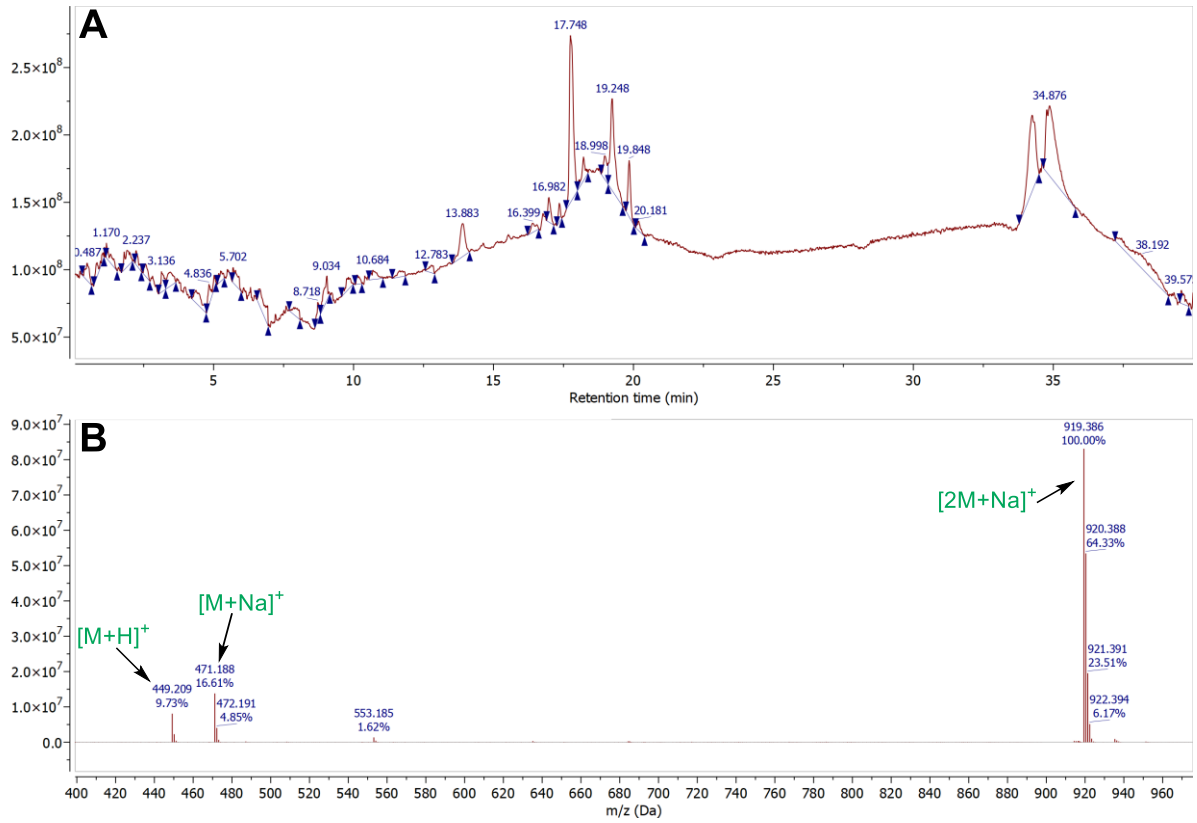

Figure 16: **A**: Total ion current chromatogram (TIC) of the HPLC-MS-run of synthesized **111**; **B**: m/z-Spectrum at the retention time of 17.75 min clearly showing signals for $[M+H]^+$, $[M+Na]^+$, and $[2M+Na]^+$.

All samples were analysed on an RP-column using a methanol/water-gradient increasing from 5% to 95% methanol over 40 min.

First, a sample containing pure **111** was examined (Figure 16). **111** showed a retention time of 17.75 min. The m/z of $[M+H]^+$ at 449 Da, $[M+Na]^+$ at 471 Da, and $[2M+Na]^+$ at 919 Da were clearly visible with the $[2M+Na]^+$ possessing the highest intensity.

It was also interesting to explore whether Cleistocaltone A (**23**) could be detected in the plant extract. Therefore, **23** was analysed with the same method to determine its retention time (Figure 17).

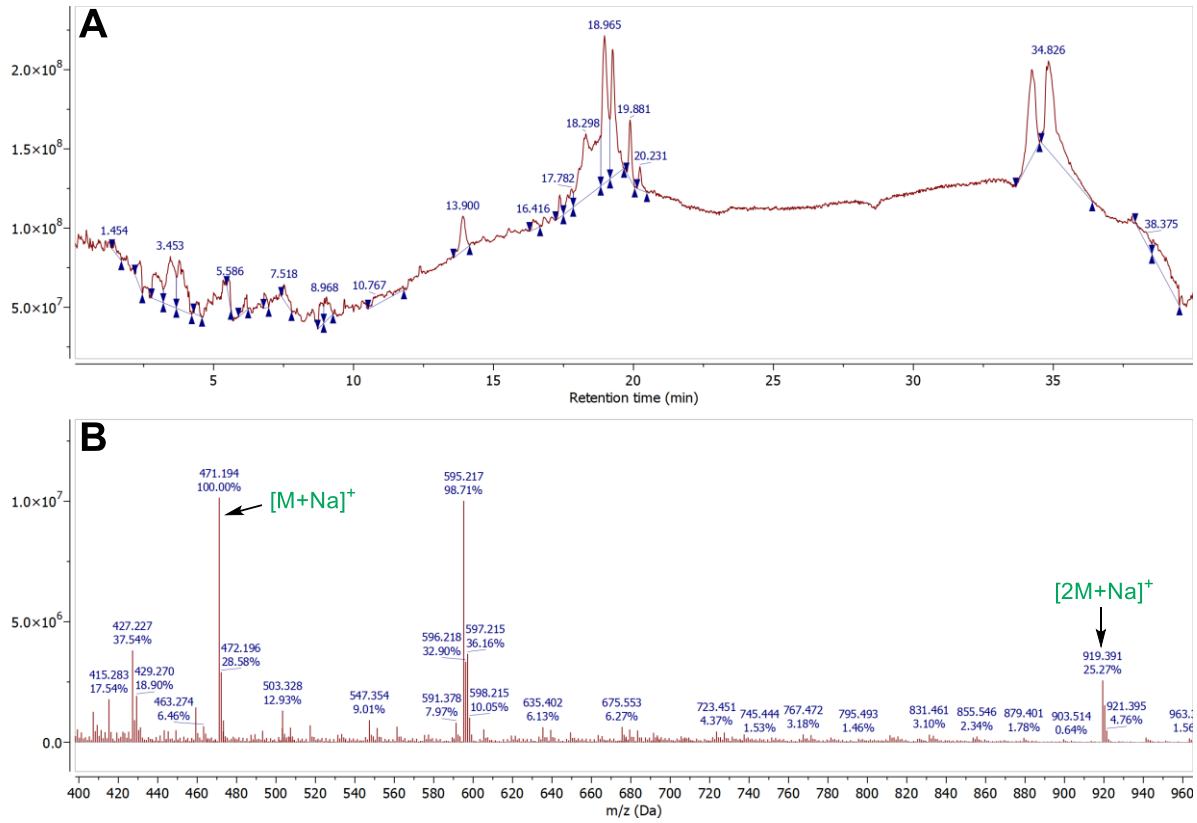

Figure 17: **A**: TIC of the HPLC-MS-run of synthesized Cleistocaltone A (**23**); **B**: m/z-Spectrum at the retention time of 18.97 min showing signals for $[M+Na]^+$ and $[2M+Na]^+$.

Cleistocaltone A (**23**) showed a retention time of 18.97 min. The signals of $[M+Na]^+$ of 471 Da and $[2M+Na]^+$ of 919 Da could be detected.

With the retention times of **111** and **23** determined, the plant material was analysed. If a compound with the mass of **111** could be found at the retention time of 17.75 min, it would be a good indication that sufficient amounts of **111** were present in the extract. This would justify further isolation efforts. First, a chromatogram of the chosen fractions shown in Scheme 51 was taken (Figure 18).

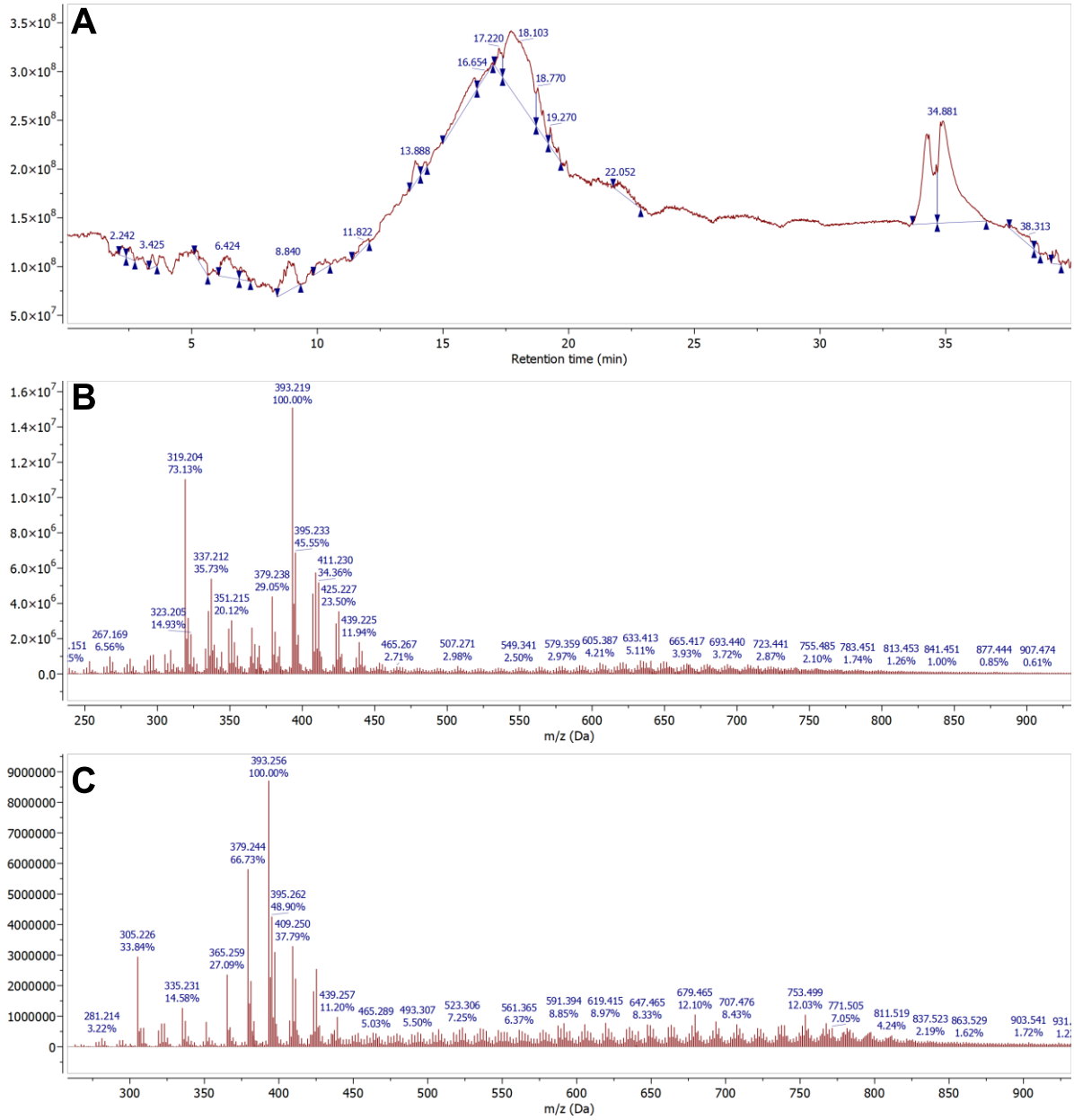

Figure 18: **A**: TIC of the HPLC-MS-run of the chosen fractions as demonstrated in Scheme 51; **B**: m/z-Spectrum at the retention time of 17.75 min; **C**: m/z-spectrum at the retention time of 18.97 min.

Unfortunately, at the retention times of 17.75 min and 18.97 min no signals with the mass of **111** or Cleistocaltone A (**23**) could be detected (Figure 18). The area around these retention times was analysed as well with similar results.

Afterwards, the crude plant extract was analysed as well to test if **111** is present in the full extract (Figure 19).

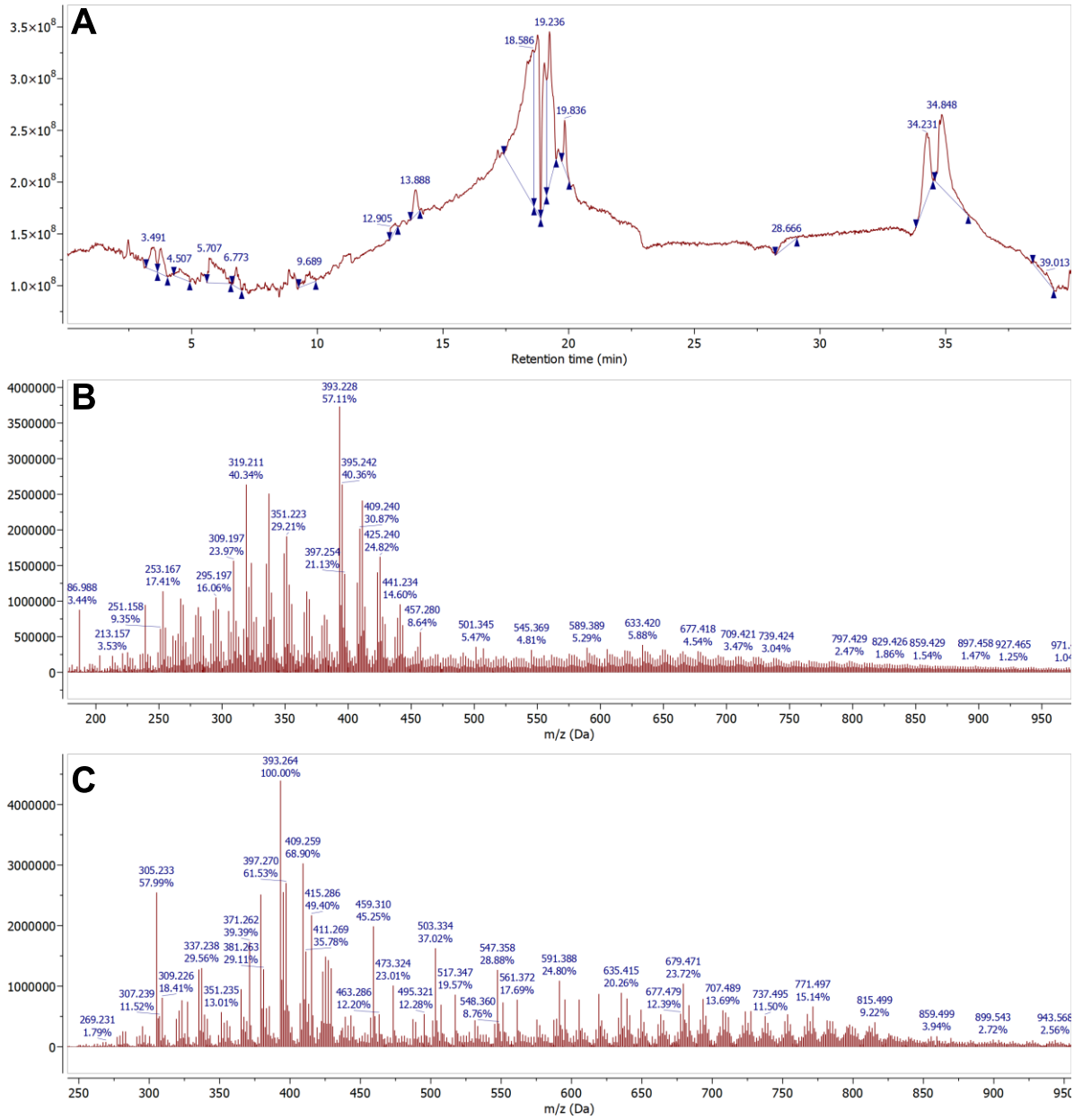

Figure 19: **A**: TIC of the HPLC-MS-run of the crude plant extract; **B**: m/z-Spectrum at the retention time of 17.75 min; **C**: m/z-spectrum at the retention time of 18.91 min.

Again, the masses of **111** or Cleistocaltone A (**23**) were not detectable.

The isolation of **111** yielded negative results, potentially due to several factors. Natural product concentration varies greatly depending on the plant's origin, influenced by factors like weather and soil composition. This variability could have resulted in undetectable levels of **111** in the specific plant material used. Additionally, insufficient material fractionation or degradation of the compounds over time from using non-fresh plant material could also have caused problems. While this attempt was unsuccessful, it doesn't conclusively disprove **111**'s presence. Future isolation efforts with fresh material from a well-defined source and potentially higher fractionation could yield better results.

3.10 Synthesis of Cleistocaltone B

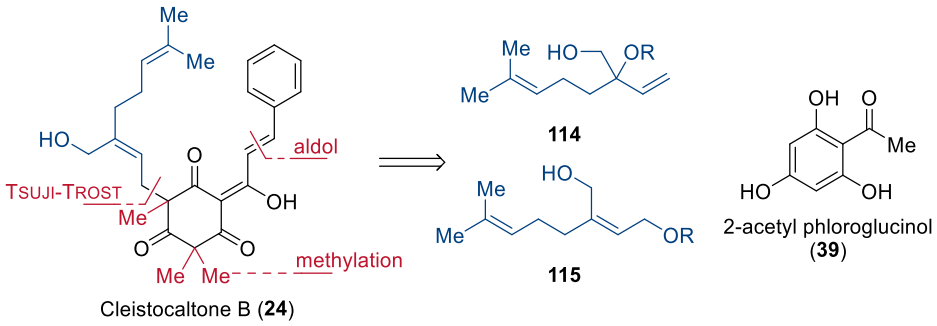

Scheme 52: Retrosynthetic analysis of Cleistocaltone B (**24**).

Cleistocaltone B (**24**) is structurally very similar to geranyl Champanone B **34** with the allylic hydroxyl group at the geranyl side chain being the only difference. Therefore, the synthesis approach was comparable to the one for geranyl Champanone B **34** (Scheme 52). Accordingly, starting from 2-acetyl phloroglucinol (**39**) after methylation, the terpene side-chain should be installed through a TSUJI-TROST coupling. Finally, the cinnamoyl moiety should be attached via an aldol condensation. For the TSUJI-TROST coupling an oxidized terpene fragment such as **114** or **115** based on linalool (**74**) or geraniol (**75**) was required. The synthesis of this fragment posed the main challenge for this route.

3.10.1 Synthesis of Terpene Fragments for Cleistocaltone B

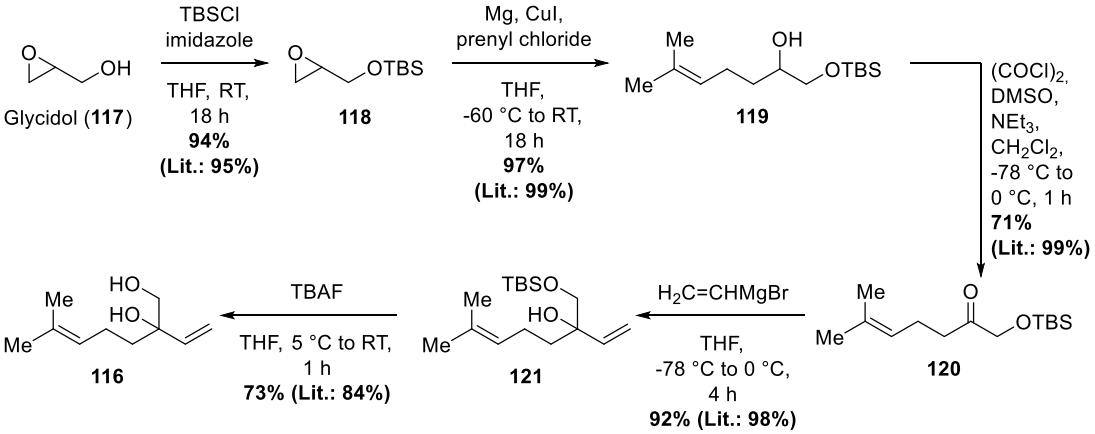

Scheme 53: Synthesis of diol (**116**) according to LÖBERMANN, TRAUNER, and coworkers.[102]

The first key-intermediate for the synthesis of terpene fragments for Cleistocaltone B (**24**) was linalyl-based diol **116**. One route to this compound was developed by LÖBERMANN, TRAUNER, and coworkers (Scheme 53).[102] This route started from glycidol (**117**) which after conversion to TBS-glycidol (**118**) was coupled with prenyl-MgCl through a copper mediated addition to obtain alcohol **119**. **119** was oxidized to the corresponding ketone **120** via a SWERN-oxidation. Vinyl-MgBr was coupled to the carbonyl group of **120** to obtain mono-TBS protected diol **121**.

Treatment of **121** with TBAF cleaved the silyl-ether to give diol **116**. While each step boasted excellent yields, the overall route suffered from a high step count. Another more step efficient route was developed by DELMOND and coworkers (Scheme 54).[103]

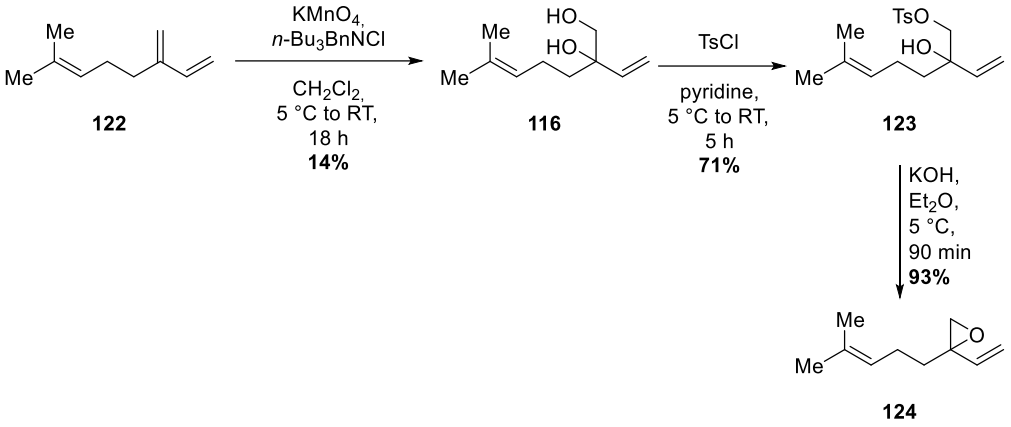

Scheme 54: Dihydroxylation of myrcene (**122**) according to DELMOND and coworkers[103] and conversion to epoxide **124**.

Diol **116** was obtained in one step by dihydroxylation of myrcene (**122**) with potassium permanganate in CH_2Cl_2 using *n*-Bu_3BnNCl as a phase-transfer reagent. Due to **122** containing multiple carbon- carbon double bonds which were oxidized with minimal selectivity, the yield of this step was suboptimal with only 14%. Thus, the route of LÖBERMANN, TRAUNER, and coworkers was much more efficient regarding the overall yield, but also much more time-consuming. The primary alcohol in diol **116** was then transformed to the tosylate **123** with 71% yield. An intramolecular nucleophilic substitution using KOH as base in Et_2O yielded the epoxide **124** with 93%.

3.10.2 TSUJI-TROST Coupling Reactions

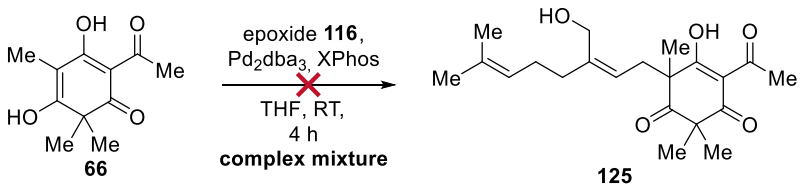

Scheme 55: Attempted TSUJI-TROST coupling of trimethylated acetyl phloroglucinol **66** with epoxide **116**.

First, using the optimized conditions for previous TSUJI-TROST couplings with XPhos and Pd_2dba_3 in THF, epoxide **116** was attempted to be coupled with trimethylated acetyl phloroglucinol **66** (Scheme 55). However, since epoxide **116** was much more reactive, the reaction proceeded already at RT and the starting material was fully consumed after 4 h. Unfortunately, only a complex mixture was obtained. The coupling did not only show a poor *E*/*Z*-selectivity, but the product also rapidly decomposed even when stored at –20 °C.

To circumvent this problem, a one-pot benzoyl-protection subsequent to the coupling reaction (Scheme 56) was performed. The benzoyl protecting group offered the strategic advantage of facile removal during the aldol-condensation step, thus streamlining the synthesis. Furthermore, its compatibility with the aldol condensation, wherein benzoic acid is a by-product, minimized potential complications.

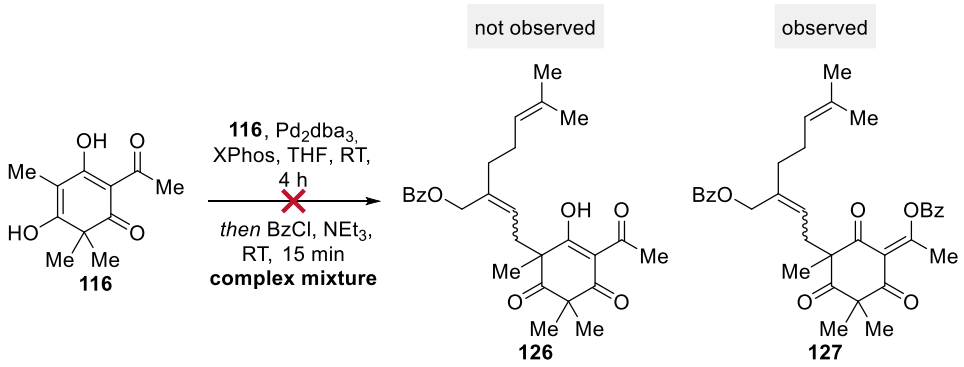

Scheme 56: Attempted TSUJI-TROST coupling of **66** with epoxide **116** with one-pot benzoyl protection.

Thus, benzoyl chloride and triethylamine were added to the reaction mixture after the coupling reaction was completed. The protection showed full conversion after only 15 min. Unfortunately, the result was a complex mixture once more. While the desired mono-protected benzoyl compound **126** was not observed, the di-protected benzoyl compound **127** was observed by mass spectrometry. Once more, a poor E/Z-selectivity and other side products made a purification impossible.

In the next attempt, the aldol condensation was performed in a one-pot procedure subsequent to the TSUJI-TROST coupling (Scheme 57). This procedure would not only simplify the synthesis, but access to the literature spectra of Cleistocaltone B (**24**) would also facilitate the analysis of the product mixture.

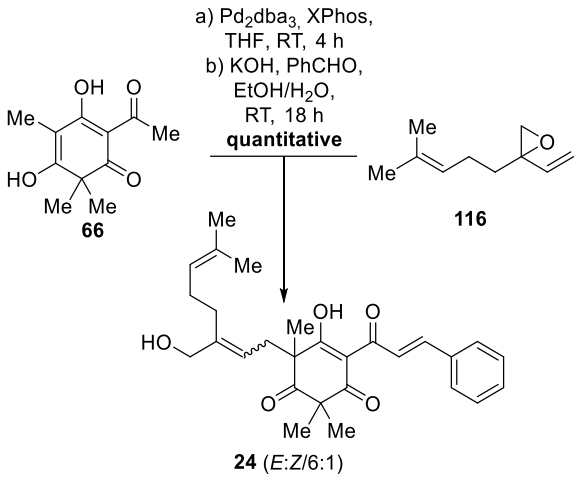

Scheme 57: One-pot TSUJI-TROST coupling of **66** with epoxide **116** with subsequent aldol condensation to obtain (E/Z)-Cleistocaltone B (**24**).

A mixture of two products was isolated with a quantitative yield. It was proposed that this mixture consisted of the *E*- and *Z*-isomer of Cleistocaltone B (**24**) with a d.r. of *E*:*Z* = 6:1. The NMR-signals of the minor isomer were mostly consistent with the literature spectra of Cleistocaltone B (**24**). Especially the characteristic signals in the low-field of the ^{13}C-NMR belonging to the carbonyl groups and the signals in the ^{1}H-NMR belonging to the enol-OH at 18.25 ppm and 18.10 ppm matched almost perfectly with the literature at 18.24 ppm and 18.10 ppm (Figure 20).[51]

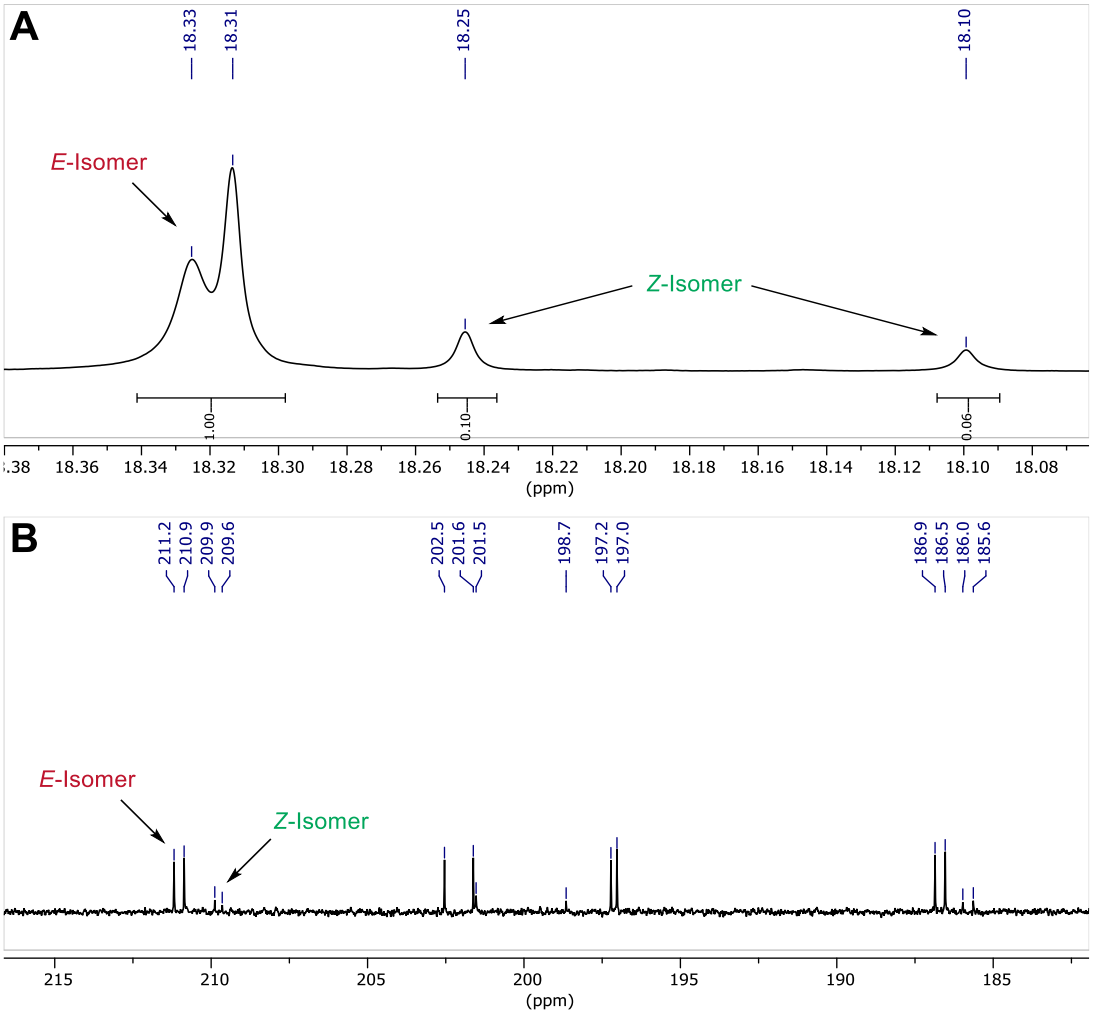

Figure 20: **A**: Low-field section of the ^{1}H-NMR of (*E*/*Z*)-Cleistocaltone B (**24**), **B**: Low-field section of the ^{13}C-NMR of (*E*/*Z*)-Cleistocaltone B (**24**).

A full comparison of the observable signals of the *Z*-isomer is shown in Table 17. However, many signals are overlapped with the signals of the supposed *E*-isomer. While in the ^{13}C-NMR most signals are distinguishable, in the ^{1}H-NMR only the enol-OH and some of the methyl-group-signals are discernible due to heavy overlap.

Table 17: Comparison of ^{1}H- and ^{13}C-NMR data for isolated and synthetic (±)-Cleistocaltone B (**24**).[a]

No.	Tautomer A		Tautomer B		Tautomer A		Tautomer B	
	Isolation[b] ^{13}C NMR (125 MHz) δ_C/ppm[c]	**Synthetic ^{13}C NMR (151 MHz)** δ_C/ppm[c]	**Isolation[b] ^{13}C NMR (125 MHz)** δ_C/ppm[c]	**Synthetic ^{13}C NMR (151 MHz)** δ_C/ppm[c]	**Isolation[b] ^{1}H NMR (500 MHz)** δ_H/ppm (*J* in Hz)[d]	**Synthetic ^{1}H NMR (600 MHz)** δ_H/ppm (*J* in Hz)[c]	**Isolation[b] ^{1}H NMR (500 MHz)** δ_H/ppm (*J* in Hz)[d]	**Isolation[b] ^{1}H NMR (600 MHz)** δ_H/ppm (*J* in Hz)[d]
1	198.5	198.7	202.7	n.o.				
2	58.2	n.o.	54.1	54.1				
3	209.8	209.9	209.6	209.6				
4	57.8	57.8	61.2	61.2				
5	201.5	201.5	197.0	198.7				
6	110.6	110.7	109.6	109.6				
7	185.7	185.6	186.0	186.0				
8	121.0	120.9	121.2	121.2	7.90 (d, 15.7)	n.o.	8.01 (d, 15.7)	n.o.
9	147.0	147.0	147.0	147.1	8.00 (d, 15.7)	n.o.	8.01 (d, 15.7)	n.o.
10	134.8	n.o.	134.9	n.o.				
11	129.2	n.o.	129.2	n.o.	7.66 (m)	n.o.	7.66 (m)	n.o.
12	129.3	129.3	129.3	129.3	7.42	n.o.	7.41	n.o.
13	131.4	131.5	131.4	131.5	7.42	n.o.	7.41	n.o.
14	129.3	n.o.	129.3	n.o.	7.42	n.o.	7.41	n.o.
15	129.2	n.o.	129.2	n.o.	7.66 (m)	n.o.	7.66 (m)	n.o.
16	21.9	21.9	21.4	21.5	1.49 (s)	1.49 (s)	1.40 (s)	n.o.
17	26.2	26.2	26.1	26.1	1.35 (s)	1.34 (s)	1.43 (s)	1.43 (s)
18	20.4	20.3	22.1	22.0	1.36 (s)	1.35 (s)	1.44 (s)	1.44 (s)
1'a	38.6	38.6	36.9	36.9	2.69	n.o.	2.68	n.o.
1'b					2.56	n.o.	2.55	n.o.
2'	119.6	119.7	119.0	119.0	5.06	n.o.	5.17	n.o.
3'	144.3	144.4	143.0					
4'	28.0	27.9	28.3	28.3	2.02	n.o.	2.02	n.o.
5'	26.9	26.8	27.0	27.0	1.99	n.o.	1.99	n.o.
6'	123.8	123.7	123.8	123.7	5.09	n.o.	5.06	n.o.
7'	132.4	132.4	132.4	132.4				
8'	25.8	n.o.	25.8	n.o.	1.67 (s)	1.66 (s)	1.65 (s)	1.65 (s)
9'	66.6	66.6	66.7	66.8	3.93	n.o.	3.91	n.o.
10'	17.8	n.o.	17.8	n.o.	1.58 (s)	1.57 (s)	1.56 (s)	1.56 (s)
1-OH					18.24	18.25	18.10	18.10

a) All data were obtained in $CDCl_3$. Overlapped signals were reported without designating multiplicity. Signals that were not observable due to overlap are indicated with a "n.o.". b) Data from reference [51]. c) Chemical shifts are reported relative to the corresponding residual non-deuterated solvent signal ($CDCl_3$: δ_H = 7.26 ppm, δ_C = 77.16 ppm). d) Chemical shifts are reported relative to TMS (δ_H = 0.00 ppm).

Unfortunately, all attempts of separation of the two isomers failed. Additionally, with the undesired isomer being in large excess, this was no viable strategy for the synthesis of Cleistocaltone B (**24**). The development of a new strategy was necessary.

3.10.3 Synthesis of Terpene Fragment with Terminal Leaving Group

The results of the studies of the TSUJI-TROST coupling in the synthesis of Cleistocaltone A (**23**) showed that the *E*/*Z*-selectivity only posed a challenge when linalyl-based terpene fragments with a tertiary leaving group were utilized. With geranyl-based coupling partners the configuration of the double-bond was conserved giving exclusively the *E*-isomer. Accordingly, an oxidized geranyl-based terpene fragment featuring a *Z*-double bond should give a better *Z*-selectivity in the synthesis of Cleistocaltone B (**24**).

The strategy to obtain such a terpene fragment commenced from butenolide **128** which contains the double bond in the desired *Z*-configuration (Scheme 58). This should be opened through saponification resulting in ester **129**. After protection of the alcohol, the ester in **130** should be reduced giving alcohol **131**. After conversion of the alcohol into a leaving group, **132** could be used in a TSUJI-TROST coupling.

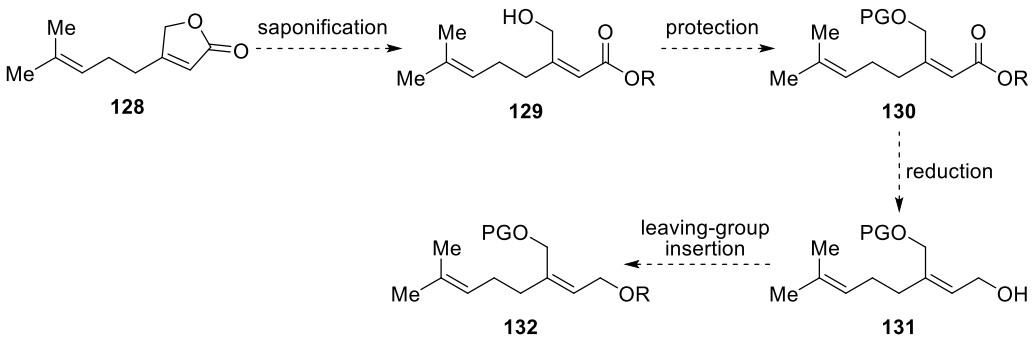

Scheme 58: Strategy for the synthesis of geranyl-based terpene fragment **132**.

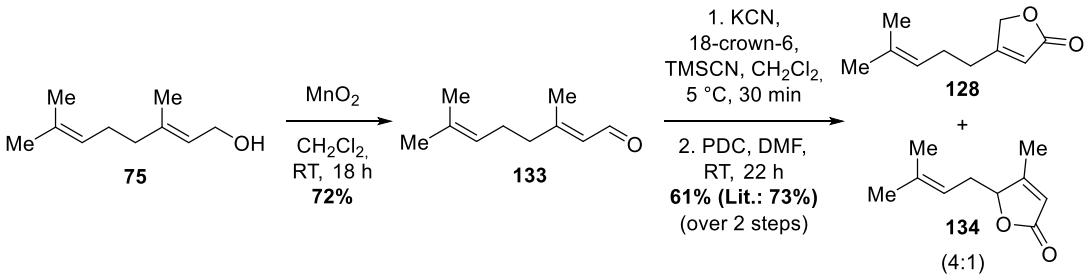

Scheme 59: Synthesis of butenolide **128** according to COREY and SCHMIDT.[104]

Butenolide **128** was obtained through a literature-known procedure (Scheme 59). First, geraniol (**75**) was oxidized using MnO_2 which yielded geranial (**133**) with 72%. Subsequently, geranial (**133**) was directly converted to butenolide **128** with a procedure developed by COREY and SCHMIDT.[104] Here, geranial (**133**) is first transformed to the corresponding *O*-trimethylsilyl-

cyanohydrin employing KCN, 18-crown-6, and TMSCN in CH_2Cl_2. After removal of the volatiles under reduced pressure it is then oxidized with PDC in DMF giving butenolide **128** and its constitutional isomer **134** with 61% yield in a 4:1 ratio.

Various bases were tested to open butenolide **128** and obtain an ester such as **135** (Table 18).

Table 18: Screening of saponification conditions of butenolide **128**.

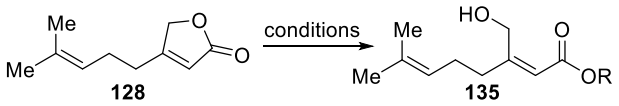

128 **135**

Entry	R	Conditions	Comment
1	Et	K_2CO_3, EtOH, 0 °C to 90 °C, 24 h	no conversion
2	H	LiOH, THF/H_2O, RT, 60 h	decomposition
3	Me	NaOMe, MeOH, 0 °C to RT, 1 h	decomposition

With the weakest base K_2CO_3 in EtOH no conversion was observable, even after heating of the reaction mixture to reflux (Table 18, entry 1). LiOH in THF/H_2O showed only decomposition (Table 18, entry 2). When attempted to open the butenolide with NaOMe, decomposition occurred within one hour (Table 18, entry 3).

No further attempts were made since it was presumed that the butenolide **128** probably cyclizes back immediately following saponification. The *Z*-configuration of the double-bond should facilitate this reaction immensely. Other strategies which hinder the cyclization were necessary, but have not been explored in this work.

4. Conclusion

4.1 Summary of Results

In conclusion, the biomimetic synthesis of the anti-RSV agent Cleistocaltone A (**23**) has been successfully executed. Two different routes have been established. The convergent route where geranyl acetate (**81**) was transformed to the diene **83** first and then coupled to the phloroglucinol fragment **66** obtained through methylation of 2-acetyl phloroglucinol (**39**) gave Cleistocaltone A (**23**) with a longest linear sequence of 6 steps and an overall yield of 1.7% (Scheme 60).

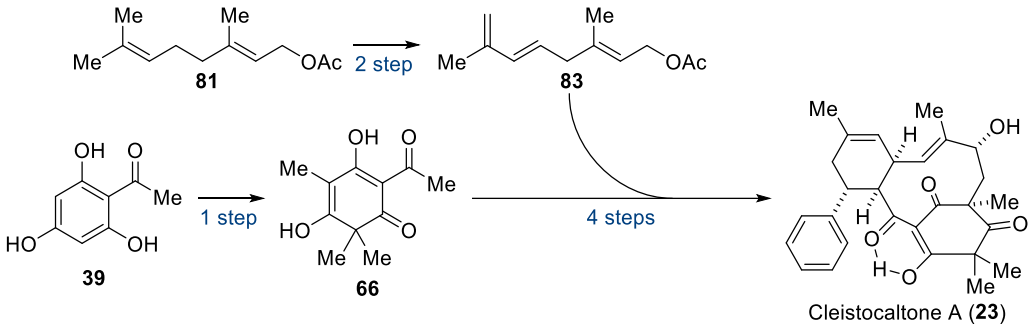

Scheme 60: Convergent route to Cleistocaltone A (**23**).

The linear route, where the geranylation of the phloroglucinol fragment **66** was performed first and the functionalization of the terpene sidechain thereafter, produced Cleistocaltone A (**23**) in 8 steps with an overall yield of 2.2% (Scheme 61). Because it was more efficient, this route was successfully scaled up to gram-scale producing 587 mg of **23**. Additionally an interesting side product **111** containing a unique tetracyclic system with an eight-membered cyclic ether was isolated and analyzed by XRD (Figure 21). It was suspected that **111** was a natural product from *C. operculatus* as well. However, all isolation attempts remained unsuccessful.

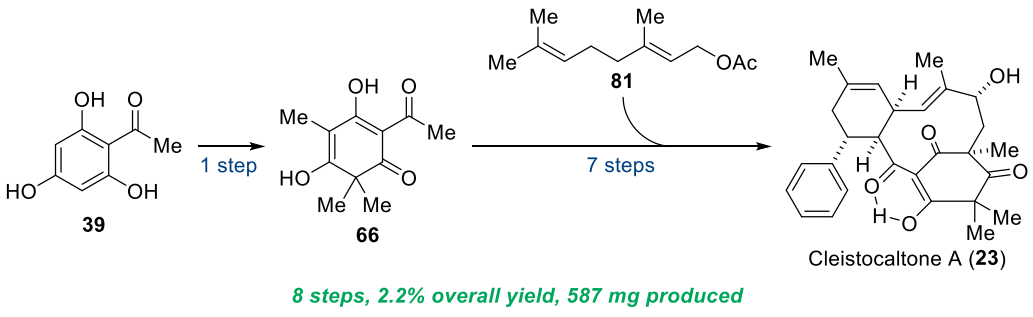

Scheme 61: Linear route to Cleistocaltone A (**23**).

Synthetic Cleistocaltone A (**23**) was tested by LUDLOW, CHRISTMANN, and coworkers for its anti-RSV activity against a contemporary recombinant RSV-A strain and showed a modestly higher IC_{50} than the isolated material by YE, WANG, and coworkers.[51,83]

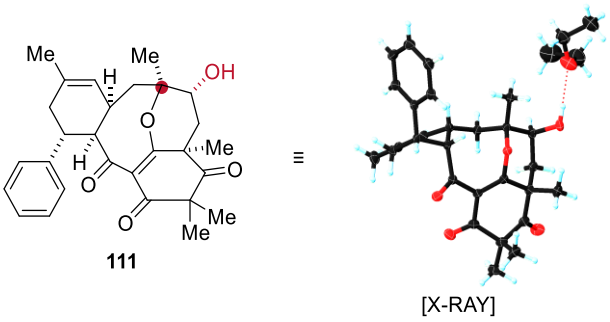

Figure 21: Isolated side product **111** and its molecular structure in a crystal.

The attempted synthesis of Cleistocaltone B (**24**) was unfortunately met with limited success. While the TSUJI-TROST coupling of phloroglucinol **66** with epoxide **124** was successful, there were *E*/*Z*-selectivity issues and the undesired *E*-isomer was produced in a large 6:1 excess (Scheme 62).

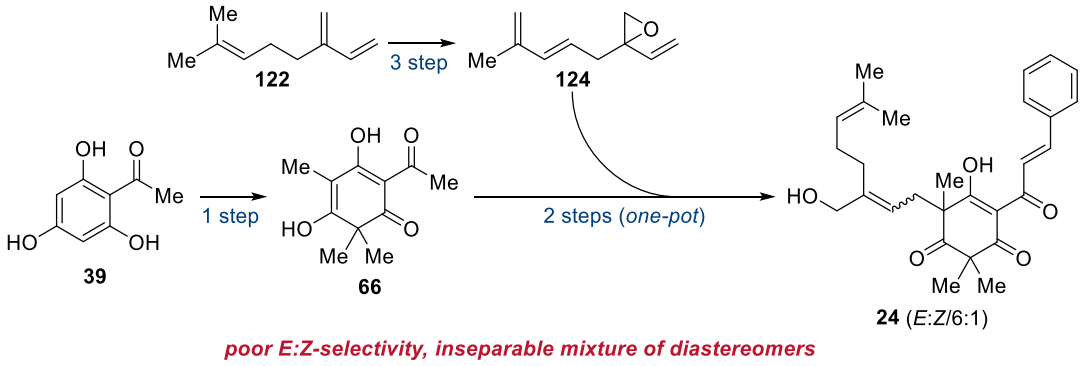

Scheme 62: Attempted synthesis of Cleistocaltone B (**24**).

4.2 Outlook

4.2.1 Further Biological Evaluations

The successful synthesis of Cleistocaltone A (**23**) gives access to many new compounds that could be used in biological evaluations (Figure 22). These derivatives may exhibit enhanced activity compared to the natural product. Although the enantioselective synthesis of **23** was not achieved, separation of the enantiomers *via* chiral column chromatography could provide (+)- and (–)-Cleistocaltone A (**23**). Subsequent testing of both enantiomers could reveal differences in biological activity which could provide insights into its mechanism of action.

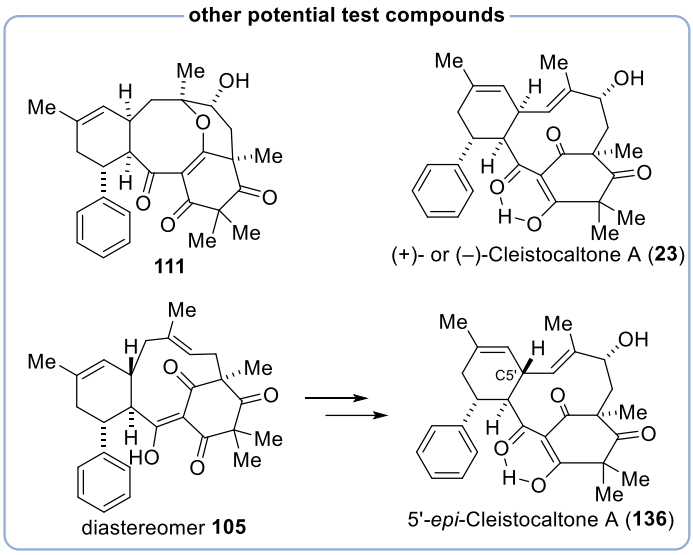

Figure 22: Other potential test compounds that emerged from the total synthesis of Cleistocaltone A (**23**).

Additionally, through the synthesis many new testing compounds became available. This includes **111** and IMDA-diastereomers **105** and **37.** Moreover, if the epoxidation and epoxide opening from the established synthesis were to be performed starting from the undesired IMDA-diastereomer **105**, an access to 5'-*epi*-Cleistocaltone A (**136**) could be realized which is another potential test compound.

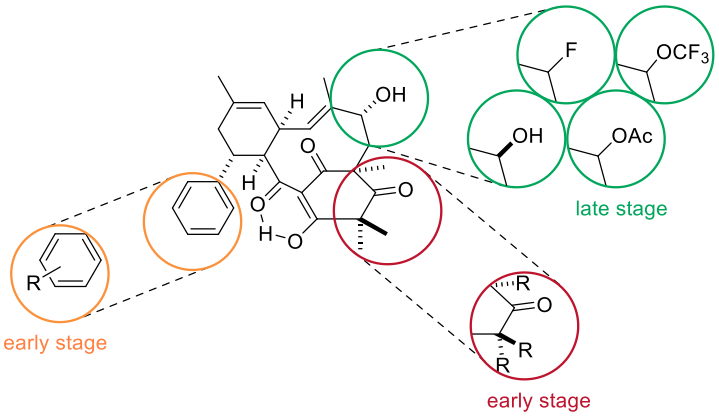

Figure 23: Possible derivatizations of Cleistocaltone A (**23**).

Furthermore, the synthesis of Cleistocaltone A (**23**) enables the exploration of various derivatizations (Figure 23). Late-stage modifications could focus on functionalization of the allylic hydroxyl group on the backbone. For instance, substitution with a fluoride or trifluoromethyl group could enhance the molecule's lipophilicity and its metabolic stability.[105,106] Alternatively, an acetylation might improve **23**'s bioavailability.[107] Early-stage modifications could involve substitutions of the alkyl groups on the phloroglucinol moiety, such as introducing trifluoromethyl groups. Additionally, alterations to the phenyl group could be considered. For example, the introduction of methyl groups at aromatic positions has been shown to increase activity in drug development.[108]

4.2.2 Synthesis of Similar Natural Products

The findings from this work could be valuable for the synthesis of structurally similar NPs. Earlier this year, TANG, YE, WANG, and coworkers isolated several new NPs from *C. operculatus* applying a blocks-based molecular network (BBMN) strategy to the phytochemical investigation of the plant.[109] One of these NPs, Cleistoperone A (**137**, Figure 24) possesses many of the same structural motifs as Cleistocaltone A (**23**). The main difference is that instead of a monoterpene backbone, **137** possesses a diterpene backbone which is presumably also tethered to the phloroglucinol moiety with an IMDA. Thus, Cleistoperone A (**137**) could be synthesized using a similar retrosynthesis. With a remarkable IC_{50} of 1.71 ± 0.61 µmol/L against RSV,[109] Cleistoperone A (**137**) would be a valuable target for a total synthesis.

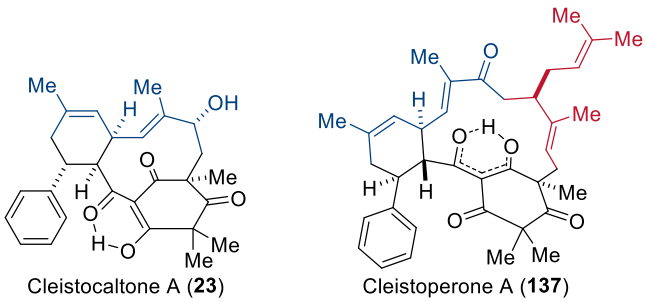

Figure 24: Structural similarities of Cleistocaltone A (**23**) and Cleistoperone A (**137**).[109]

5. Experimental Procedures and Analytical Data

5.1 General Information

5.1.1 Materials and Methods

Reactions with air- or moisture-sensitive substances were carried out under an argon atmosphere using standard SCHLENK technique. Ambient or room temperature (RT) refers to 18–23 °C. Heating of reactions was performed with an oil bath unless otherwise noted. “Brine” refers to a sat. aq. NaCl solution.

Unless otherwise noted, all starting materials and reagents were purchased from commercial distributors and used without further purification. Anhydrous dichloromethane and tetrahydrofuran were provided by purification with a MBraun SPS-800 solvent system (BRAUN) using solvents of HPLC grade purchased from FISHER Scientific and ROTH. 2-Acetyl phloroglucinol monohydrate was dried for 16 h at 60 °C under high vacuum to obtain dry 2-acetyl phloroglucinol which was stored under argon. Solvents for extraction, crystallization and flash column chromatography were purchased in technical grade and distilled under reduced pressure prior to use.

Column chromatography was performed on silica 60 M (0.040-0.063 mm, 230-400 mesh, MACHEREY-NAGEL).

Medium pressure liquid chromatography (MPLC) was performed with a TELEDYNE ISCO Combi-Flash Rf200 using prepacked silica columns and cartridges from TELDYNE. UV response was monitored at 254 nm and 280 nm. As eluents, cyclohexane (99.5+% quality) and EtOAc (HPLC grade) were used.

5.1.2 Analysis

Reaction monitoring: Reactions were monitored by thin layer chromatography (TLC). TLC-analysis was performed on silica gel coated aluminium plates ALUGRAM® Xtra SIL G/UV_{254} purchased from MACHEREY-NAGEL. Products were visualized by UV light at 254 nm and by using staining reagents (based on $Ce(SO_4)_2$ and anisaldehyde).

NMR spectroscopy: ^{1}H NMR and ^{13}C NMR spectral data were recorded on JEOL (ECX 400, ECP 500), VARIAN (Inova 600), and BRUKER (AVANCE III 500, AVANCE III 700) spectrometers in the reported deuterated solvents. The chemical shifts (δ) are listed in parts per million (ppm) and are reported relative to the corresponding residual non-deuterated solvent signal ($CDCl_3$: δ_H =

7.26 ppm, δ_C = 77.2 ppm; CD_2Cl_2: δ_H = 5.32 ppm, δ_C = 53.8 ppm; DMSO-d_6: δ_H = 2.50 ppm, δ_C = 39.5 ppm). Integrals are in accordance with assignments; coupling constants (*J*) are given in Hz. Multiplicity is indicated as follows: s (singlet), d (doublet), t (triplet), q (quartet), p (quintet), br (broad), and combinations thereof. In the case where no multiplicity could be identified, the chemical shift range of the signal is given as m (multiplet). ^{13}C NMR spectra are ^{1}H-broadband decoupled.

High resolution mass spectrometry: High resolution mass spectra (HRMS) were measured with an AGILENT 6210 ESI-TOF (10 µL/min, 1.0 bar, 4 kV) instrument.

Infrared spectroscopy: Infrared (IR) spectra were measured on a Jasco FT/IR-4100 Type A spectrometer with a TGS detector. Wavenumbers $\tilde{\nu}$ are given in cm^{-1}.

X-ray: X-ray diffraction data was collected on a BRUKER D8 Venture CMOS area detector (Photon 100) diffractometer with Cu Kα radiation. Single crystals were coated with perfluoroether oil and mounted on a 0.2 mm Micromount. The structures were solved with the ShelXT[110] structure solution program using intrinsic phasing and refined with the ShelXL[111] refinement package using least squares on weighted F2 values for all reflections using OLEX2.[112] Crystallographic data for compounds **105**, **37**, and **111** have been deposited with the Cambridge Crystallographic Data Centre under CCDC2352922, CCDC2352924, and CCDC2352923.

5.2 Synthesis of Champanone B

5.2 1 Route 1

1-(2-Hydroxy-4,6-bis(methoxymethoxy)phenyl)ethan-1-one (69)

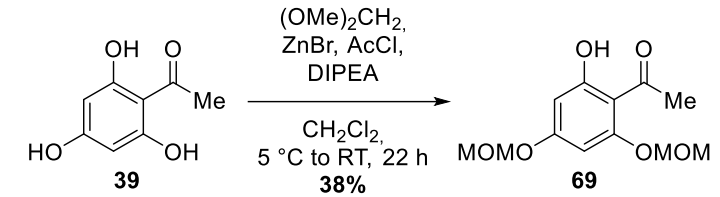

MOMCl was generated *in situ* through a literature-known procedure.[75] A SCHLENK tube was charged with $ZnBr_2$ (54.0 mg, 0.238 mmol, 0.40 equiv.) which was then dried *in vacuo* by heating of the tube with a heat gun at 630 °C. Afterwards, anhydrous CH_2Cl_2 (20 mL) and anhydrous dimethoxymethane (2.10 mL, 1.81 g, 23.8 mmol, 4.00 equiv.) were added subsequently and the mixture was cooled to 5 °C using an ice-water bath. Then, acetyl chloride (1.70 mL, 3.08 g, 23.8 mmol, 4.00 equiv.) was added dropwise. After complete addition, the mixture was allowed to warm up to RT and stirred for 36 h. This MOMCl solution was used directly in the next step.

In a SCHLENK tube, anhydrous acetyl phloroglucinol **39** (1.00 g, 5.95 mmol, 1.00 equiv.) was suspended in anhydrous CH_2Cl_2 (15 mL) and cooled to 5 °C using an ice-water bath. The previously produced MOMCl solution was added dropwise. After complete addition, DIPEA (4.16 mL, 3.08 g, 23.8 mmol, 4.00 equiv.) was added dropwise and the mixture was allowed to warm up to RT. During this time, the mixture became a clear solution. After 18 h, the excess MOMCl was quenched by addition of sat. aq. NH_4Cl (50 mL) and vigorous stirring for 10 min. The phases were separated and the organic phase was washed with 10% aq. citric acid (50 mL) and brine (50 mL), dried over Na_2SO_4, filtered, and concentrated under reduced pressure. The crude product was purified by column chromatography (SiO_2, EtOAc:cyclohexane/1:1) to afford MOM-protected acetyl phloroglucinol **69** (590 mg, 2.29 mmol, 38%) as a colourless oil.

^{1}H NMR (700 MHz, $CDCl_3$): δ = 13.70 (s, 1H), 6.26 (d, *J* = 2.3 Hz, 1H), 6.24 (d, *J* = 2.4 Hz, 1H), 5.25 (s, 2H), 5.16 (s, 2H), 3.51 (s, 3H), 3.47 (s, 3H), 2.65 (s, 3H) ppm.

^{13}C NMR (176 MHz, $CDCl_3$): δ = 203.4, 167.0, 163.6, 160.5, 107.1, 97.3, 94.6, 94.2, 56.8, 56.6, 33.1 ppm.

The spectroscopic data are in accordance with the literature.[113]

1-(2-Hydroxy-4,6-bis(methoxymethoxy)phenyl)-3-phenylprop-2-en-1-one (70)

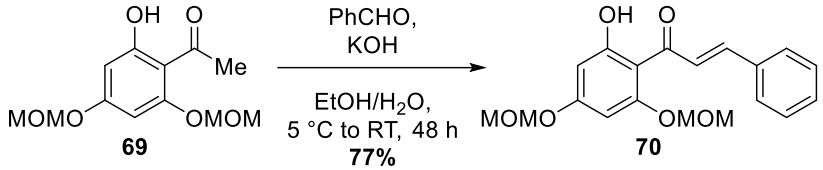

69
$C_{12}H_{16}O_6$ (256.25 g/mol)

70
$C_{19}H_{20}O_6$ (344.36 g/mol)

In a round-bottom flask, KOH (23.8 g, 424 mmol, 24.0 equiv.) was dissolved in water (50 mL). EtOH (50 mL) was added and the mixture was cooled down to 5 °C using an ice-water bath. To the cooled mixture a solution of MOM-protected acetyl-phloroglucinol **69** (4.53 g, 17.7 mmol, 1.00 equiv.) and benzaldehyde (1.82 mL, 1.91 g, 18.0 mmol, 1.02 equiv.) in EtOH (50 mL) was added dropwise and the mixture was allowed to warm up to RT. After 24 h, more benzaldehyde (3.57 mL, 3.74 g, 35.3 mmol, 2.00 equiv.) was added and stirring was continued for another 24 h. Afterwards, ice-water was added to the mixture and the pH was adjusted to 3 using 1 M aq. HCl. The mixture was extracted with EtOAc (3 x 100 mL). The combined organic layers were washed with water (200 mL) and brine (200 mL), dried over Na_2SO_4, filtered, and concentrated under reduced pressure. The crude product was recrystallized from EtOH:pentane/1:1 and filtered. The filtrate was concentrated and recrystallized again to recover more material. The collected solids were combined to afford MOM-protected cinnamoyl phloroglucinol **70** (4.70 g, 13.6 mmol, 77%) as an orange, amorphous solid.

^{1}H NMR (700 MHz, $CDCl_3$): δ = 13.82 (s, 1H), 7.93 (d, *J* = 15.6 Hz, 1H), 7.79 (d, *J* = 15.6 Hz, 1H), 7.62 – 7.59 (m, 2H), 7.42 – 7.38 (m, 3H), 6.32 (d, *J* = 2.4 Hz, 1H), 6.26 (d, *J* = 2.4 Hz, 1H), 5.29 (s, 2H), 5.19 (s, 2H), 3.54 (s, 3H), 3.49 (s, 3H) ppm.

^{13}C NMR (176 MHz, $CDCl_3$): δ = 193.1, 167.5, 163.7, 160.0, 142.6, 135.6, 130.3, 129.1, 128.5, 127.5, 107.7, 97.6, 95.3, 94.9, 94.2, 57.0, 56.6 ppm.

The spectroscopic data are in accordance with the literature.[114]

3-Phenyl-1-(2,4,6-trihydroxyphenyl)prop-2-en-1-one (71)

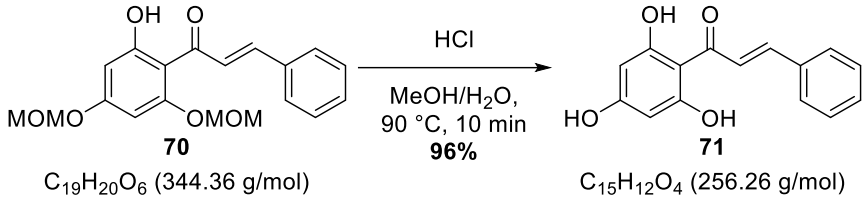

$C_{19}H_{20}O_6$ (344.36 g/mol) $C_{15}H_{12}O_4$ (256.26 g/mol)

In a round-bottom flask, MOM-protected cinnamoyl-phloroglucinol **70** (52.0 mg, 0.151 mmol, 1.00 equiv.) was dissolved in MeOH (3 mL). Aq. HCl (3 M, 1.26 mL, 25.0 equiv.) was added and the mixture was heated to 90 °C for 10 min. Afterwards, the mixture was diluted with water (20 mL) and extracted with EtOAc (2 x 10 mL). The combined organic layers were dried over Na_2SO_4, filtered, and concentrated under reduced pressure. The residue was suspended in CH_2Cl_2 and filtered. The filter cake was washed with additional CH_2Cl_2, dissolved in EtOH, and concentrated under reduced pressure to afford cinnamoyl phlorogucinol **71** (37.0 mg, 0.144 mmol, 96%) as a yellow amorphous solid.

^{1}H NMR (600 MHz, methanol-d_4): δ = 8.21 (d, *J* = 15.6 Hz, 1H), 7.71 (d, *J* = 15.7 Hz, 1H), 7.62 – 7.59 (m, 2H), 7.40 – 7.36 (m, 3H), 5.86 (s, 2H) ppm.

^{13}C NMR (151 MHz, methanol-d_4): δ = 194.0, 166.6, 166.1, 142.9, 137.0, 131.1, 130.0, 129.3, 128.9, 105.9, 96.0 ppm.

The spectroscopic data are in accordance with the literature.[114]

5.2.2 Route 2

2-Acetyl-3,5-dihydroxy-4,6,6-trimethylcyclohexa-2,4-dien-1-one (66) (Reproduced (adapted) from Ref.[83] with permission from the Royal Society of Chemistry.)

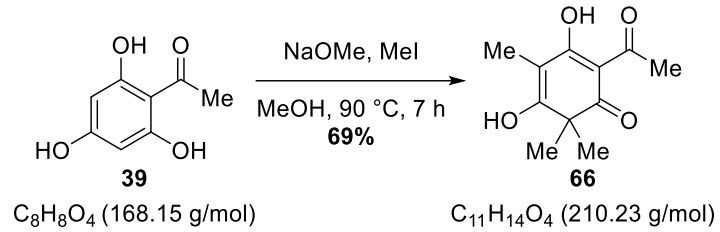

39 $C_8H_8O_4$ (168.15 g/mol)

66 $C_{11}H_{14}O_4$ (210.23 g/mol)

The methylation of 2-acetyl phloroglucinol (**39**) was performed according to a literature-known procedure.[72] Sodium (7.59 g, 330 mmol, 3.70 equiv.) was added to anhydrous methanol (250 mL) in a three-necked round-bottom flask equipped with a reflux-condenser. After the sodium had reacted completely, anhydrous 2-acetyl phloroglucinol (**39**, 15.0 g, 89.2 mmol, 1.00 equiv.) dissolved in anhydrous methanol (200 mL) was added slowly. Afterwards, methyl iodide (18.2 mL, 41.8 g, 294 mmol, 3.30 equiv.) was added slowly. Then, the mixture was heated to 90 °C and stirred at this temperature for 7 h. Afterwards, the mixture was cooled down to 5 °C using an ice/water-bath. The mixture was acidified to pH = 2-3 with 1 M aq. HCl. The precipitated solid was filtered off, washed with water, and dried under high vacuum. Trimethylated acetyl phloroglucinol **66** (12.9 g, 61.6 mmol, 69%) was isolated as an off-white powder and used without further purification.

^{1}H NMR (600 MHz, DMSO-d_6): δ = 18.96 (s, 1H), 2.46 (s, 3H), 1.77 (s, 3H), 1.27 (s, 6H) ppm.

^{13}C NMR (151 MHz, DMSO-d_6): δ = 199.4, 196.0, 188.9, 176.0, 105.1, 101.9, 48.2, 27.8, 24.3, 7.2 ppm.

The spectroscopic data are in accordance with the literature.[115]

2-Acetyl-3-hydroxy-5-(methoxymethoxy)-4,6,6-trimethylcyclohexa-2,4-dien-1-one (72)

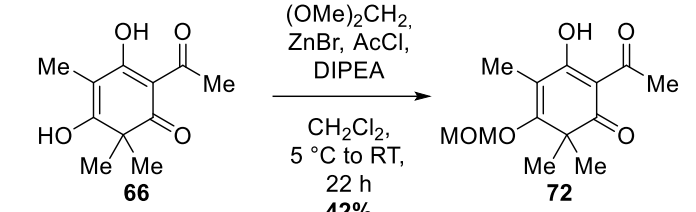

MOMCl was generated *in situ* through a literature-known procedure.[75] A SCHLENK tube was charged with $ZnBr_2$ (305 mg, 1.36 mmol, 10 mol%) which was then dried *in vacuo* by heating of the tube with a heat gun at 630 °C. Afterwards, anhydrous CH_2Cl_2 (50 mL) and anhydrous dimethoxymethane (2.40 mL, 2.06 g, 27.1 mmol, 2.00 equiv.) were added subsequently and the mixture was cooled to 5 °C using an ice-water bath. Then, acetyl chloride (1.93 mL, 2.13 g, 27.1 mmol, 2.00 equiv.) was added dropwise. After complete addition, the mixture was allowed to warm up to RT and stirred for 4 h. Afterwards, the mixture was diluted with anhydrous CH_2Cl_2 (85 mL) and cooled down to 5 °C using an ice-water bath. Trimethylated acetyl phloroglucinol **66** (2.85 g, 13.6 mmol, 1.00 equiv.) and DIPEA (4.74 mL, 3.50 g, 27.1 mmol, 2.00 equiv.) were added to the mixture subsequently. Then, the mixture was allowed to warm up to RT over 18 h. Afterwards, the excess MOMCl was quenched by addition of sat. aq. NH_4Cl (50 mL) and vigorous stirring for 10 min. The phases were separated and the organic phase was washed with 10% aq. citric acid (50 mL) and brine (50 mL), dried over Na_2SO_4, filtered, and concentrated under reduced pressure. The crude product was purified by column chromatography (SiO_2, EtOAc:cyclohexane/1:9) to afford MOM-protected, trimethylated acetyl phloroglucinol **72** (1.45 g, 5.70 mmol, 42%) as a colourless oil.

The product was isolated as a mixture of two interconverting tautomers (tautomer A : tautomer B = 1:0.6) which gave two sets of signals in the ^{1}H- and ^{13}C-NMR in which many signals overlapped.

Tautomer A:

^{1}H NMR (600 MHz, $CDCl_3$): δ = 18.89 (s, 1H), 5.11 (s, 2H), 3.58 (s, 3H), 2.61 (s, 3H), 1.92 (s, 3H), 1.34 (s, 6H) ppm.

^{13}C NMR (151 MHz, $CDCl_3$): δ = 201.5, 197.5, 190.1, 174.9, 112.8, 107.4, 99.6, 57.6, 50.1, 28.2, 24.3, 10.0 ppm.

Tautomer B:

^{1}H NMR (600 MHz, $CDCl_3$): δ = 18.17 (s, 1H), 5.04 (s, 2H), 3.58 (s, 3H), 2.69 (s, 3H), 1.87 (s, 3H), 1.46 (s, 6H) ppm.

^{13}C NMR (151 MHz, $CDCl_3$): δ = 204.3, 197.6, 185.6, 169.0, 118.6, 109.6, 99.8, 57.4, 44.8, 29.5, 24.4, 10.5 ppm.

HRMS (ESI, pos.): *m/z* calcd for $C_{13}H_{18}NaO_5^+$ $[M+Na^+]^+$: 277.1046, found 277.1057.

IR (ATR): $\tilde{\nu}$ = 2979, 2935, 2830, 1656, 1634, 1530, 1441, 1372, 1362, 1337, 1299, 1261, 1215, 1162, 1132, 1065, 1029, 1004, 968, 934, 894, 814, 786, 721 cm^{-1}.

2-Cinnamoyl-3-hydroxy-5-(methoxymethoxy)-4,6,6-trimethylcyclohexa-2,4-dien-1-one (73)

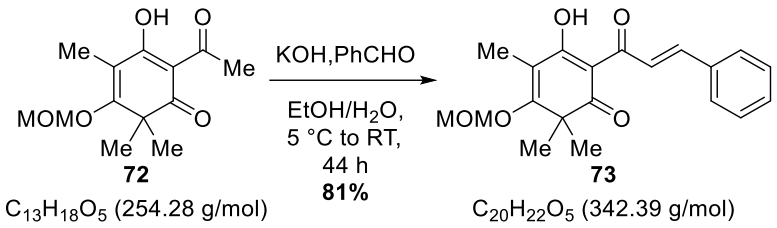

$C_{13}H_{18}O_5$ (254.28 g/mol) $C_{20}H_{22}O_5$ (342.39 g/mol)

In a round-bottom flask, MOM-protected trimethylated acetyl phloroglucinol **72** (1.37 g, 5.39 mmol, 1.00 equiv.) and freshly distilled benzaldehyde (1.09 mL, 1.14 g, 10.8 mmol, 2.00 equiv.) were dissolved in EtOH (175 mL). The mixture was cooled down to 5 °C using an ice-water bath and a solution of KOH (7 M, 18.5 mL) mixed with EtOH (16 mL) was added dropwise through a dropping funnel. After complete addition, the mixture was allowed to warm up to RT and stirred for 18 h. Afterwards, more benzaldehyde (1.09 mL, 1.14 g, 10.8 mmol, 2.00 equiv.) was added and stirring was continued. After 8 h, more benzaldehyde (1.09 mL, 1.14 g, 10.8 mmol, 2.00 equiv.) was added and stirring was continued for 18 h. Then, the mixture was cooled down to 5 °C using an ice-water bath and a sat. aq. solution of NH_4Cl (50 mL) was added dropwise through the dropping funnel. The mixture was extracted with cyclohexane (3 x 300 mL). The combined organic layers were dried over Na_2SO_4, filtered, and concentrated under reduced pressure. The residue was dried while stirring under high vacuum for 3 h to remove parts of the excess benzaldehyde. The crude product was purified by column chromatography (SiO_2, EtOAc:pentane/1:9). After purification, remaining traces of benzaldehyde were removed by stirring under high vacuum at 40 °C overnight upon which MOM-protected cinnamoyl phloroglucinol **73** (1.49 g, 4.36 mmol, 81%) solidified as a bright yellow, amorphous solid.

The product was isolated as a mixture of two interconverting tautomers (tautomer A : tautomer B = 1:0.5) which gave two sets of signals in the ^{1}H- and ^{13}C-NMR in which many signals overlapped.

Tautomer A:

^{1}H NMR (600 MHz, $CDCl_3$): δ = 19.11 (s, 1H), 8.32 (d, J = 15.8 Hz, 1H), 7.93 (d, J = 15.8 Hz, 1H), 7.69 – 7.65 (m, 2H), 7.39 – 7.37 (m, 3H), 5.12 (s, 2H), 3.59 (s, 3H), 1.95 (s, 3H), 1.40 (s, 6H) ppm.

^{13}C NMR (151 MHz, $CDCl_3$): δ = 198.1, 192.2, 187.3, 174.6, 145.1, 135.3, 130.7, 129.0, 129.0, 123.2, 114.3, 106.7, 99.6, 57.5, 50.2, 24.4, 10.2 ppm.

Tautomer B:

^{1}H NMR (600 MHz, $CDCl_3$): δ = 18.76 (s, 1H), 8.53 (d, J = 15.8 Hz, 1H), 7.95 (d, J = 15.8 Hz, 1H), 7.69 – 7.65 (m, 2H), 7.39 – 7.37 (m, 3H), 5.06 (s, 2H), 3.58 (s, 3H), 1.91 (s, 3H), 1.49 (s, 6H) ppm.

^{13}C NMR (151 MHz, $CDCl_3$): δ = 201.8, 189.5, 186.1, 169.3, 145.6, 135.2, 130.9, 129.1, 129.0, 123.6, 119.0, 108.4, 99.7, 57.4, 45.8, 24.5, 10.7 ppm.

HRMS (ESI, pos.): *m/z* calcd for $C_{20}H_{22}NaO_5^+$ $[M+Na^+]^+$: 365.1359, found 365.1373.

IR (ATR): $\tilde{\nu}$ = 3101, 3084, 3060, 3026, 2979, 2932, 2828, 1655, 1621, 1576, 1509, 1468, 1447, 1427, 1372, 1353, 1335, 1304, 1242, 1214, 1149, 1065, 1011, 980, 911, 873, 825, 797, 758, 741, 719 cm^{-1}.

Champanone B (25)

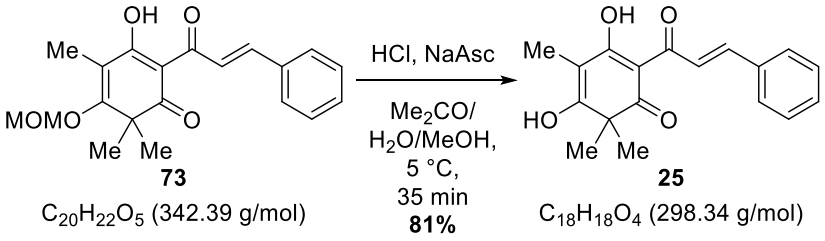

In a round-bottom flask, HCl (37%, 5.37 mL, 6.44 g, 65.3 mmol, 45.0 equiv.) and sodium ascorbate (575 mg, 2.90 mmol, 2.00 equiv.) were dissolved in MeOH while cooling the mixture to 5 °C using an ice-water bath. Then, MOM-protected cinnamoyl-phloroglucinol **73** (500 mg, 1.45 mmol, 1.00 equiv.) dissolved in acetone (32 mL) was added to the mixture over 30 min using a syringe pump. After full addition, stirring was continued for 5 min. Then, the mixture was diluted with water upon which a yellow solid precipitated. The solid was filtered off through a glass filter and washed with water. The filter cake was dissolved in MeOH and concentrated under reduced pressure. The crude product was purified by column chromatography (SiO_2, EtOAc:pentane/1:1) to afford Champanone B (**25**, 352 mg, 1.18 mmol, 81%) as a yellow, amorphous solid.

^{1}H NMR (600 MHz, acetone-d_6): δ = 8.38 (d, J = 15.9 Hz, 1H), 7.89 (d, J = 15.9 Hz, 1H), 7.73 – 7.71 (m, 2H), 7.49 – 7.44 (m, 3H), 1.91 (s, 3H), 1.42 (s, 6H) ppm.

^{13}C NMR (151 MHz, acetone-d_6): δ = 197.6, 192.2, 187.1, 175.2, 144.1, 136.4, 131.3, 129.9, 129.4, 124.6, 106.2, 105.2, 49.4, 24.8, 7.5 ppm.

The spectroscopic data are in accordance with the literature.[71]

5.3 Synthesis of Terpene Fragments

5.3.1 Synthesis of Hotrienyl Derivatives

6-Chloro-3,7-dimethylocta-1,7-dien-3-yl acetate (78)

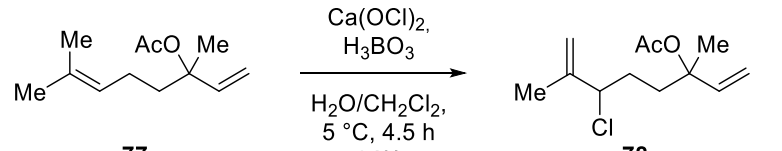

77
$C_{12}H_{20}O_2$ (196.29 g/mol)

78
$C_{12}H_{19}ClO_2$ (230.73 g/mol)

The chlorination of linalyl acetate (**77**) was performed according to a literature procedure.[79] In an ERLENMEYER flask equipped with a large stirring bar, linalyl acetate (**77**, 11.3 mL, 10.15 g, 51.7 mmol, 1.00 equiv.) was dissolved in CH_2Cl_2 (50 mL). The mixture was cooled down to 5 °C using an ice-water bath. Calcium hypochlorite (67 w%, 6.62 g, 31.0 mmol, 0.60 equiv.) and boric acid (6.40 g, 103 mmol, 2.00 equiv.) were added subsequently. Afterwards, water (10 mL) was added over a period of 4 h using a syringe pump while stirring the mixture vigorously. After stirring for an additional 30 min the reaction showed complete conversion. Na_2SO_4 was added and the inorganic salts were filtered off through celite. The filtrate was washed with a 10% aq. NaCl solution (2 x 100 mL), dried over Na_2SO_4, filtered, and concentrated under reduced pressure. The crude product was purified by column chromatography (SiO_2, EtOAc:pentane/1:20) to afford allyl chloride **78** (7.58 g, 32.9 mmol, 64%) as a yellowish oil.

The product was obtained as an inseparable mixture of two diastereomers which gave two sets of signals in the ^{1}H- and ^{13}C-NMR in which many signals overlapped.

Diastereomer A:

^{1}H NMR (700 MHz, $CDCl_3$): δ = 5.96 – 5.90 (m, 1H), 5.18 – 5.13 (m, 2H), 5.01 – 5.01 (m, 1H), 4.91 – 4.90 (m, 1H), 4.35 – 4.32 (m, 1H), 2.01 (s, 3H), 1.99 – 1.90 (m, 1H), 1.90 – 1.80 (m, 3H), 1.79 – 1.79 (m, 3H), 1.54 (s, 3H) ppm.

^{13}C NMR (176 MHz, $CDCl_3$): δ = 170.0, 144.1, 141.5, 114.7, 113.7, 82.4, 66.7, 37.3, 30.9, 23.8, 22.3, 17.0 ppm.

Diastereomer B:

^{1}H NMR (700 MHz, $CDCl_3$): δ = 5.96 – 5.90 (m, 1H), 5.18 – 5.13 (m, 2H), 5.01 – 5.01 (m, 1H), 4.91 – 4.90 (m, 1H), 4.35 – 4.32 (m, 1H), 2.01 (s, 3H), 1.99 – 1.90 (m, 1H), 1.90 – 1.80 (m, 3H), 1.79 – 1.79 (m, 3H), 1.55 (s, 3H) ppm.

^{13}C NMR (176 MHz, $CDCl_3$): δ = 170.0, 144.2, 141.4, 114.7, 113.8, 82.5, 66.8, 37.2, 30.9, 24.0, 22.3, 17.0 ppm.

The spectroscopic data are in accordance with the literature.[79]

Hotrienyl acetate (79)

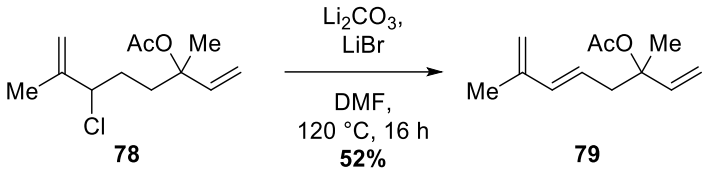

The dehydrochlorination of allylic chloride **78** was performed according to a literature procedure.[79] A SCHLENK tube was charged with lithium carbonate (5.42 g, 73.4 mmol, 2.50 equiv.) and lithium bromide (3.82 g, 44.0 mmol, 1.50 equiv.). The salts were dried *in vacuo* using a heat gun at 630 °C for 30 min. After allowing the salts to cool down to RT, anhydrous DMF (25 mL) and allylic chloride **78** (6.77 g, 29.3 mmol, 1.00 equiv.) were added. The mixture was heated to 120 °C and stirred at that temperature for 16 h. After complete conversion the mixture was diluted with water (20 mL) and extracted with cyclohexane (3 x 30 mL). The combined organic layers were washed with water (50 mL) and brine (50 mL), dried over Na_2SO_4, filtered, and concentrated under reduced pressure. The crude product was purified by column chromatography (SiO_2, EtOAc:cyclohexane/1:19) to afford hotrienyl acetate (**79**, 2.97 g, 15.3 mmol, 52%) as a yellowish, fruity smelling oil.

^{1}H NMR (600 MHz, $CDCl_3$): δ = 6.17 (d, J = 15.5 Hz, 1H), 6.01 (dd, J = 17.5, 11.0 Hz, 1H), 5.56 (dt, J = 15.6, 7.4 Hz, 1H), 5.18 – 5.13 (m, 2H), 4.91 – 4.90 (m, 2H), 2.67 – 2.59 (m, 2H), 1.99 (s, 3H), 1.83 – 1.83 (m, 3H), 1.52 (s, 3H) ppm.

^{13}C NMR (151 MHz, $CDCl_3$): δ = 170.1, 142.0, 141.7, 136.6, 124.4, 115.5, 113.7, 82.6, 43.0, 23.8, 22.3, 18.8 ppm.

The spectroscopic data are in accordance with the literature.[79]

Hotrienol (76)

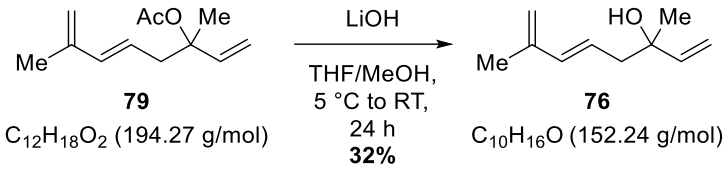

79
$C_{12}H_{18}O_2$ (194.27 g/mol)

76
$C_{10}H_{16}O$ (152.24 g/mol)

In a round-bottom flask, hotrienyl acetate (**79**, 530 mg, 2.73 mmol, 1.00 equiv.) was dissolved in a 1:1-mixture of THF and methanol (12 mL) and cooled down to 5 °C using an ice-water bath. To the mixture was added aq. LiOH (2 M, 2.73 mL, 5.46 mmol, 2.00 equiv.) slowly. The mixture was allowed to warm up to RT and stirred for 24 h. Then the mixture was diluted with aq. NaOH (1 M, 200 mL) and extracted with EtOAc (3 x 100 mL). The combined organic layers were dried over Na_2SO_4, filtered, and concentrated under reduced pressure. The crude product was purified by column chromatography (SiO_2, EtOAc:pentane/1:9) to afford hotrienol (**76**, 134 mg, 0.879 mmol, 32%) as a yellowish, fruity smelling oil.

The compound contained some inseparable impurities which, however, did not interfere in the following reaction and were removed after the next step.

^{1}H NMR (600 MHz, $CDCl_3$): δ = 6.21 (d, J = 15.5 Hz, 1H), 5.94 (dd, J = 17.3, 10.7 Hz, 1H), 5.65 – 5.59 (m, 1H), 5.22 (dd, J = 17.3, 1.2 Hz, 1H), 5.07 (dd, J = 10.8, 1.3 Hz, 1H), 4.93 – 4.91 (m, 2H), 2.40 – 2.31 (m, 2H), 1.83 (s, 3H), 1.29 (s, 3H) ppm.

^{13}C NMR (151 MHz, $CDCl_3$): δ = 144.9, 141.9, 137.2, 125.0, 115.8, 112.2, 73.0, 45.9, 27.7, 18.8 ppm.

The spectroscopic data are in accordance with the literature.[79]

Hotrienyl *tert*-butyl carbonate (80)

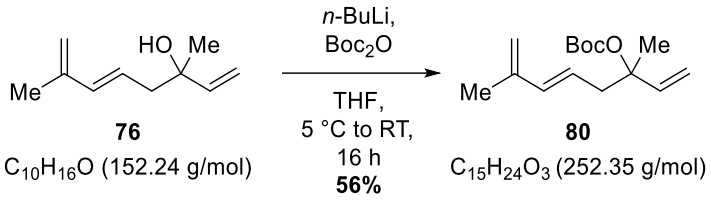

In a SCHLENK tube, hotrienol (**76**, 80.0 mg, 0.526 mmol, 1.00 equiv.) was dissolved in anhydrous THF (2 mL) and cooled down to 5 °C using an ice-water bath. *n*-BuLi (2.5 M solution in *n*-hexane, 0.252 mL, 0.631 mmol, 1.20 equiv.) was added dropwise, followed by Boc_2O (0.112 mL, 115 mg, 0.526 mmol, 1.00 equiv.) and the mixture was allowed to warm up to RT over 16 h. Excess *n*-BuLi was quenched by addition of sat. aq. $NaHCO_3$ (5 mL) and the mixture was extracted with EtOAc (3 x 10 mL). The combined organic layers were dried over Na_2SO_4, filtered, and concentrated under reduced pressure. The crude product was purified by column chromatography (SiO_2, EtOAc:pentane/1:9) to afford hotrienyl *tert*-butyl carbonate (**80**, 74.0 mg, 0.294 mmol, 56%) as a colourless oil.

^{1}H NMR (600 MHz, $CDCl_3$): δ = 6.18 (d, J = 15.6 Hz, 1H), 6.05 (dd, J = 17.6, 11.0 Hz, 1H), 5.61 – 5.56 (m, 1H), 5.19 (d, J = 11.8 Hz, 1H), 5.17 (d, J = 5.2 Hz, 1H), 4.89 (d, J = 11.6 Hz, 2H), 2.73 (dd, J = 14.0, 7.6 Hz, 1H), 2.60 (dd, J = 14.0, 7.4 Hz, 1H), 1.83 (s, 3H), 1.52 (s, 3H), 1.46 (s, 9H) ppm.

5.3.2 Synthesis of Terpene Fragments Containing a Terminal Leaving Group

6-Chloro-3,7-dimethylocta-2,7-dien-1-yl acetate (82) (Reproduced (adapted) from Ref.[83] with permission from the Royal Society of Chemistry.)

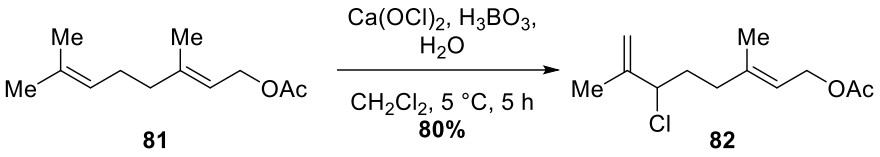

Calcium hypochlorite (67 w%, 6.47 g, 30.6 mmol, 0.60 equiv.) and boric acid (7.58 g, 122 mmol, 2.40 equiv.) were suspended in anhydrous CH_2Cl_2 (50 mL) in an ERLENMEYER flask. The resulting mixture was cooled down to 5 °C using an ice-water bath and geranyl acetate (**81** ,11.0 mL, 10.0 g, 50.9 mmol, 1.00 equiv.) was added. Under vigorous stirring, water (13.8 mL) was added over 5 h using a syringe pump. Afterwards, solid Na_2SO_3 was added, the inorganic salts were filtered off through a plug of celite and the filtrate was concentrated under reduced pressure. The crude product was purified by column chromatography (SiO_2, EtOAc/pentane, 1:19 to 1:9) to afford allylic chloride **82** (9.37 g, 40.6 mmol, 80%) as a colourless oil.

^{1}H NMR (600 MHz, $CDCl_3$): δ = 5.37 (tq, *J* = 7.0, 1.3 Hz, 1H), 5.01 – 5.00 (m, 1H), 4.90 (p, *J* = 1.5 Hz, 1H), 4.58 (d, *J* = 7.1 Hz, 2H), 4.35 – 4.32 (m, 1H), 2.19 – 2.13 (m, 2H), 2.05 (s, 3H), 2.01 – 1.88 (m, 2H), 1.81 (s, 3H), 1.71 (s, 3H) ppm.

^{13}C NMR (151 MHz, $CDCl_3$): δ = 171.2, 144.3, 140.7, 119.5, 114.5, 66.3, 61.3, 36.6, 34.5, 21.2, 17.1, 16.6 ppm.

The spectroscopic data are in accordance with the literature.[116]

3,7-Dimethylocta-2,5,7-trien-1-yl acetate (83) (Reproduced (adapted) from Ref.[83] with permission from the Royal Society of Chemistry.)

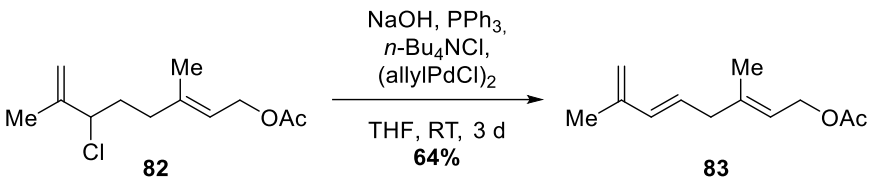

The dehydrochlorination of allylic chloride **82** was performed according to a literature-known procedure.[80] Freshly ground NaOH (3.57 g, 89.2 mmol, 1.10 equiv.), PPh_3 (1.06 g, 4.05 mmol, 5 mol%), and *n*-Bu_4NCl (676 mg, 2.43 mmol, 3 mol%) were loaded into a SCHLENK flask. The flask was evacuated and backfilled with argon three times. Afterwards, anhydrous THF (60 mL) and allylic chloride **82** (18.7 g, 81.0 mmol, 1.00 equiv.) dissolved in anhydrous THF (100 mL) were added to the mixture subsequently while keeping the temperature under 25 °C using a water bath. The mixture was stirred for three days. Afterwards, water (100 mL) was added, the phases were separated and the aqueous phase was extracted with diethyl ether (3 x 100 mL). The combined organic layers were washed with water, brine, dried over Na_2SO_4, filtered, and concentrated under reduced pressure. The crude product was purified by column chromatography (SiO_2, EtOAc/pentane, 1:19) to afford diene **83** (10.0 g, 51.5 mmol, 64%) as a yellowish oil.

^{1}H NMR (600 MHz, $CDCl_3$): δ = 6.16 (d, *J* = 15.6 Hz, 1H), 5.61 (dt, *J* = 15.5, 7.1 Hz, 1H), 5.37 (tq, *J* = 7.1, 1.4 Hz, 1H), 4.91 – 4.90 (m, 2H), 4.60 (d, *J* = 7.3 Hz, 2H), 2.82 (d, *J* = 7.1 Hz, 2H), 2.06 (s, 3H), 1.84 (s, 3H), 1.70 (s, 3H) ppm.

^{13}C NMR (151 MHz, $CDCl_3$): δ = 171.3, 142.0, 141.2, 135.0, 127.5, 119.3, 115.3, 61.5, 42.8, 21.2, 18.8, 16.8 ppm.

HRMS (ESI, pos.): *m/z* calcd for $C_{12}H_{18}O_2Na^+$ $[M+Na^+]^+$: 217.1199, found 217.1193.

IR (ATR): $\tilde{\nu}$ = 3081, 3022, 2975, 2942, 2919, 1737, 1672, 1649, 1608, 1438, 1380, 1365, 1319, 1227, 1109, 1021, 966, 884, 826, 793, 777, 747, 719 cm^{-1}.

3,7-Dimethylocta-2,5,7-trien-1-ol (84)

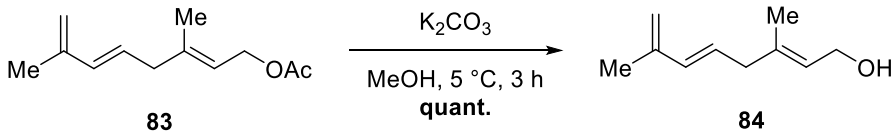

83
$C_{12}H_{18}O_2$ (194.27 g/mol)

84
$C_{10}H_{16}O$ (152.24 g/mol)

In a round-bottom flask, allylic acetate **83** (1.00 g, 5.15 mmol, 1.00 equiv.) was dissolved in methanol (5 mL). The mixture was cooled down to 5 °C using an ice-water bath and K_2CO_3 (213 mg, 1.54 mmol, 0.30 equiv.) was added. After 3 h the mixture was neutralized by adding sat. aq. NH_4Cl (5 mL). Afterwards, the mixture was extracted with EtOAc (3 x 10 mL). The combined organic layers were dried over Na_2SO_4, filtered, and concentrated under reduced pressure to afford allylic alcohol **84** (780 mg, 5.12 mmol, quant.) as a colourless oil.

^{1}H NMR (600 MHz, $CDCl_3$): δ = 6.16 (d, J = 15.5 Hz, 1H), 5.62 (dt, J = 15.5, 7.1 Hz, 1H), 5.48 – 5.42 (m, 1H), 4.90 (s, 2H), 4.17 (d, J = 5.8 Hz, 2H), 2.80 (d, J = 7.2 Hz, 2H), 1.84 (s, 3H), 1.68 (s, 3H) ppm.

***tert*-Butyl (3,7-dimethylocta-2,5,7-trien-1-yl) carbonate (85)**

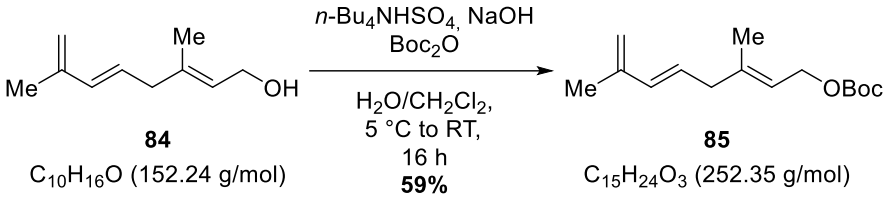

In a test tube, allylic alcohol **84** (100 mg, 0.657 mmol, 1.00 equiv.) was dissolved in CH_2Cl_2 (0.33 mL). *n*-Bu_4NHSO_4 (4.46 mg, 0.013 mmol, 20 mol%), and Boc_2O (0.169 mL, 172 mg, 0.788 mmol, 1.20 equiv.) were added and the mixture was cooled down to 5 °C using an ice-water bath. Afterwards, aq. NaOH (10 M, 0.363 mL, 5.50 equiv.) was added and the mixture was allowed to warm up to RT over 16 h. Then, the mixture was diluted with Et_2O (2 mL) and water (2 mL). The phases were separated and the aqueous phase was extracted with Et_2O (2 x 2 mL). The combined organic layers were washed with aq. HCl (1 M, 5 mL), water (5 mL), brine (5 mL), dried over Na_2SO_4, filtered, and concentrated under reduced pressure. The crude product was purified by column chromatography (SiO_2, Et_2O/pentane, 1:99) to afford *tert*-butyl carbonate **85** (97.0 mg, 0.384 mmol, 59%) as a colourless oil.

^{1}H NMR (600 MHz, $CDCl_3$): δ = 6.15 (d, J = 15.6 Hz, 1H), 5.60 (dt, J = 15.6, 7.1 Hz, 1H), 5.40 (tq, J = 7.1, 1.3 Hz, 1H), 4.89 (s, 2H), 4.59 (d, J = 7.1 Hz, 2H), 2.81 (d, J = 7.1 Hz, 2H), 1.83 (s, 3H), 1.70 (s, 3H), 1.48 (s, 9H) ppm.

^{13}C NMR (151 MHz, $CDCl_3$): δ = 153.7, 142.0, 141.4, 135.0, 127.4, 119.1, 115.3, 82.1, 63.8, 42.8, 27.9, 18.8, 16.8 ppm.

***tert*-Butyl (3,7-dimethylocta-2,6-dien-1-yl) carbonate (91)**

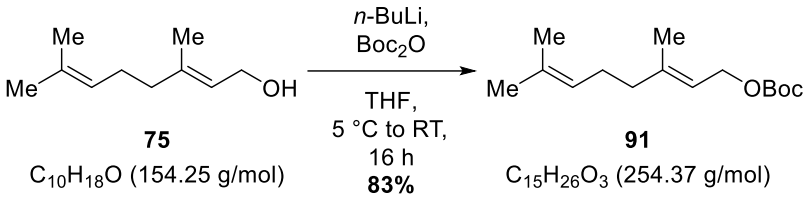

The Boc-substitution of geraniol (**75**) was performed according to a literature-known procedure.[59] In a SCHLENK tube, geraniol (**75**, 2.26 mL, 2.00 g, 13.0 mmol, 1.00 equiv.) was dissolved in anhydrous THF (50 mL). The solution was cooled down to 5 °C using an ice-water bath. Afterwards, *n*-BuLi (2.50 M in hexane, 5.71 mL, 14.3 mmol, 1.10 equiv.) was added over 1 h using a syringe pump. Then, Boc_2O (2.78 mL, 2.83 g, 13.0 mmol, 1.00 equiv.) was added and the mixture was allowed to warm up to RT over 16 h. The reaction was stopped by addition of sat. aq. NaHCO3 (50 mL). The mixture was extracted with EtOAc (3 x 100 mL). The combined organic layers were dried over Na_2SO_4, filtered, and concentrated under reduced pressure. The crude product was purified by column chromatography (SiO_2, Et_2O/pentane, 1:9) to afford geranyl *tert*-butyl carbonate **91** (2.73 g, 10.7 mmol, 83%) as a colourless oil.

^{1}H NMR (600 MHz, $CDCl_3$): δ = 5.37 (tq, J = 7.1, 1.3 Hz, 1H), 5.08 (tt, J = 6.9, 1.4 Hz, 1H), 4.58 (dd, J = 7.2, 0.7 Hz, 2H), 2.11 – 2.08 (m, 2H), 2.05 – 2.02 (m, 2H), 1.70 (s, 3H), 1.68 (d, J = 1.4 Hz, 3H), 1.59 (s, 3H), 1.48 (s, 9H) ppm.

^{13}C NMR (151 MHz, $CDCl_3$): δ = 153.8, 142.7, 132.0, 123.9, 118.2, 82.0, 63.9, 39.7, 28.0, 26.4, 25.8, 17.8, 16.6 ppm.

The spectroscopic data are in accordance with the literature.[59]

***tert*-Butyl (3,7-dimethylocta-1,6-dien-3-yl) carbonate (86)**

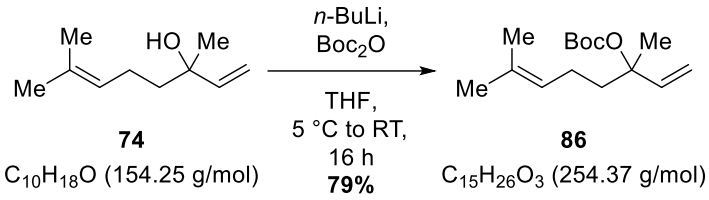

The Boc-substitution of linalool (**74**) was performed according to a literature-known procedure.[59] In a SCHLENK tube, linalool (**74**, 2.32 mL, 2.00 g, 13.0 mmol, 1.00 equiv.) was dissolved in anhydrous THF (50 mL). The solution was cooled down to 5 °C using an ice-water bath. Afterwards, *n*-BuLi (2.50 M in hexane, 5.71 mL, 14.3 mmol, 1.10 equiv.) was added over 1 h using a syringe pump. Then, Boc_2O (2.78 mL, 2.83 g, 13.0 mmol, 1.00 equiv.) was added and the mixture was allowed to warm up to RT over 16 h. The reaction was stopped by addition of sat. aq. $NaHCO_3$ (50 mL). The mixture was extracted with EtOAc (3 x 100 mL). The combined organic layers were dried over Na_2SO_4, filtered, and concentrated under reduced pressure. The crude product was purified by column chromatography (SiO_2, Et_2O/pentane, 1:9) to afford linalyl *tert*-butyl carbonate **86** (2.60 g, 10.2 mmol, 79%) as a colourless oil.

^{1}H NMR (600 MHz, $CDCl_3$): δ = 6.02 (dd, J = 17.6, 11.0 Hz, 1H), 5.18 – 5.14 (m, 2H), 5.08 (tt, J = 7.2, 1.4 Hz, 1H), 2.01 – 1.97 (m, 2H), 1.87 – 1.78 (m, 2H), 1.67 (s, 3H), 1.59 (s, 3H), 1.53 (s, 3H), 1.46 (s, 9H) ppm.

^{13}C NMR (151 MHz, $CDCl_3$): δ = 152.0, 141.8, 132.1, 123.8, 113.7, 83.7, 81.5, 39.6, 28.0, 25.8, 23.5, 22.5, 17.7 ppm.

The spectroscopic data are in accordance with the literature.[59]

5.4 Linear Route to Key-Intermediate 38 (Reproduced (adapted) from Ref.[83] with permission from the Royal Society of Chemistry.)

4-Acetyl-6-(3,7-dimethylocta-2,6-dien-1-yl)-5-hydroxy-2,2,6-trimethylcyclohex-4-ene-1,3-dione (90)

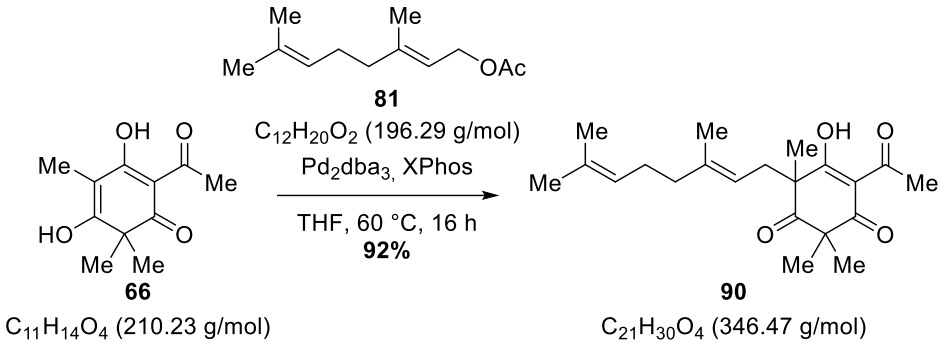

A SCHLENK flask was loaded with trimethylated acetyl-phloroglucinol **66** (11.8 g, 56.0 mmol, 1.00 equiv.), $Pd_2(dba)_3$ (1.28 g, 1.40 mmol, 2.5 mol%), and XPhos (2.67 g, 5.60 mmol, 10 mol%). The flask was evacuated and backfilled with argon three times. Afterwards, anhydrous THF (500 mL) and geranyl acetate (**81**, 18.1 mL, 16.5 g, 84.1 mmol, 1.50 equiv.) were added subsequently and the mixture was heated to 60 °C. After stirring at this temperature for 16 h, the mixture was allowed to cool down to RT and filtered through a plug of silica. The silica was thoroughly rinsed with CH_2Cl_2. The filtrate was concentrated under reduced pressure and the crude product was purified by column chromatography (SiO_2, EtOAc:pentane/2% to 5%) to afford geranylated acetyl phloroglucinol **90** (17.8 g, 51.4 mmol, 92%) as a yellowish oil.

The product was isolated as a mixture of two interconverting tautomers (tautomer A : tautomer B = 1:0.7) which gave two sets of signals in the ^{1}H- and ^{13}C-NMR in which many signals overlapped.

Tautomer A:

^{1}H NMR (600 MHz, $CDCl_3$): δ = 18.23 (s, 1H), 4.98 – 4.95 (m, 1H), 4.75 – 4.71 (m, 1H), 2.70 – 2.66 (m, 1H), 2.57 (s, 3H), 2.50 – 2.47 (m, 1H), 1.95 – 1.82 (m, 4H), 1.62 (s, 3H), 1.53 (s, 3H), 1.48 (s, 3H), 1.43 (s, 3H), 1.28 (s, 3H), 1.26 (s, 3H) ppm.

^{13}C NMR (151 MHz, $CDCl_3$): δ = 210.3, 201.8, 197.9, 196.6, 140.8, 131.7, 123.9, 117.3, 111.3, 57.1, 56.2, 39.9, 38.7, 27.8, 26.5, 26.2, 25.7, 22.6, 20.6, 17.7, 16.2 ppm.

Tautomer B

^{1}H NMR (600 MHz, $CDCl_3$): δ = 18.19 (s, 1H), 4.98 – 4.95 (m, 1H), 4.79 – 4.76 (m, 1H), 2.59 – 2.55 (m, 1H), 2.57 (s, 3H), 2.42 – 2.39 (m, 1H), 1.95 – 1.82 (m, 4H), 1.62 (s, 3H), 1.53 (s, 3H), 1.51 (s, 3H), 1.40 (s, 3H), 1.38 (s, 3H), 1.30 (s, 3H) ppm.

^{13}C NMR (151 MHz, $CDCl_3$): δ = 210.0, 201.5, 199.3, 196.5, 139.6, 131.7, 123.9, 118.0, 110.7, 60.9, 52.2, 39.9, 38.2, 27.5, 26.6, 26.4, 25.7, 22.0, 21.2, 17.7, 16.3 ppm.

HRMS (ESI, pos.): *m/z* calcd for $C_{21}H_{31}O_4^+$ $[M+H^+]^+$: 347.2217, found 347.2216.

IR (ATR): $\tilde{\nu}$ = 2979, 2927, 2874, 1717, 1667, 1555, 1426, 1378, 1360, 1326, 1288, 1234, 1178, 1128, 1108, 1027, 955, 932, 863, 834, 804, 781, 741 cm^{-1}.

4-Acetyl-6-(6-chloro-3,7-dimethylocta-2,7-dien-1-yl)-5-hydroxy-2,2,6-trimethylcyclohex-4-ene-1,3-dione (102)

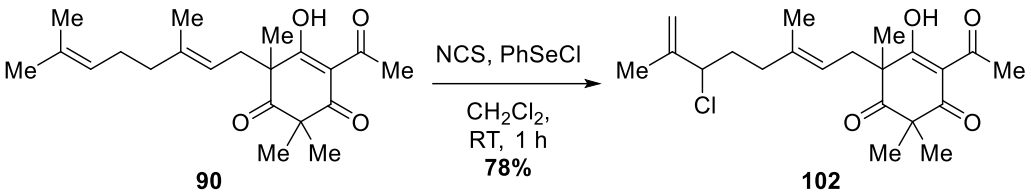

90
$C_{21}H_{30}O_4$ (346.47 g/mol)

102
$C_{21}H_{29}ClO_4$ (380.91 g/mol)

In a SCHLENK flask, geranyl acetyl phloroglucinol **90** (50.0 mg, 0.144 mmol, 1.00 equiv.) was dissolved in anhydrous CH_2Cl_2 (1.5 mL). PhSeCl (2.76 mg, 0.0144 mmol, 10 mol%) and NCS (21.2 mg, 0.159 mmol, 1.10 equiv.) were added and the mixture was stirred for 1 h at RT. Afterwards, the mixture was concentrated under reduced pressure. The residue was diluted with Et_2O (10 mL) and washed with water (3 x 10 mL), brine (3 x 10 mL), dried over Na_2SO_4, filtered, and concentrated under reduced pressure. The crude product was purified by column chromatography (SiO_2, EtOAc/pentane, 1:19) to afford allylic chloride **102** (43.0 mg, 0.113 mmol, 78%) as a yellowish oil.

The product was isolated as a mixture of two diastereomers which were also interconverting tautomers. Therefore, there are four sets of signals in the ^{1}H- and ^{13}C-NMR. As a result of this, many signals are overlapping which makes a distinguishment between the different sets very complicated. The signals are given without assignment.

^{1}H NMR (600 MHz, $CDCl_3$): δ = 18.27 – 18.23 (m, 2H), 4.98 – 4.96 (m, 2H), 4.87 – 4.78 (m, 4H), 4.27 – 4.19 (m, 2H), 2.73 – 2.60 (m, 2H), 2.60 – 2.59 (m, 6H), 2.55 – 2.42 (m, 2H), 2.03 – 1.78 (m, 8H), 1.77 (brs, 6H), 1.55 (s, 3H), 1.51 (s, 3H), 1.46 (s, 3H), 1.42 – 1.41 (m, 6H), 1.33 – 1.32 (m, 3H), 1.32 (brs, 3H), 1.29 – 1.28 (m, 3H) ppm.

^{13}C NMR (151 MHz, $CDCl_3$): δ = 210.3, 210.2, 209.9, 209.9, 202.0, 201.9, 201.7, 199.4, 199.4, 197.9, 197.9, 196.6, 196.6, 196.3, 196.3, 144.4, 144.3, 139.3, 139.1, 138.0, 119.4, 118.8, 118.6, 114.4, 114.4, 114.4, 114.3, 111.3, 110.6, 110.6, 66.2, 66.1, 66.1, 60.9, 60.9, 57.3, 57.2, 56.2, 56.2, 52.2, 52.1, 38.4, 38.4, 37.6, 37.6, 36.9, 36.9, 34.7, 34.7, 34.6, 32.1, 32.0, 29.8, 27.8, 27.8, 27.7, 26.3, 26.3, 26.3, 26.3, 23.0, 22.9, 22.4, 22.3, 21.7, 21.6, 20.7, 20.6, 17.1, 17.1, 16.3, 16.2, 16.2 ppm.

4-Cinnamoyl-6-(3,7-dimethylocta-2,5,7-trien-1-yl)-5-hydroxy-2,2,6-trimethylcyclohex-4-ene-1,3-dione (34)

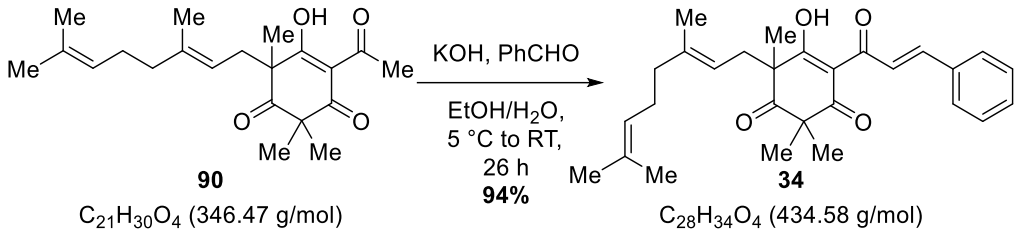

In a round-bottom flask, geranylated acyl phloroglucinol **90** (17.8 g, 51.4 mmol, 1.00 equiv.) and freshly distilled benzaldehyde (20.8 mL, 21.8 g, 206 mmol, 4.00 equiv.) were dissolved in EtOH (175 mL). The mixture was cooled down to 5 °C using an ice/water-bath and a solution of KOH (7 M, 176 mL) mixed with EtOH (75 mL) was added dropwise through a dropping funnel. After complete addition, the mixture was allowed to warm up to RT and stirred for 18 h. Afterwards, more benzaldehyde (10.4 mL, 10.9 g, 103 mmol, 2.00 equiv.) was added and stirring was continued. After 8 h, crude ^{1}H-NMR indicated complete consumption of the starting material. The mixture was cooled down to 5 °C using an ice/water-bath and a sat. aq. NH_4Cl (500 mL) was added dropwise through the dropping funnel. The mixture was extracted with cyclohexane (3 x 300 mL). The combined organic layers were dried over Na_2SO_4, filtered, and concentrated under reduced pressure. The residue was dried while stirring under high vacuum for 3 h to remove parts of the excess benzaldehyde. The crude product was purified by column chromatography (SiO_2, EtOAc:pentane/1:9). After purification, remaining traces of benzaldehyde were removed by stirring under high vacuum at 40 °C overnight to afford cinnamoyl phloroglucinol **34** (20.9 g, 48.2 mmol, 94%) as an orange, viscous oil.

The product was isolated as a mixture of two interconverting tautomers (tautomer A : tautomer B = 1:0.8) which gave two sets of signals in the ^{1}H- and ^{13}C-NMR in which many signals overlapped.

Tautomer A:

^{1}H NMR (600 MHz, $CDCl_3$): δ = 18.38 (s, 1H), 8.05 – 7.97 (m, 2H), 7.67 – 7.65 (m, 2H), 7.42 – 7.39 (m, 3H), 5.00 – 4.95 (m, 1H), 4.83 – 4.79 (m, 1H), 2.70 – 2.67 (m, 1H), 2.53 – 2.49 (m, 2H), 1.96 – 1.90 (m, 2H), 1.88 – 1.84 (m, 2H), 1.62 (s, 3H), 1.53 (s, 3H), 1.51 (s, 3H), 1.46 (s, 3H), 1.35 (s, 3H), 1.34 (s, 3H) ppm.

^{13}C NMR (151 MHz, $CDCl_3$): δ = 210.2, 201.8, 197.3, 186.3, 146.7, 140.8, 134.9, 131.7, 131.3, 129.2, 129.1, 124.0, 121.5, 117.3, 110.1, 57.9, 57.8, 39.9, 39.0, 26.6, 26.5, 25.7, 21.9, 20.7, 17.7, 16.3 ppm.

Tautomer B:

^{1}H NMR (600 MHz, $CDCl_3$): δ = 18.11 (s, 1H), 8.05 – 7.97 (m, 2H), 7.67 – 7.65 (m, 2H), 7.42 – 7.39 (m, 3H), 5.00 – 4.95 (m, 1H), 4.88 – 4.85 (m, 1H), 2.65 – 2.61 (m, 1H), 2.46 – 2.42 (m, 2H), 1.96 – 1.90 (m, 2H), 1.88 – 1.84 (m, 2H), 1.63 (s, 3H), 1.51 (s, 6H), 1.44 (s, 3H), 1.40 (s, 3H), 1.38 (s, 3H) ppm.

^{13}C NMR (151 MHz, $CDCl_3$): δ = 209.8, 202.7, 197.4, 185.7, 146.7, 139.8, 134.9, 131.7, 131.3, 129.2, 129.1, 124.0, 121.2, 117.8, 109.8, 61.4, 54.1, 39.9, 38.5, 26.6, 26.2, 25.7, 21.3, 21.0, 17.7, 16.4 ppm.

HRMS (ESI, pos.): *m/z* calcd for $C_{28}H_{34}NaO_4^+$ $[M+Na^+]^+$: 457.2349, found 457.2344.

IR (ATR): $\tilde{\nu}$ = 3101, 3058, 2979, 2920, 2878, 2857, 1717, 1665, 1620, 1577, 1518, 1448, 1412, 1378, 1326, 1268, 1209, 1180, 1157, 1108, 1069, 1027, 979, 959, 945, 873, 851, 836, 793, 752 cm^{-1}.

2-(6-Chloro-3,7-dimethylocta-2,7-dien-1-yl)-4-cinnamoyl-5-hydroxy-2,6,6-trimethylcyclohex-4-ene-1,3-dione (103)

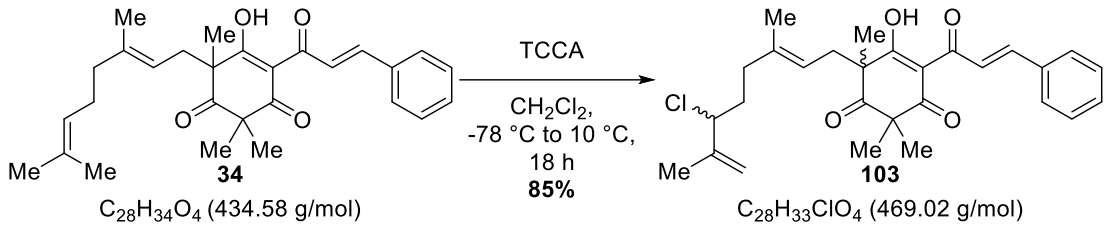

$C_{28}H_{34}O_4$ (434.58 g/mol) $C_{28}H_{33}ClO_4$ (469.02 g/mol)

Gram-scale:

In a SCHLENK flask geranylated Champanone B **34** (20.9 g, 48.1 mmol, 1.00 equiv.) was dissolved in anhydrous CH_2Cl_2 (500 mL) and the mixture was cooled down to –78 °C using a dry ice/isopropanol bath. Then, trichloroisocyanuric acid (TCCA, 5.15 g, 22.2 mmol, 0.46 equiv.) was added and the mixture was allowed to warm up to 10 °C over 18 h. Afterwards, the mixture was diluted with pentane (500 mL) and filtered through a plug of silica. The silica was thoroughly rinsed with EtOAc:pentane/1:9. The filtrate was concentrated under reduced pressure and the crude product was purified by column chromatography (SiO_2, Et_2O:pentane/1:19) to afford allylic chloride **103** (11.2 g, 23.9 mmol, 50%) as a yellow oil.

Milligram-scale:

According to the above described procedure geranylated Champanone B **34** (98.0 mg, 226 µmol, 1.00 equiv.) was reacted with trichloroisocyanuric acid (TCCA, 24.1 mg, 104 µmol, 0.46 equiv.) in anhydrous CH_2Cl_2 (2.3 mL). The mixture was diluted with pentane and filtered through a plug of silica which was rinsed with EtOAc:pentane/1:9 until all of the yellow colour was washed out of the silica to afford the pure allylic chloride **103** (90.0 mg, 192 µmol, 85%) as a yellow oil.

The product was isolated as a mixture of two diastereomers which were also interconverting tautomers. Therefore, there are four sets of signals in the ^{1}H- and ^{13}C-NMR. As a result of this, many signals are overlapping which makes a distinguishment between the different sets very complicated. The signals are given without assignment.

^{1}H NMR (600 MHz, $CDCl_3$): δ = 18.34 – 18.11 (m, 1H), 8.04 – 7.99 (m, 2H), 7.67 – 7.65 (m, 2H), 7.43 – 7.41 (m, 3H), 4.96 – 4.93 (m, 1H), 4.92 – 4.83 (m, 1H), 4.83 – 4.79 (m, 1H), 4.25 – 4.20 (m, 1H), 2.71 – 2.60 (m, 1H), 2.54 – 2.42 (m, 1H), 2.01 – 1.95 (m, 1H), 1.91 – 1.85 (m, 1H), 1.84 – 1.75 (m, 2H), 1.74 – 1.71 (m, 3H), 1.52 (s, 3H), 1.47 – 1.44 (m, 3H), 1.41 – 1.38 (m, 3H), 1.36 – 1.34 (m, 3H) ppm.

^{13}C NMR (176 MHz, $CDCl_3$): δ = 210.1, 210.1, 209.7, 209.7, 202.7, 201.8, 201.8, 197.3, 197.2, 197.2, 197.1, 186.3, 186.2, 185.8, 185.8, 146.9, 146.9, 146.9, 144.3, 144.3, 144.3, 139.3, 139.3, 138.2, 134.8, 134.8, 131.4, 131.3, 129.3, 129.2, 129.2, 129.2, 129.2, 129.2, 129.1, 129.1, 121.4, 121.4, 121.1, 121.1, 119.1, 119.0, 118.6, 118.6, 114.4, 114.3, 114.3, 110.1, 109.6, 109.6, 66.2, 66.2, 66.1, 57.9, 57.8, 57.8, 54.1, 54.1, 38.7, 38.7, 38.0, 38.0, 37.0, 36.9, 36.9, 34.7, 34.7, 34.6, 26.5, 26.5, 26.3, 26.3, 22.2, 22.1, 21.5, 21.5, 21.2, 21.2, 20.7, 17.1, 17.0, 16.3, 16.2 ppm.

HRMS (ESI, pos.): *m/z* calcd for $C_{28}H_{33}ClNaO_4^+$ $[M+Na^+]^+$: 491.1959, found 491.1966.

IR (ATR): $\tilde{\nu}$ = 3101, 3058, 2979, 2920, 2878, 2857, 1717, 1665, 1620, 1577, 1518, 1448, 1412, 1378, 1326, 1268, 1209, 1180, 1157, 1108, 1069, 1027, 979, 959, 945, 873, 851, 836, 793, 752 cm^{-1}.

4-Cinnamoyl-2-(3,7-dimethylocta-2,5,7-trien-1-yl)-5-hydroxy-2,6,6-trimethylcyclohex-4-ene-1,3-dione (38)

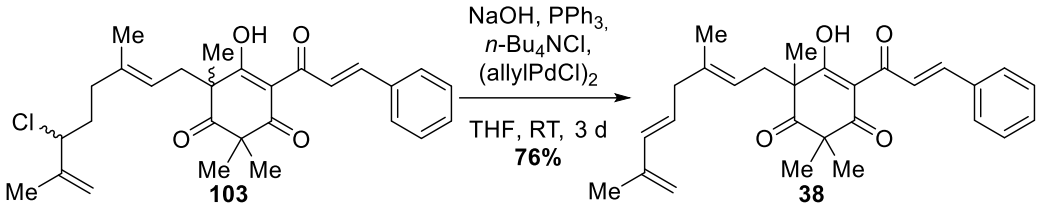

$C_{28}H_{33}ClO_4$ (469.02 g/mol) $C_{28}H_{32}O_4$ (432.56 g/mol)

A SCHLENK flask was loaded with freshly ground NaOH (2.34 g, 58.6 mmol, 2.50 equiv.), PPh_3 (308 mg, 1.17 mmol, 5 mol%), and allylpalladium chloride dimer (85.8 mg, 235 µmol, 1 mol%). The flask was evacuated and backfilled with argon three times. Afterwards, anhydrous THF (40 mL) and an anhydrous THF solution of tetrabutylammonium chloride (40 mM, 16.8 mL, 704 µmol, 3 mol%) were added subsequently. The mixture was stirred vigorously and a solution of allylic chloride **103** (11.0 g, 23.5 mmol, 1.00 equiv.) in anhydrous THF (50 mL) was added slowly while keeping the mixture at 20 °C using a water bath. Then, the mixture was stirred at RT for 3 d. Afterwards, water (100 mL) was added and the mixture was extracted with EtOAc (3 x 100 mL). The combined organic layers were washed with water, brine, dried over Na_2SO_4, filtered, and concentrated under reduced pressure. The crude product was purified by column chromatography (SiO_2, EtOAc:cyclohexane/1:9) to afford diene **38** (7.74 g, 17.8 mmol, 76%) as a yellow oil.

The product was isolated as a mixture of two interconverting tautomers (tautomer A : tautomer B = 1:0.75) which gave two sets of signals in the ^{1}H- and ^{13}C-NMR in which many signals overlapped.

Tautomer A:

^{1}H NMR (600 MHz, $CDCl_3$): δ = 18.42 (s, 1H), 8.04 – 7.98 (m, 2H), 7.67 – 7.65 (m, 2H), 7.43 – 7.40 (m, 3H), 6.05 – 6.00 (m, 1H), 5.46 – 5.40 (m, 1H), 4.90 – 4.80 (m, 3H), 2.73 – 2.66 (m, 1H), 2.64 – 2.61 (m, 2H), 2.54 – 2.44 (m, 1H), 1.75 (s, 3H), 1.51 (s, 3H), 1.48 (s, 3H), 1.35 (s, 3H), 1.33 (s, 3H) ppm.

^{13}C NMR (151 MHz, $CDCl_3$): δ = 210.3, 201.7, 197.2, 186.4, 146.8, 142.0, 139.7, 134.9, 134.8, 131.3, 129.2, 129.1, 127.7, 121.5, 118.3, 115.0, 110.3, 58.0, 57.6, 43.0, 39.2, 26.4, 22.3, 20.3, 18.7, 16.5 ppm.

Tautomer B:

^{1}H NMR (600 MHz, $CDCl_3$): δ = 18.12 (s, 1H), 8.04 – 7.98 (m, 2H), 7.67 – 7.65 (m, 2H), 7.43 – 7.40 (m, 3H), 6.05 – 6.00 (m, 1H), 5.46 – 5.40 (m, 1H), 4.90 – 4.80 (m, 3H), 2.73 – 2.66 (m, 1H), 2.64 – 2.61 (m, 2H), 2.54 – 2.44 (m, 1H), 1.74 (s, 3H), 1.51 (s, 3H), 1.42 (s, 3H), 1.40 (s, 6H) ppm.

^{13}C NMR (151 MHz, $CDCl_3$): δ = 210.0, 202.7, 197.4, 185.7, 146.8, 141.9, 138.6, 134.9, 134.8, 131.3, 129.2, 129.2, 127.6, 121.2, 118.9, 115.1, 109.9, 61.1, 54.3, 43.0, 38.6, 26.6, 21.6, 21.1, 18.7, 16.6 ppm.

HRMS (ESI, pos.): *m/z* calcd for $C_{28}H_{32}NaO_4^+$ $[M+Na^+]^+$: 455.2193, found 455.2201.

IR (ATR): $\tilde{\nu}$ = 3101, 3082, 3024, 2980, 2931, 2871, 2853, 1717, 1666, 1620, 1577, 1519, 1449, 1415, 1380, 1327, 1305, 1266, 1209, 1181, 1158, 1118, 1026, 966, 946, 884, 854, 839, 794, 752 cm^{-1}.

5.5 Convergent Route to Key-Intermediate 38 (Reproduced (adapted) from Ref.[83] with permission from the Royal Society of Chemistry.)

4-Acetyl-6-(3,7-dimethylocta-2,5,7-trien-1-yl)-5-hydroxy-2,2,6-trimethylcyclohex-4-ene-1,3-dione (95)

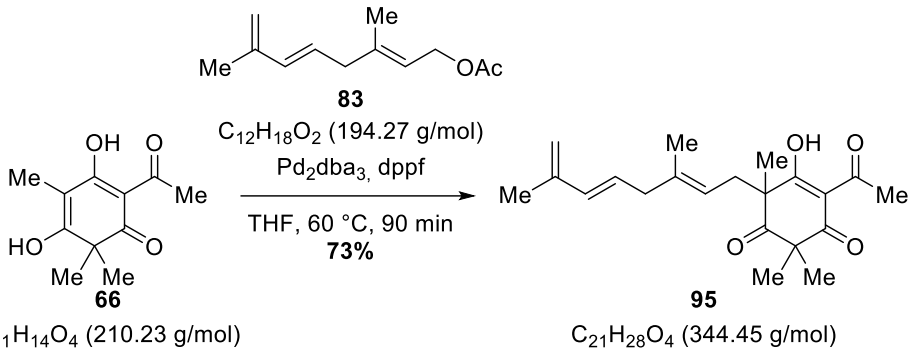

A SCHLENK flask was loaded with trimethylated acetyl-phloroglucinol **66** (5.80 g, 27.6 mmol, 1.00 equiv.), $Pd_2(dba)_3$ (632 mg, 690 µmol, 2.5 mol%), and dppf (765 mg, 1.38 mmol, 5 mol%). The flask was evacuated and backfilled with argon three times. Afterwards, anhydrous THF (200 mL) and allylic acetate **83** (8.04 g, 41.4 mmol, 1.50 equiv.) were added subsequently and the mixture was heated to 60 °C. After stirring at this temperature for 90 min, the mixture was allowed to cool down to RT and filtered through a plug of silica. The silica was thoroughly rinsed with EtOAc. The filtrate was concentrated under reduced pressure and the crude product was purified by column chromatography (SiO_2, Et_2O/pentane, 1:19 to 1:9) to afford diene **95** (6.90 g, 20.0 mmol, 73%) as a yellowish oil.

The product was isolated as a mixture of two interconverting tautomers (tautomer A : tautomer B = 1:0.7) which gave two sets of signals in the ^{1}H- and ^{13}C-NMR in which many signals overlapped.

Tautomer A:

^{1}H NMR (600 MHz, CD_2Cl_2): δ = 18.23 (s, 1H), 6.08 – 6.04 (m, 1H), 5.51 – 5.43 (m, 1H), 4.88 – 4.78 (m, 3H), 2.73 – 2.58 (m, 3H), 2.56 (s, 3H), 2.53 – 2.41 (m, 1H), 1.80 (s, 3H), 1.50 (s, 3H), 1.45 (s, 3H), 1.29 (s, 3H), 1.24 (s, 3H) ppm.

^{13}C NMR (151 MHz, CD_2Cl_2): δ = 210.5, 202.2, 197.9, 196.6, 142.5, 139.8, 134.9, 128.1, 118.7, 115.0, 111.7, 57.6, 56.3, 43.2, 39.0, 27.8, 26.4, 23.0, 20.4, 18.8, 16.5 ppm.

Tautomer B

^{1}H NMR (600 MHz, CD_2Cl_2): δ = 18.20 (s, 1H), 6.08 – 6.04 (m, 1H), 5.51 – 5.43 (m, 1H), 4.88 – 4.78 (m, 3H), 2.73 – 2.58 (m, 3H), 2.56 (s, 3H), 2.53 – 2.41 (m, 1H), 1.79 (s, 3H), 1.53 (s, 3H), 1.39 (s, 6H), 1.31 (s, 3H) ppm.

^{13}C NMR (151 MHz, CD_2Cl_2): δ = 210.2, 201.7, 199.6, 196.5, 142.4, 138.6, 134.9, 128.2, 119.4, 115.1, 111.1, 60.9, 52.5, 43.2, 38.4, 27.6, 26.6, 22.0, 21.6, 18.8, 16.5 ppm.

HRMS (ESI, pos.): *m/z* calcd for $C_{21}H_{28}NaO_4^+$ $[M+Na^+]^+$: 367.1880, found 367.1896.

IR (ATR): $\tilde{\nu}$ = 3082, 2976, 2936, 2874, 2853, 1739, 1718, 1670, 1607, 1556, 1453, 1434, 1381, 1364, 1323, 1229, 1177, 1124, 1025, 966, 928, 882, 861, 836, 794, 779, 743, 722 cm^{-1}.

4-Cinnamoyl-6-(3,7-dimethylocta-2,5,7-trien-1-yl)-5-hydroxy-2,2,6-trimethylcyclohex-4-ene-1,3-dione (38)

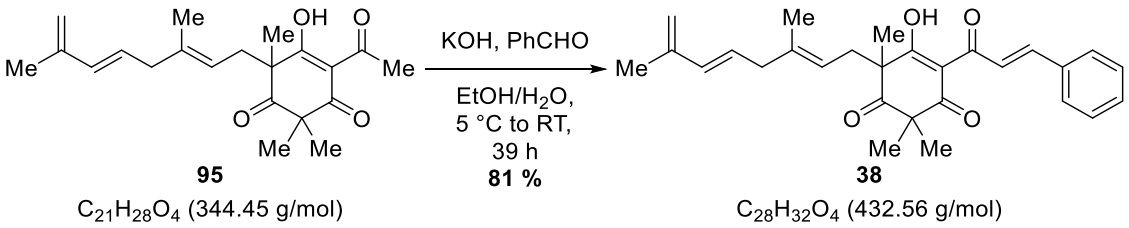

95
$C_{21}H_{28}O_4$ (344.45 g/mol)

38
$C_{28}H_{32}O_4$ (432.56 g/mol)

In a round-bottom flask, a mixture of aq. KOH (7 M, 15 mL, 24.0 equiv.) and EtOH (15 mL) was cooled down to 5 °C using an ice-water bath. Acetyl phloroglucinol **95** (1.70 g, 4.94 mmol, 1.00 equiv.) and benzaldehyde (1.00 mL, 1.05 g, 9.87 mmol, 2.00 equiv.) dissolved in EtOH (15 mL) were added slowly. Then, the mixture was allowed to warm up to RT. After stirring the mixture at this temperature for 16 h, more benzaldehyde (1.00 mL, 1.05 g, 9.87 mmol, 2.00 equiv.) was added. Stirring was continued for 7 h. Then, more benzaldehyde (1.00 mL, 1.05 g, 9.87 mmol, 2.00 equiv.) was added. After another 16 h the starting material was consumed completely. The mixture was poured into ice-cold sat. aq. NH_4Cl (100 mL) and extracted with EtOAc (3 x 100 mL). The combined organic layers were washed with water (100 mL) and brine (100 mL), dried over Na_2SO_4, filtered, and concentrated under reduced pressure. The residue was dried while stirring under high vacuum for 3 h to remove parts of the excess benzaldehyde. The crude product was purified by column chromatography (SiO_2, Et_2O/pentane, 1:19). After purification, the product was once more dried while stirring under high vacuum over night to remove the remaining traces of benzaldehyde to afford cinnamoyl phloroglucinol **38** (1,73 g, 4.00 mmol, 81%) as a yellow, thick oil.

The product was isolated as a mixture of two interconverting tautomers (tautomer A : tautomer B = 1:0.75) which gave two sets of signals in the ^{1}H- and ^{13}C-NMR in which many signals overlapped.

Tautomer A:

^{1}H NMR (600 MHz, $CDCl_3$): δ = 18.42 (s, 1H), 8.04 – 7.98 (m, 2H), 7.67 – 7.65 (m, 2H), 7.43 – 7.40 (m, 3H), 6.05 – 6.00 (m, 1H), 5.46 – 5.40 (m, 1H), 4.90 – 4.80 (m, 3H), 2.73 – 2.66 (m, 1H), 2.64 – 2.61 (m, 2H), 2.54 – 2.44 (m, 1H), 1.75 (s, 3H), 1.51 (s, 3H), 1.48 (s, 3H), 1.35 (s, 3H), 1.33 (s, 3H) ppm.

^{13}C NMR (151 MHz, $CDCl_3$): δ = 210.3, 201.7, 197.2, 186.4, 146.8, 142.0, 139.7, 134.9, 134.8, 131.3, 129.2, 129.1, 127.7, 121.5, 118.3, 115.0, 110.3, 58.0, 57.6, 43.0, 39.2, 26.4, 22.3, 20.3, 18.7, 16.5 ppm.

Tautomer B:

^{1}H NMR (600 MHz, $CDCl_3$): δ = 18.12 (s, 1H), 8.04 – 7.98 (m, 2H), 7.67 – 7.65 (m, 2H), 7.43 – 7.40 (m, 3H), 6.05 – 6.00 (m, 1H), 5.46 – 5.40 (m, 1H), 4.90 – 4.80 (m, 3H), 2.73 – 2.66 (m, 1H), 2.64 – 2.61 (m, 2H), 2.54 – 2.44 (m, 1H), 1.74 (s, 3H), 1.51 (s, 3H), 1.42 (s, 3H), 1.40 (s, 6H) ppm.

^{13}C NMR (151 MHz, $CDCl_3$): δ = 210.0, 202.7, 197.4, 185.7, 146.8, 141.9, 138.6, 134.9, 134.8, 131.3, 129.2, 129.2, 127.6, 121.2, 118.9, 115.1, 109.9, 61.1, 54.3, 43.0, 38.6, 26.6, 21.6, 21.1, 18.7, 16.6 ppm.

HRMS (ESI, pos.): *m/z* calcd for $C_{28}H_{32}NaO_4^+$ $[M+Na^+]^+$: 455.2193, found 455.2201.

IR (ATR): $\tilde{\nu}$ = 3101, 3082, 3024, 2980, 2931, 2871, 2853, 1717, 1666, 1620, 1577, 1519, 1449, 1415, 1380, 1327, 1305, 1266, 1209, 1181, 1158, 1118, 1026, 966, 946, 884, 854, 839, 794, 752 cm^{-1}.

5.6 Intramolecular DIELS-ALDER Cycloaddition and Backbone Oxidation (Reproduced (adapted) from Ref.[83] with permission from the Royal Society of Chemistry.)

IMDA-diastereomers 105 and 37

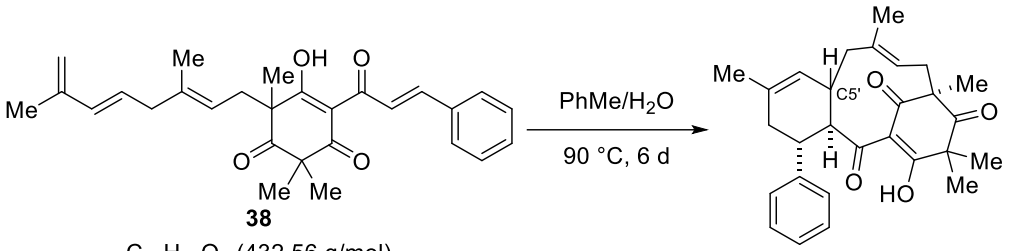

38

$C_{28}H_{32}O_4$ (432.56 g/mol)

5'*S** = **105** (**20%**)
5'*R** = **37** (**26%**)
$C_{28}H_{32}O_4$ (432.56 g/mol)

In a two-necked round-bottom flask equipped with a reflux condenser, diene **38** (7.70 g, 17.8 mmol, 1.00 equiv.) was dissolved in toluene (500 mL). Water (500 mL) was added and the mixture was degassed by bubbling through a stream of argon while stirring vigorously for 5 h. Afterwards, the mixture was heated to 90 °C for 6 d. After allowing the mixture to cool down to RT, the phases were separated and the aqueous phase was extracted with EtOAc (3 x 100 mL). The combined organic layers were washed with brine, dried over Na_2SO_4, filtered, and concentrated under reduced pressure. Pentane was added to the residue and the mixture was filtered. The solids were collected, cyclohexane was added, and the suspension was sonicated for 30 min. The mixture was filtered again and the solid was dried in the high vacuum to afford diastereomer **37** (2.00 g, 4.64 mmol, 26%) as a white, amorphous solid. The filtrate of the second filtration was concentrated under reduced pressure, pentane was added, and the suspension was sonicated for 10 min. The solid was filtered off and dried in the high vacuum to afford diastereomer **105** (1.55 g, 3.58 mmol, 20%) as a white, amorphous solid.

Analytical data for compound **105**:

^{1}H NMR (600 MHz, $CDCl_3$): δ = 17.50 (s, 1H), 7.40 – 7.39 (m, 2H), 7.19 – 7.16 (m, 2H), 7.08 – 7.05 (m, 1H), 5.20 – 5.18 (m, 1H), 5.00 – 4.97 (m, 1H), 3.44 (dd, *J* = 11.0, 9.8 Hz, 1H), 3.19 (td, *J* = 11.7, 4.4 Hz, 1H), 3.12 – 3.06 (m, 1H), 2.41 – 2.34 (m, 1H), 2.33 – 2.29 (m, 1H), 2.19 (dd, *J* = 13.8, 12.1 Hz, 1H), 2.14 – 2.10 (m, 1H), 1.99 – 1.95 (m, 1H), 1.80 (t, *J* = 12.5 Hz, 1H), 1.72 (s, 3H), 1.40 (s, 3H), 1.34 (s, 3H), 1.33 (s, 3H), 0.98 (s, 3H) ppm.

^{13}C NMR (151 MHz, $CDCl_3$): δ = 206.3, 202.6, 196.4, 195.8, 142.3, 140.5, 133.6, 128.9, 127.9, 126.4, 124.8, 120.1, 114.4, 60.5, 52.0, 49.0, 48.3, 46.0, 42.2, 38.6, 37.1, 28.2, 23.4, 20.0, 16.6, 15.5 ppm.

HRMS (ESI, pos.): *m/z* calcd for $C_{28}H_{32}KO_4^+$ $[M+K^+]^+$: 471.1933, found 471.1914.

IR (ATR): $\tilde{\nu}$ = 3029, 2979, 2913, 2878, 2850, 1722, 1684, 1539, 1495, 1454, 1387, 1376, 1361, 1345, 1310, 1217, 1162, 1141, 1103, 1082, 1025, 950, 923, 907, 897, 881, 840, 800, 753 cm^{-1}.

X-ray: Crystals were grown by the vapor diffusion technique of a solution of **105** in CH_2Cl_2 with *n*-pentane at ambient temperature.

Analytical data for compound **37**:

^{1}H NMR (600 MHz, $CDCl_3$): δ = 17.96 (s, 1H), 7.37 – 7.32 (m, 4H), 7.23 – 7.21 (m, 1H), 5.18 (brs, 1H), 4.59 – 4.56 (m, 1H), 3.55 – 3.54 (m, 1H), 3.38 – 3.36 (m, 1H), 2.86 – 2.83 (m, 1H), 2.81 – 2.76 (m, 1H), 2.38 (t, *J* = 12.7 Hz, 1H), 2.29 – 2.26 (m, 1H), 2.24 – 2.18 (m, 2H), 1.89 (s, 3H), 1.78 – 1.74 (m, 1H), 1.45 (s, 3H), 1.44 (s, 3H), 1.38 (s, 3H), 1.16 (s, 3H) ppm.

^{13}C NMR (151 MHz, $CDCl_3$): δ = 209.2, 201.3, 200.7, 194.7, 144.9, 134.8, 134.4, 128.5, 127.3, 126.5, 124.9, 123.4, 117.0, 59.1, 56.0, 43.4, 43.0, 39.5, 39.5, 32.1, 30.8, 28.2, 23.6, 22.9, 16.7, 14.2 ppm.

HRMS (ESI, pos.): *m/z* calcd for $C_{28}H_{32}NaO_4^+$ $[M+Na^+]^+$: 455.2193, found 455.2181.

IR (ATR): $\tilde{\nu}$ = 3062, 3024, 2979, 2906, 2852, 1722, 1675, 1541, 1495, 1466, 1450, 1370, 1360, 1316, 1296, 1268, 1216, 1180, 1153, 1081, 1068, 1030, 993, 958, 930, 881, 841, 756, 703 cm^{-1}.

X-ray: Crystals were grown by the vapor diffusion technique of a solution of **37** in CH_2Cl_2 with *n*-pentane at ambient temperature.

Epoxide 110

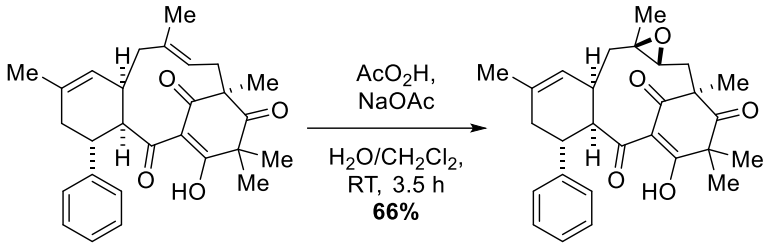

37
$C_{28}H_{32}O_4$ (432.56 g/mol)

110
$C_{28}H_{32}O_5$ (448.56 g/mol)

In a round-bottom flask, **37** (2.00 g, 4.64 mmol, 1.00 equiv.) was dissolved in CH_2Cl_2 (14 mL). 1 M aq. NaOAc (23 mL) was added to the mixture. Under vigorous stirring, acetic acid peroxide (35 w% in acetic acid, 2.95 mL, 3.33 g, 15.3 mmol, 3.33 equiv.) was added over 3.5 h. Afterwards, the mixture was cooled down to 5 °C using an ice/water-bath and sat. aq. $Na_2S_2O_3$ (50 mL) was added slowly under vigorously stirring. Then, the phases were separated and the aqueous phase was extracted with CH_2Cl_2 (3 x 20 mL). The combined organic layers were washed with sat. aq. $NaHCO_3$ (50 mL), water (50 mL), and brine (50 mL), dried over Na_2SO_4, filtered, and concentrated under reduced pressure. The crude product was purified by column chromatography (SiO_2, CH_2Cl_2) to afford epoxide **110** (1.38 g, 3.08 mmol, 66%) as a white, amorphous solid.

^{1}H NMR (600 MHz, $CDCl_3$): δ = 17.95 (s, 1H), 7.40 – 7.39 (m, 2H), 7.36 – 7.34 (m, 2H), 7.25 – 7.23 (m, 1H), 5.14 (s, 1H), 3.95 (d, *J* = 6.0 Hz, 1H), 3.45 (d, *J* = 6.6 Hz, 1H), 2.80 – 2.75 (m, 1H), 2.68 (d, *J* = 13.2 Hz, 1H), 2.30 – 2.27 (m, 1H), 2.21 – 2.19 (m, 1H), 2.14 – 2.10 (m, 1H), 1.97 (dd, *J* = 13.8, 5.1 Hz, 1H), 1.86 (s, 3H), 1.48 (s, 3H), 1.44 (s, 3H), 1.38 (s, 3H),1.35 – 1.34 (m, 1H), 0.85 (t, *J* = 13.8 Hz, 1H), 0.74 (s, 3H) ppm.

^{13}C NMR (151 MHz, $CDCl_3$): δ = 209.0, 200.0, 199.5, 199.1, 144.9, 134.7, 128.8, 127.5, 126.9, 123.4, 115.5, 64.3, 60.0, 58.6, 57.0, 42.7, 40.7, 39.7, 37.8, 33.2, 30.9, 28.1, 23.5, 23.2, 16.7, 16.1 ppm.

HRMS (ESI, neg.): *m/z* calcd for $C_{28}H_{31}O_5^-$ $[M\text{-}H^+]^-$: 447.2177, found 447.2169.

IR (ATR): $\tilde{\nu}$ = 3024, 2976, 2908, 2861, 1724, 1672, 1542, 1495, 1450, 1427, 1386, 1370, 1318, 1297, 1280, 1254, 1218, 1183, 1166, 1117, 1065, 1050, 1028, 990, 978, 967, 945, 926, 883, 865, 813, 753, 702 cm^{-1}.

(±)-Cleistocaltone A (23)

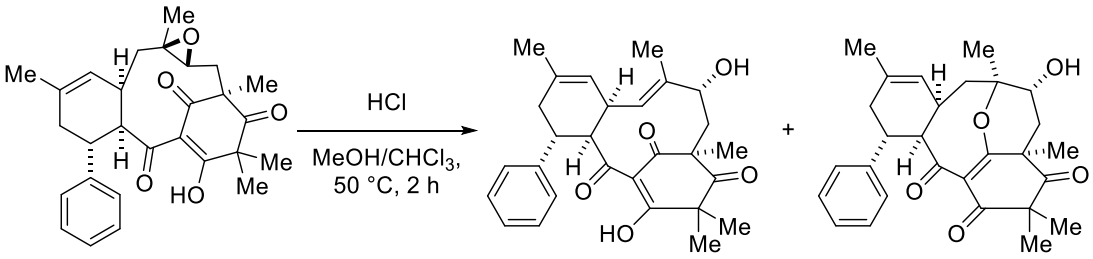

110
$C_{28}H_{32}O_5$ (448.56 g/mol)

23 (**33%**)
$C_{28}H_{32}O_5$ (448.56 g/mol)

111 (**9%**)
$C_{28}H_{32}O_5$ (448.56 g/mol)

In a two-necked round-bottom flask equipped with a dropping funnel, epoxide **110** (1.74 g, 4.02 mmol, 1.00 equiv.) was dissolved in $CHCl_3$ (150 mL). The reaction vessel was capped and the mixture was heated to 50 °C. HCl (1 w% in MeOH, 92.9 mL, 20.1 mmol, 5.00 equiv.) was added through the dropping funnel and the mixture was stirred for 2 h. Afterwards, the mixture was concentrated under reduced pressure. The crude product was purified by flash column chromatography (SiO_2, EtOAc/pentane, 1:4) to afford (±)-Cleistocaltone A (**23**) (587 mg, 1.30 mmol, 33%) as a white amorphous solid and side product **111** (162 mg, 361 µmol, 9%) as a white amorphous solid.

Analytical data of (±)-Cleistocaltone A (**23**):

^{1}H NMR (700 MHz, $CDCl_3$): δ = 16.46 (s, 1H), 7.33 – 7.31 (m, 2H), 7.24 – 7.22 (m, 1H), 7.21 – 7.20 (m, 2H), 5.09 – 5.08 (m, 1H), 4.85 (dd, *J* = 9.8, 1.6 Hz, 1H), 4.22 – 4.21 (m, 1H), 3.75 (dd, *J* = 11.4, 2.8 Hz, 1H), 3.48 – 3.46 (m, 1H), 3.06 – 3.02 (m, 2H), 2.50 (dd, *J* = 13.1, 2.8 Hz, 1H), 2.21 – 2.18 (m, 1H), 2.13 (dd, *J* = 13.2, 11.4 Hz, 1H), 1.81 (s, 3H), 1.50 (s, 3H), 1.47 (s, 3H), 1.32 (s, 3H), 1.18 (d, *J* = 1.4 Hz, 3H) ppm.

^{13}C NMR (151 MHz, $CDCl_3$): δ = 210.9, 207.1, 196.4, 187.3, 146.0, 138.2, 136.2, 131.5, 128.6, 127.4, 126.5, 120.3, 116.3, 75.0, 56.7, 51.0, 47.9, 45.2, 38.1, 32.3, 32.0, 28.8, 27.5, 23.7, 20.1, 8.9 ppm.

HRMS (ESI, pos.): *m/z* calcd for $C_{28}H_{32}NaO_5^+$ $[M+Na^+]^+$: 471.2142, found 471.2147.

IR (ATR): $\tilde{\nu}$ = 3474, 3394, 2924, 2851, 1716, 1659, 1568, 1495, 1451, 1402, 1378, 1243, 1102, 1031, 956, 864, 767, 737 cm^{-1}.

The spectroscopic data are in accordance with the literature (comparison in Table 19).[51]

Analytical data of sideproduct **111**:

^{1}H NMR (700 MHz, $CDCl_3$) δ = 7.30 – 7.28 (m, 2H), 7.22 – 7.20 (m, 1H), 7.16 – 7.15 (m, 2H), 5.04 (brs, 1H), 3.85 (brs, 1H), 3.59 (dd, *J* = 4.3, 2.2 Hz, 1H), 3.54 (dd, *J* = 5.4, 3.7 Hz, 1H), 2.72 – 2.68 (m, 1H), 2.46 – 2.44 (m, 1H), 2.34 (dd, *J* = 15.0, 2.2 Hz, 1H), 2.15 – 2.09 (m, 3H), 2.05 – 2.01 (m, 1H), 1.71 (s, 3H), 1.70 (s, 3H), 1.45 (s, 3H), 1.38 (dd, *J* = 15.1, 6.1 Hz, 1H), 1.27 (s, 3H), 1.25 (s, 3H) ppm.

^{13}C NMR (176 MHz, $CDCl_3$) δ = 210.6, 198.1, 195.0, 175.6, 145.5, 135.6, 128.5, 127.6, 127.4, 126.3, 123.7, 89.7, 70.5, 59.1, 56.1, 46.6, 39.0, 37.9, 36.7, 31.9, 27.7, 27.2, 23.9, 23.3, 19.2, 19.1 ppm.

HRMS (ESI, pos.): *m/z* calcd for $C_{28}H_{32}NaO_5^+$ $[M+Na^+]^+$: 471.2142, found 471.2157.

IR (ATR): $\tilde{\nu}$ = 3467, 2982, 2961, 2924, 2855, 1718, 1689, 1645, 1622, 1495, 1453, 1381, 1353, 1320, 1246, 1220, 1178, 1145, 1092, 1050, 1010, 992, 971, 940, 921, 902, 852, 822, 795, 754, 712, 702 cm^{-1}.

X-ray: Crystals were grown by slow evaporation of a solution of **111** in diethyl ether at ambient temperature. The compound crystallized with one diethyl ether molecule in the cell.

Table 19: Comparison of ^{1}H- and ^{13}C-NMR data for isolated and synthetic (±)-Cleistocaltone A (**23**).[a] (Reproduced (adapted) from Ref.[83] with permission from the Royal Society of Chemistry.)

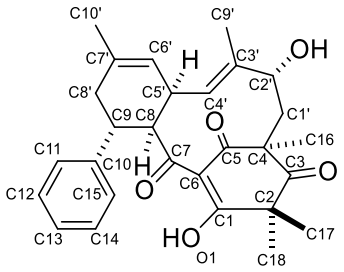

No.	**Isolation[b] ^{13}C NMR (125 MHz)** δ_C/ppm[c]	**Synthetic ^{13}C NMR (176 MHz)** δ_C/ppm[c]	Δ/ppm	**Isolation[b] ^{1}H NMR (500 MHz)** δ_H/ppm (*J* in Hz)[d]	**Synthetic ^{1}H NMR (700 MHz)** δ_H/ppm (*J* in Hz)[c]	Δ/ppm
1	187.1	187.3	0.2			
2	50.9	51.0	0.1			
3	210.9	210.9	0.0			
4	56.6	56.7	0.1			
5	196.2	196.4	0.2			
6	116.2	116.3	0.1			
7	206.9	207.1	0.2			
8	38.0	38.1	0.1	3.53 m	3.47 m	0.06
9	47.9	47.9	0.0	4.27 m	4.21 m	0.06
10	145.9	146.0	0.1			
11	127.2	127.4	0.2	7.28 m	7.20 m	0.08
12	128.5	128.6	0.1	7.37	7.32	0.05
13	126.4	126.5	0.1	7.28	7.23	0.05
14	128.5	128.6	0.1	7.37	7.32	0.05
15	127.3	127.4	0.1	7.28 m	7.20 m	0.08
16	27.4	27.5	0.1	1.37s	1.32 s	0.05
17	28.6	28.8	0.2	1.56 s	1.50 s	0.06
18	20.0	20.1	0.1	1.52 s	1.47 s	0.05
1'a	45.2	45.2	0.0	2.54 dd (13.2, 2.7)	2.50 dd (13.1, 2.8)	0.04
1'b				2.16 dd (13.2, 11.3)	2.13 dd (13.2, 11.4)	0.03
2'	74.8	75.0	0.2	3.80 dd (11.3, 2.7)	3.75 dd (11.4, 2.8)	0.05
3'	138.3	138.2	0.1			
4'	131.2	131.5	0.3	4.90 d (9.9)	4.85 dd (9.8, 1.6)	0.05
5'	31.9	32.0	0.1	3.10	3.04	0.06
6'	120.3	120.3	0.0	5.15 m	5.09 m	0.06
7'	136.0	136.2	0.2			
8'a	32.2	32.3	0.1	3.10	3.04	0.06
8'b				2.26 m	2.20 m	0.06
9'	8.8	8.9	0.1	1.23 s	1.18 d (1.4)	0.05
10'	23.5	23.7	0.2	1.87 s	1.81 s	0.06
1-OH				16.51 s	16.46 s	0.05

a) All data were obtained in $CDCl_3$. Overlapped signals were reported without designating multiplicity. b) Data from reference [51]. c) Chemical shifts are reported relative to the corresponding residual non-deuterated solvent signal ($CDCl_3$: δ_H = 7.26 ppm, δ_C = 77.16 ppm). d) Chemical shifts are reported relative to TMS (δ_H = 0.00 ppm).

5.7 Synthesis of Cleistocaltone B

tert-Butyldimethyl(oxiran-2-ylmethoxy)silane (118)

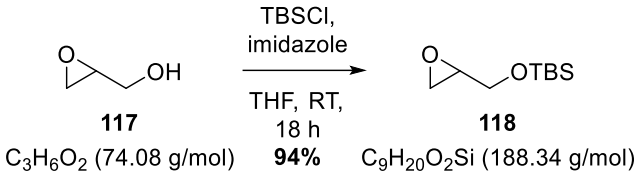

The TBS-protection of glycidol (**117**) was performed according to a literature-known procedure.[102] In a SCHLENK tube, glycidol (**117**, 4.48 mL, 5.00 g, 67.5 mmol, 1.00 equiv.) was dissolved in anhydrous THF (100 mL). TBSCl (15.3 g, 101 mmol, 1.50 equiv.) and imidazole (6.89 g, 101 mmol, 1.50 equiv.) were added and the mixture was stirred for 18 h. Afterwards, the precipitated solids were filtered off through a plug of celite. The filtrate was concentrated under reduced pressure. The crude product was purified by flash column chromatography (SiO_2, EtOAc/pentane, 1:9) to afford silyl ether **118** (11.9 g, 63.2 mmol, 94%) as a colourless oil.

^{1}H NMR (500 MHz, $CDCl_3$) δ = 3.85 (dd, J = 11.9, 3.2 Hz, 1H), 3.66 (dd, J = 11.9, 4.8 Hz, 1H), 3.10 – 3.07 (m, 1H), 2.78 – 2.76 (m, 1H), 2.64 – 2.63 (dd, J = 5.2, 2.7 Hz, 1H), 0.90 (s, 9H), 0.08 (s, 3H), 0.07 (s, 3H) ppm.

^{13}C NMR (126 MHz, $CDCl_3$) δ = 64.4, 52.6, 44.6, 26.0, 18.5, -5.2, -5.2 ppm.

The spectroscopic data are in accordance with the literature.[102]

1-((*tert*-Butyldimethylsilyl)oxy)-6-methylhept-5-en-2-ol (119)

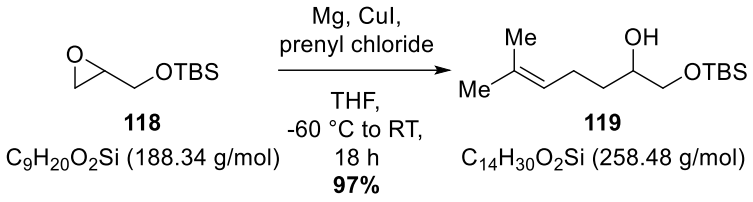

118
$C_9H_{20}O_2Si$ (188.34 g/mol)

119
$C_{14}H_{30}O_2Si$ (258.48 g/mol)

The GRIGNARD reaction of epoxide **118** with prenyl magnesium chloride was performed according to a literature-known procedure.[102]

Preparation of the GRIGNARD reagent:

In a two-necked round-bottom flask equipped with a reflux condenser, magnesium turnings (1.61 g, 66.4 mmol, 2.00 equiv.) were stirred for 10 min under an argon atmosphere. Afterwards, anhydrous THF (27 mL) and one iodine crystal were added and the mixture was heated to etch the magnesium until the yellow colour disappeared. In a separate SCHLENK flask, prenyl chloride (5.99 mL, 5.55 g, 53.1 mmol, 1.60 equiv.) was dissolved in anhydrous THF (13 mL). The prenyl chloride solution (4 mL) was added to the suspension of magnesium at RT. Once the reaction initiated, the mixture was immediately cooled down to –15 °C using an ice-NaCl-water bath. The remaining prenyl chloride solution was added to the mixture over 2 h using a syringe pump. After the addition was complete, stirring at –15 °C was continued for 30 min. Then, the mixture was allowed to warm up to RT. The black Grignard solution was stored at 5 °C and used within an hour.

GRIGNARD-reaction:

In a SCHLENK flask, epoxide **118** (6.25 g, 33.2 mmol, 1.00 equiv.) was dissolved in anhydrous THF (150 mL). Then, CuI (758 mg, 3.98 mmol, 12 mol%) was added and the mixture was cooled to –60 °C using an dry ice/isopropanol bath. The prenyl magnesium chloride solution was decantated from the excess magnesium turnings with a syringe and added to the mixture over 1 h using a syringe pump. The mixture was allowed to warm up to RT over 18 h. The reaction was terminated by adding crushed ice. After allowing the mixture to warm up to RT, sat. aq. NH_4Cl (70 mL) was added. The phases were separated and the aqueous phase was extracted with EtOAc (3 x 50 mL). The combined organic layers were washed with sat. aq. $NaHCO_3$ (100 mL) and brine (100 mL), dried over Na_2SO_4, filtered, and concentrated under reduced pressure to afford alcohol **119** (8.35 g, 32.3 mmol, 97%) as a colourless oil which was used in the next step without further purification.

^{1}H NMR (500 MHz, $CDCl_3$) δ = 5.13 – 5.10 (m, 1H), 3.65 – 3.59 (m, 2H), 3.41 – 3.38 (m, 1H), 2.40 (d, J = 3.2 Hz, 1H), 2.15 – 2.05 (d, J = 53.0 Hz, 2H), 1.68 (s, 3H), 1.62 (s, 3H), 1.50 – 1.38 (m, 2H), 0.90 (s, 9H), 0.07 (s, 6H) ppm.

^{13}C NMR (126 MHz, $CDCl_3$) δ = 132.1, 124.2, 71.6, 67.4, 33.0, 26.0, 25.8, 24.3, 18.4, 17.8, -5.2, -5.3 ppm.

The spectroscopic data are in accordance with the literature.[102]

1-((*tert*-Butyldimethylsilyl)oxy)-6-methylhept-5-en-2-one (120)

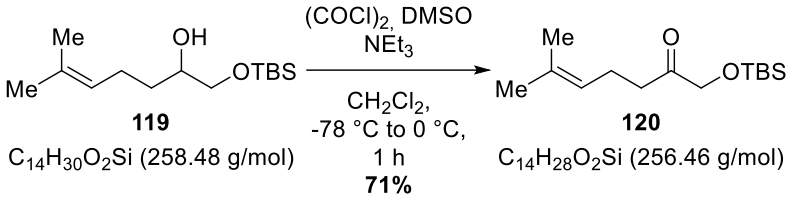

The SWERN oxidation of alcohol **119** was performed according to a literature-known procedure.[102] In a SCHLENK flask, oxalyl chloride (3.37 mL, 4.98 g, 39.2 mmol, 1.30 equiv.) was dissolved in anhydrous CH_2Cl_2 (154 mL). The mixture was cooled down to −78 °C using a dry ice/isopropanol bath and a solution of anhydrous DMSO (5.64 mL, 6.20 g, 81.5 mmol, 2.70 equiv.) in anhydrous CH_2Cl_2 (40 mL) was added over 1 mmol, 5.00 equiv.) was added. The mixture was allowed to warm up to 0 °C over 1 h. Then, the reaction was stopped by addition of sat. aq. $NaHCO_3$ (100 mL). The mixture was extracted with CH_2Cl_2 (4 x 100 mL). The combined organic layers were dried over Na_2SO_4, filtered, and concentrated under reduced pressure. The crude product was purified by flash column chromatography (SiO_2, EtOAc/pentane, 1:9) to afford ketone **120** (5.48 g, 21.4 mmol, 71%) as a colourless oil.

^{1}H NMR (500 MHz, $CDCl_3$) δ = 5.08 – 5.05 (m, 1H), 4.17 (s, 2H), 2.51 (t, J = 7.4 Hz, 2H), 2.26 (q, J = 7.5 Hz, 2H), 1.67 (s, 3H), 1.61 (s, 3H), 0.92 (s, 9H), 0.08 (s, 6H) ppm.

^{13}C NMR (126 MHz, $CDCl_3$) δ = 211.0, 132.9, 122.9, 69.6, 38.6, 25.9, 25.8, 22.2, 17.8, -5.4 ppm.

The spectroscopic data are in accordance with the literature.[102]

3-(((*tert*-Butyldimethylsilyl)oxy)methyl)-7-methylocta-1,6-dien-3-ol (121)

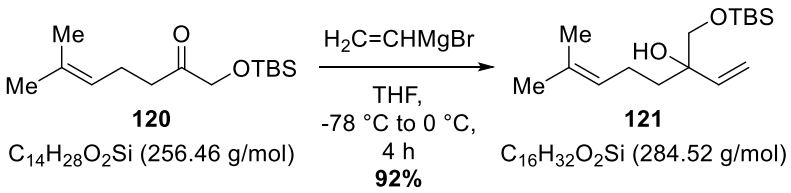

The GRIGNARD reaction of ketone **120** with vinyl magnesium bromide was performed according to a literature-known procedure.[102] In a SCHLENK tube, ketone **120** (5.30 g, 20.7 mmol, 1.00 equiv.) was dissolved in anhydrous THF (46 mL) and cooled down to –78 °C using an dry ice/isopropanol-bath. Then, vinyl magnesium bromide (1.0 M in THF, 24.8 mL, 24.8 mmol 1.20 equiv.) was added over 1 h using a syringe pump. After another 3 h of stirring at –78 °C, the mixture was allowed to warm up to 0 °C and quenched with sat. aq. NH_4Cl (40 mL). The phases were separated and the aqueous phase was extracted with EtOAc (3 x 40 mL). The combined organic layers were dried over Na_2SO_4, filtered, and concentrated under reduced pressure. The crude product was purified by flash column chromatography (SiO_2, EtOAc/pentane, 7:93) to afford alcohol **121** (5.39 g, 18.9 mmol, 92%) as a colourless oil.

^{1}H NMR (500 MHz, $CDCl_3$) δ = 5.78 (dd, J = 17.3, 10.8 Hz, 1H), 5.30 (dd, J = 17.3, 1.6 Hz, 1H), 5.17 (dd, J = 10.8, 1.6 Hz, 1H), 5.12 – 5.08 (m, 1H), 3.46 (s, 2H), 2.47 (s, 1H), 2.09 – 1.94 (m, 2H), 1.67 (s, 3H), 1.63 – 1.58 (m, 1H), 1.59 (s, 3H), 1.48 – 1.42 (m, 1H), 0.89 (s, 9H), 0.06 (s, 3H), 0.05 (s, 3H) ppm.

^{13}C NMR (126 MHz, $CDCl_3$) δ = 141.2, 131.7, 124.7, 114.3, 75.4, 69.6, 37.2, 26.0, 25.8, 22.2, 18.4, 17.8, -5.3, -5.3 ppm.

The spectroscopic data are in accordance with the literature.[102]

6-Methyl-2-vinylhept-5-ene-1,2-diol (116)

Synthesis of dihydroxymyrcene **116** according to LÖBERMANN, TRAUNER, and coworkers:[102]

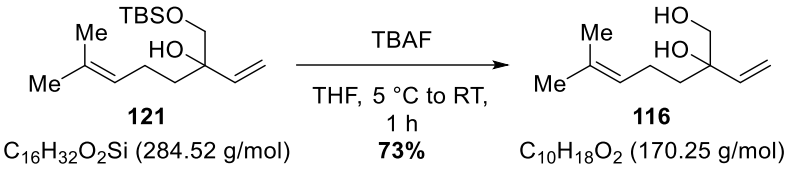

In a SCHLENK flask, silyl ether **121** (1.00 g, 3.52 mmol, 1.00 equiv.) was dissolved in THF (9 mL) and the mixture was cooled down to 0 °C using an ice-water-NaCl bath. Then, TBAF (1.0 M in THF, 10.5 mL, 10.5 mmol, 3.00 equiv.) was added, the mixture was allowed to warm up to RT and stirred for 1 h. Afterwards, the mixture was diluted with EtOAc (20 mL) and washed with sat. aq. $NaHCO_3$ (40 mL). The phases were separated and the aqueous phase was extracted with EtOAc (3 x 40 mL). The combined organic layers were dried over Na_2SO_4, filtered, and concentrated under reduced pressure. The crude product was purified by flash column chromatography (SiO_2, EtOAc/pentane, 1:2) to afford dihydroxymyrcene **116** (440 mg, 2.60 mmol, 73%) as a colourless oil.

One-step procedure of the dihydroxylation of myrcene (**122**) according to DELMOND and coworkers:[103]

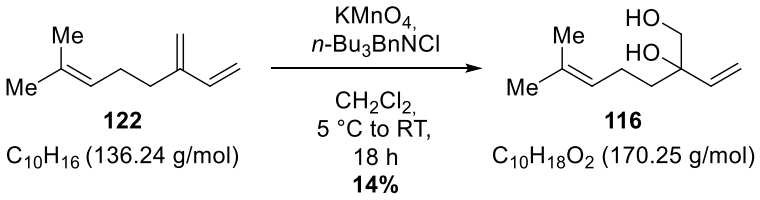

In three separate 1L-SCHLENK flasks, *n*-Bu_3BnNCl (35.5 g, 114 mmol, 1.00 equiv.; total: 107 g, 342 mmol) was dissolved in anhydrous CH_2Cl_2 (370 mL; total: 1.11 L) and cooled down to 5 °C using an ice-water bath. To the solution was added potassium permanganate (18.0 g, 114 mmol, 1.00 equiv.; total: 54.0 g, 342 mmol). The mixture was stirred for 3 h. Then, myrcene (**122**, 34.9 mL, 27.9 g, 205 mmol, 1.80 equiv.; total: 105 mL, 83.7 g, 615 mmol) was added and the mixture was allowed to warm up to RT over 18 h. The reaction mixture was quenched by subsequent addition of aq. NaOH (1.5 M, 200 mL; total: 600 mL), aq. Na_2SO_3 (0.6 M, 200 mL; total: 600 mL), and aq. H_2SO_4 (1.5 M, 200 mL; total: 600 mL) under vigorous stirring. The contents of the three flasks were combined in a 6 L-separatory funnel. The funnel was shaken vigorously once more and the phases were separated. The aqueous phase was extracted with CH_2Cl_2 (3 x 500 mL) The combined organic layers were washed with sat. aq. $NaHCO_3$ (1 L), dried over Na_2SO_4, filtered, and concentrated under reduced pressure. The crude product was purified by flash column

chromatography (SiO_2, EtOAc/pentane, 1:5 to 1:1). The polar fractions were collected, concentrated under reduced pressure and the residue was subjected to column chromatography (SiO_2, EtOAc/pentane, 1:3) once more to afford dihydroxymyrcene **116** (2.63 g, 15.4 mmol, 14%) as a colourless oil.

^{1}H NMR (500 MHz, $CDCl_3$) δ = 5.15 (p, J = 1.0 Hz, 1H), 5.11 (ddq, J = 8.4, 5.7, 1.4 Hz, 1H), 5.00 – 4.99 (m, 1H), 4.20 (ddq, J = 7.3, 3.5, 0.7 Hz, 1H), 3.70 (dd, J = 11.2, 3.4 Hz, 1H), 3.54 (dd, J = 11.3, 7.2 Hz, 1H), 2.19 – 2.14 (m, 2H), 2.13 – 2.00 (m, 2H), 1.69 (d, J = 1.4 Hz, 3H), 1.61 (s, 3H) ppm.

^{13}C NMR (126 MHz, $CDCl_3$) δ = 140.1, 132.4, 126.1, 116.0, 76.4, 69.0, 36.9, 25.8, 22.1, 17.9.

The spectroscopic data are in accordance with the literature.[103]

2-Hydroxy-6-methyl-2-vinylhept-5-en-1-yl 4-methylbenzenesulfonate (123)

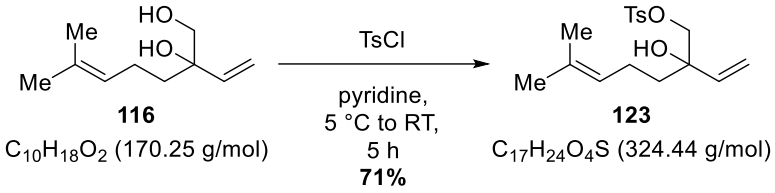

The tosylation of dihydroxymyrcene **116** was performed according to a literature-known procedure.[103] In a SCHLENK tube, dihydroxymyrcene **116** (2.60 g, 15.3 mmol, 1.00 equiv.) was dissolved in anhydrous pyridine (15 mL) which was previously cooled down to 5 °C using an ice-water bath. Then, TsCl (3.78 g, 19.9 mmol, 1.30 equiv.) was added and the mixture allowed to warm up to RT over 5 h. The reaction was stopped by addition of 10% aq. HCl (10 mL). The mixture was extracted with Et_2O (3 x 20 mL). The combined organic layers were washed with sat. aq. $NaHCO_3$ (50 mL) and brine (50 mL), dried over Na_2SO_4, filtered, and concentrated under reduced pressure. The crude product was purified by flash column chromatography (SiO_2, EtOAc/pentane, 1:9) to afford tosylate **123** (3.54 g, 10.9 mmol, 71%) as a colourless oil.

^{1}H NMR (500 MHz, $CDCl_3$) δ = 7.80 – 7.77 (m, 2H), 7.36 – 7.34 (m, 2H), 5.72 (dd, J = 17.3, 10.8 Hz, 1H), 5.33 (dd, J = 17.3, 1.1 Hz, 1H), 5.23 (dd, J = 10.8, 1.1 Hz, 1H), 5.05 (ddq, J = 8.7, 5.7, 1.4 Hz, 1H), 3.89 (s, 2H), 2.45 (s, 3H), 2.10 – 1.90 (m, 3H), 1.66 (s, 3H), 1.65 – 1.60 (m, 1H), 1.55 (s, 3H), 1.49 (ddd, J = 13.9, 10.5, 5.5 Hz, 1H) ppm.

^{13}C NMR (126 MHz, $CDCl_3$) δ = 145.1, 139.0, 132.9, 132.7, 130.1, 128.1, 123.8, 120.1, 116.1, 75.3, 74.5, 36.9, 25.8, 21.9, 21.8, 17.8 ppm.

The spectroscopic data are in accordance with the literature.[103]

2-(4-Methylpent-3-en-1-yl)-2-vinyloxirane (124)

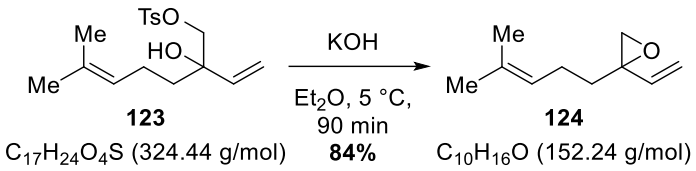

123 $C_{17}H_{24}O_4S$ (324.44 g/mol) **84%** **124** $C_{10}H_{16}O$ (152.24 g/mol)

The epoxide formation out of **123** was performed according to a literature-known procedure.[102] In a SCHLENK tube, tosylate **123** (48.0 mg, 0.148 mmol, 1.00 equiv.) was dissolved in anhydrous Et_2O (1.5 mL) and cooled down to 5 °C using an ice-water bath. Freshly ground KOH (16.6 mg, 0.296 mmol, 2.00 equiv.) was added and the mixture was stirred for 90 min. Afterwards, the mixture was filtered through a plug of silica which was rinsed with a 10% solution of Et_2O in pentane. The filtrate was concentrated under reduced pressure (min. 185 mbar at 5 °C) to afford epoxide **124** (19.0 mg, 12.5 mmol, 84%) as a colourless oil.

^{1}H NMR (500 MHz, $CDCl_3$) δ = 5.76 (dd, J = 17.4, 10.8 Hz, 1H), 5.35 (dd, J = 17.4, 1.3 Hz, 1H), 5.22 (dd, J = 10.8, 1.3 Hz, 1H), 5.10 (tdt, J = 7.1, 2.8, 1.4 Hz, 1H), 2.82 (d, J = 5.3 Hz, 1H), 2.67 (d, J = 5.4 Hz, 1H), 2.09 (dd, J = 15.6, 7.9 Hz, 2H), 1.75 – 1.70 (m, 2H), 1.68 (d, J = 1.4 Hz, 3H), 1.60 (s, 3H) ppm.

^{13}C NMR (126 MHz, $CDCl_3$) δ = 137.7, 132.2, 123.7, 116.6, 58.6, 55.2, 33.7, 25.8, 23.8, 17.8 ppm.

The spectroscopic data are in accordance with the literature.[103]

(*E*)-Cleistocaltone B (24)

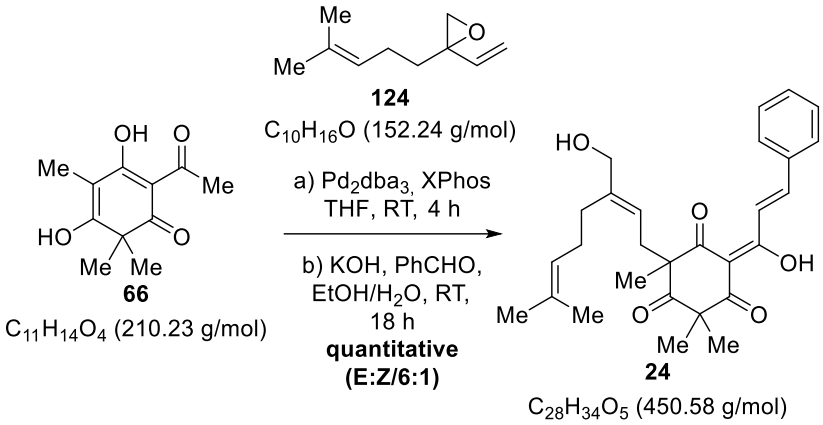

A SCHLENK tube was charged with acetyl phloroglucinol **66** (15.0 mg, 71.4 µmol, 1.00 equiv.), Pd_2dba_3 (1.63 mg, 1.78 µmol, 2.50 mol%), and XPhos (3.40 mg, 7.14 µmol, 0.10). The tube was evacuated and backfilled with argon three times. Then, the contents of the tube were dissolved in anhydrous THF (0.5 mL). The mixture was stirred for 10 min and epoxide **124** (21.7 mg, 0.143 mmol, 2.00 equiv.) dissolved in anhydrous THF (0.5 mL) was added. The resulting mixture was stirred for 4 h at RT. Afterwards, the mixture was cooled down to 5 °C and diluted with EtOH (2 mL). Then, benzaldehyde (43.2 µL, 45.4 mg, 0.428 mmol, 6.00 equiv.) and aq. KOH (7 M, 1.12 mL) were added subsequently and the mixture was stirred for 16 h. Afterwards, the mixture was diluted with diethyl ether (10 mL) and neutralized with sat. aq. NH_4Cl (10 mL). The phases were separated and the organic phase was washed with sat. aq. $NaHCO_3$ (15 mL), water (15 mL), and brine (15 mL), dried over Na_2SO_4, filtered, and concentrated under reduced pressure. The crude product was purified by flash column chromatography (SiO_2, EtOAc/pentane, 1:9 to 1:1) to afford (*E*)-Cleistocaltone B (**24**, 26.0 mg, 71.7 µmol, quantitative) as a bright yellow thick oil.

The product contained about 14% of the (*Z*)-diastereomer which was not separable. Both the (*E*)- and the (*Z*)-diastereomer were isolated as a mixture of tautomers. Therefore, four sets of signals were present in the ^{1}H- and ^{13}C-NMR in which many signals overlapped. Many signals of the (*Z*)-diastereomer where not visible under the much larger signals of the (*E*)-diastereomer. Therefore, only the signals of the (*E*)-diastereomer are given. The mixture of tautomers for the (*E*)-diastereomer was 1:1 which made a distinction between the two sets of the (*E*)-diastereomer almost impossible. Therefore the signals are given without designation.

^{1}H NMR (600 MHz, $CDCl_3$) δ = 18.33 (s, 1H), 18.31 (s, 1H), 8.05 – 8.03 (m, 2H, *overlap of sets*), 7.69 – 7.65 (m, 2H, *overlap of sets*), 7.45 – 7.41 (m, 3H, *overlap of sets*), 5.02 – 4.97 (m, 2H, *overlap of sets*), 4.16 (d, J = 12.1 Hz, 1H), 4.11 – 4.06 (m, 2H), 3.97 (d, J = 12.2 Hz, 1H), 2.88 – 2.64 (m, 2H,

overlap of sets), 2.05 – 1.97 (m, 4H, *overlap of sets*), 1.62 (s, 3H, *overlap of sets*), 1.53 (s, 3H), 1.52 (s, 3H), 1.48 (s, 3H), 1.48 (s, 3H), 1.41 (s, 3H), 1.40 (s, 3H), 1.32 (s, 3H), 1.25 (s, 3H) ppm.

^{13}C NMR (151 MHz, $CDCl_3$) δ = 211.2, 210.9, 202.5, 201.6, 197.2, 197.0, 186.9, 186.5, 147.5, 147.3, 143.4, 142.5, 134.8, 134.8, 132.1, 132.0, 131.5, 131.5, 129.3 (*overlap of sets*), 129.2, 129.2, 123.9, 123.9, 122.3, 121.4, 121.3, 121.3, 109.9, 109.3, 61.6, 60.3, 60.2, 58.3, 57.9, 53.9, 36.5, 35.9, 35.6, 35.5, 32.1, 30.9, 26.9, 26.9, 25.8, 25.0, 24.5, 24.2, 23.7, 22.0, 17.8 (*overlap of sets*) ppm.

HRMS (ESI, pos.): *m/z* calcd for $C_{28}H_{34}NaO_5^+$ $[M+Na^+]^+$: 473.2298, found 473.2316.

***tert*-Butyl (3-(((*tert*-butyldimethylsilyl)oxy)methyl)-7-methylocta-1,6-dien-3-yl) carbonate (138)**

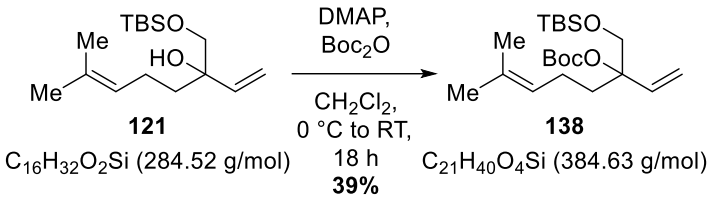

In a SCHLENK flask, alcohol **121** (1.00 g, 3.52 mmol, 1.00 equiv.) was dissolved in anhydrous CH_2Cl_2 (87 mL). The mixture was cooled down to 0 °C using an ice-NaCl-water bath. Then, Boc_2O (1.21 mL, 1.15 g, 1.50 equiv.) and DMAP (42.9 mg, 351 mmol, 10 mol%) were added and the mixture was allowed to warm up to RT over 18 h. Afterwards, the solvent was removed under reduced pressure and the crude product was purified by flash column chromatography (SiO_2, EtOAc/pentane, 1:19) to afford *tert*-butyl carbonate **138** (530 mg, 1.38 mmol, 39%) as a colourless oil.

^{1}H NMR (500 MHz, $CDCl_3$) δ = 5.93 (dd, J = 17.7, 11.3 Hz, 1H), 5.22 – 5.20 (m, 1H), 5.20 – 5.17 (m, 1H), 5.12 – 5.08 (m, 1H), 3.95 (d, J = 10.1 Hz, 1H), 3.76 (d, J = 10.1 Hz, 1H), 2.00 – 1.88 (m, 4H), 1.67 (s, 3H), 1.59 (s, 3H), 1.46 (s, 9H), 0.88 (s, 9H), 0.04 (s, 3H), 0.03 (s, 3H) ppm.

^{13}C NMR (126 MHz, $CDCl_3$) δ = 151.8, 139.1, 131.9, 124.1, 114.8, 85.3, 81.5, 64.9, 33.7, 28.0, 26.0, 25.8, 21.9, 18.4, 14.3, -5.4 ppm.

5.7.1 Synthesis of Butenolide 128

Geranial (133)

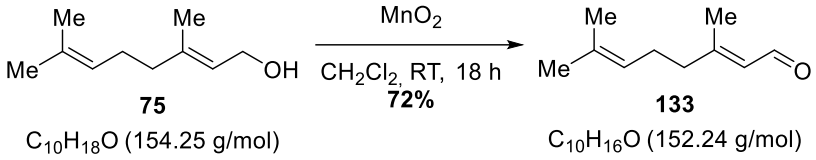

75
$C_{10}H_{18}O$ (154.25 g/mol)

133
$C_{10}H_{16}O$ (152.24 g/mol)

In a round-bottom flask, geraniol (**75**, 5.68 mL, 5.00 g, 32.4 mmol, 1.00 equiv.) was dissolved in CH_2Cl_2 (50 mL). Then, MnO_2 (portion: 28.2 g, 324 mmol, 10.0 equiv.; total: 84.5 g, 972 mmol, 30.0 equiv.) was added in three portions with intervals of 30 min. The reaction mixture was stirred for 16 h and filtered through a patch of celite. The filtrate was washed with water (3 x 20 mL) and brine (3 x 20 mL), dried over Na_2SO_4, filtered, and concentrated under reduced pressure to afford geranial (**133**, 3.54 g, 23.3 mmol, 72%) as a yellowish oil.

^{1}H NMR (500 MHz, CD_3CN) δ = 9.96 (d, J = 8.1 Hz, 1H), 5.79 (ddq, J = 8.1, 2.4, 1.2 Hz, 1H), 5.12 – 5.08 (m, 1H), 2.26 – 2.20 (m, 4H), 2.15 (d, J = 1.3 Hz, 3H), 1.67 (s, 3H), 1.61 (s, 3H) ppm.

The spectroscopic data are in accordance with the literature.[117]

4-(4-Methylpent-3-en-1-yl)furan-2(5H)-one (128)

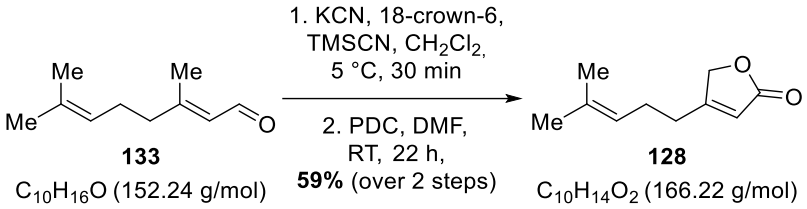

The oxidation of geranial (**133**) to butenolide **128** was performed according to a literature-known procedure.[104] A SCHLENK tube was charged with 18-crown-6 (86.8 mg, 0.328 mmol, 10 mol%) and KCN (21.4 mg, 0.328 mmol, 10 mol%). The tube was evacuated and backfilled with argon three times. Then, anhydrous CH_2Cl_2 (2 mL) and TMSCN (358 mg, 3.61 mmol, 1.10 equiv.) were added subsequently. The mixture was cooled down to 5 °C using an ice-water bath and geranial (**133**, 500 mg, 3.28 mmol, 1.00 equiv.) was added dropwise. After 3 h, the reaction mixture was concentrated under reduced pressure using the SCHLENK line while cooling to 5 °C continued. The residue was dissolved in anhydrous DMF (8 mL) and PDC (3.71 g, 9.85 mmol, 3.00 equiv.) was added. The mixture was stirred for 22 h at RT. Afterwards, the mixture was filtered through a patch of celite. The filter cake was thoroughly washed with CH_2Cl_2. The filtrate was washed with water (6 x 20 mL) and brine (6 x 20 mL), dried over Na_2SO_4, filtered, and concentrated under reduced pressure. The crude product was purified by flash column chromatography (SiO_2, EtOAc/pentane, 1:9) to afford butenolide **128** (320 mg, 1.93 mmol, 59%) as a colourless oil.

^{1}H NMR (500 MHz, $CDCl_3$) δ = 5.85 – 5.84 (m, 1H), 5.08 – 5.05 (m, 1H), 4.73 (s, 2H), 2.46 – 2.43 (m, 2H), 2.31 – 2.26 (m, 2H), 1.70 (s, 3H), 1.62 (s, 3H) ppm.

The spectroscopic data are in accordance with the literature.[104]

6. References

[1] K. Rogers, *The Components of Life: From Nucleic Acids to Carbohydrates*, The Rosen Publishing Group, Inc, New York, NY, **2011**.

[2] D. H. Boal, *Mechanics of the Cell*, Cambridge University Press, **2002**.

[3] A. L. Demain, A. Fang, in *History of Modern Biotechnology I* (Ed.: A. Fiechter), Springer Science & Business Media, Berlin Heidelberg New York, **2000**, pp. 1–39.

[4] J.-M. Mérillon, K. G. Ramawat, *Co-Evolution of Secondary Metabolites*, Springer, Cham, Switzerland, **2022**.

[5] H. Yuan, Q. Ma, L. Ye, G. Piao, *Molecules* **2016**, *21*, 559.

[6] D. J. Newman, G. M. Cragg, *J. Nat. Prod.* **2016**, *79*, 629–661.

[7] M. C. Wani, H. L. Taylor, M. E. Wall, P. Coggon, A. T. McPhail, *J. Am. Chem. Soc.* **1971**, *93*, 2325–2327.

[8] J. Wang, C. Xu, Y. K. Wong, Y. Li, F. Liao, T. Jiang, Y. Tu, *Engineering* **2019**, *5*, 32–39.

[9] R. A. Holton, C. Somoza, H. Kim, F. Liang, R. J. Biediger, P. D. Boatman, M. Shindo, C. C. Smith, S. Kim, H. Nadizadeh, Y. Suzuki, C. Tao, P. Vu, S. Tang, P. Zhang, K. K. Murthi, L. N. Gentile, J. H. Liu, *J. Am. Chem. Soc.* **1994**, *116*, 1597–1598.

[10] R. A. Holton, H. Kim, C. Somoza, F. Liang, R. J. Biediger, P. D. Boatman, M. Shindo, C. C. Smith, S. Kim, H. Nadizadeh, Y. Suzuki, C. Tao, P. Vu, S. Tang, P. Zhang, K. K. Murthi, L. N. Gentile, J. H. Liu, *J. Am. Chem. Soc.* **1994**, *116*, 1599–1600.

[11] Y. Kanda, H. Nakamura, S. Umemiya, R. K. Puthukanoori, V. R. Murthy Appala, G. K. Gaddamanugu, B. R. Paraselli, P. S. Baran, *J. Am. Chem. Soc.* **2020**, *142*, 10526–10533.

[12] Y. J. Hu, C. C. Gu, X. F. Wang, L. Min, C. C. Li, *J. Am. Chem. Soc.* **2021**, *143*, 17862–17870.

[13] K. C. Nicolaou, Z. Yang, J. J. Liu, H. Ueno, P. G. Nantermet, R. K. Guy, C. F. Claiborne, J. Renaud, E. A. Couladouros, K. Paulvannan, E. J. Sorensen, *Nature* **1994**, *367*, 630–634.

[14] K. C. Nicolaou, J. Renaud, P. G. Nantermet, E. A. Couladouros, R. K. Guy, W. Wrasidlo, *J. Am. Chem. Soc.* **1995**, *117*, 2409–2420.

[15] P. A. Wender, N. F. Badham, S. P. Conway, P. E. Floreancig, T. E. Glass, J. B. Houze, N. E. Krauss, D. Lee, D. G. Marquess, P. L. McGrane, W. Meng, M. G. Natchus, A. J. Shuker, J. C. Sutton, R. E. Taylor, *J. Am. Chem. Soc.* **1997**, *119*, 2757–2758.

[16] K. Morihira, R. Hara, S. Kawahara, T. Nishimori, N. Nakamura, H. Kusama, I. Kuwajima, *J. Am. Chem. Soc.* **1998**, *120*, 12980–12981.

[17] H. Kusama, R. Hara, S. Kawahara, T. Nishimori, H. Kashima, N. Nakamura, K. Morihira, I. Kuwajima, *J. Am. Chem. Soc.* **2000**, *122*, 3811–3820.

[18] T. Doi, S. Fuse, S. Miyamoto, K. Nakai, D. Sasuga, T. Takahashi, *Chem.: Asian J.* **2006**, *1*, 370–383.

[19] K. Fukaya, Y. Tanaka, A. C. Sato, K. Kodama, H. Yamazaki, T. Ishimoto, Y. Nozaki, Y. M. Iwaki, Y. Yuki, K. Umei, T. Sugai, Y. Yamaguchi, A. Watanabe, T. Oishi, T. Sato, N. Chida, *Org. Lett.* **2015**, *17*, 2570–2573.

[20] K. Fukaya, K. Kodama, Y. Tanaka, H. Yamazaki, T. Sugai, Y. Yamaguchi, A. Watanabe, T. Oishi, T. Sato, N. Chida, *Org. Lett.* **2015**, *17*, 2574–2577.

[21] M. A. Avery, W. K. M. Chong, C. Jennings-White, *J. Am. Chem. Soc.* **1992**, *114*, 974–979.

[22] W. S. Zhou, X. X. Xu, *Acc. Chem. Res.* **1994**, *27*, 211–216.

[23] C. Zhu, S. P. Cook, *J. Am. Chem. Soc.* **2012**, *134*, 13577–13579.

[24] F. Lévesque, P. H. Seeberger, *Angew. Chem. Int. Ed.* **2012**, *51*, 1706–1709.

[25] D. Kopetzki, F. Lévesque, P. H. Seeberger, *Chem. Eur. J.* **2013**, *19*, 5450–5456.

[26] W. Xiao, F. Lei, Z. Hengqiang, L. Xiaojing, in *Natural Product Extraction: Principles and Applications* (Eds.: J. Prado, M. Rostagno), The Royal Society Of Chemistry, London, **2022**, pp. 544–590.

[27] K. C. Nicolaou, D. Vourloumis, N. Winssinger, P. S. Baran, *Angew. Chem. Int. Ed.* **2000**, *39*, 44–122.

[28] T. Seitz, P. Fu, F. L. Haut, L. Adam, M. Habicht, D. Lentz, J. B. MacMillan, M. Christmann, *Org. Lett.* **2016**, *18*, 3070–3073.

[29] H. Itoh, M. Inoue, *Chem. Rev.* **2019**, *119*, 10002–10031.

[30] J. Schwan, M. Christmann, *Chem. Soc. Rev.* **2018**, *47*, 7985–7995.

[31] R. Bao, H. Zhang, Y. Tang, *Acc. Chem. Res.* **2021**, *54*, 3720–3733.

[32] T. V. de Castro, D. M. Huang, C. J. Sumby, A. L. Lawrence, J. H. George, *Chem. Sci.* **2023**, *14*, 950–954.

[33] S. A. French, C. J. Sumby, D. M. Huang, J. H. George, *J. Am. Chem. Soc.* **2022**, *144*, 22844–22849.

[34] A. Jha, H. Jarvis, C. Fraser, P. J. M. Openshaw, in *SARS, MERS and Other Viral Lung Infections*, European Respiratory Society, Sheffield, **2016**, pp. 1–38.

[35] J. A. Morris, R. E. Blount, R. E. Savage, *Proc. Soc. Exp. Biol. Med.* **1956**, *92*, 544–549.

[36] Y. Li, X. Wang, D. M. Blau, M. T. Caballero, D. R. Feikin, C. J. Gill, S. A. Madhi, S. B. Omer, E. A. F. Simões, H. Campbell, A. B. Pariente, D. Bardach, Q. Bassat, J. S. Casalegno, G. Chakhunashvili, N. Crawford, D. Danilenko, L. A. H. Do, M. Echavarria, A. Gentile, A. Gordon, T. Heikkinen, Q. S. Huang, S. Jullien, A. Krishnan, E. L. Lopez, J. Markić, A. Mira-Iglesias, H. C. Moore, J. Moyes, L. Mwananyanda, D. J. Nokes, F. Noordeen, E. Obodai, N. Palani, C. Romero, V. Salimi, A. Satav, E. Seo, Z. Shchomak, R. Singleton, K. Stolyarov, S. K. Stoszek, A. von Gottberg, D. Wurzel, L. M. Yoshida, C. F. Yung, H. J. Zar, M. Abram, J. Aerssens, A. Alafaci, A. Balmaseda, T. Bandeira, I. Barr, E. Batinović, P. Beutels, J. Bhiman, C. C. Blyth, L. Bont, S. S. Bressler, C. Cohen, R. Cohen, A. M. Costa, R. Crow, A. Daley, D. A. Dang, C. Demont, C. Desnoyers, J. Díez-Domingo, M. Divarathna, M. du Plessis, M. Edgoose, F. M. Ferolla, T. K. Fischer, A. Gebremedhin, C. Giaquinto, Y. Gillet, R. Hernandez, C. Horvat, E. Javouhey, I. Karseladze, J. Kubale, R. Kumar, B. Lina, F. Lucion, R. MacGinty, F. Martinon-Torres, A. McMinn, A. Meijer, P. Milić, A. Morel, K. Mulholland, T. Mungun, N. Murunga, C. Newbern, M. P. Nicol, J. K. Odoom, P. Openshaw, D. Ploin, F. P. Polack, A. J. Pollard, N. Prasad, J. Puig-Barberà, J. Reiche, N. Reyes, B. Rizkalla, S. Satao, T. Shi, S. Sistla, M. Snape, Y. Song, G. Soto, F. Tavakoli, M. Toizumi, N. Tsedenbal, M. van den Berge, C. Vernhes, C. von Mollendorf, S. Walaza, G. Walker, H. Nair, *Lancet* **2022**, *399*, 2047–2064.

[37] M. Savic, Y. Penders, T. Shi, A. Branche, J. Y. Pirçon, *Influenza Other Respir. Viruses* **2022**, 1–10.

[38] G. den Hartog, P. B. van Kasteren, R. M. Schepp, A. C. Teirlinck, F. R. M. van der Klis, R. S. van Binnendijk, *Lancet Infect. Dis.* **2023**, *23*, 23–25.

[39] A. C. Langedijk, L. J. Bont, *Nat. Rev. Microbiol.* **2023**, *21*, 734–749.

[40] G. N. Pham, T. T. T. Nguyen, H. Nguyen-Ngoc, *Evid. Based Complement. Alternat. Med.* **2020**, *2020*, Article ID 8263670.

[41] A. Y. H. Woo, M. M. Y. Waye, H. S. Kwan, M. C. Y. Chan, C. F. Chau, C. H. K. Cheng, *Vasc. Pharmacol.* **2002**, *38*, 163–168.

[42] P. L. Tran, O. Kim, H. N. K. Tran, M. H. Tran, B. S. Min, C. Hwangbo, J. H. Lee, *Food Chem. Toxicol.* **2019**, *129*, 125–137.

[43] C.-L. Ye, J.-W. Liu, D.-Z. Wei, Y.-H. Lu, F. Qian, *Pharmacol. Res.* **2004**, *50*, 505–510.

[44] C. Wang, P. Wu, X.-L. Shen, X.-Y. Wei, Z.-H. Jiang, *RSC Adv.* **2017**, *7*, 48031–48038.

[45] H. N. Tuan, B. H. Minh, P. T. Tran, J. H. Lee, H. Van Oanh, Q. M. T. Ngo, Y. N. Nguyen, P. T. K. Lien, M. H. Tran, *Molecules* **2019**, *24*, 2538.

[46] J. W. Choi, M. Kim, H. Song, C. S. Lee, W. K. Oh, I. Mook-Jung, S. S. Chung, K. S. Park, *Metab.: Clin. Exp.* **2016**, *65*, 533–542.

[47] M.-Y. Su, H.-Y. Huang, L. Li, Y.-H. Lu, *J. Agric. Food Chem.* **2011**, *59*, 521–527.

[48] W.-G. Yu, H. He, J. Qian, Y.-H. Lu, *J. Agric. Food Chem.* **2014**, *62*, 11949–11056.

[49] W. G. Yu, H. He, J. Y. Yao, Y. X. Zhu, Y. H. Lu, *Biomol. Ther.* **2015**, *23*, 549–556.

[50] J. C. Su, S. Wang, W. Cheng, X. J. Huang, M. M. Li, R. W. Jiang, Y. L. Li, L. Wang, W. C. Ye, Y. Wang, *J. Org. Chem.* **2018**, *83*, 8522–8532.

[51] J. G. Song, J. C. Su, Q. Y. Song, R. L. Huang, W. Tang, L. J. Hu, X. J. Huang, R. W. Jiang, Y. L. Li, W. C. Ye, Y. Wang, *Org. Lett.* **2019**, *21*, 9579–9583.

[52] Q. J. Li, P. F. Tang, X. Zhou, W. J. Lu, W. J. Xu, J. Luo, L. Y. Kong, *Bioorg. Chem.* **2020**, *104*, 104275.

[53] L. Hu, Y. Xue, J. Zhang, H. Zhu, C. Chen, X. N. Li, J. Liu, Z. Wang, Y. Zhang, Y. Zhang, *J. Nat. Prod.* **2016**, *79*, 1322–1328.

[54] B. M. Trost, *Tetrahedron* **2015**, *71*, 5708–5733.

[55] J. Tsuji, H. Takahashi, M. Morikawa, *Tetrahedron Lett.* **1965**, *6*, 4387–4388.

[56] L. Kürti, B. Czakó, in *Strategic Applications of Named Reactions in Organic Synthesis*, Elsevier Academic Press, Burlington, MA, USA; San Diego, California, USA; London, UK, **2005**, pp.

458–459.

[57] B. M. Trost, T. Zhang, J. D. Sieber, *Chem. Sci.* **2010**, *1*, 427–440.

[58] B. M. Trost, D. L. Van Vranken, *Chem. Rev.* **1996**, *96*, 395–422.

[59] B. M. Trost, S. Malhotra, W. H. Chan, *J. Am. Chem. Soc.* **2011**, *133*, 7328–7331.

[60] B. M. Trost, G. A. Molander, *J. Am. Chem. Soc.* **1981**, *103*, 5969–5972.

[61] B. M. Trost, G. M. Schroeder, *J. Am. Chem. Soc.* **1999**, *121*, 6759–6760.

[62] O. Diels, K. Alder, *Liebigs Ann. Chem.* **1927**, 98–122.

[63] R. Sustmann, *Pure Appl. Chem.* **1974**, *40*, 569–593.

[64] L. Kürti, B. Czakó, in *Strategic Applications of Named Reactions in Organic Synthesis*, Elsevier Academic Press, Burlington, MA, USA; San Diego, California, USA; London, UK, **2005**, pp. 140–141.

[65] K. Alder, G. Stein, *Angew. Chem.* **1937**, *50*, 510–519.

[66] A. G. Fallis, *Acc. Chem. Res.* **1999**, *32*, 464–474.

[67] M. Juhl, D. Tanner, *Chem. Soc. Rev.* **2009**, *38*, 2983–2992.

[68] M. Miyashita, M. Sasaki, I. Hattori, M. Sakai, K. Tanino, *Science* **2004**, *305*, 495–499.

[69] J. Sauer, R. Sustmann, *Angew. Chem. Int. Ed.* **1980**, *19*, 779–807.

[70] A. Mendoza, Y. Ishihara, P. S. Baran, *Nat. Chem.* **2012**, *4*, 21–25.

[71] A. Bonilla, C. Duque, C. Garzón, Y. Takaishi, K. Yamaguchi, N. Hara, Y. Fujimoto, *Phytochemistry* **2005**, *66*, 1736–1740.

[72] K. Nakagawa-Goto, J. H. Wu, K. H. Lee, *Synth. Commun.* **2005**, *35*, 1735–1739.

[73] K. Nakagawa-Goto, K. F. Bastow, J. H. Wu, H. Tokuda, K. H. Lee, *Bioorg. Med. Chem. Lett.* **2005**, *15*, 3016–3019.

[74] J. H. Wu, A. T. McPhail, K. F. Bastow, H. Shiraki, J. Ito, K. H. Lee, *Tetrahedron Lett.* **2002**, *43*, 1391–1393.

[75] M. A. Berliner, K. Belecki, *J. Org. Chem.* **2005**, *70*, 9618–9621.

[76] J.-H. Sohn, N. Waizumi, H. M. Zhong, V. H. Rawal, *J. Am. Chem. Soc.* **2005**, *127*, 7290–7291.

[77] J. H. Han, Y. E. Kwon, J. H. Sohn, D. H. Ryu, *Tetrahedron* **2010**, *66*, 1673–1677.

[78] T. Yoshida, S. Muraki, H. Kawamura, A. Komatsu, *Agric. Biol. Chem.* **1969**, *33*, 343–352.

[79] Y. Yuasa, Y. Kato, *J. Agric. Food Chem.* **2003**, *51*, 4036–4039.

[80] K. Naoto, S. Shinzo, *Process for Producing Lycopene and Intermediate Thereof*, **2001**, EP 1 072 589 A2.

[81] R. Appel, *Angew. Chem. Int. Ed.* **1975**, *14*, 801–811.

[82] E. J. Corey, C. U. Kim, M. Takeda, *Tetrahedron Lett.* **1972**, 4339–4342.

[83] L. Wiese, S. M. Kolbe, M. Weber, M. Ludlow, M. Christmann, *Chem. Sci.* **2024**, *15*, 10121–10125.

[84] Solvias AG, "Solvias Ligands and Catalysts Library," can be found under https://ligands.solvias.com/library/index, **2024**. (Accessed: 21.03.2024)

[85] J. F. Stevens, A. W. Taylor, J. E. Clawson, M. L. Deinzer, *J. Agric. Food Chem.* **1999**, *47*, 2421–2428.

[86] S. M. Wilkinson, J. Price, M. Kassiou, *Tetrahedron Lett.* **2013**, *54*, 52–54.

[87] K. Ito, M. Nakanishi, W. C. Lee, Y. Zhi, H. Sasaki, S. Zenno, K. Saigo, Y. Kitade, M. Tanokura, *J. Biol. Chem.* **2008**, *283*, 13889–13896.

[88] R. L. Yong, X. Li, H. K. Jung, *J. Org. Chem.* **2008**, *73*, 5662.

[89] S. Cannizzaro, *Ber. Dtsch. Chem. Ges.* **1853**, *88*, 129–130.

[90] S. Narayan, J. Muldoon, M. G. Finn, V. V. Fokin, H. C. Kolb, K. B. Sharpless, *Angew. Chem. Int. Ed.* **2005**, *44*, 3275–3279.

[91] L. Gao, J. Han, X. Lei, *Org. Lett.* **2016**, *18*, 360–363.

[92] Z. Ding, W. E. G. Osminski, H. Ren, W. D. Wulff, *Org. Process Res. Dev.* **2011**, *15*, 1089–1107.

[93] V. VanRheenen, R. C. Kelly, D. Y. Cha, *Tetrahedron Lett.* **1976**, 1973–1976.

[94] W. K. Jo, A. Schadenhofer, A. Habierski, F. K. Kaiser, G. Saletti, T. Ganzenmueller, E. Hage, S.

Haid, T. Pietschmann, G. Hansen, T. F. Schulz, G. F. Rimmelzwaan, A. D. M. E. Osterhaus, M. Ludlow, *Proc. Natl. Acad. Sci. U. S. A.* **2021**, *118*, e2026558118.

[95] J. P. DeVincenzo, R. J. Whitley, R. L. Mackman, C. Scaglioni-Weinlich, L. Harrison, E. Farrell, S. McBride, R. Lambkin-Williams, R. Jordan, Y. Xin, S. Ramanathan, T. O'Riordan, S. A. Lewis, X. Li, S. L. Toback, S.-L. Lin, J. W. Chien, *N. Engl. J. Med.* **2014**, *371*, 711–722.

[96] B. E. Hetzler, D. Trauner, A. L. Lawrence, *Nat. Rev. Chem.* **2022**, *6*, 170–181.

[97] R. Willstätter, *Ber. Dtsch. Chem. Ges.* **1900**, *33*, 1160–1166.

[98] E. Fischer, E. Abderhalden, *Biol. Chem.* **1903**, *39*, 81–94.

[99] P. Ellerbrock, N. Armanino, M. K. Ilg, R. Webster, D. Trauner, *Nat. Chem.* **2015**, *7*, 879–882.

[100] Z. Yan, J. Li, G. Ye, T. Chen, M. Li, Y. Liang, Y. Long, *RSC Adv.* **2020**, *10*, 28560–28566.

[101] D. Van Nguyen, *Medicinal Plants of Vietnam, Cambodia, and Laos*, Mekong Printing, Santa Monica, CA, **1993**.

[102] F. Löbermann, L. Weisheit, D. Trauner, *Org. Lett.* **2013**, *15*, 4324–4326.

[103] B. Delmond, V. Fauchel, B. A. S. Miguel, M. Taran, *Synth. Commun.* **1993**, *23*, 2503–2510.

[104] E. J. Corey, G. Schmidt, *Tetrahedron Lett.* **1980**, *21*, 731–734.

[105] H. J. Böhm, D. Banner, S. Bendels, M. Kansy, B. Kuhn, K. Müller, U. Obst-Sander, M. Stahl, *ChemBioChem* **2004**, *5*, 637–643.

[106] A. Tlili, F. Toulgoat, T. Billard, *Angew. Chem. Int. Ed.* **2016**, *55*, 11726–11735.

[107] H. Y. Tsai, J. F. Yang, Y. B. Chen, J. L. Guo, S. Li, G. J. Wei, C. T. Ho, J. L. Hsu, C. I. Chang, Y. S. Liang, H. S. Yu, Y. K. Chen, *Int. J. Mol. Sci.* **2022**, *23*, 13284.

[108] P. de S. M. Pinheiro, L. S. Franco, C. A. M. Fraga, *Pharmaceuticals* **2023**, *16*, 1157.

[109] J. Song, R. Huang, J. Cai, Z. Wu, L. Hu, W. Sun, X. Huang, R. He, W. Tang, W. Ye, Y. Wang, *Acta Pharm. Sin. B* **2024**, *14*, 4443–4460.

[110] G. M. Sheldrick, *Acta Crystallogr. A* **2008**, *64*, 112–122.

[111] G. M. Sheldrick, *Acta Crystallogr. C* **2015**, *71*, 3–8.

[112] O. V. Dolomanov, L. J. Bourhis, R. J. Gildea, J. A. K. Howard, H. Puschmann, *J. Appl. Crystallogr.* **2009**, *42*, 339–341.

[113] T. Kuwano, M. Watanabe, D. Kagawa, T. Murase, *J. Agric. Food Chem.* **2015**, *63*, 7937–7944.

[114] M. Thévenin, E. Mouray, P. Grellier, J. Dubois, *Eur. J. Org. Chem.* **2014**, 2986–2992.

[115] J. Q. Hou, C. Guo, J. J. Zhao, Q. W. He, B. B. Zhang, H. Wang, *J. Org. Chem.* **2017**, *82*, 1448–1457.

[116] E. Nakamura, S. Aoki, K. Sekiya, H. Oshino, I. Kuwajima, *J. Am. Chem. Soc.* **1987**, *109*, 8056–8066.

[117] N. Furukawa, X. Chen, S. Asano, M. Matsumoto, Y. Wu, K. Murata, A. Takeuchi, C. Tode, T. Homma, R. Koharazawa, K. Usami, J. K. Tie, Y. Hirota, Y. Suhara, *J. Mol. Struct.* **2023**, *1276*, 134614.

7. Appendix

7.1 List of Abbreviations

Ac	acetyl
aq.	aqueous
Ar	arene
ARI	acute respiratory infection
Asc	ascorbate
BBMN	blocks-based molecular network
BINAP	2,2′-bis(diphenylphosphino)-1,1′-binaphthyl
BINOL	1,1′-bi-2-naphthol
Bn	benzyl
Boc	*tert*-butyloxycarbonyl
br	broad
brsm	based on recovered starting material
Bu	butyl
Bz	benzoyl
CAM	ceric ammonium molybdate
COVID-19	coronavirus disease 2019
Cp	cyclopentadienyl
d	doublet
d.r.	diastereomeric ratio
Da	Dalton
DABCO	1,4-diazabicyclo[2.2.2]octan
DACH	1,2-diaminocyclohexane
dba	dibenzylideneacetone
DBU	1,8-diazabicyclo[5.4.0]undec-7-ene

DIPEA	*N*,*N*-diisopropylethylamine
DMAP	4-dimethylaminopyridine
DME	1,2-dimethoxyethane
DMC	2',4'-dihydroxy-6'-methoxy-3',5'-dimethylchalcone
DMF	dimethylformamide
DMSO	dimethylsulfoxide
dppf	1,1′-bis(diphenylphosphino)ferrocene
dppp	1,3-bis(diphenylphosphino)propane
DuPhos	1,2-bis[2,5-dimethylphospholano]benzol
EDG	electron donating group
ee	enantiomeric excess
equiv.	equivalents
ESI	electrospray ionization
Et	ethyl
EWG	electron withdrawing group
Ger	geranyl
h	hours
HOMO	highest occupied molecular orbital
HPLC-MS	high performance liquid chromatography / mass spectrometry
HRMS	high resolution mass spectrometry
HSV	herpes simplex virus
i	*iso*
IC_{50}	half maximal inhibitory concentration
IMDA	intramolecular DIELS-ALDER cycloaddition
IR	infrared spectroscopy
L	ligand
LDA	lithium diisopropylamide
LUMO	lowest unoccupied molecular orbital

M	molar
m	multiplet
m-CPBA	*meta*-chloroperbenzoic acid
Me	methyl
min	minutes
MOM	methoxymethyl
n	unbranched
NCS	*N*-chlorosuccinimide
NMO	*N*-methylmorpholine *N*-oxide
NMR	nuclear magnetic resonance
NOE	nuclear overhauser effect
NP	natural product
Nu	nucleophile
o	ortho
OPP	pyro phosphate
p	quintet
PDC	pyridinium dichromate
PG	protecting group
Ph	phenyl
ppm	parts per million
Pr	propyl
PTSA	*para*-toluenesulfonic acid
q	quartet
quant.	quantitative
Ref.	Reference
RNA	ribonucleic acid
RP	reversed-phase
RSV	respiratory syncytial virus

RT	room temperature
s	singlet
SAR	structure-activity relationship
SARS-CoV-2	severe acute respiratory syndrome coronavirus 2
sat.	saturated
S_N	nucleophilic substitution
t	*tert*
t	triplet
TBAF	tetra-*n*-butylammonium fluoride
TBS	*tert*-butyldimethylsilyl
TCCA	trichloroisocyanuric acid
TCM	traditional Chinese medicine
THF	tetrahydrofuran
TIC	total ion current chromatogram
TLC	thin layer chromatography
TMS	trimethylsilyl
TOF	time of flight
Troc	2,2,2-trichloroethyloxycarbonyl
Ts	*para*-toluenesulfonyl
VANOL	3,3′-diphenyl-2,2′-bi-(1-naphthalol)
VAPOL	2,2′-diphenyl-(4-biphenanthrol)
w%	weight-%
XPhos	2-dicyclohexylphosphin-2′,4′,6′-triisopropylbiphenyl
Xantphos	4,5-bis-(diphenylphosphino)-9,9-dimethylxanthen
XRD	X-ray diffraction

7.2 X-Ray Data (Reproduced (adapted) from Ref.[83] with permission from the Royal Society of Chemistry.)

7.2.1 IMDA-Diastereomer 105 (CCDC2352924)

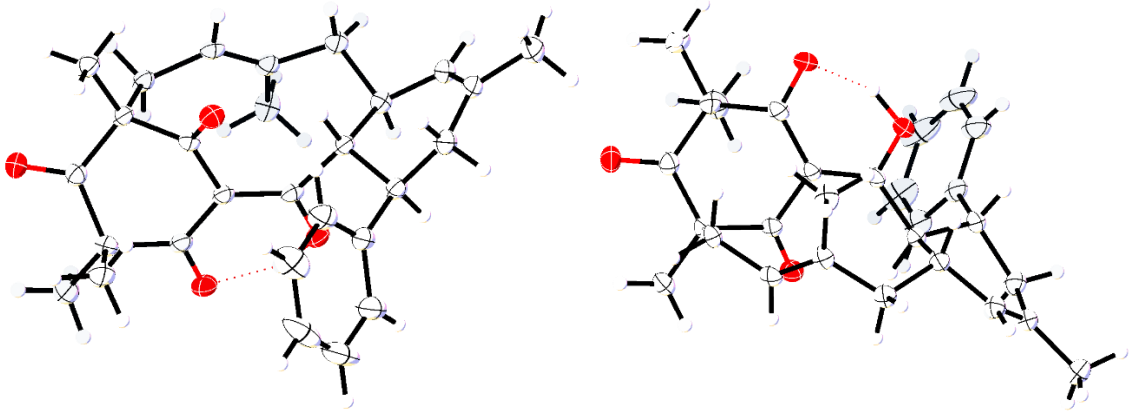

Table 20: Crystal data of IMDA-diastereomer **105**.

Empirical formula	$C_{28}H_{32}O_4$
Formula weight	432.53
Temperature/K	140(2)
Crystal system	monoclinic
Space group	$P2_1/n$
a/Å	9.53542(6)
b/Å	18.20996(12)
c/Å	14.54563(9)
α/°	90
β/°	105.5556(2)
γ/°	90
Volume/Å^3	2433.18(3)
Z	4
ρ_{calc}g/cm^3	1.181
μ/mm^{-1}	0.617
F(000)	928.0
Crystal size/mm^3	0.44 × 0.25 × 0.14
Radiation	CuKα (λ = 1.54178)
2Θ range for data collection/°	7.96 to 144.238
Index ranges	-11 ≤ h ≤ 11, -22 ≤ k ≤ 22, -14 ≤ l ≤ 17
Reflections collected	33228
Independent reflections	4766 [R_{int} = 0.0376, R_{sigma} = 0.0210]
Data/restraints/parameters	4766/0/296
Goodness-of-fit on F^2	1.049
Final R indexes [I>=2σ (I)]	R_1 = 0.0392, wR_2 = 0.0938
Final R indexes [all data]	R_1 = 0.0402, wR_2 = 0.0943
Largest diff. peak/hole / e Å^{-3}	0.22/-0.30

7.2.2 IMDA-Diastereomer 37 (CCDC2352922)

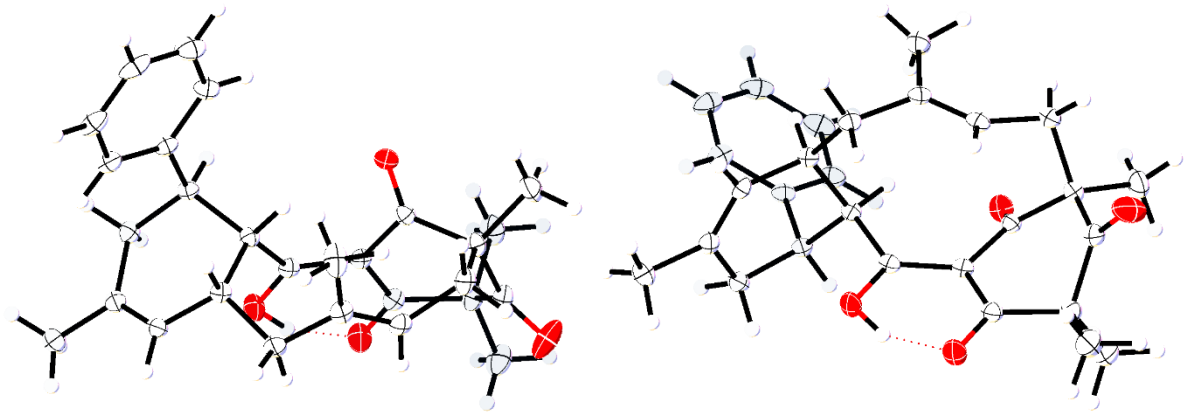

Table 21: Crystal data of IMDA-diastereomer **37**.

Empirical formula	$C_{28}H_{32}O_4$
Formula weight	432.53
Temperature/K	140(2)
Crystal system	monoclinic
Space group	$P2_1/n$
a/Å	8.38079(5)
b/Å	23.63124(15)
c/Å	12.06328(8)
α/°	90
β/°	106.2413(2)
γ/°	90
Volume/Å^3	2293.77(3)
Z	4
ρ_{calc}g/cm^3	1.253
μ/mm^{-1}	0.655
F(000)	928.0
Crystal size/mm^3	0.39 × 0.23 × 0.1
Radiation	CuKα (λ = 1.54178)
2Θ range for data collection/°	7.482 to 144.09
Index ranges	-10 ≤ h ≤ 9, -28 ≤ k ≤ 29, -14 ≤ l ≤ 14
Reflections collected	34216
Independent reflections	4516 [R_{int} = 0.0478, R_{sigma} = 0.0240]
Data/restraints/parameters	4516/0/296
Goodness-of-fit on F^2	1.046
Final R indexes [I>=2σ (I)]	R_1 = 0.0432, wR_2 = 0.1117
Final R indexes [all data]	R_1 = 0.0439, wR_2 = 0.1123
Largest diff. peak/hole / e Å^{-3}	0.41/-0.31

7.2.3 Side Product 111 (CCDC2352923)

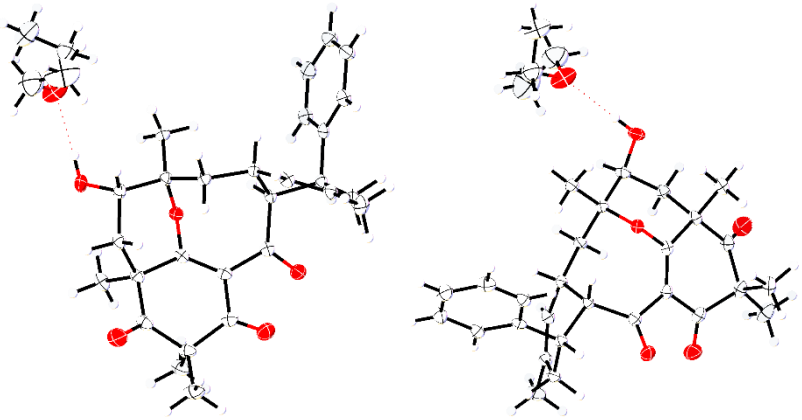

Table 22: Crystal data of side product **111**.

Empirical formula	$C_{32}H_{42}O_6$
Formula weight	522.65
Temperature/K	150(2)
Crystal system	orthorhombic
Space group	$P2_12_12_1$
a/Å	10.10314(7)
b/Å	10.72852(8)
c/Å	25.70876(18)
α/°	90
β/°	90
γ/°	90
Volume/Å^3	2786.62(3)
Z	4
ρ_{calc}g/cm^3	1.246
μ/mm^{-1}	0.679
F(000)	1128.0
Crystal size/mm^3	0.22 × 0.16 × 0.12
Radiation	CuKα (λ = 1.54178)
2Θ range for data collection/°	6.876 to 140.684
Index ranges	-12 ≤ h ≤ 12, -13 ≤ k ≤ 13, -31 ≤ l ≤ 31
Reflections collected	73519
Independent reflections	5283 [R_{int} = 0.0383, R_{sigma} = 0.0184]
Data/restraints/parameters	5283/0/351
Goodness-of-fit on F^2	1.043
Final R indexes [I>=2σ (I)]	R_1 = 0.0327, wR_2 = 0.0870
Final R indexes [all data]	R_1 = 0.0330, wR_2 = 0.0872
Largest diff. peak/hole / e Å^{-3}	0.60/-0.25
Flack parameter	0.00(3)

7.3 NMR spectra

MOM-Protected Acetyl Phloroglucinol 69

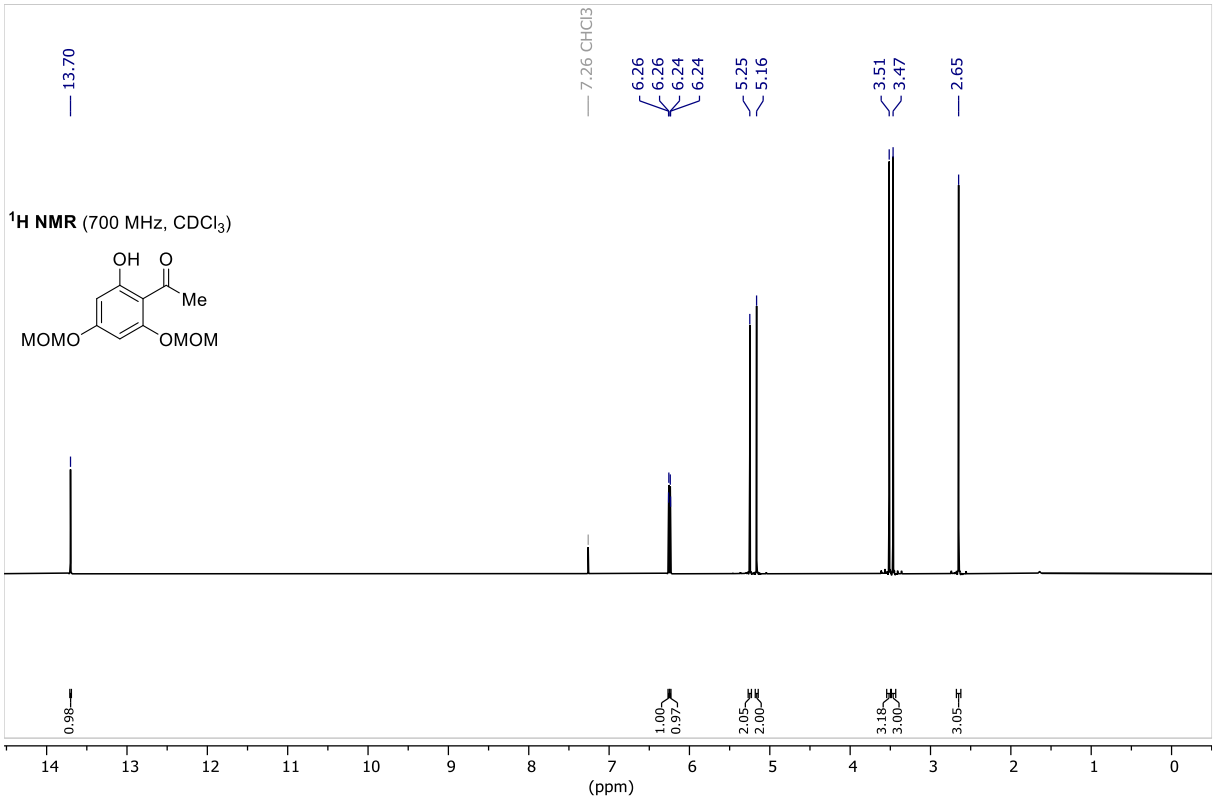

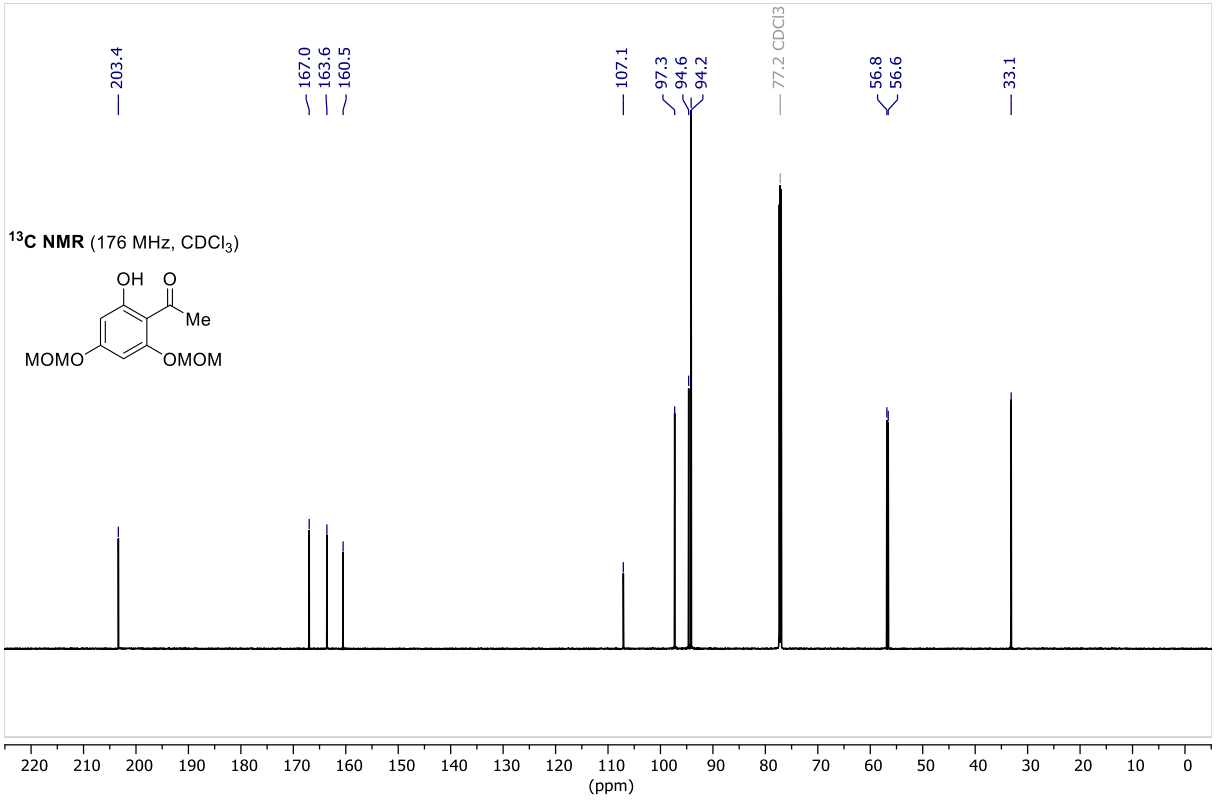

MOM-Protected Cinnamoyl Phloroglucinol 70

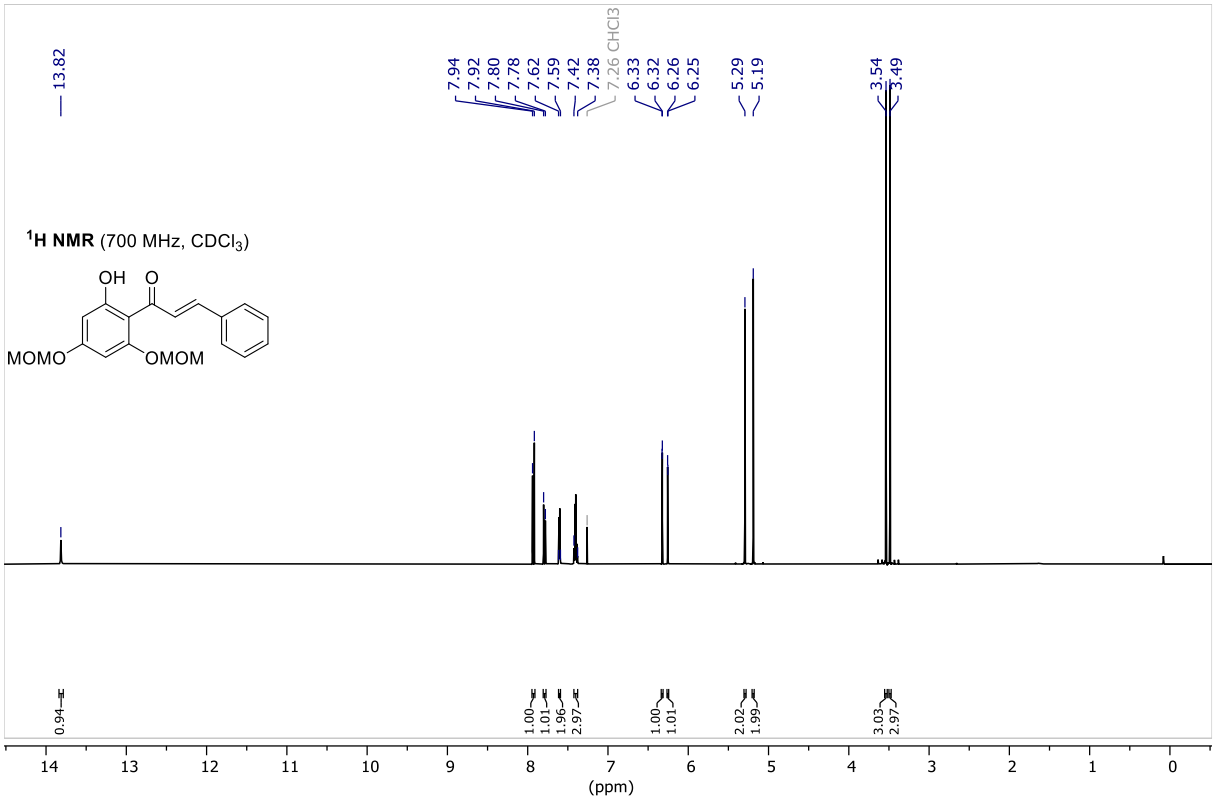

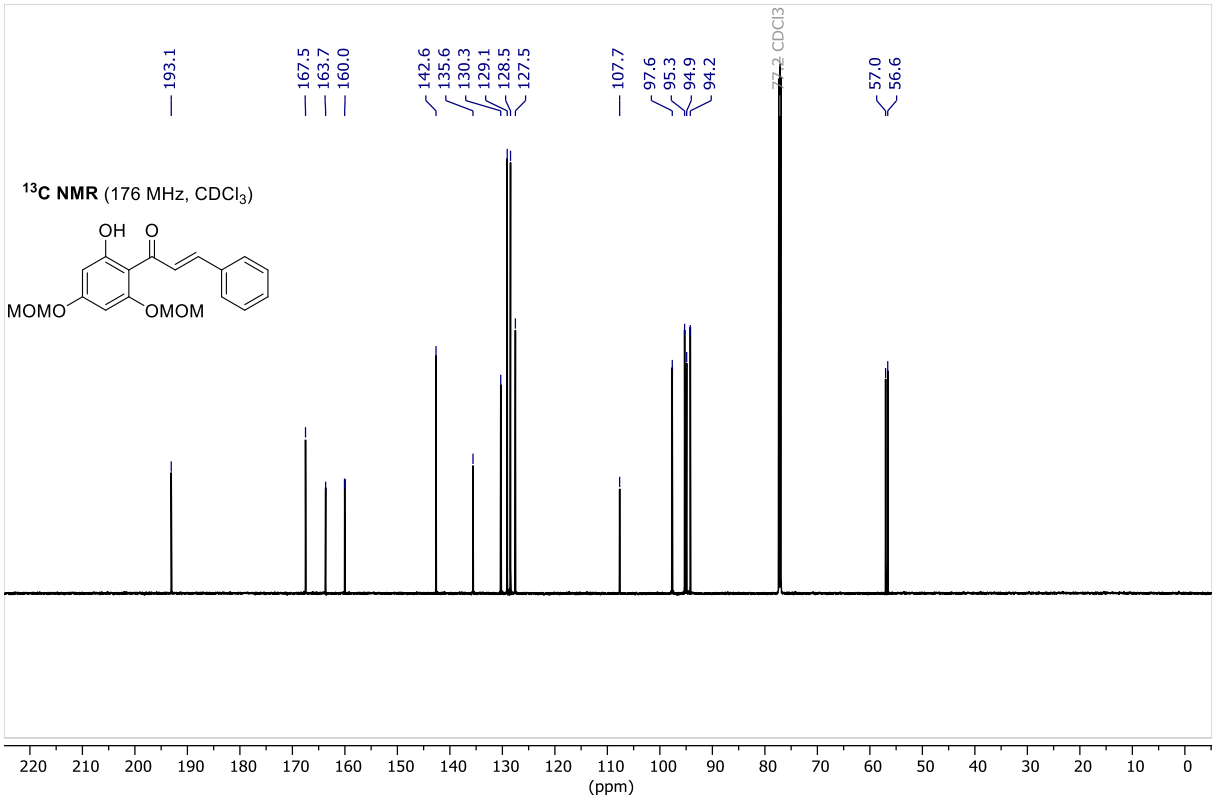

Cinnamoyl Phloroglucinol 71

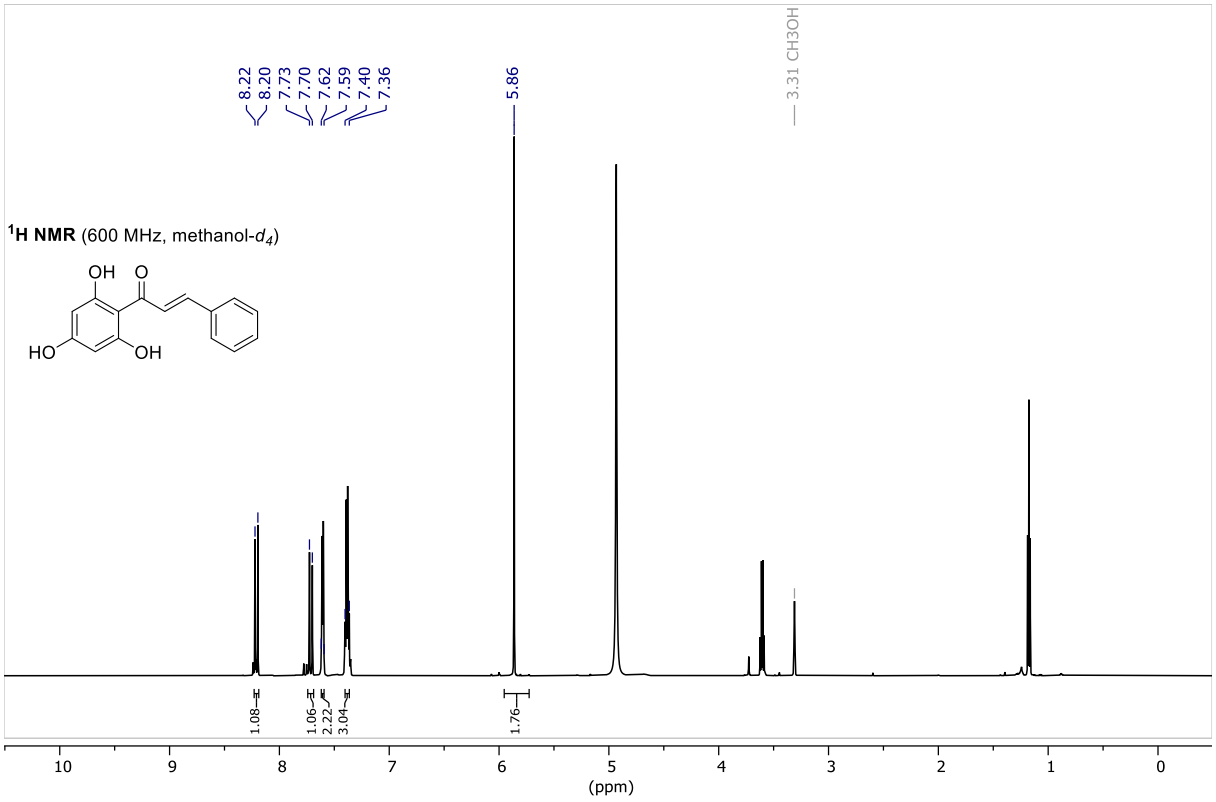

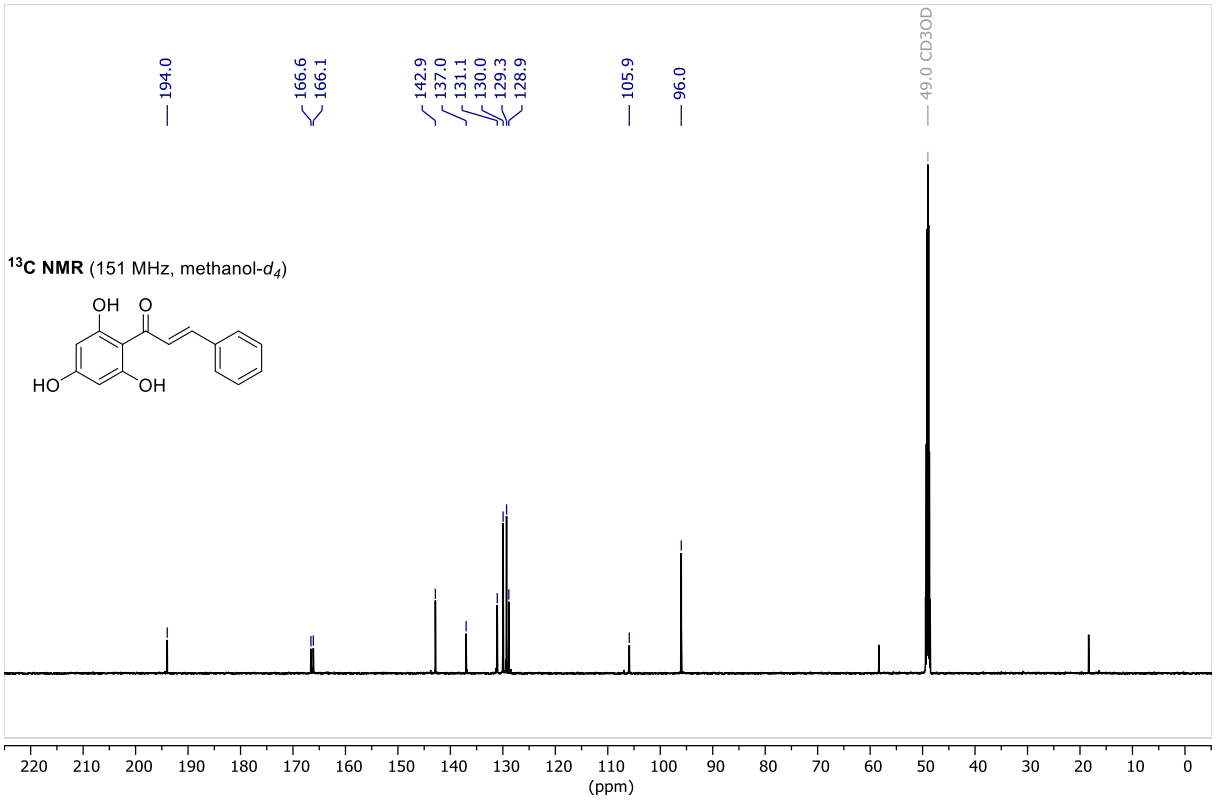

Methylated Acetyl Phloroglucinol 66 (Reproduced from Ref.[83] with permission from the Royal Society of Chemistry.)

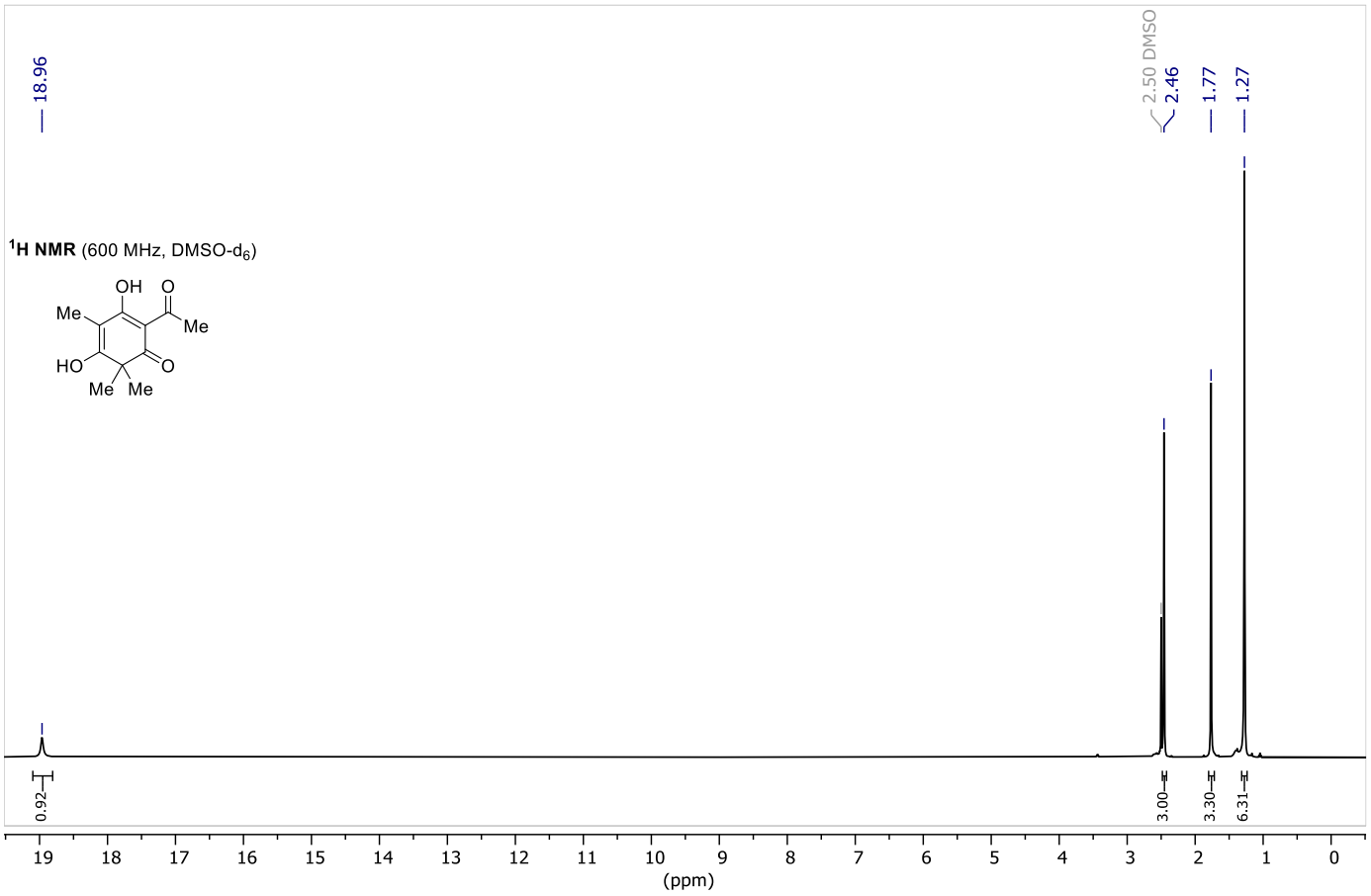

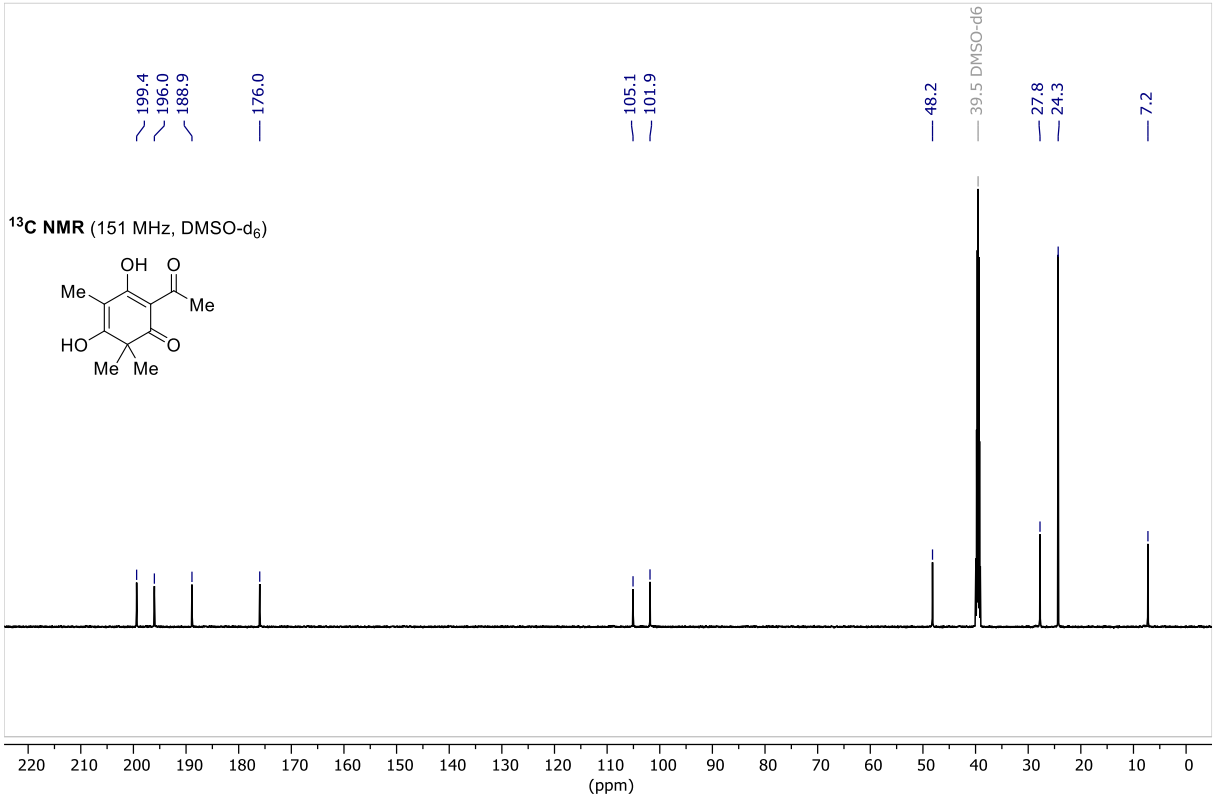

MOM-Protected Methylated Acetyl Phloroglucinol 72

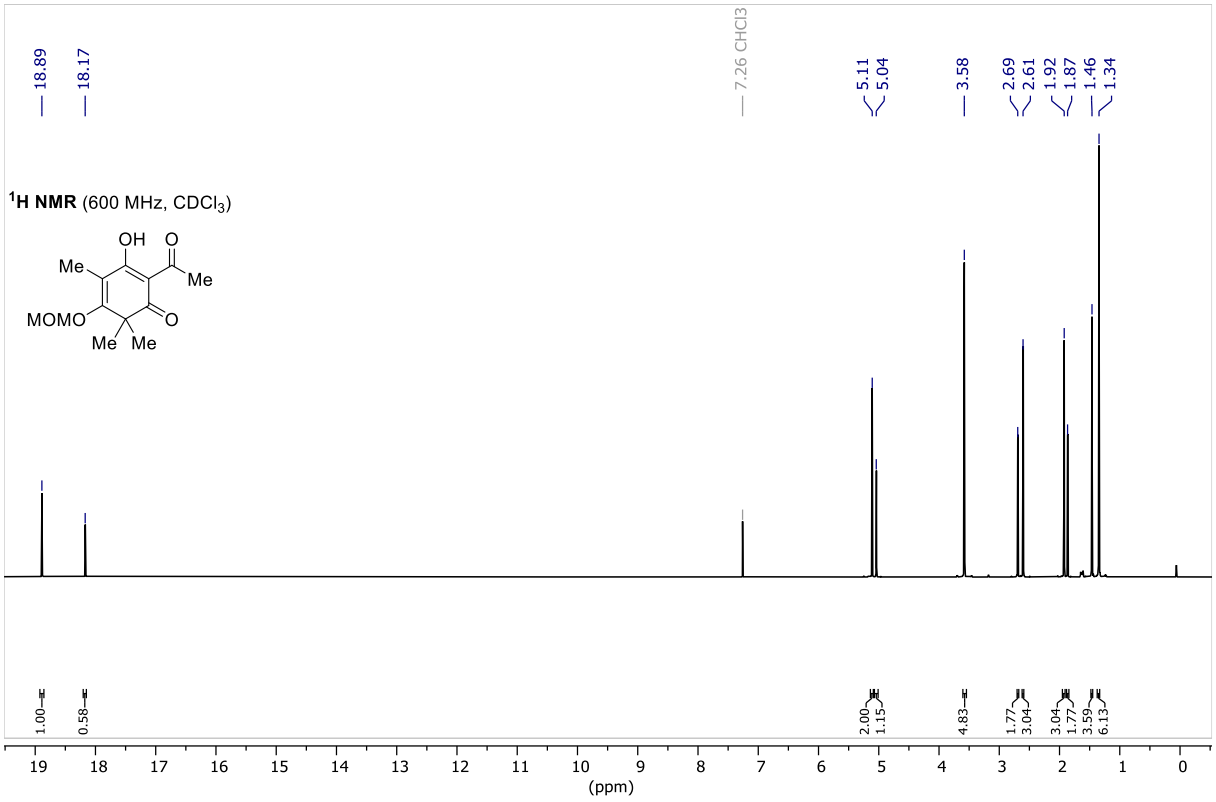

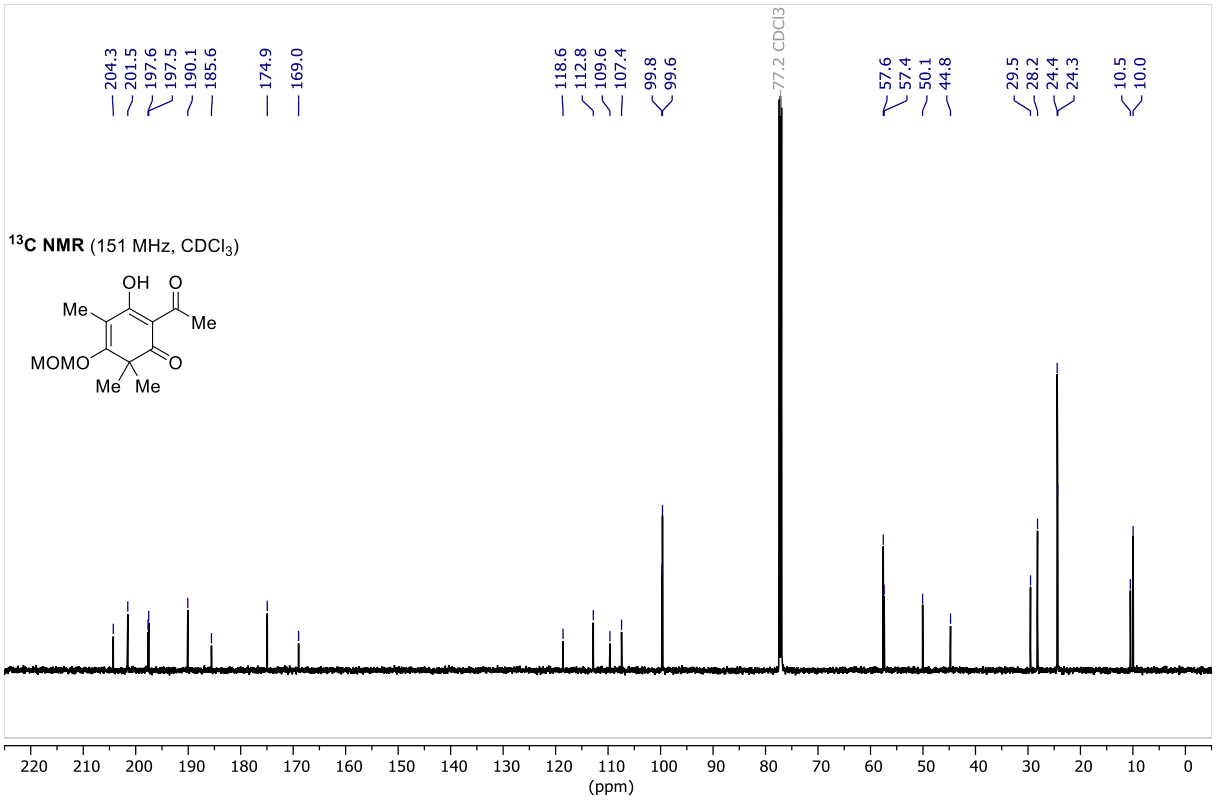

MOM-Protected Methylated Cinnamoyl Phloroglucinol 73

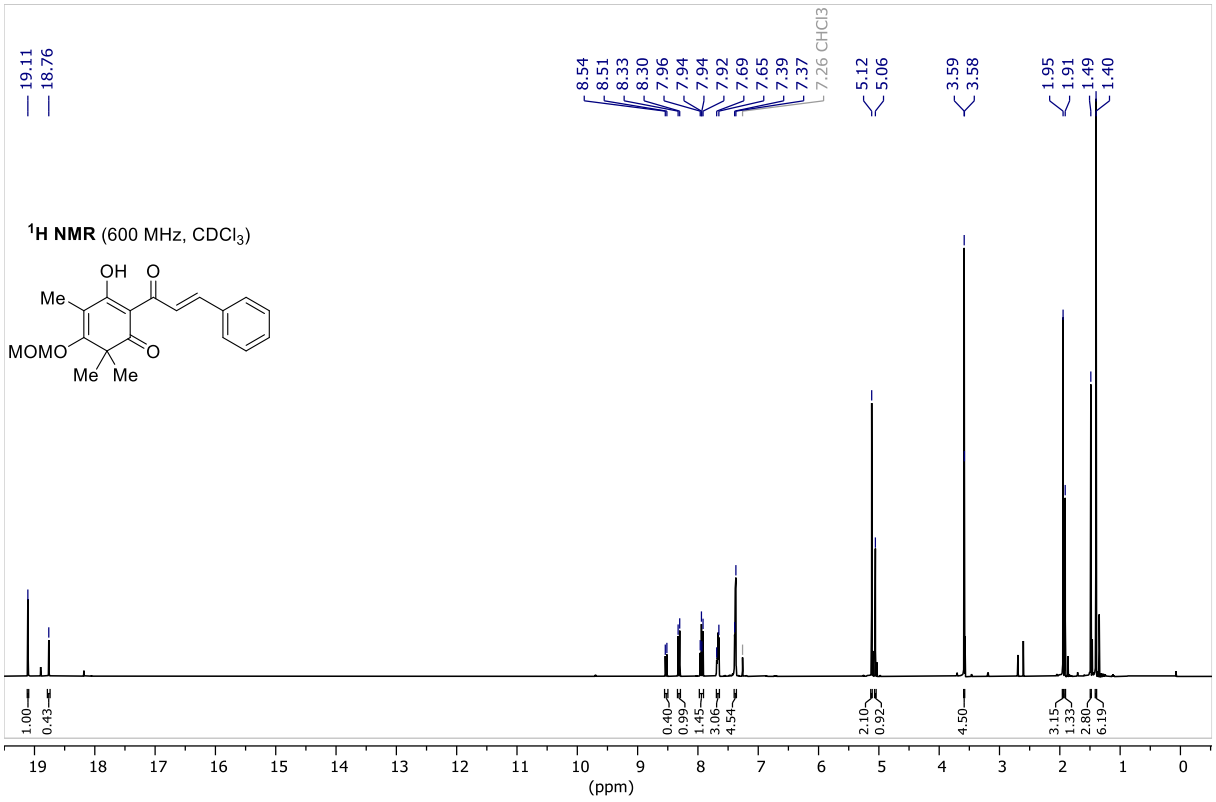

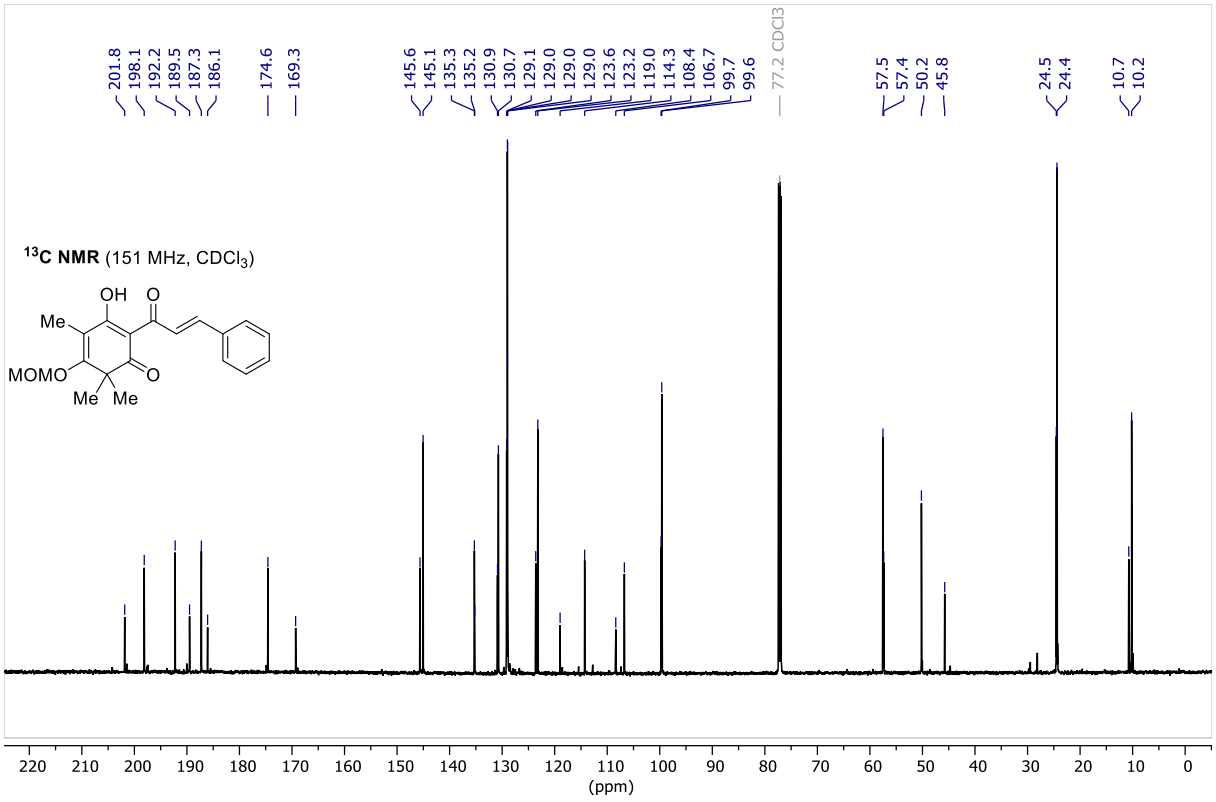

Champanone B (25)

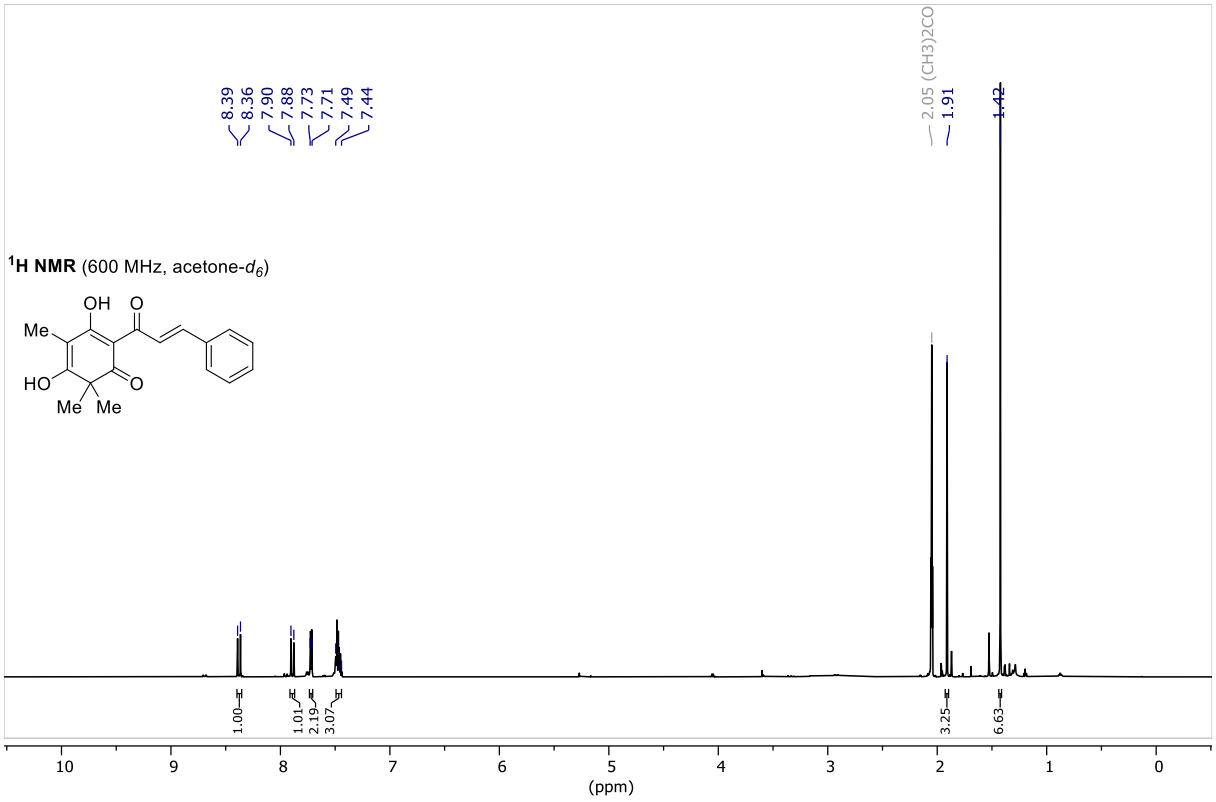

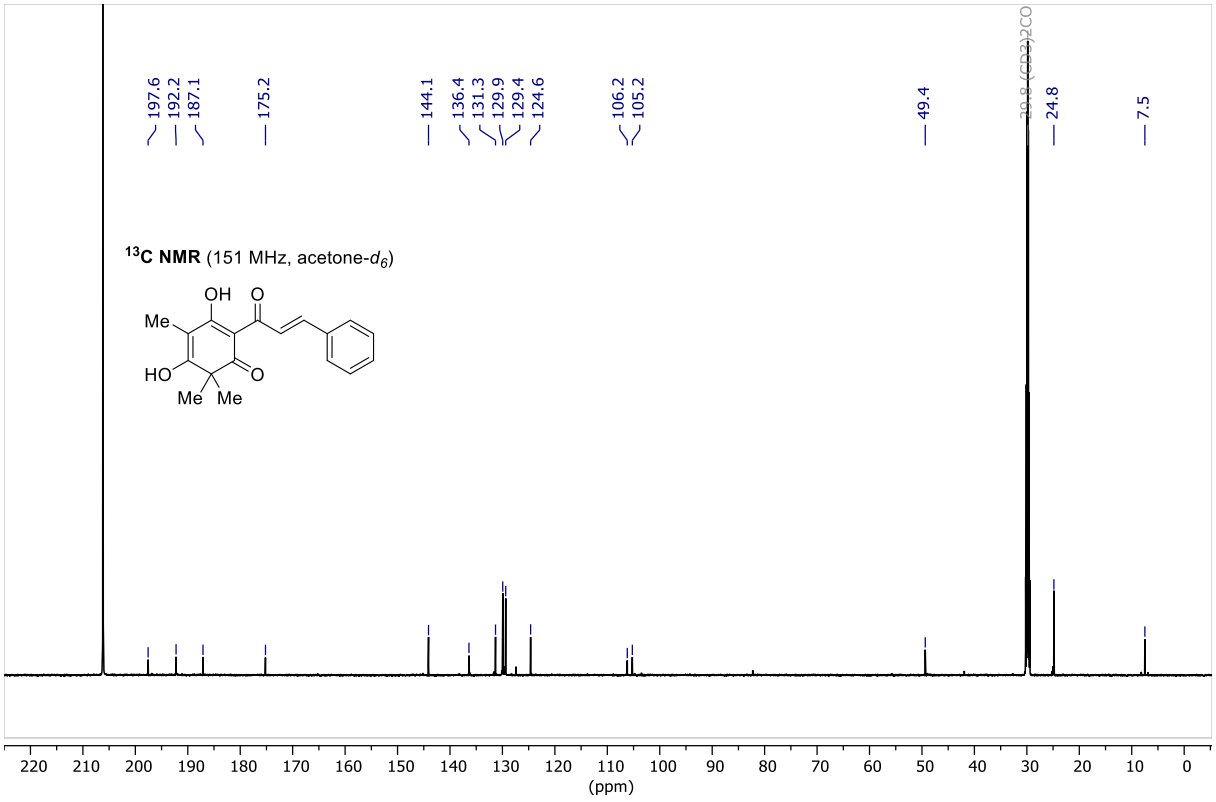

Allyl Chloride 78

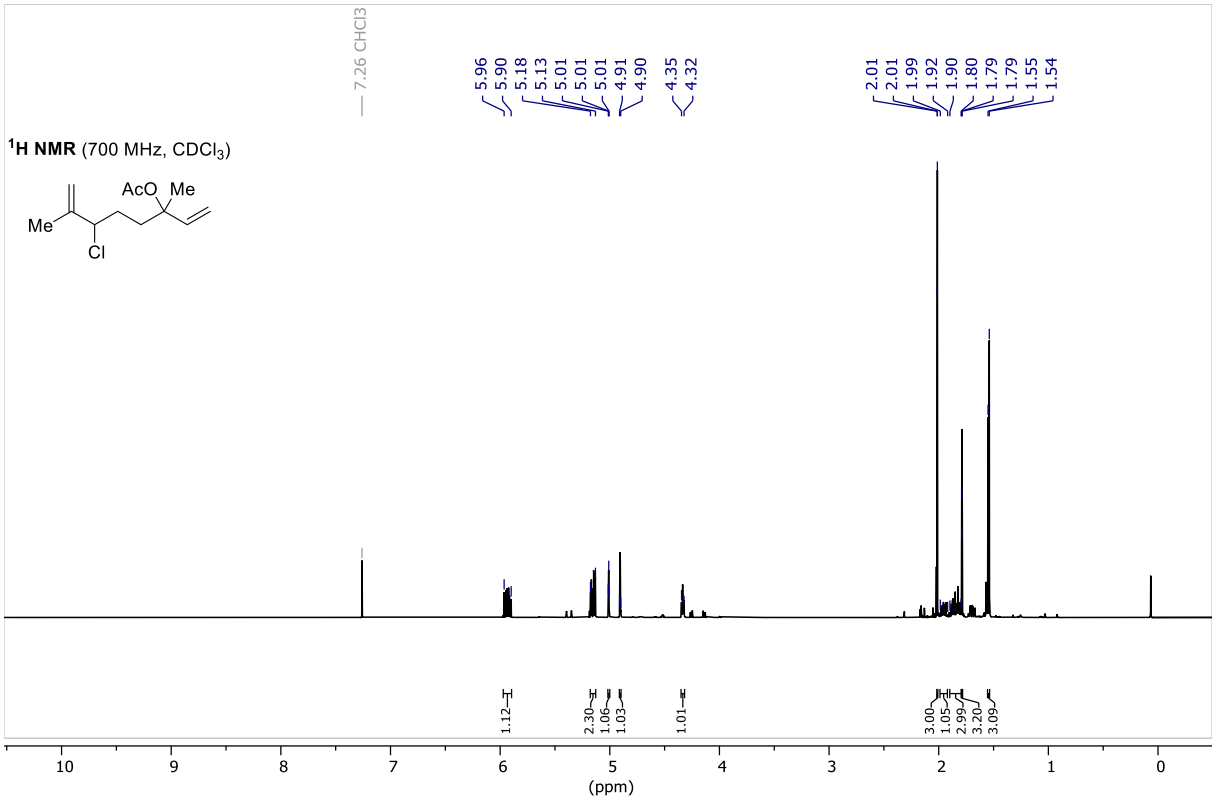

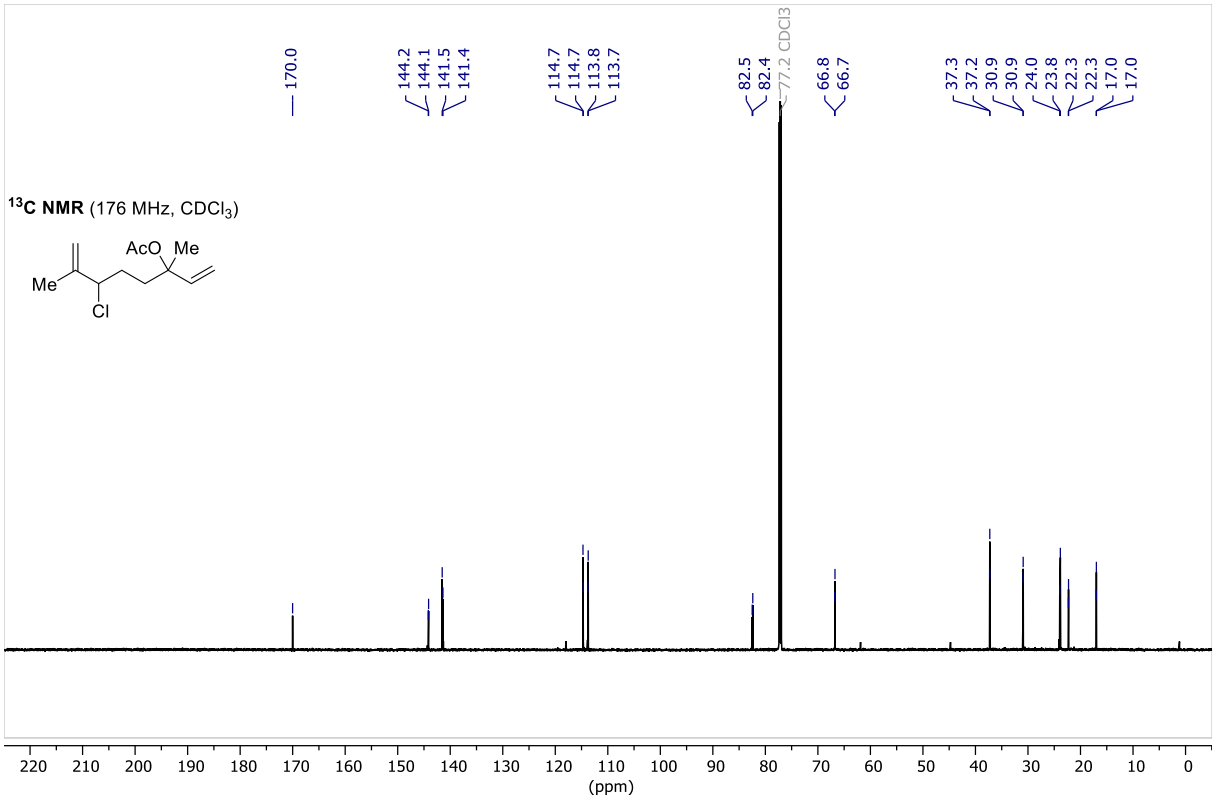

Hotrienyl Acetate (79)

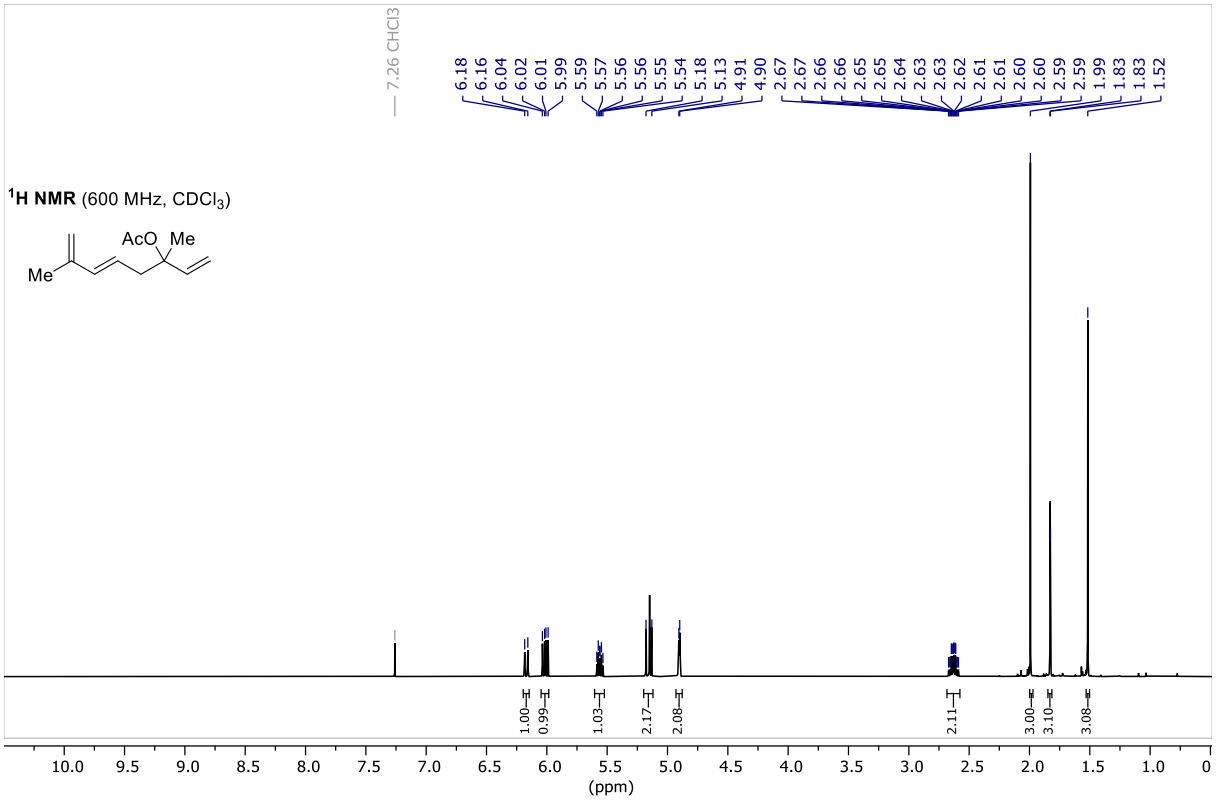

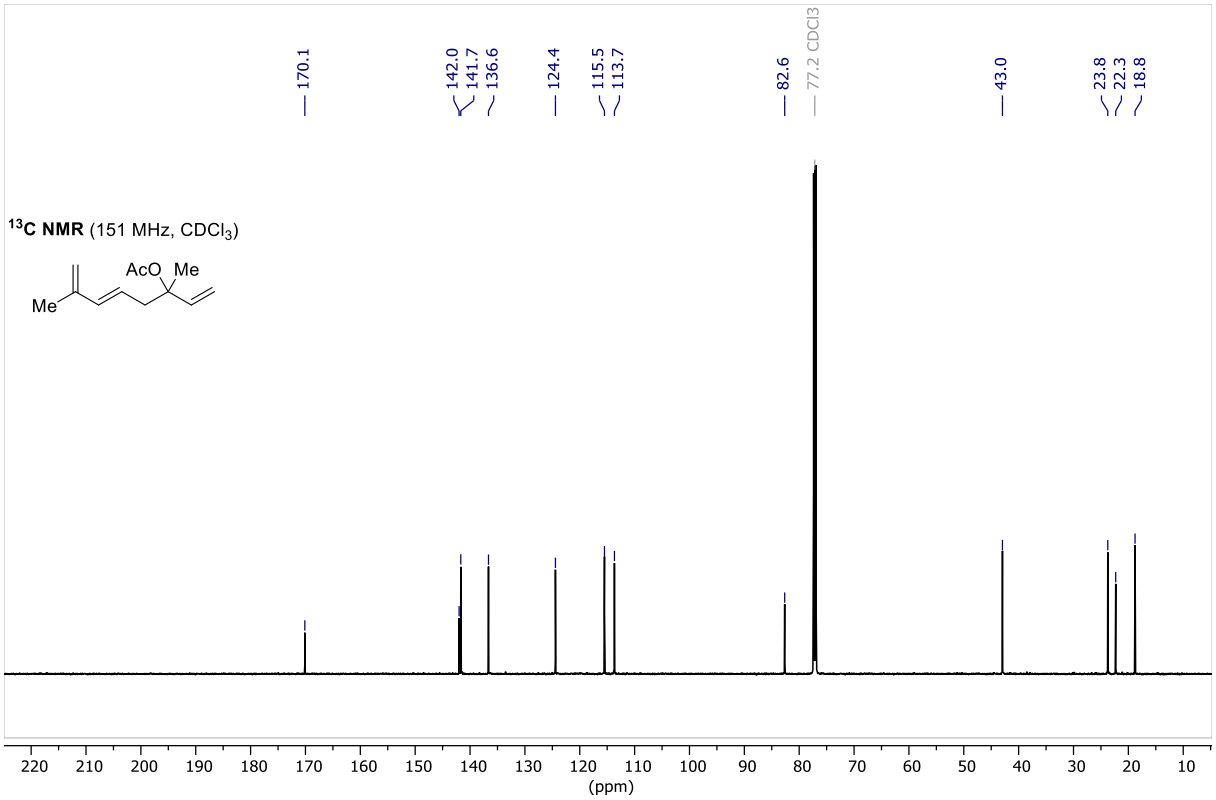

Hotrienol (76)

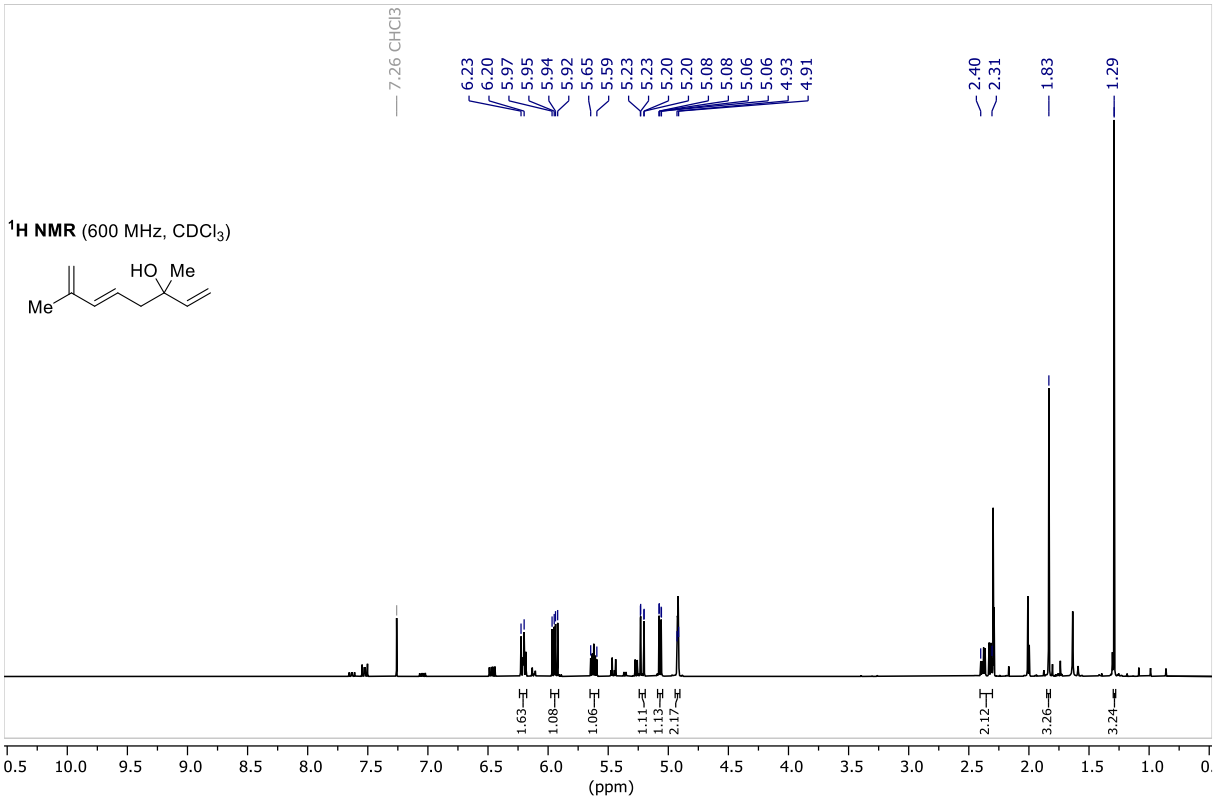

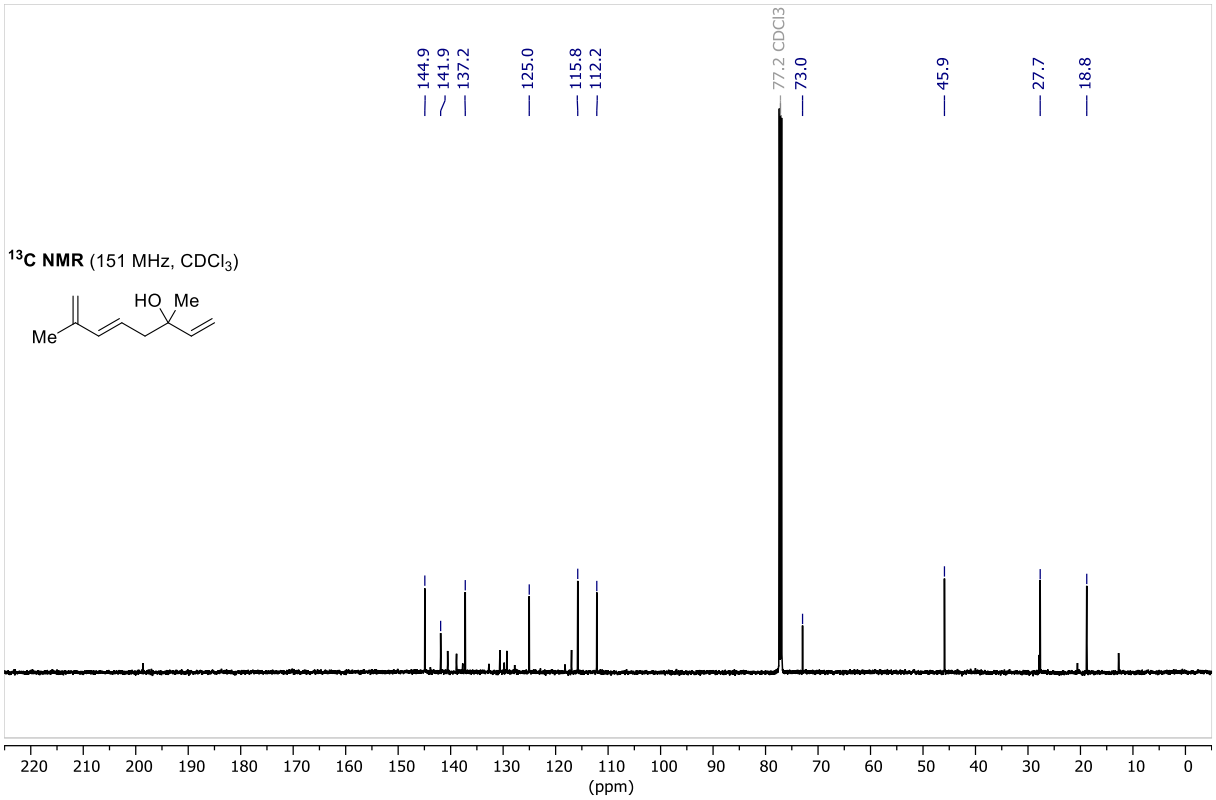

Hotrienol *tert*-Butyl Carbonate (80)

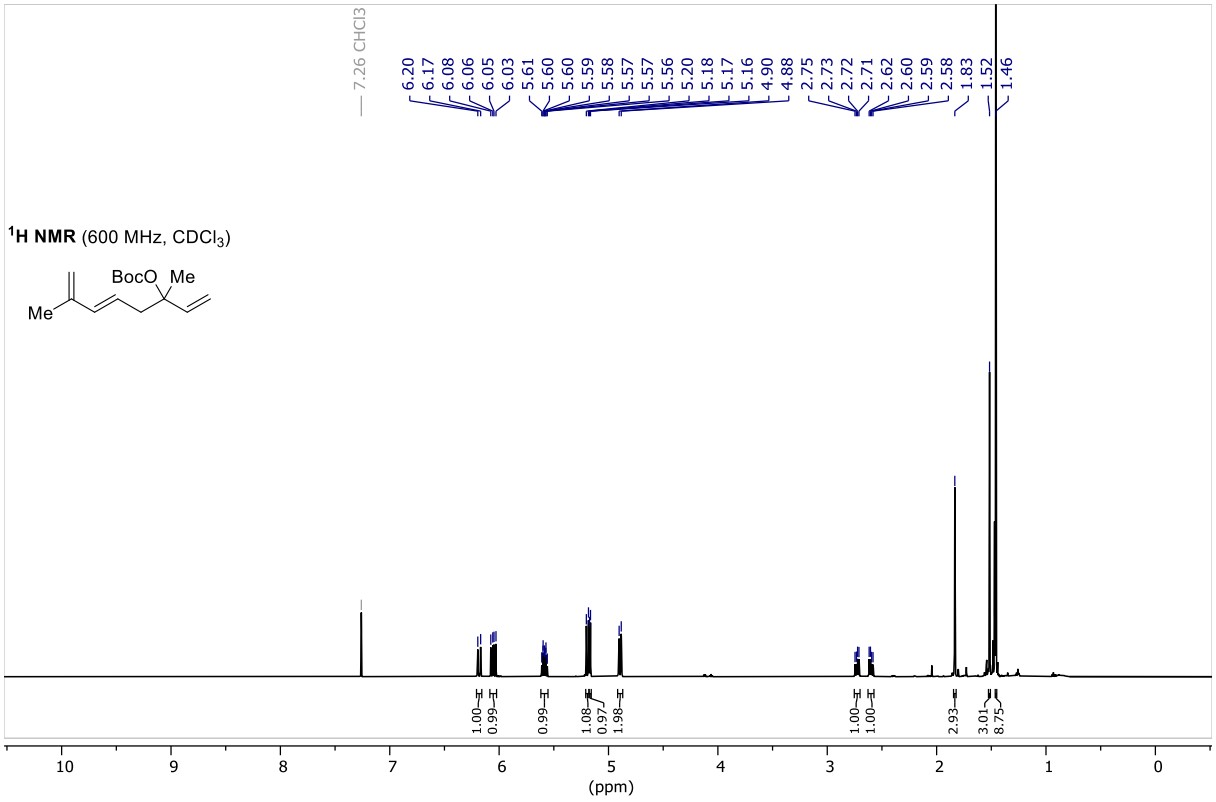

Allylic Chloride 82 (Reproduced from Ref.[83] with permission from the Royal Society of Chemistry.)

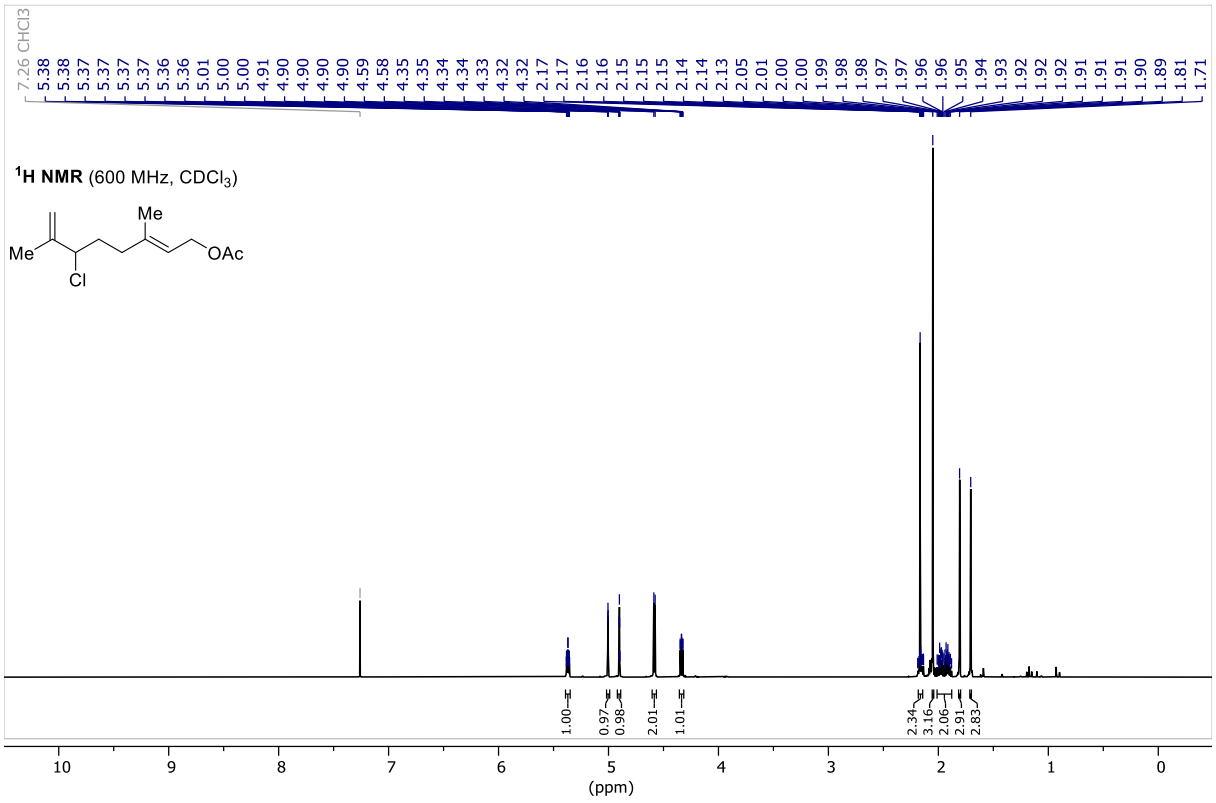

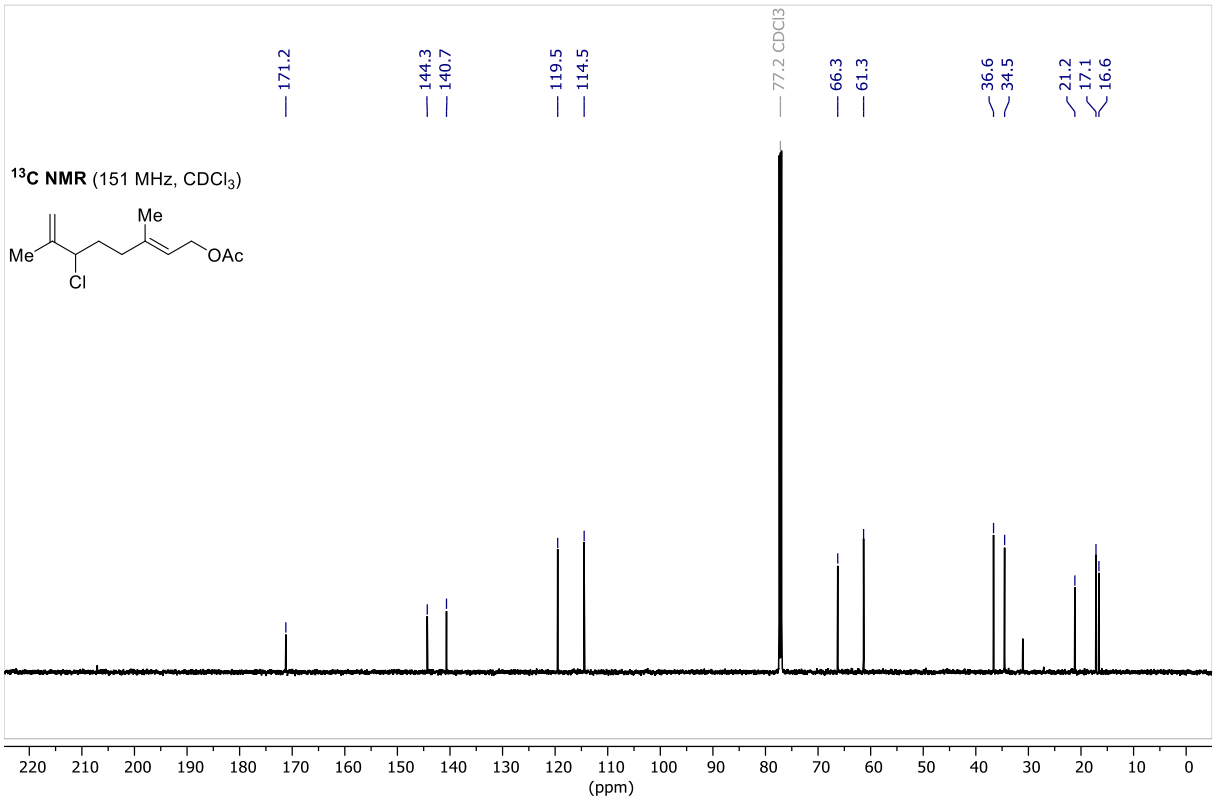

Diene 83 (Reproduced from Ref.[83] with permission from the Royal Society of Chemistry.)

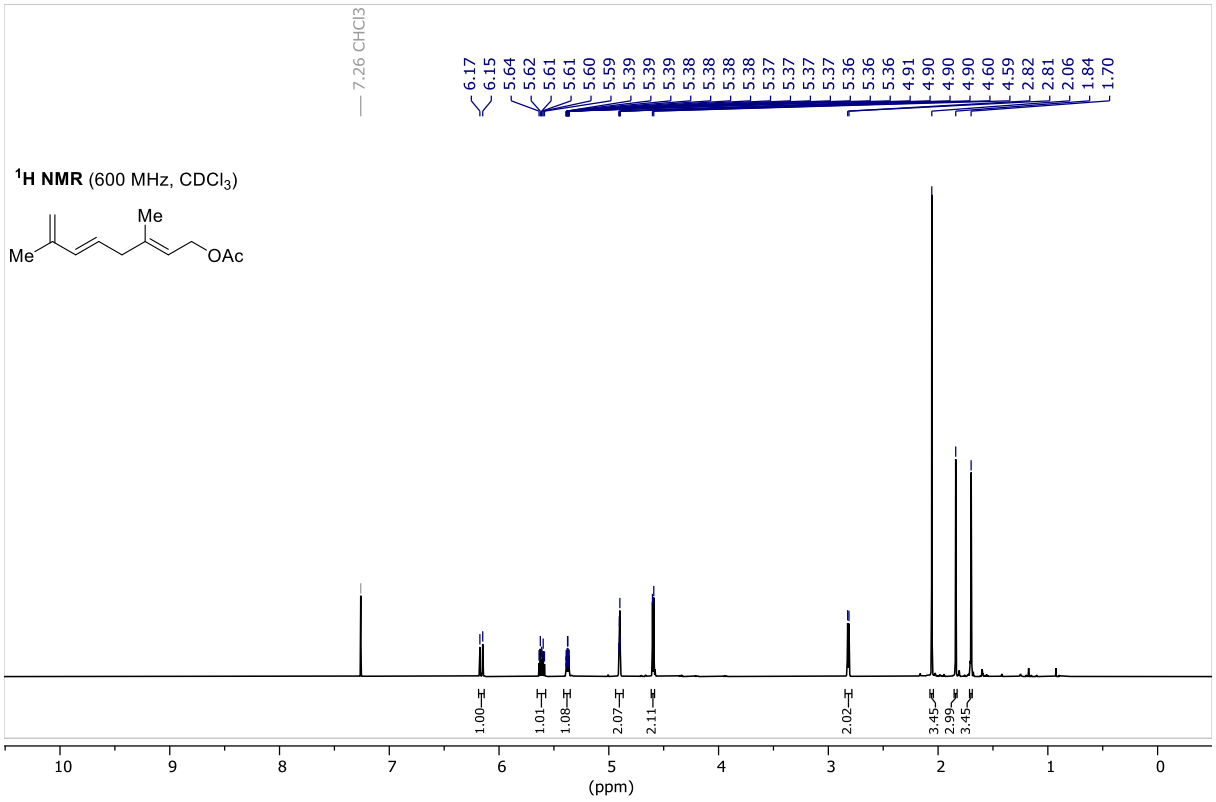

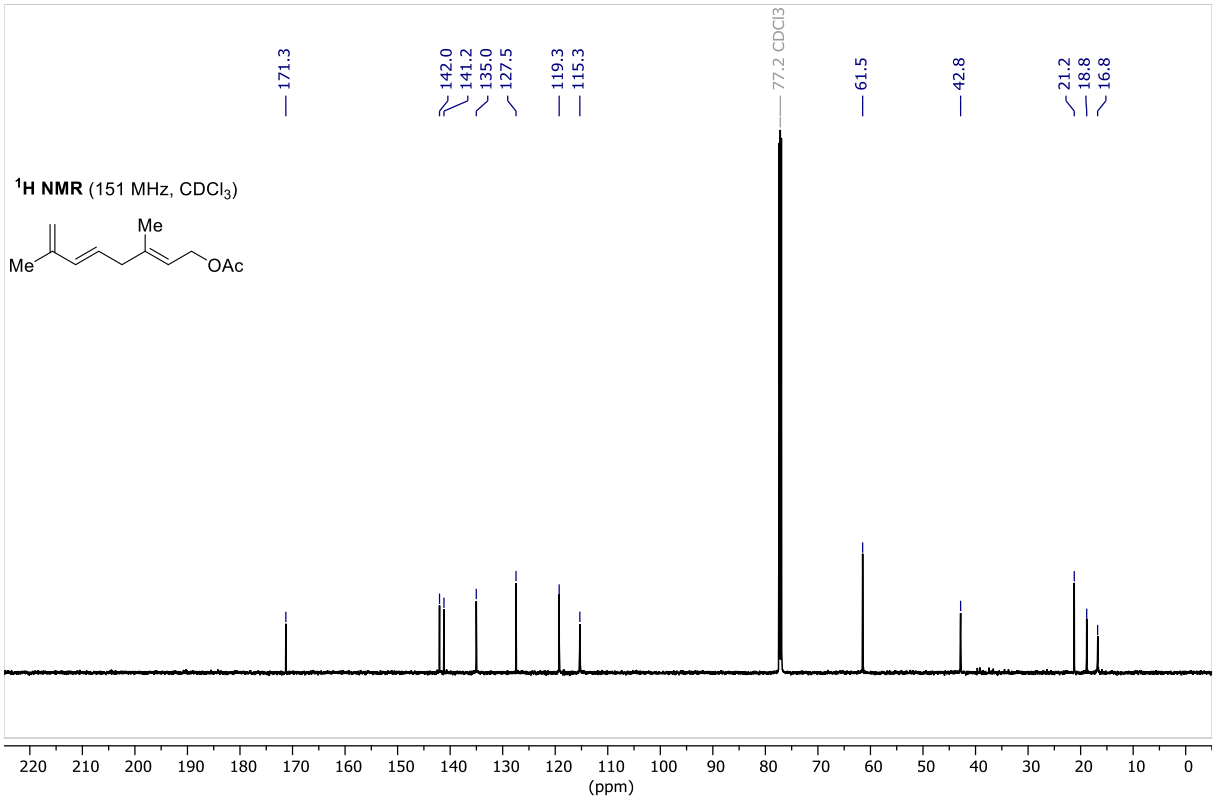

Allylic Alcohol 84

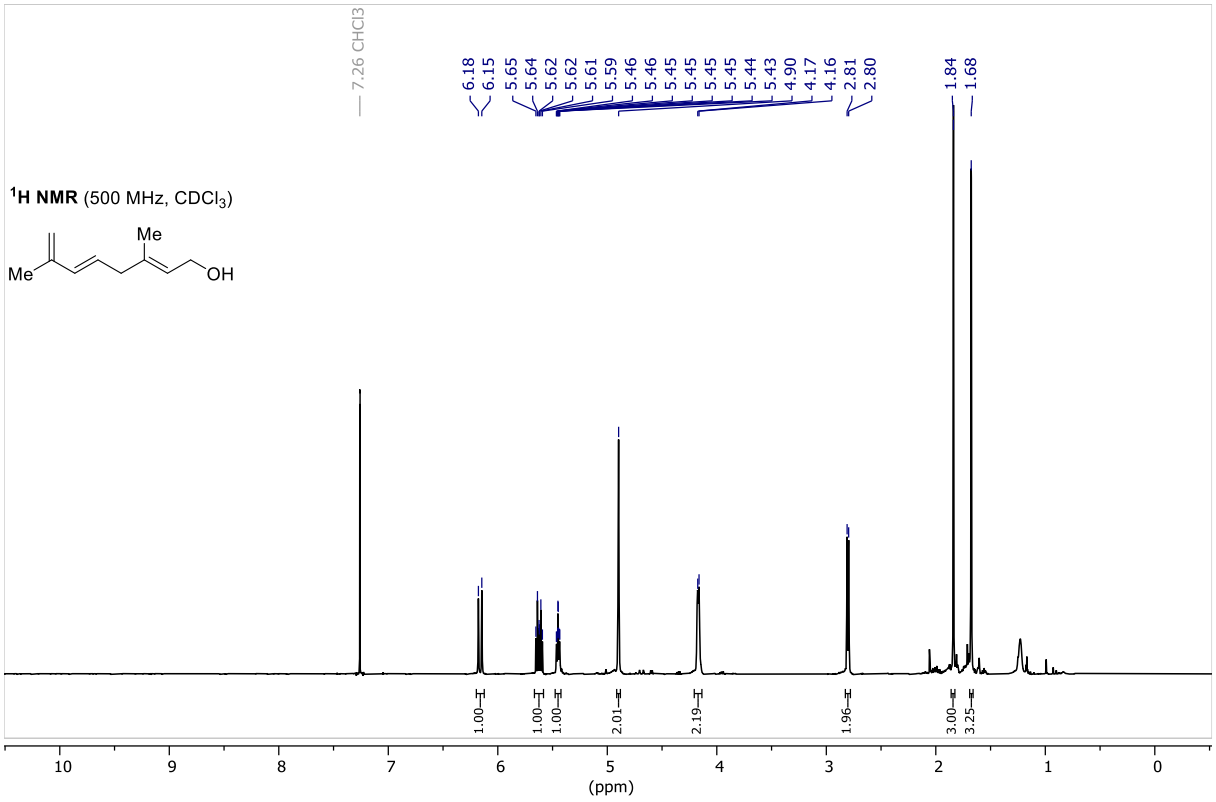

tert-Butyl Carbonate 85

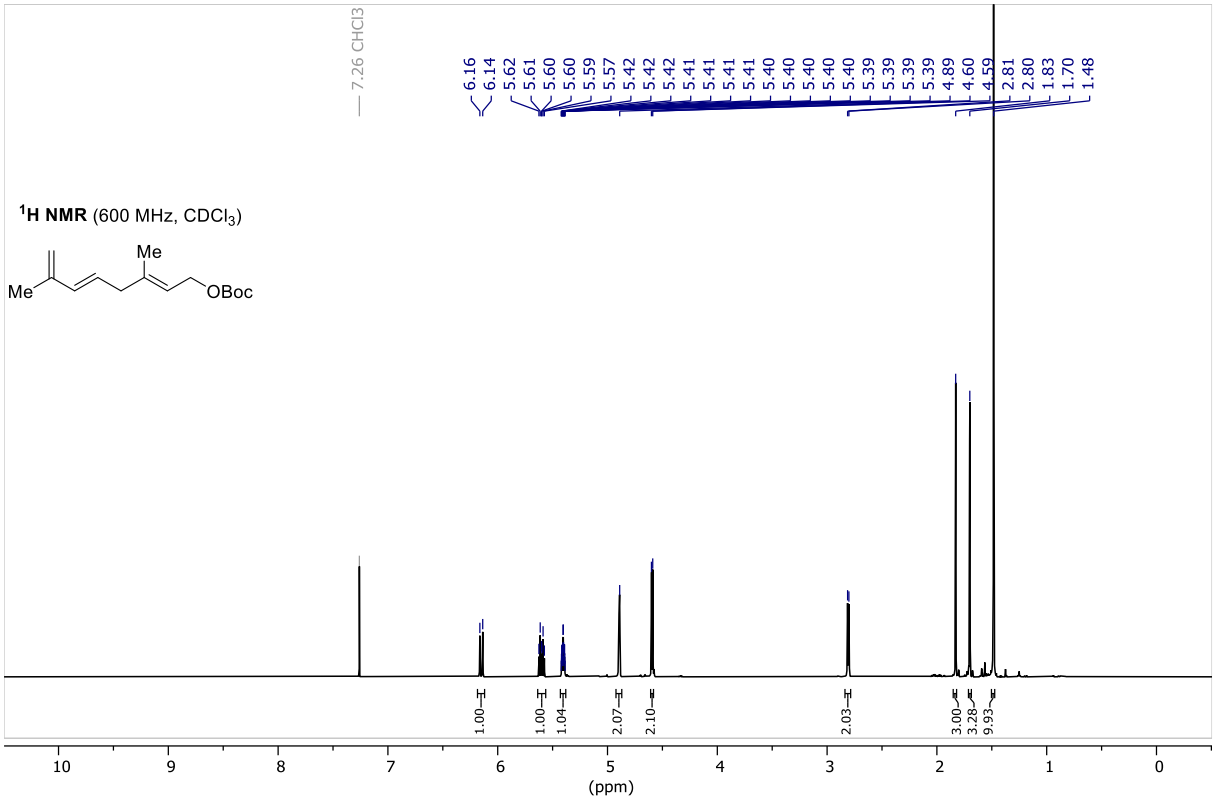

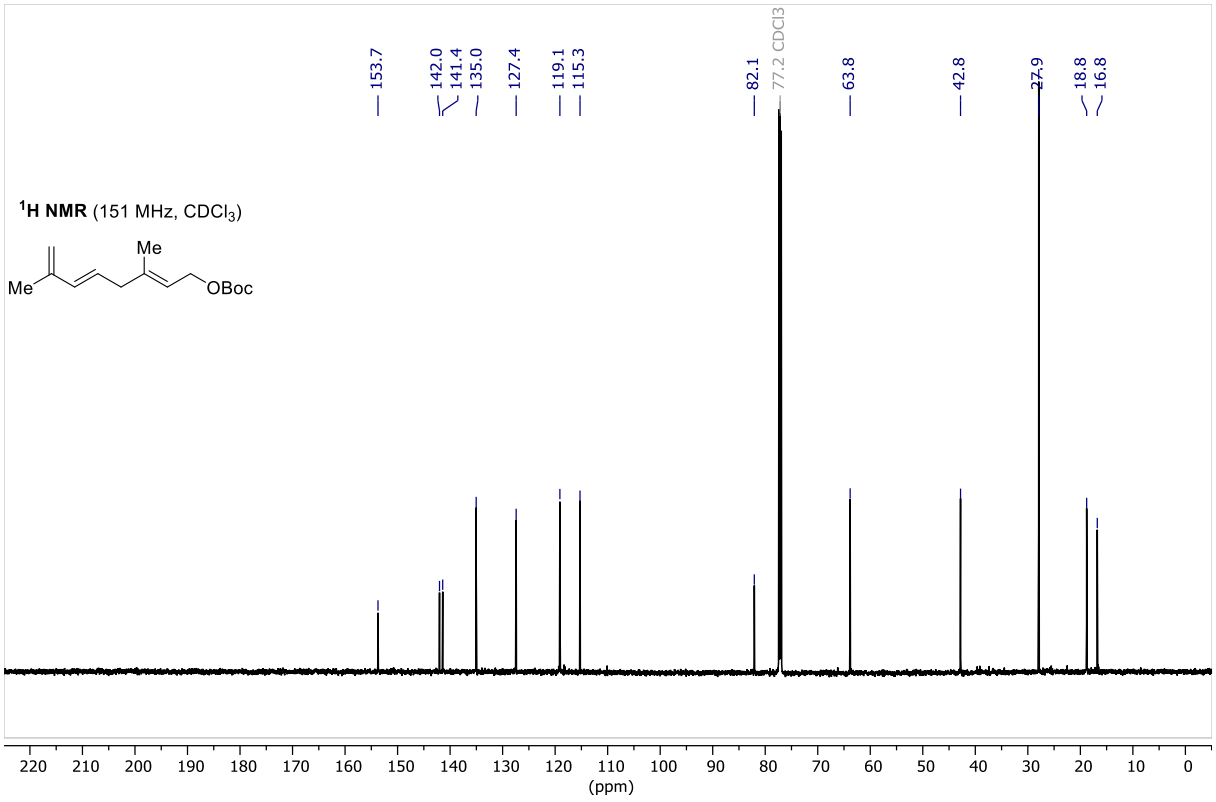

Geranyl *tert*-Butyl Carbonate 91

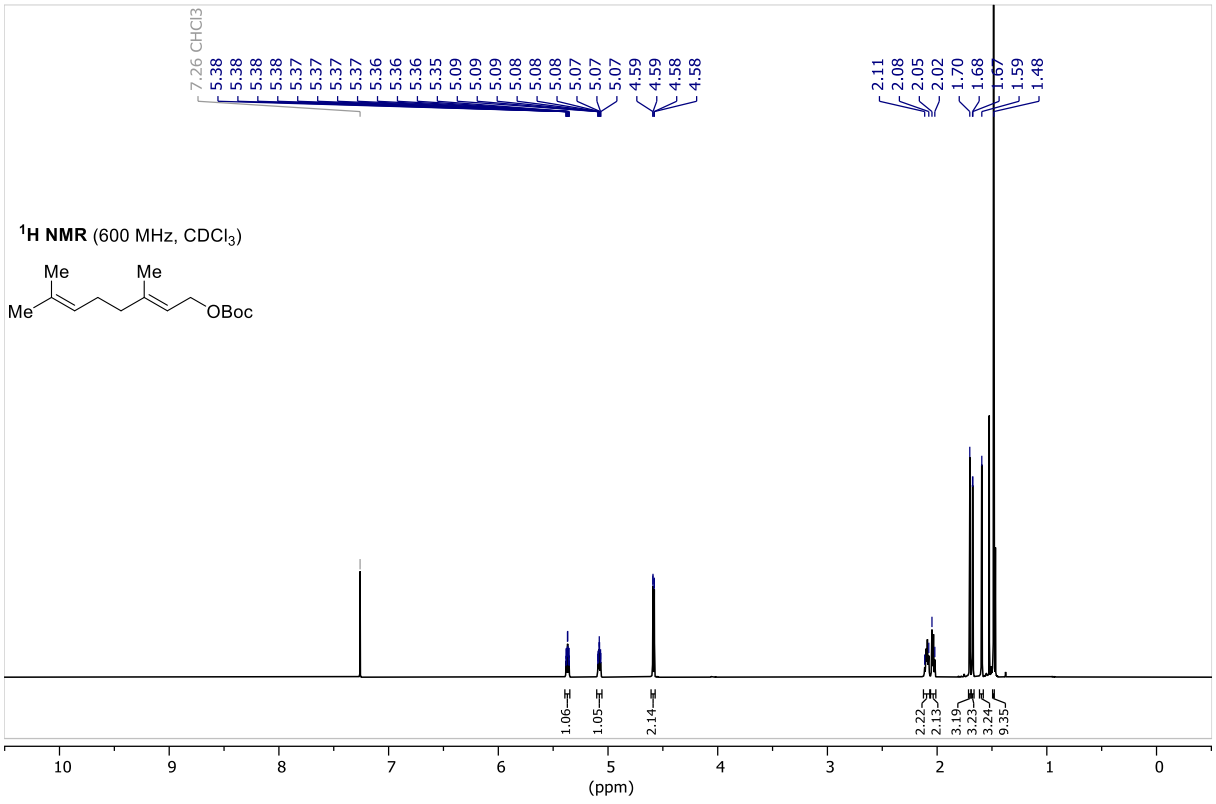

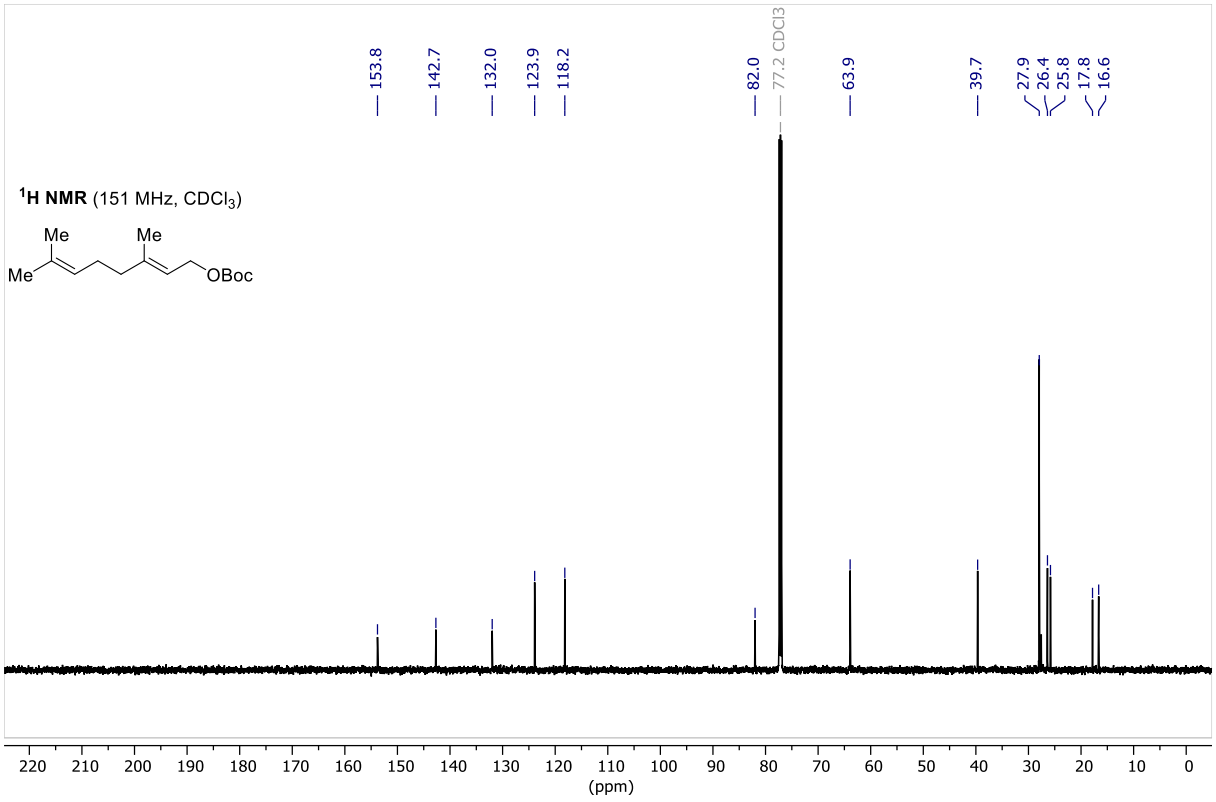

Linalyl *tert*-Butyl Carbonate 86

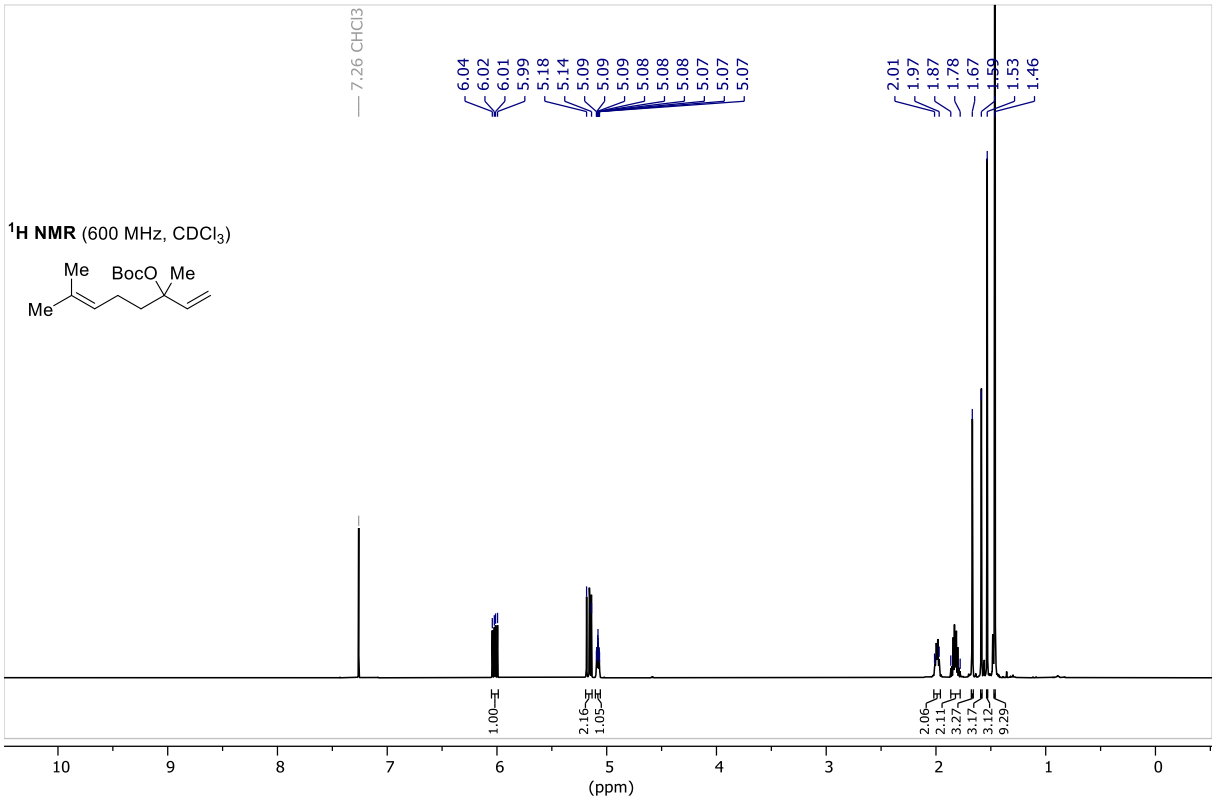

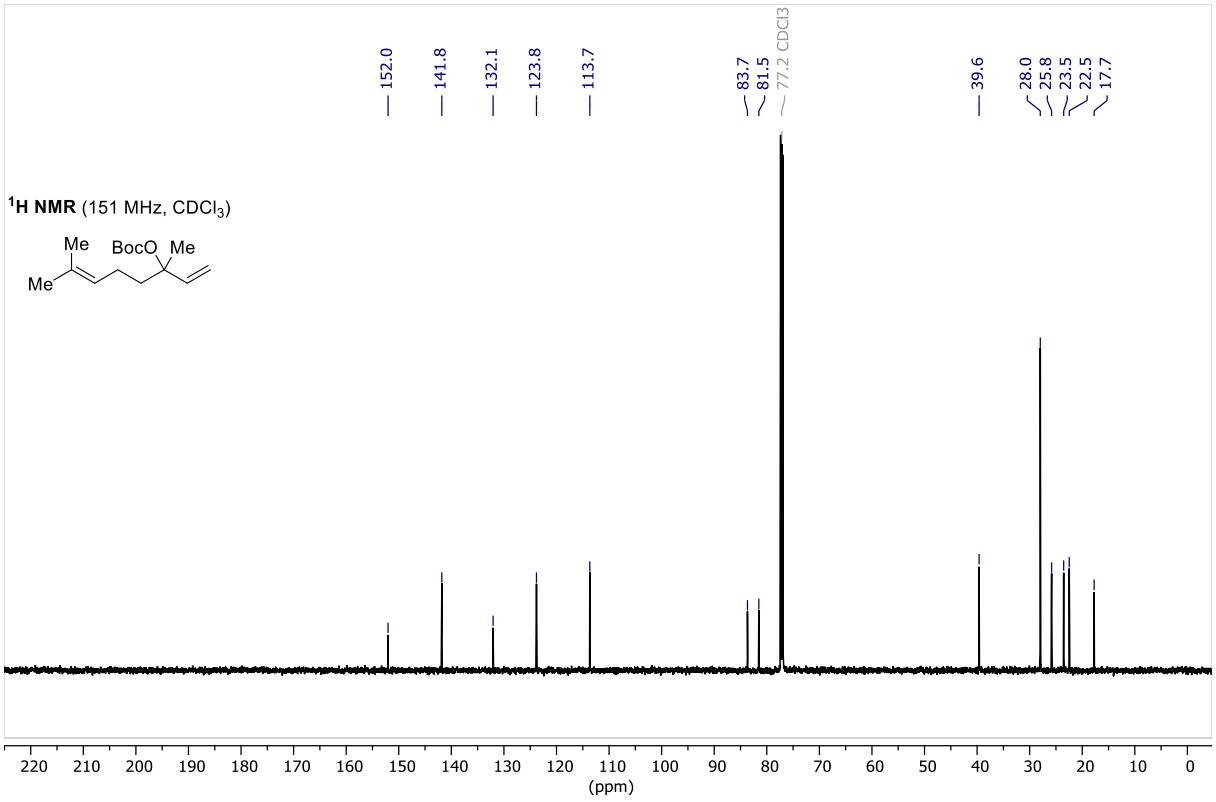

Geranylated Acetyl Phloroglucinol 90 (Reproduced from Ref.[83] with permission from the Royal Society of Chemistry.)

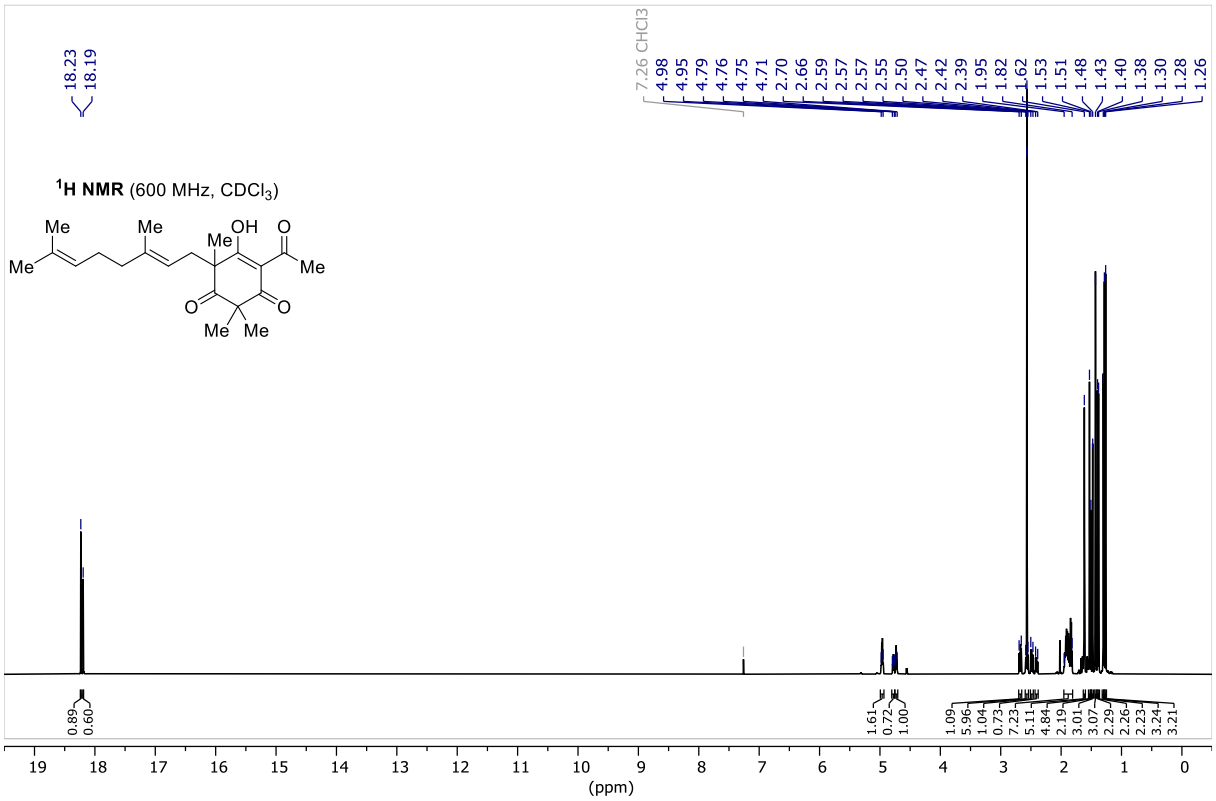

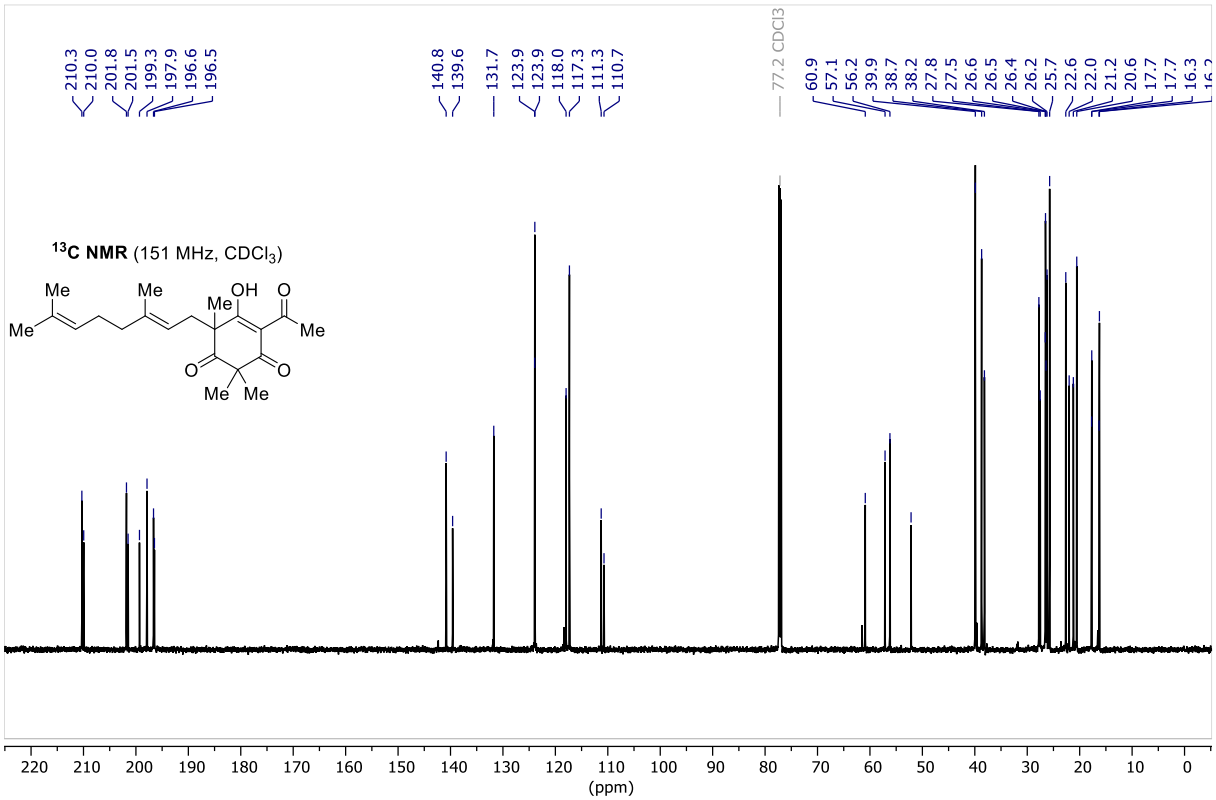

Alyllic Chloride 102

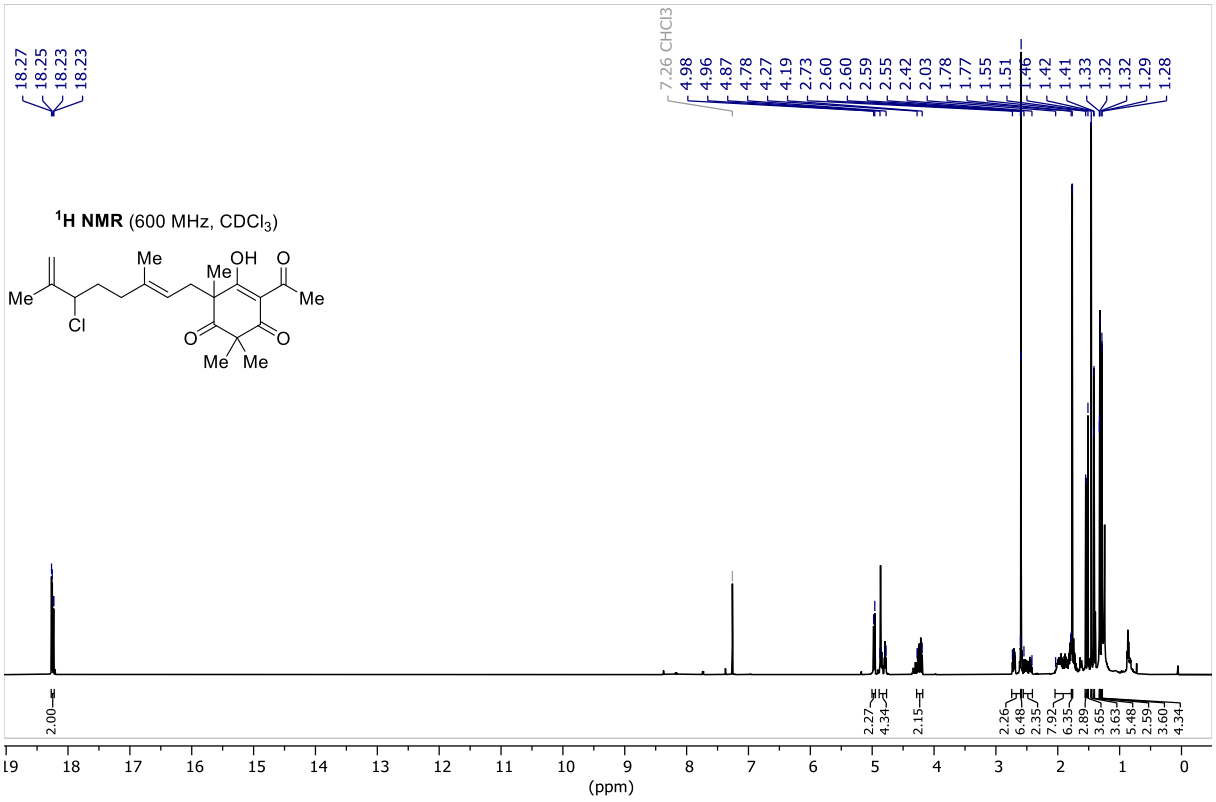

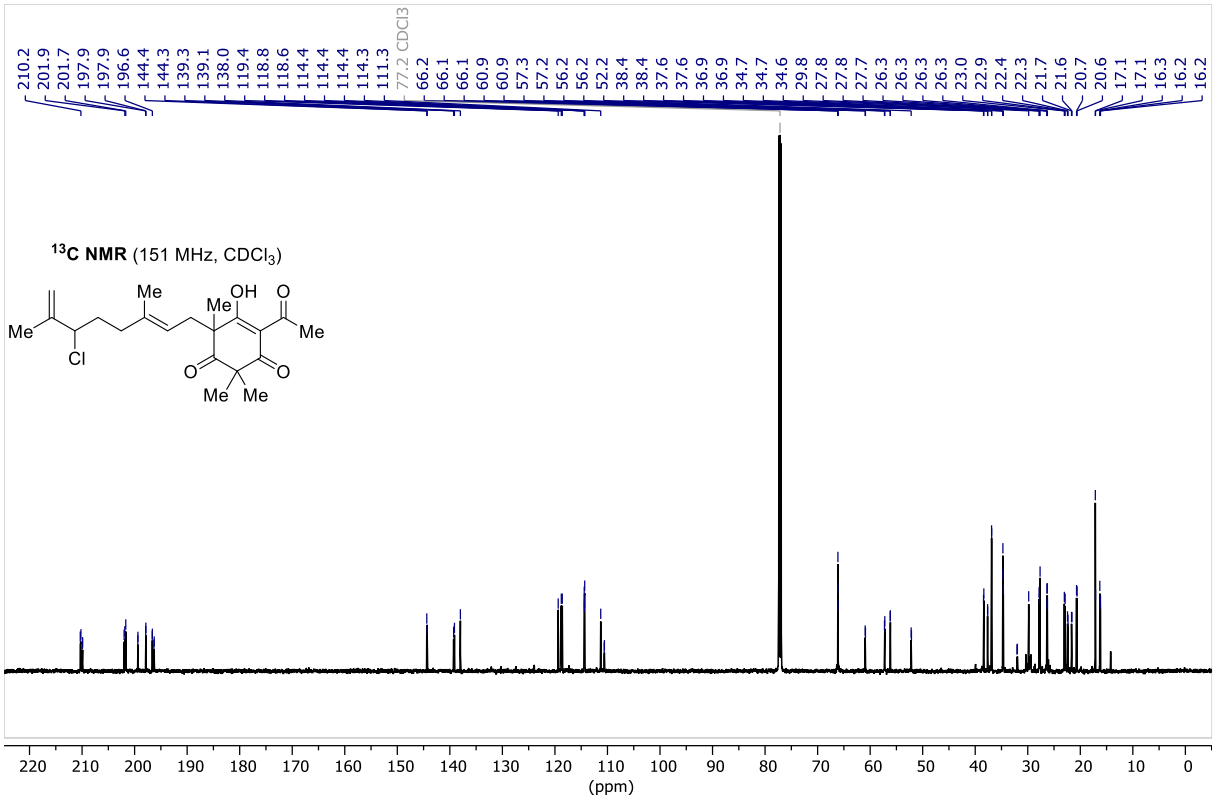

Geranylated Champanone B 34 (Reproduced from Ref.[83] with permission from the Royal Society of Chemistry.)

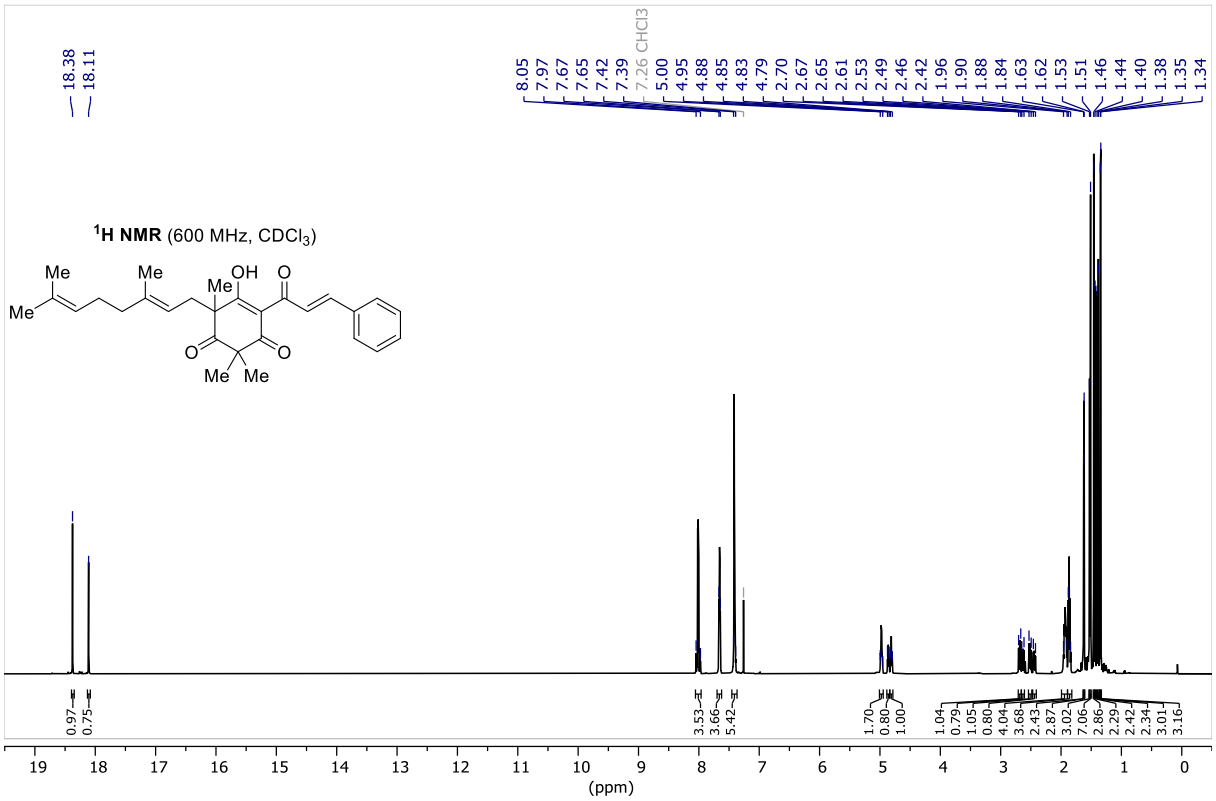

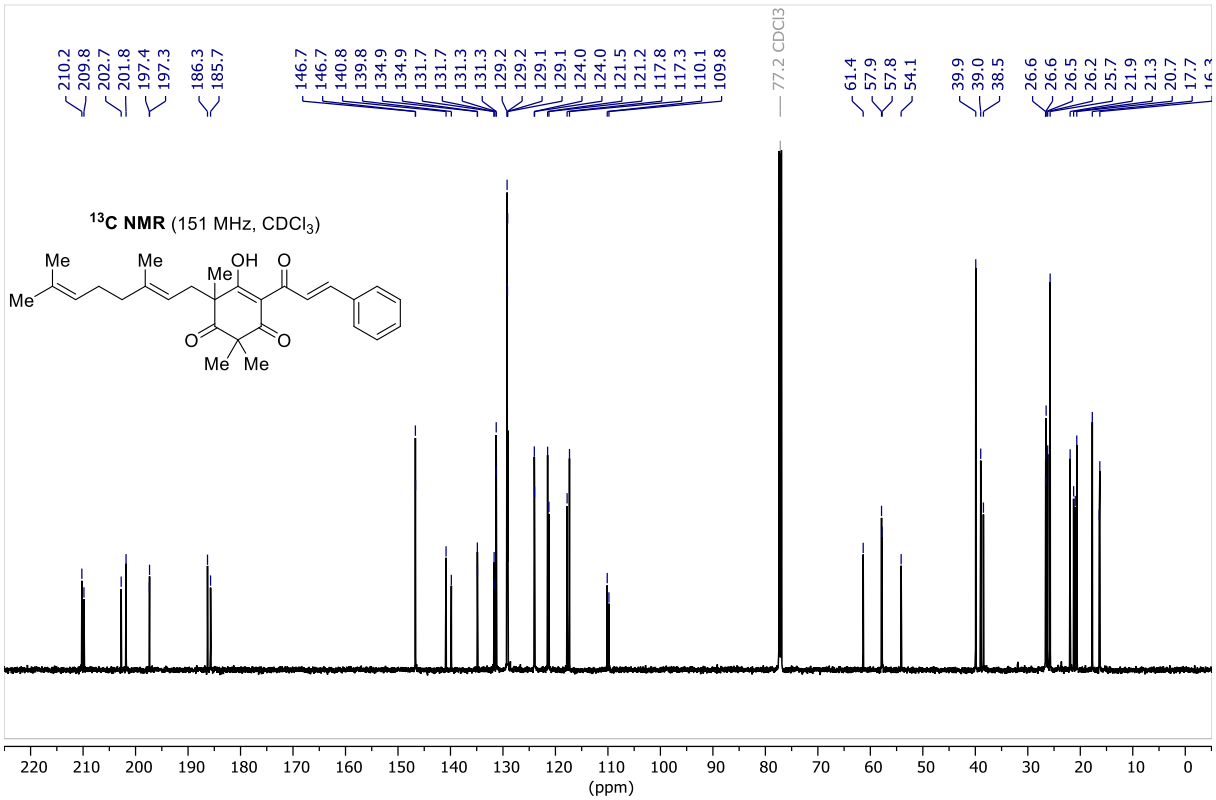

Allylic Chloride 103 (Reproduced from Ref.[83] with permission from the Royal Society of Chemistry.)

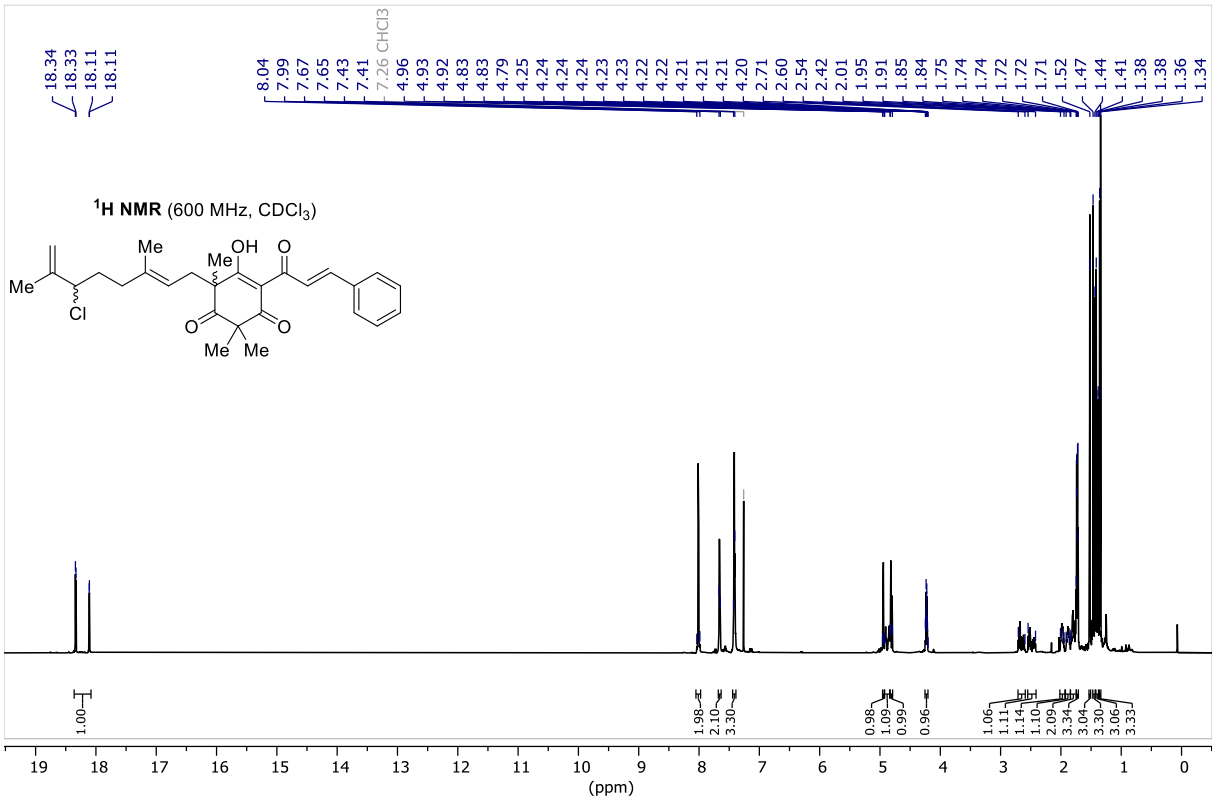

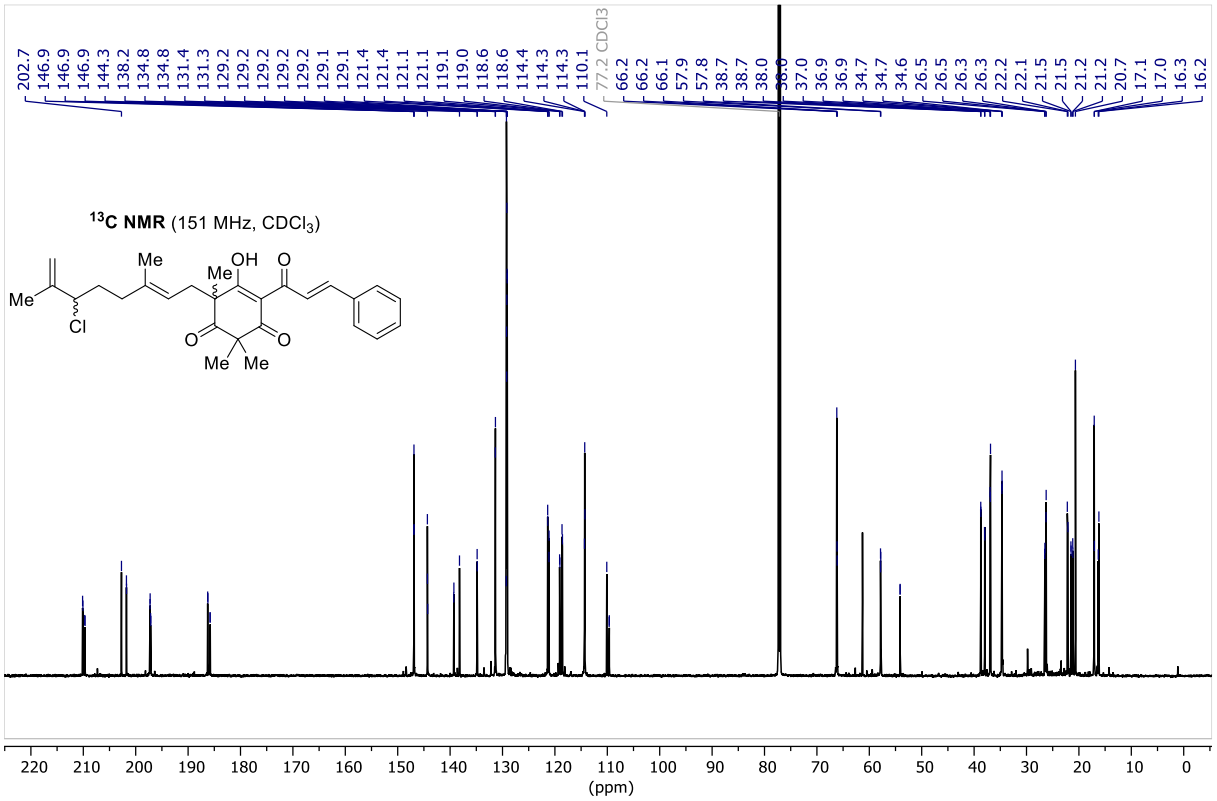

Diene 95 (Reproduced from Ref.[83] with permission from the Royal Society of Chemistry.)

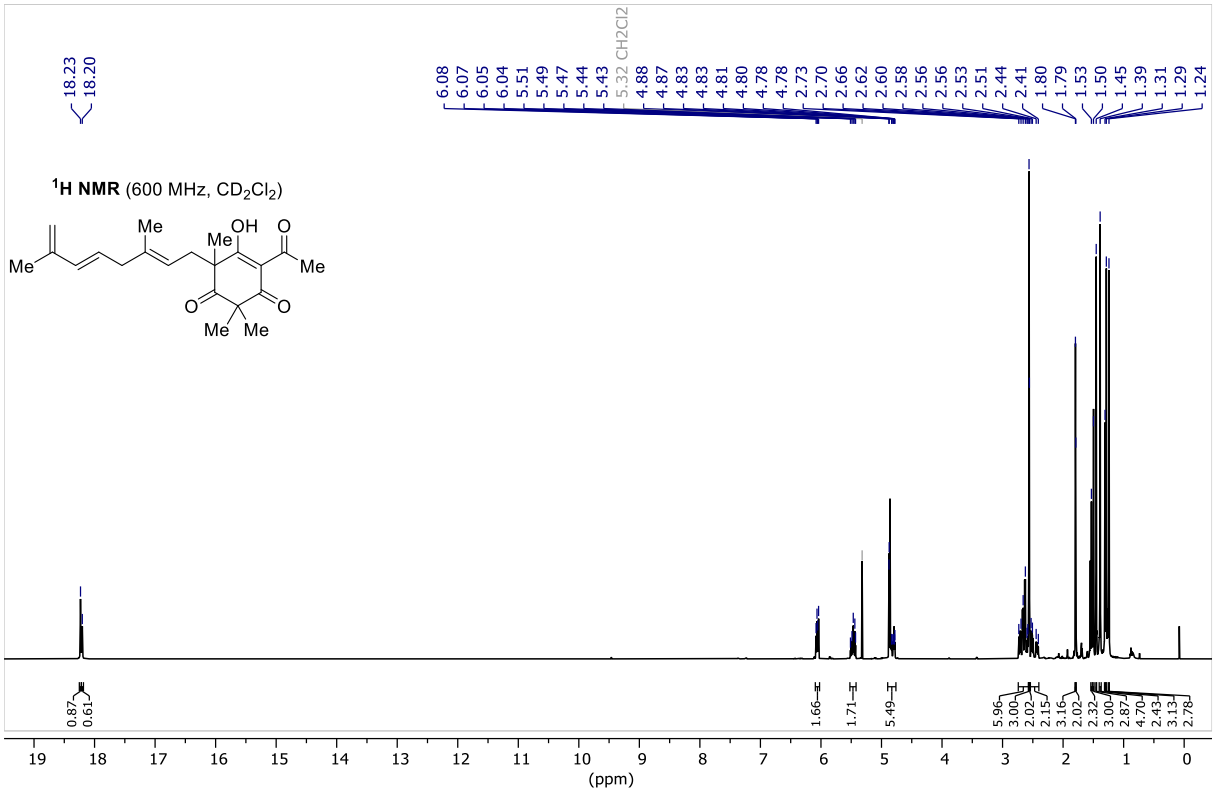

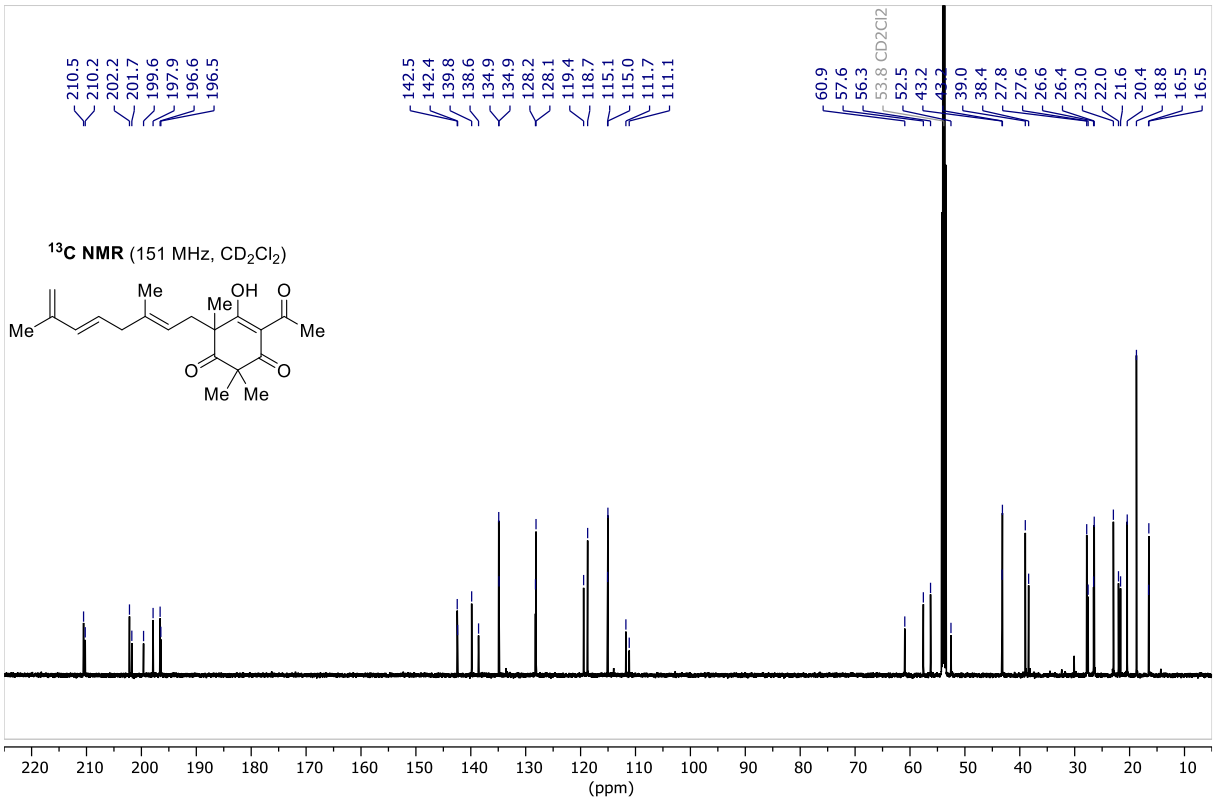

Diene 38 (Reproduced from Ref.[83] with permission from the Royal Society of Chemistry.)

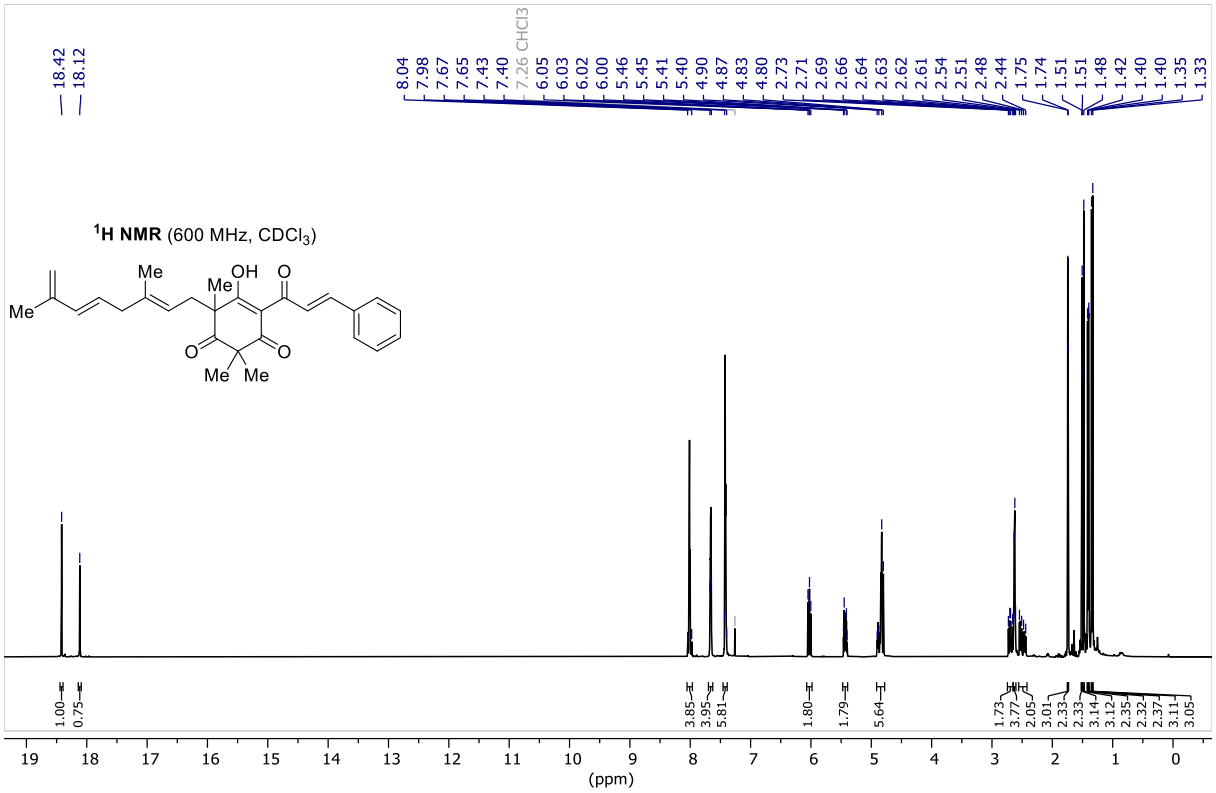

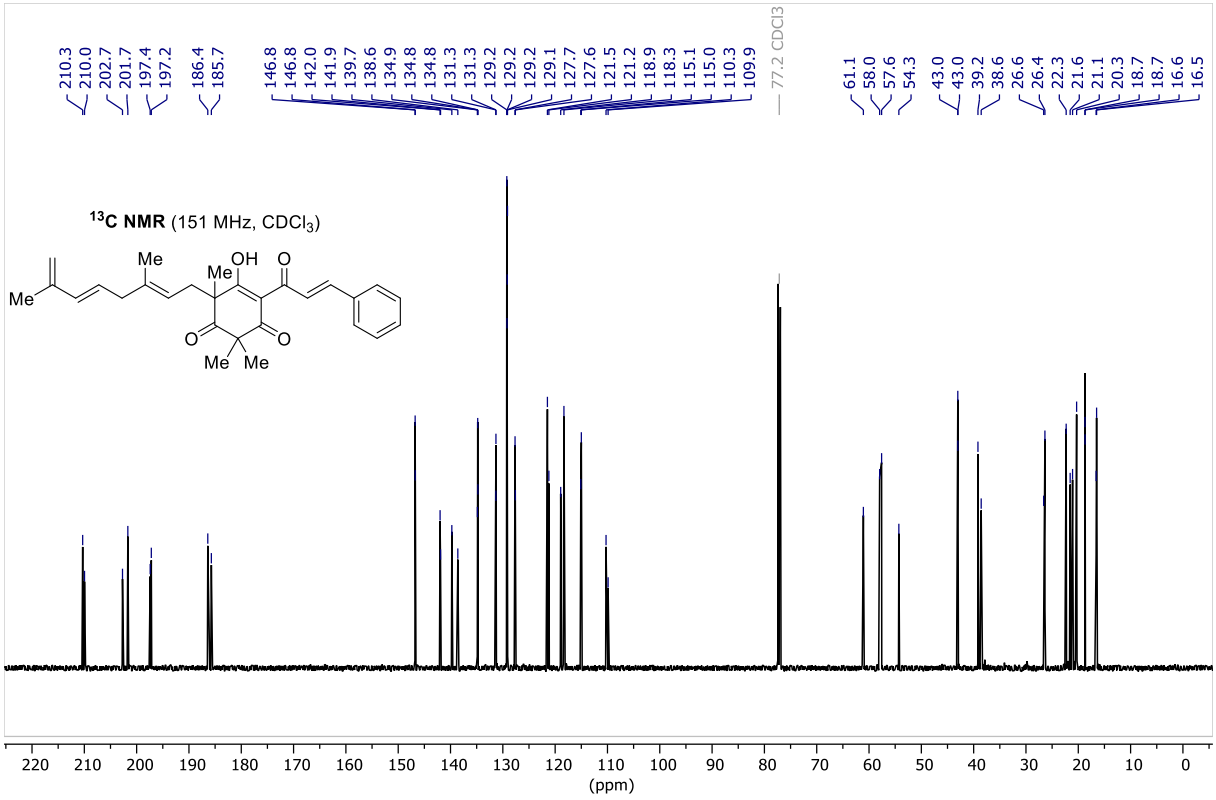

IMDA Diastereomer 105 (Reproduced from Ref.[83] with permission from the Royal Society of Chemistry.)

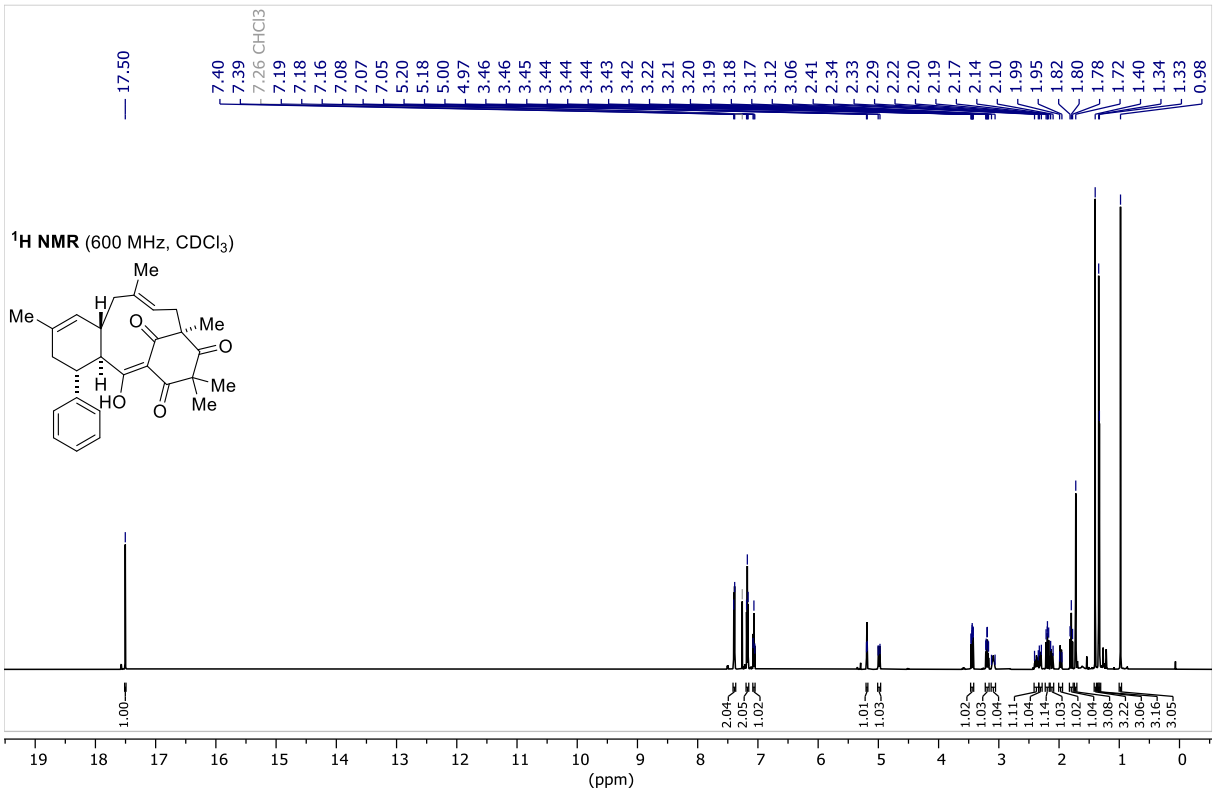

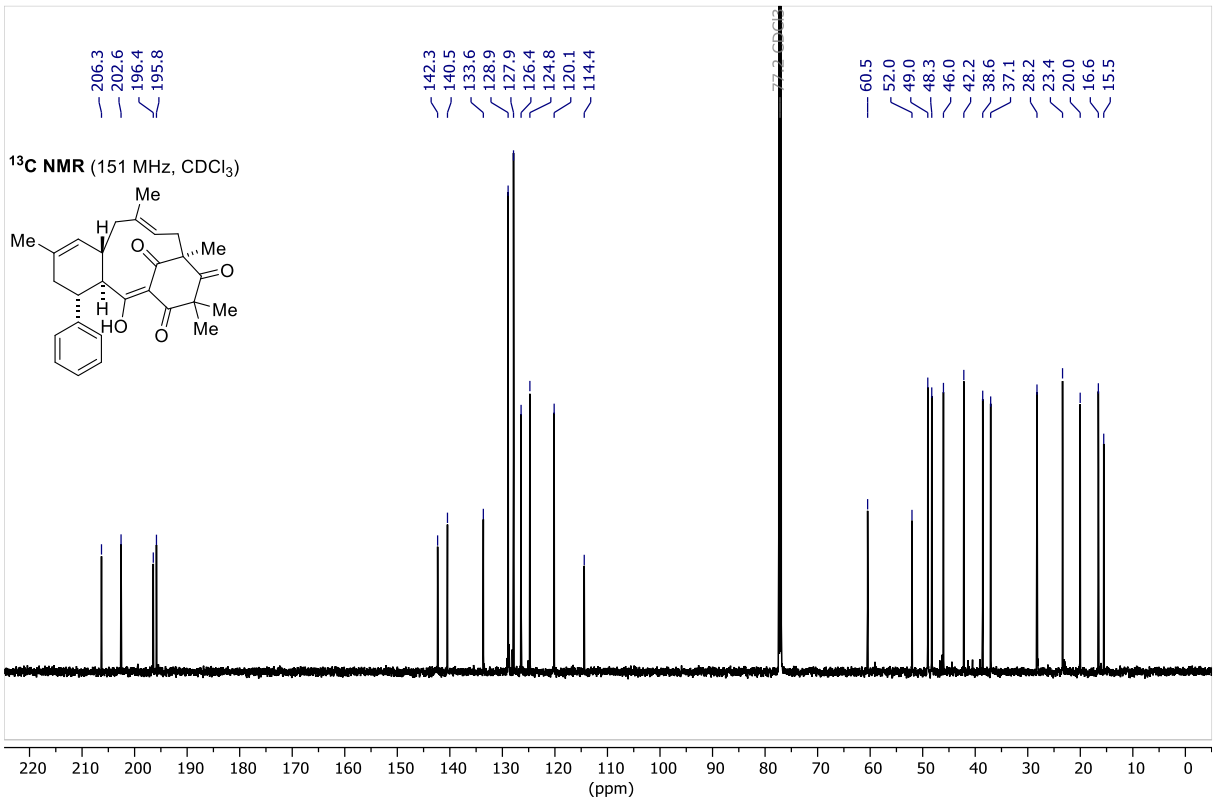

IMDA Diastereomer 37 (Reproduced from Ref.[83] with permission from the Royal Society of Chemistry.)

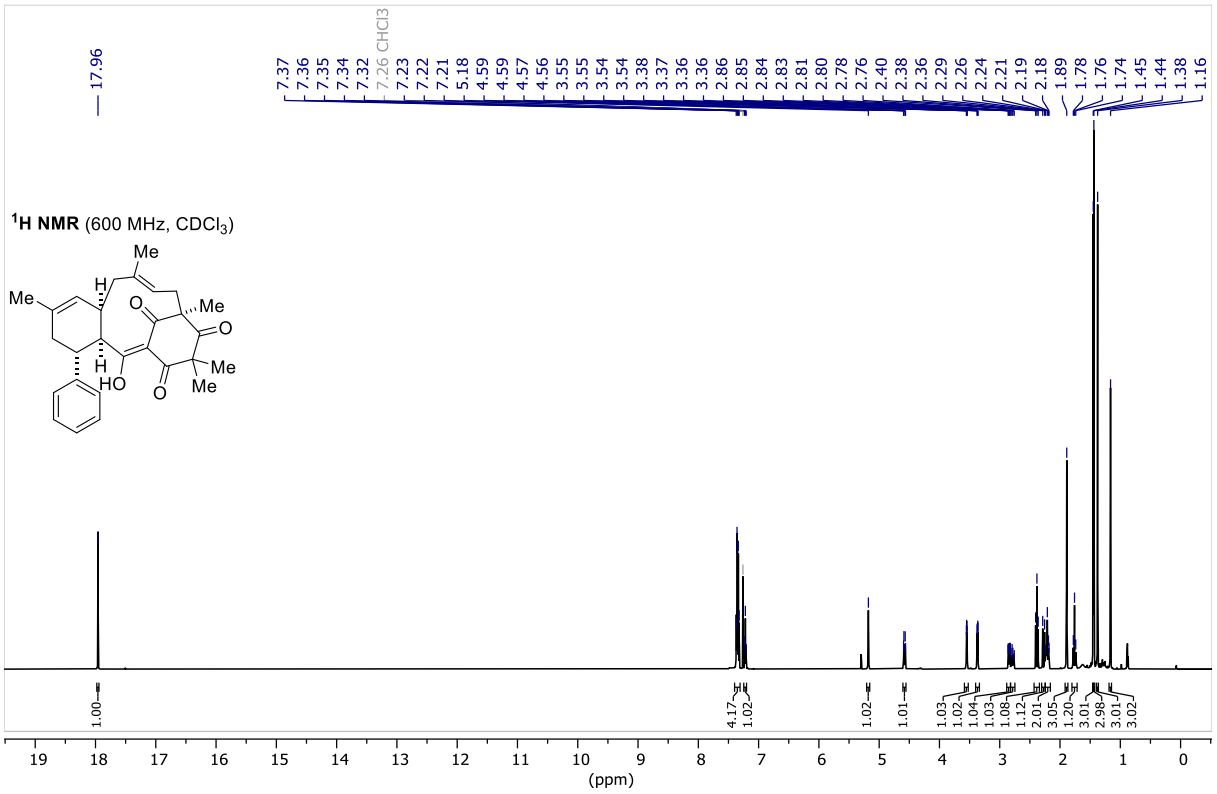

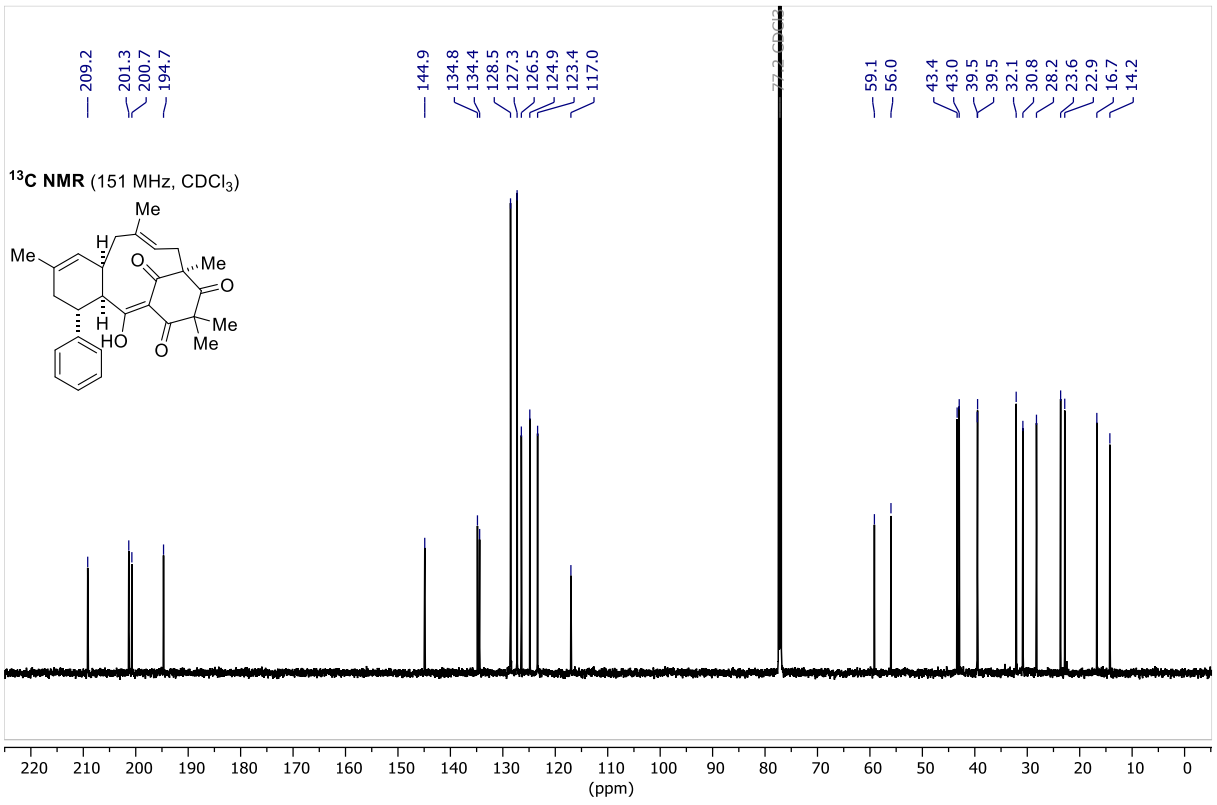

Epoxide 110 (Reproduced from Ref.[83] with permission from the Royal Society of Chemistry.)

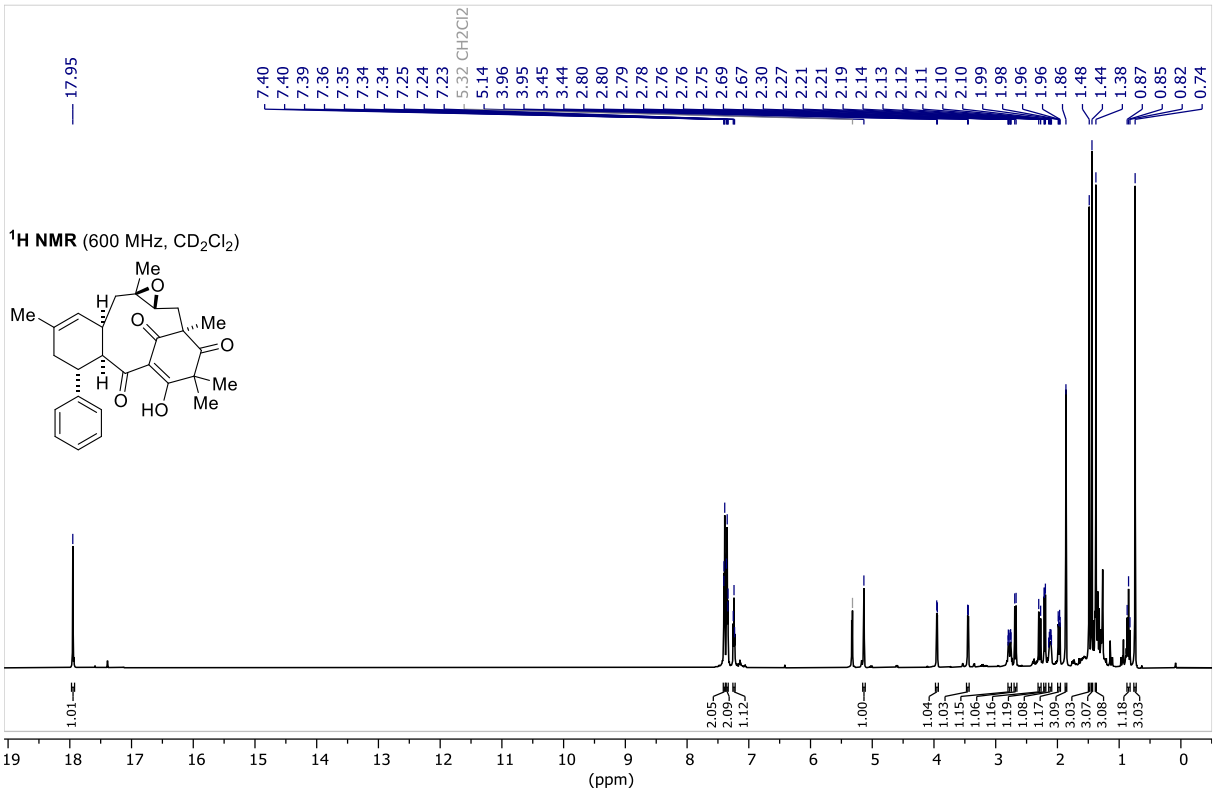

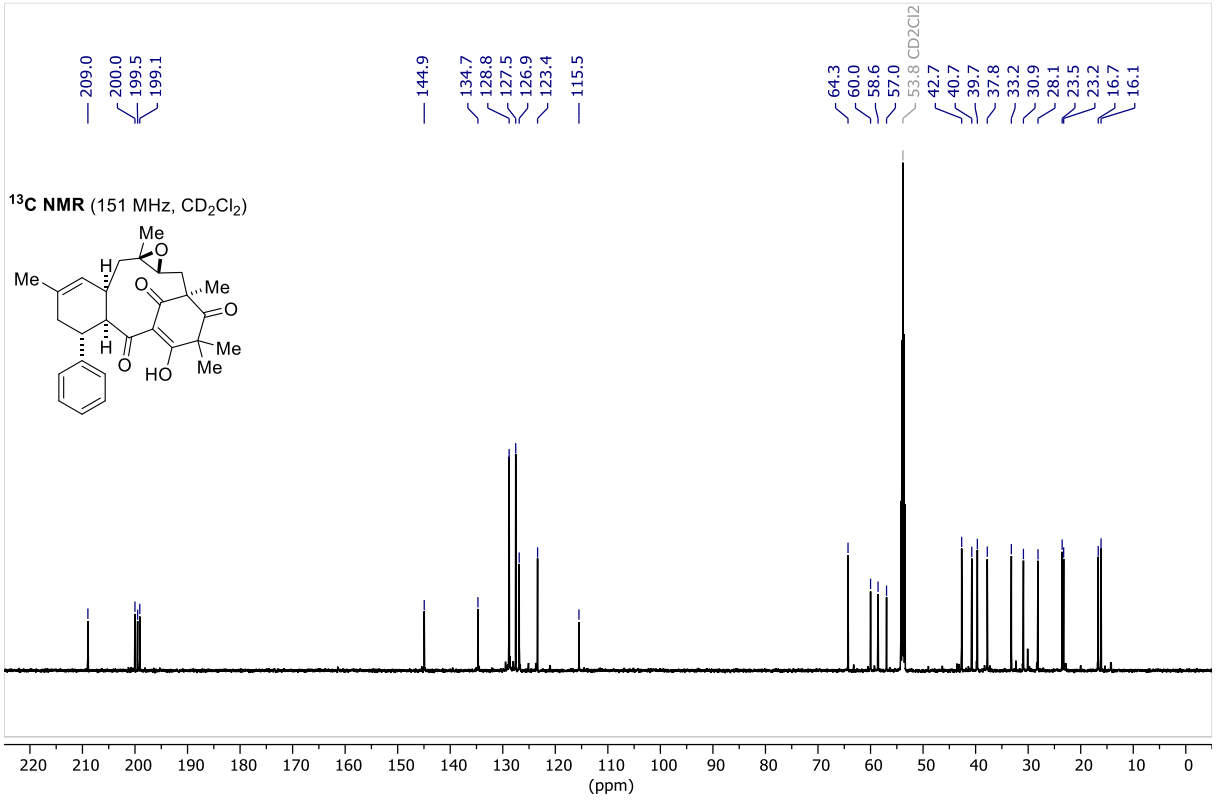

(±)-Cleistocaltone A (23) (Reproduced from Ref.[83] with permission from the Royal Society of Chemistry.)

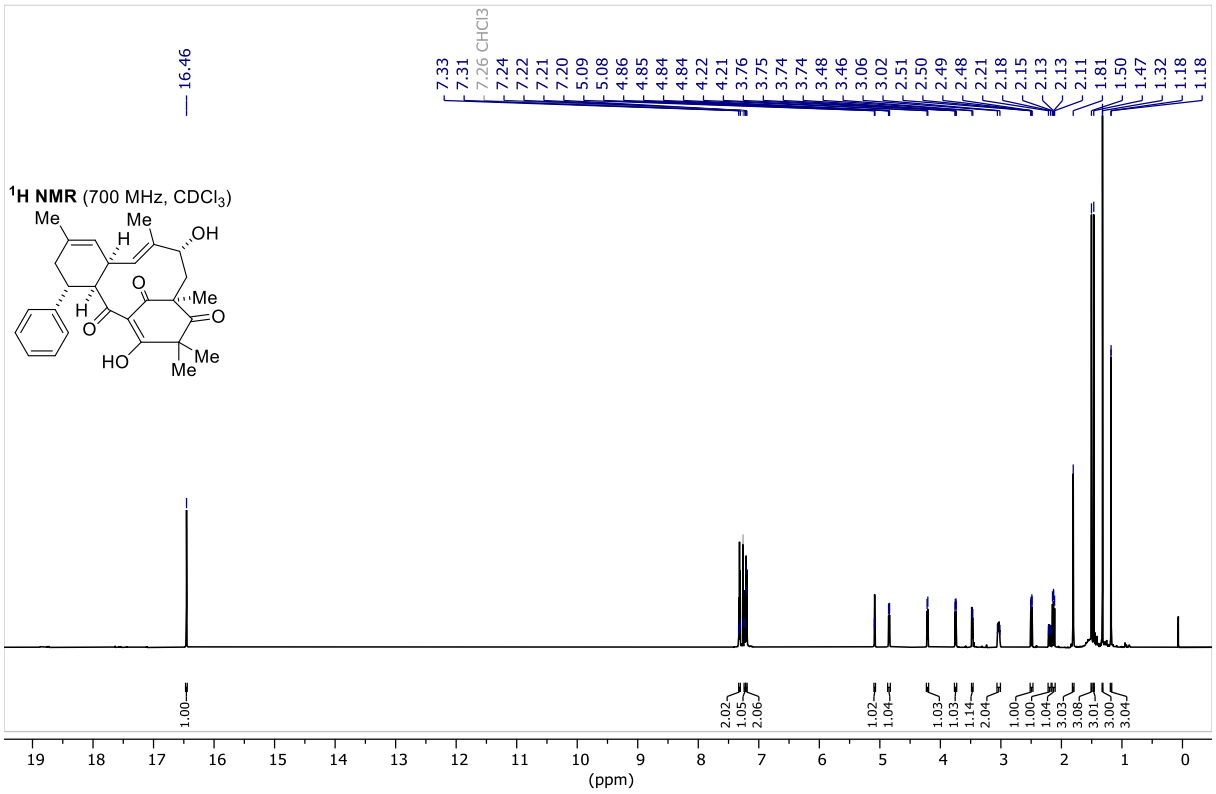

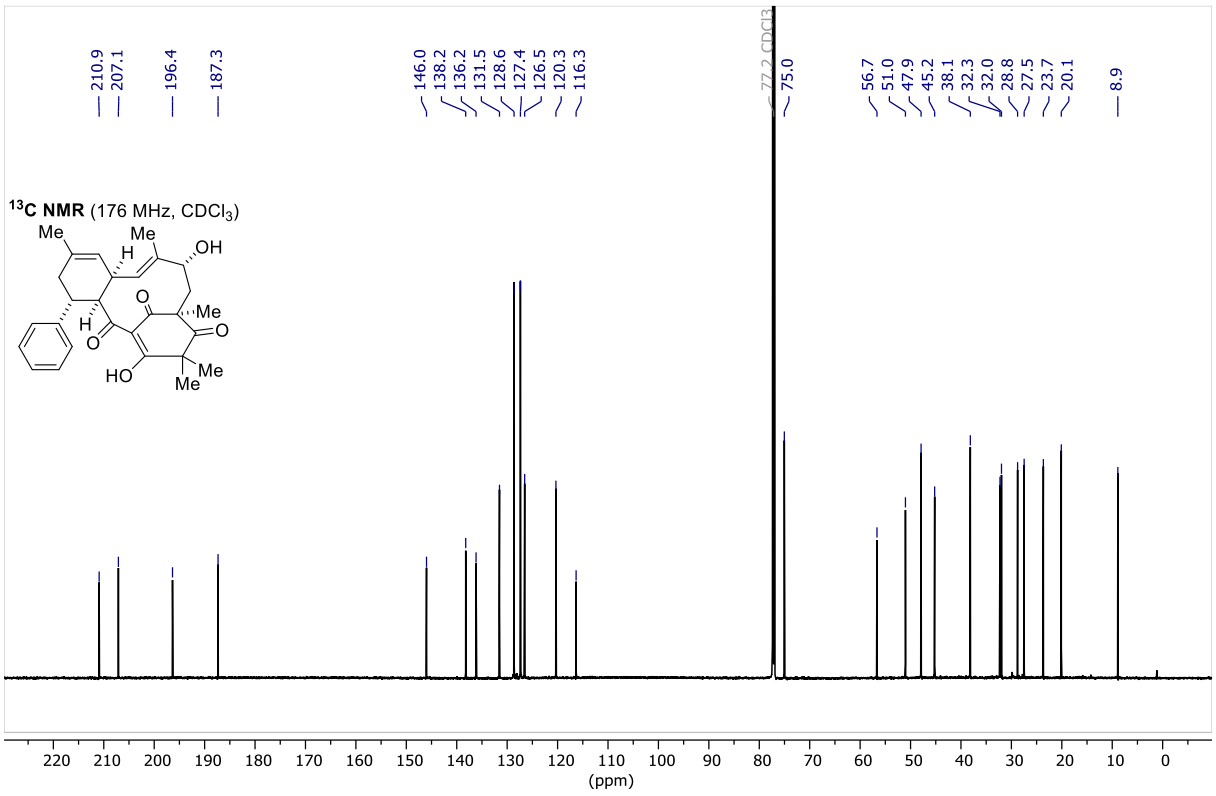

Side Product 111 (Reproduced from Ref.[83] with permission from the Royal Society of Chemistry.)

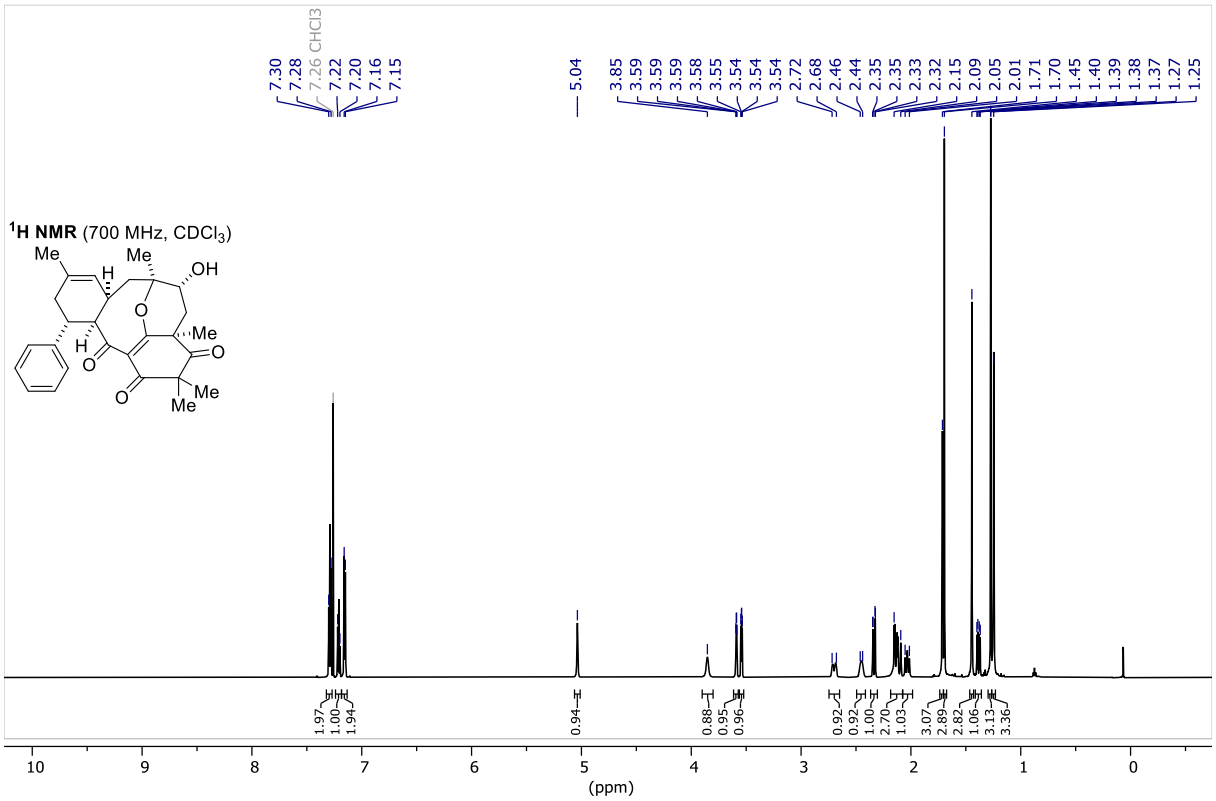

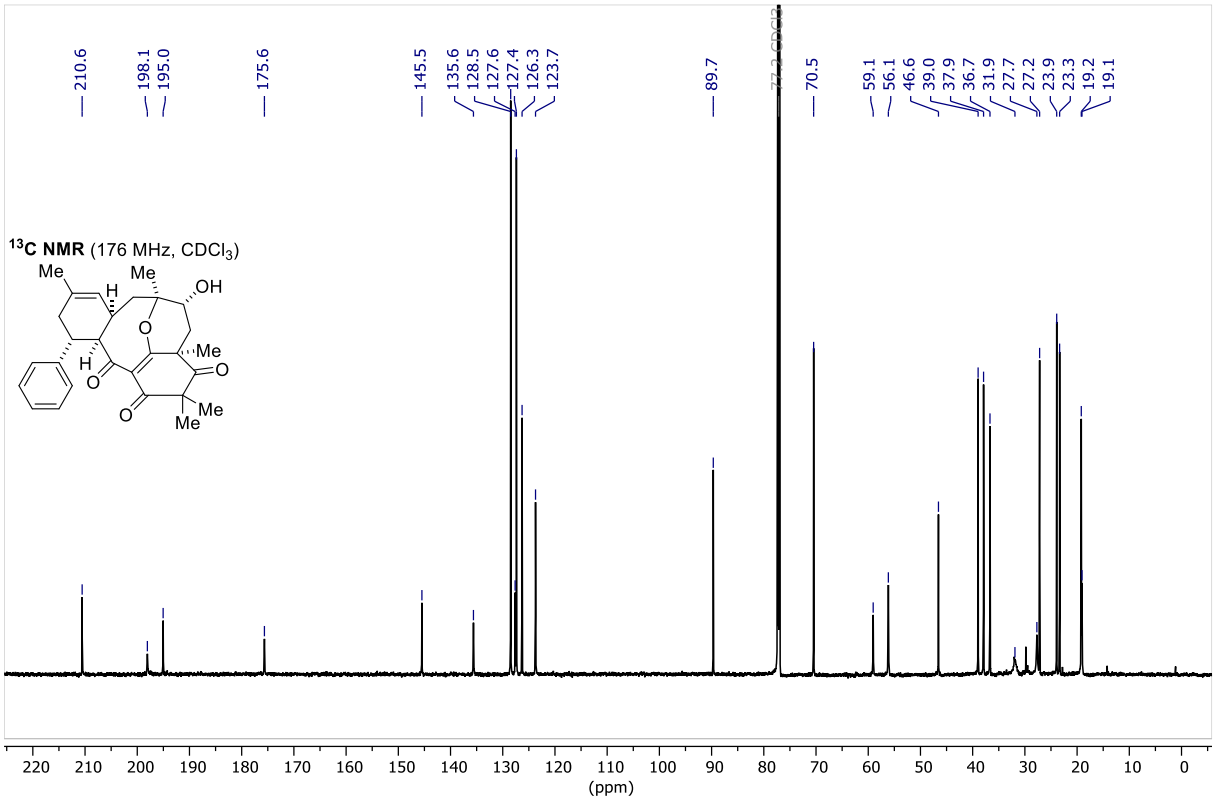

Epoxide 118

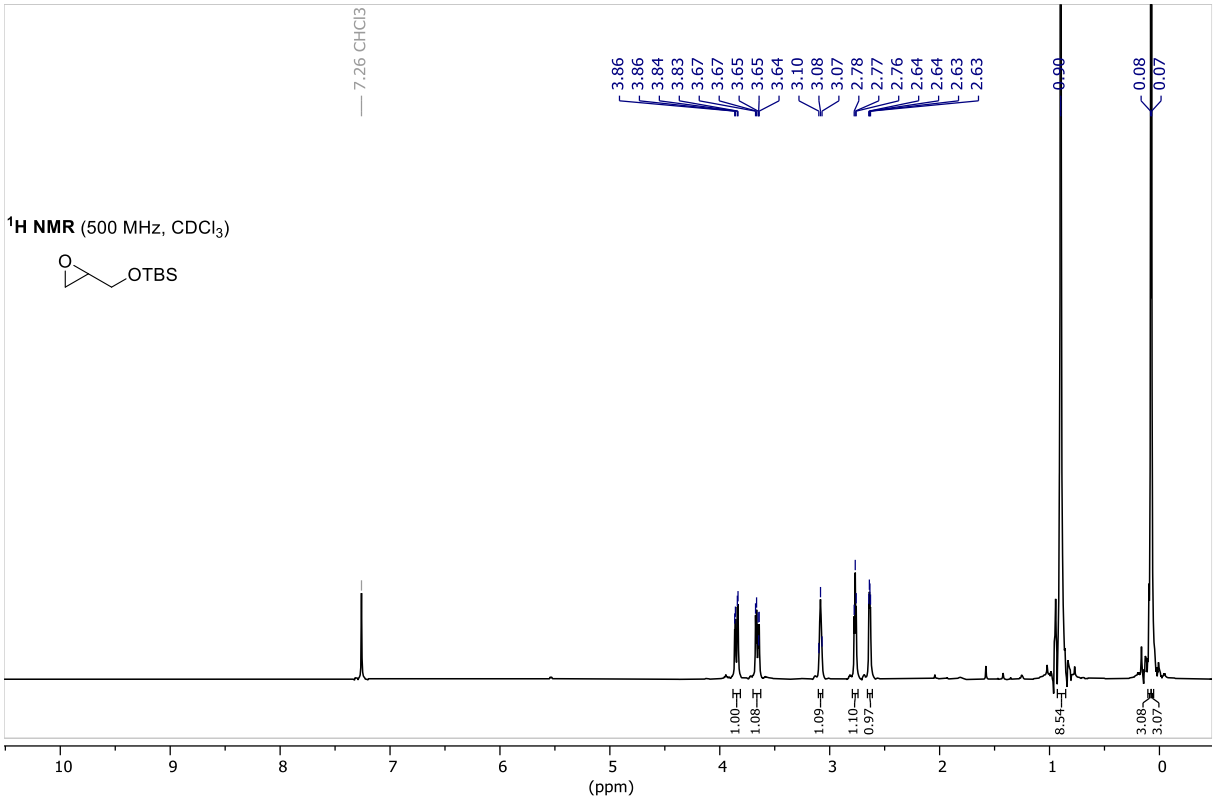
7.26 CHCl3
3.86
3.86
3.84
3.83
3.67
3.67
3.65
3.65
3.64
3.10
3.08
3.07
2.78
2.77
2.76
2.64
2.64
2.63
2.63
0.90
0.08
0.07
1H NMR (500 MHz, CDCl3)
OTBS
1.00
1.08
1.09
1.10
0.97
8.54
3.08
3.07
(ppm)

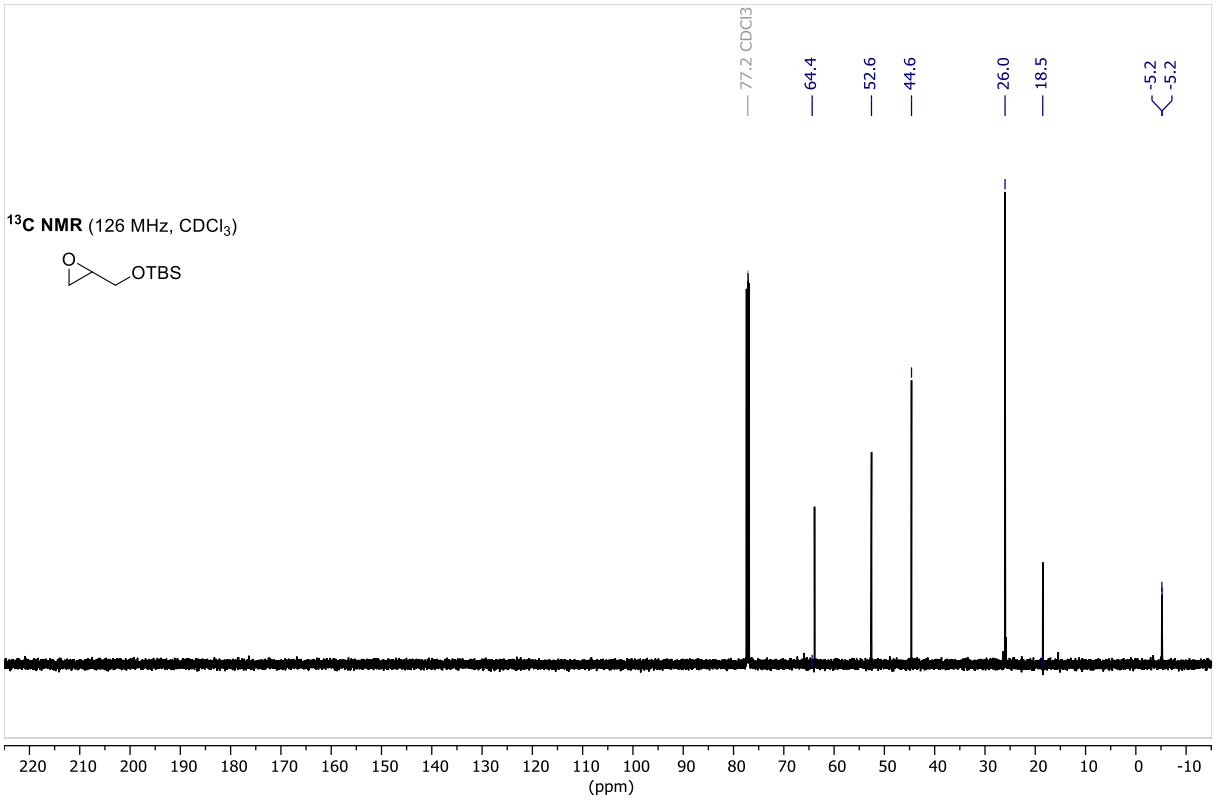
77.2 CDCl3
64.4
52.6
44.6
26.0
18.5
-5.2
-5.2
13C NMR (126 MHz, CDCl3)
OTBS
(ppm)

Alcohol 119

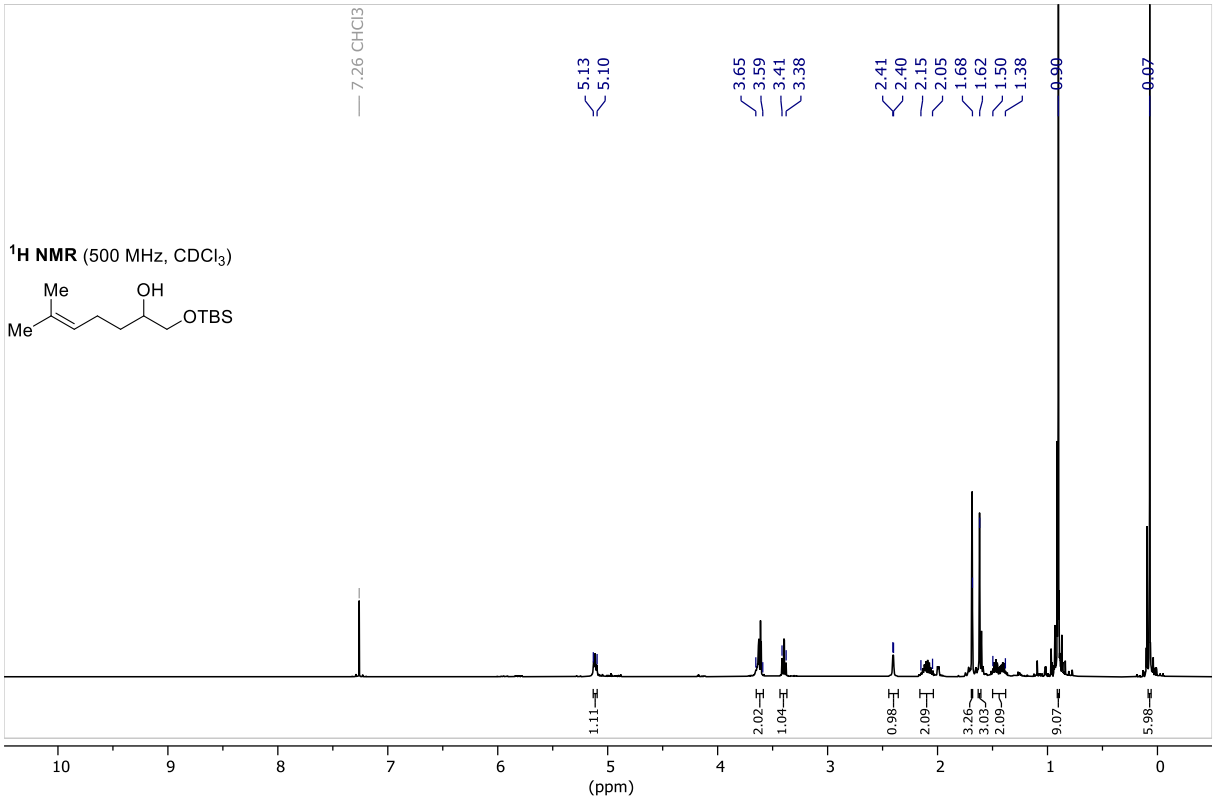
7.26 CHCl3
5.13
5.10
3.65
3.59
3.41
3.38
2.41
2.40
2.15
2.05
1.68
1.62
1.50
1.38
0.90
0.07
1H NMR (500 MHz, CDCl3)
Me
OH
OTBS
Me
1.11
2.02
1.04
0.98
2.09
3.26
3.03
2.09
9.07
5.98
10
9
8
7
6
5
4
3
2
1
0
(ppm)

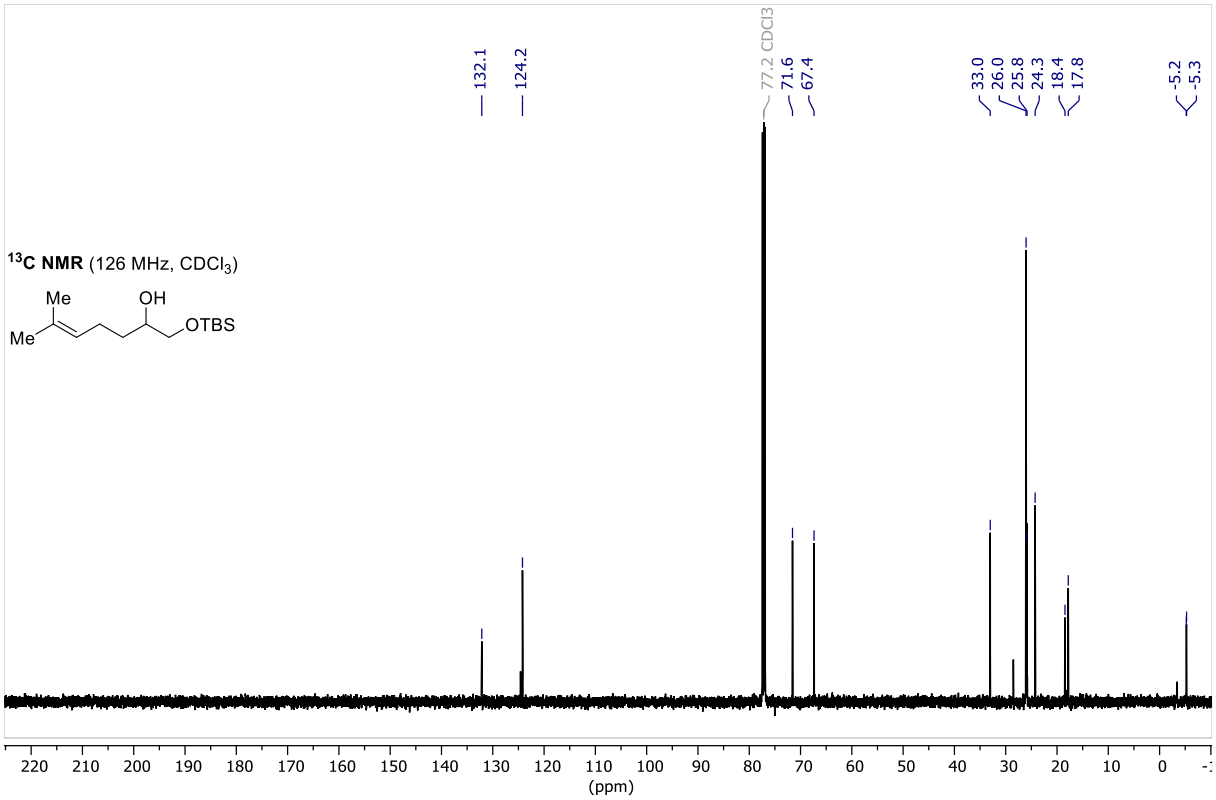
132.1
124.2
77.2 CDCl3
71.6
67.4
33.0
26.0
25.8
24.3
18.4
17.8
-5.2
-5.3
13C NMR (126 MHz, CDCl3)
Me
OH
OTBS
Me
220
210
200
190
180
170
160
150
140
130
120
110
100
90
80
70
60
50
40
30
20
10
0
(ppm)

Ketone 120

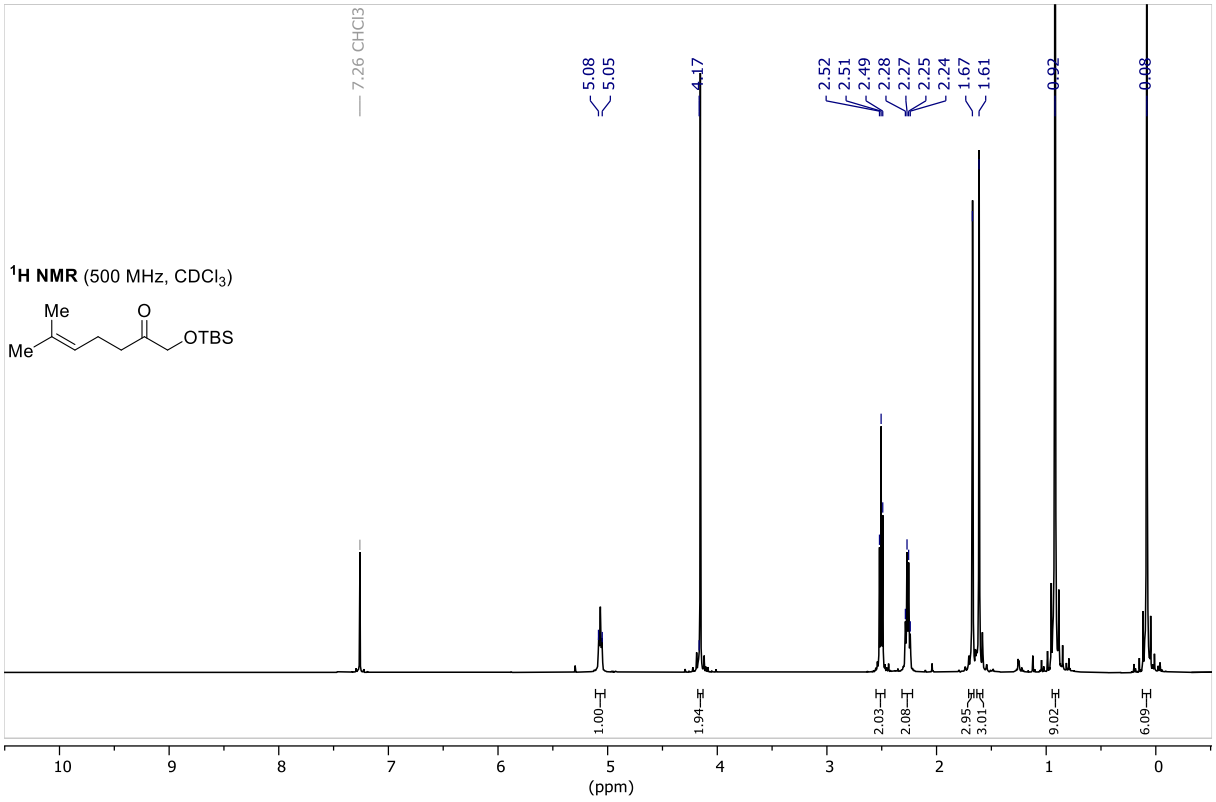
7.26 CHCl3
5.08
5.05
4.17
2.52
2.51
2.49
2.28
2.27
2.25
2.24
1.67
1.61
0.92
0.08
1H NMR (500 MHz, CDCl3)
Me
O
Me
OTBS
1.00
1.94
2.03
2.08
2.95
3.01
9.02
6.09
(ppm)

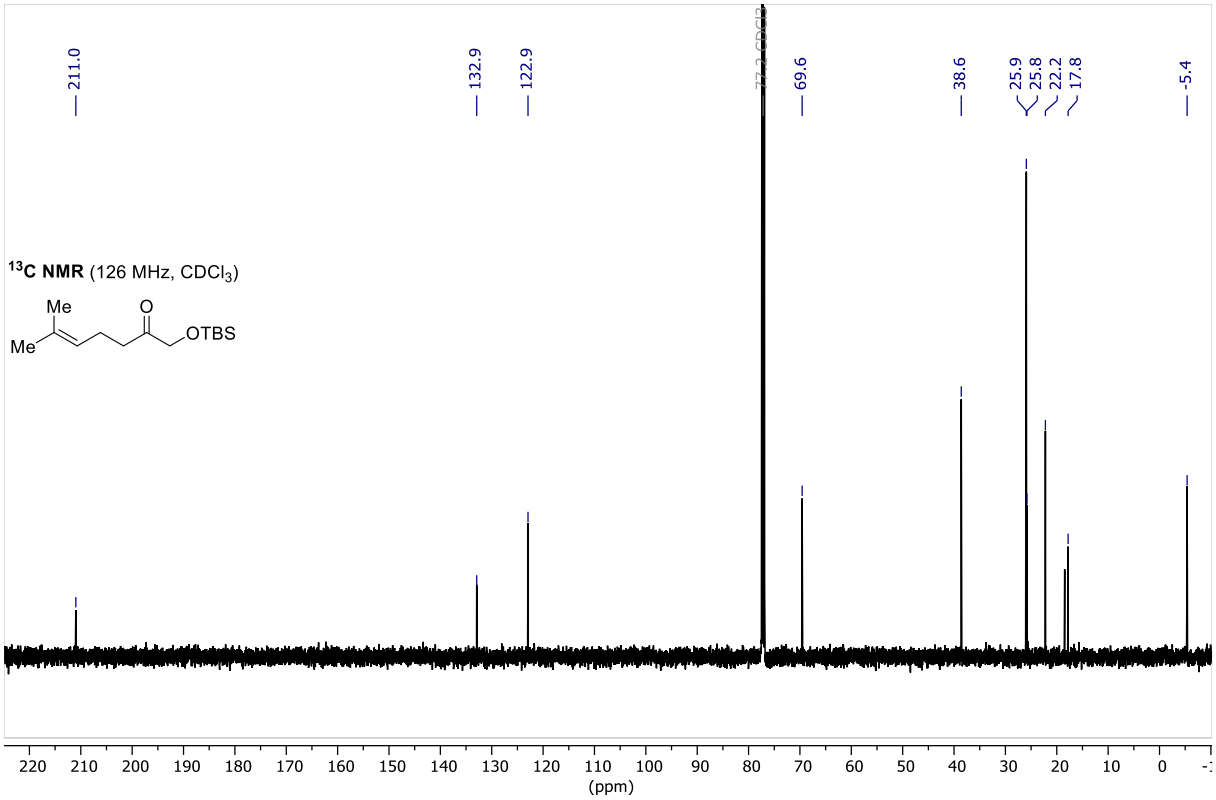
211.0
132.9
122.9
77.2 CDCl3
69.6
38.6
25.9
25.8
22.2
17.8
-5.4
13C NMR (126 MHz, CDCl3)
Me
O
Me
OTBS
(ppm)

Alcohol 121

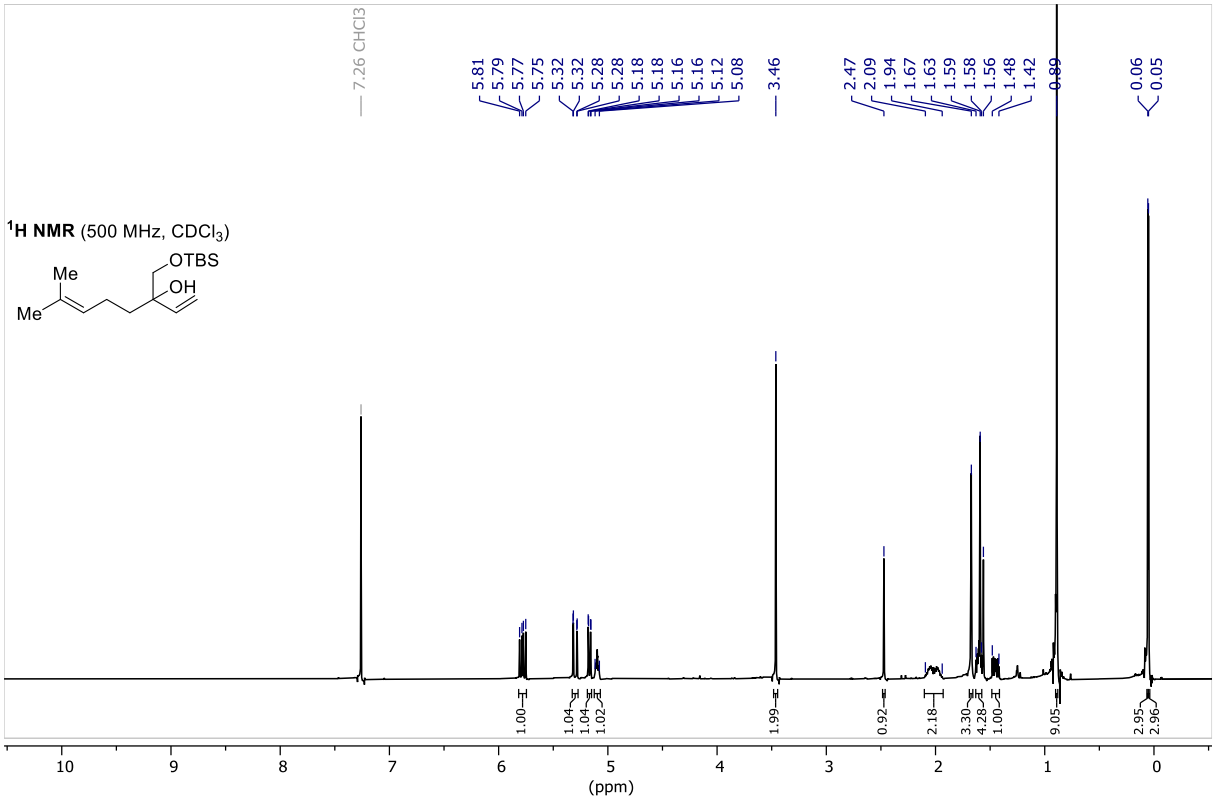
7.26 CHCl3
5.81
5.79
5.77
5.75
5.32
5.32
5.28
5.28
5.18
5.18
5.16
5.16
5.12
5.08
3.46
2.47
2.09
1.94
1.67
1.63
1.59
1.58
1.56
1.48
1.42
0.89
0.06
0.05
1H NMR (500 MHz, CDCl3)
OTBS
OH
Me
Me
1.00
1.04
1.04
1.02
1.99
0.92
2.18
3.30
4.28
1.00
9.05
2.95
2.96
10
9
8
7
6
5
4
3
2
1
0
(ppm)

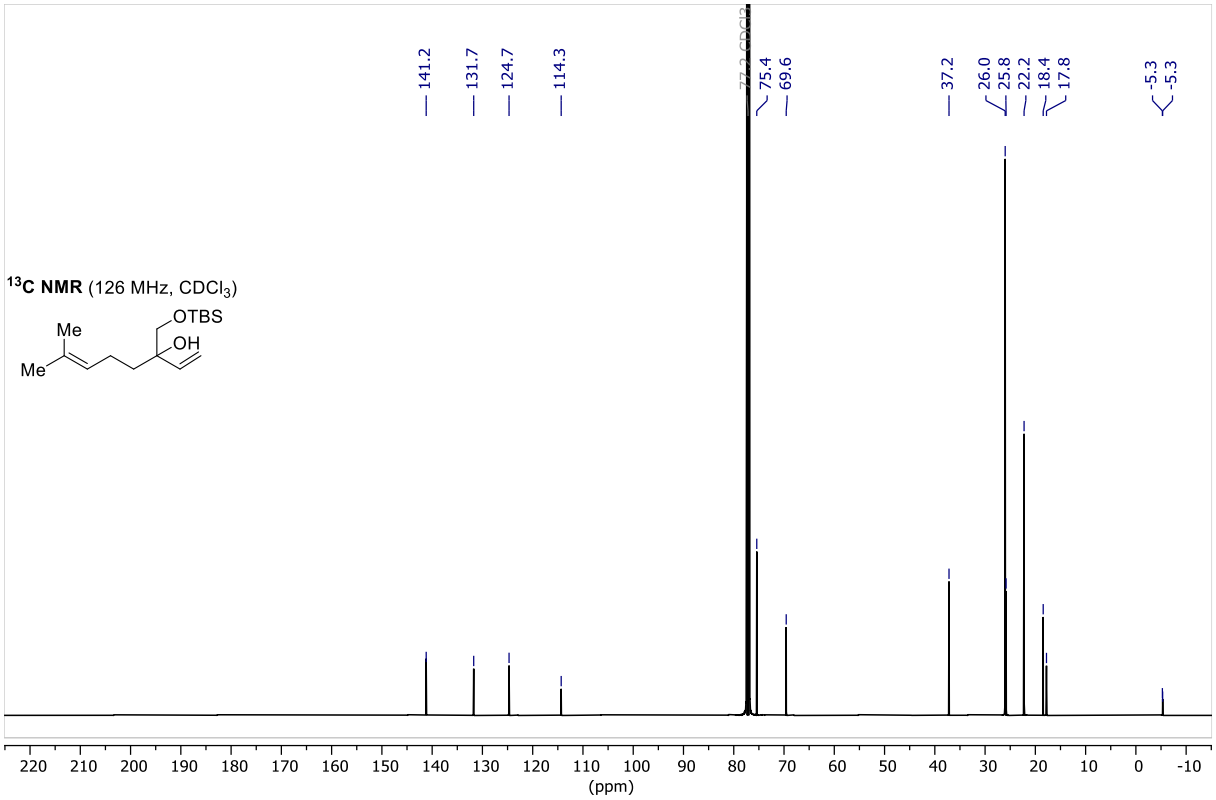
141.2
131.7
124.7
114.3
77.2 CDCl3
75.4
69.6
37.2
26.0
25.8
22.2
18.4
17.8
-5.3
-5.3
13C NMR (126 MHz, CDCl3)
OTBS
OH
Me
Me
220
210
200
190
180
170
160
150
140
130
120
110
100
90
80
70
60
50
40
30
20
10
0
-10
(ppm)

Dihydroxymyrcene 116

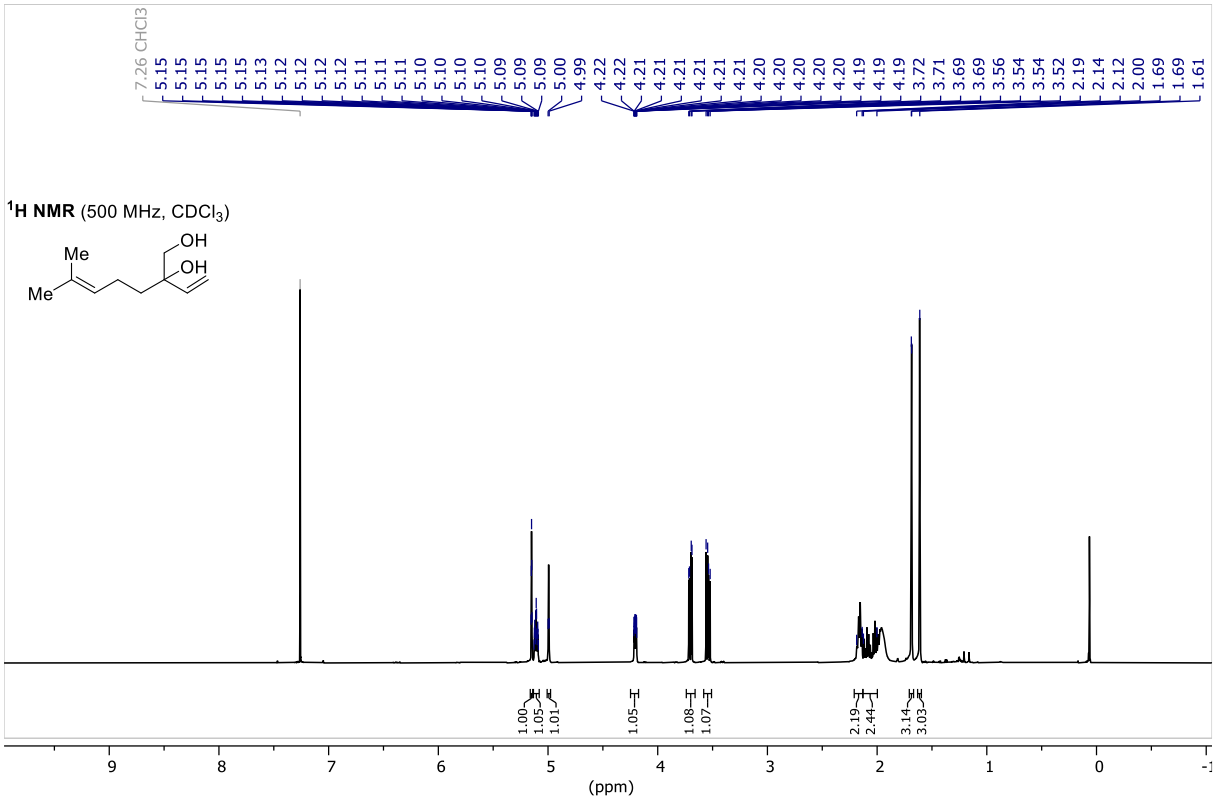

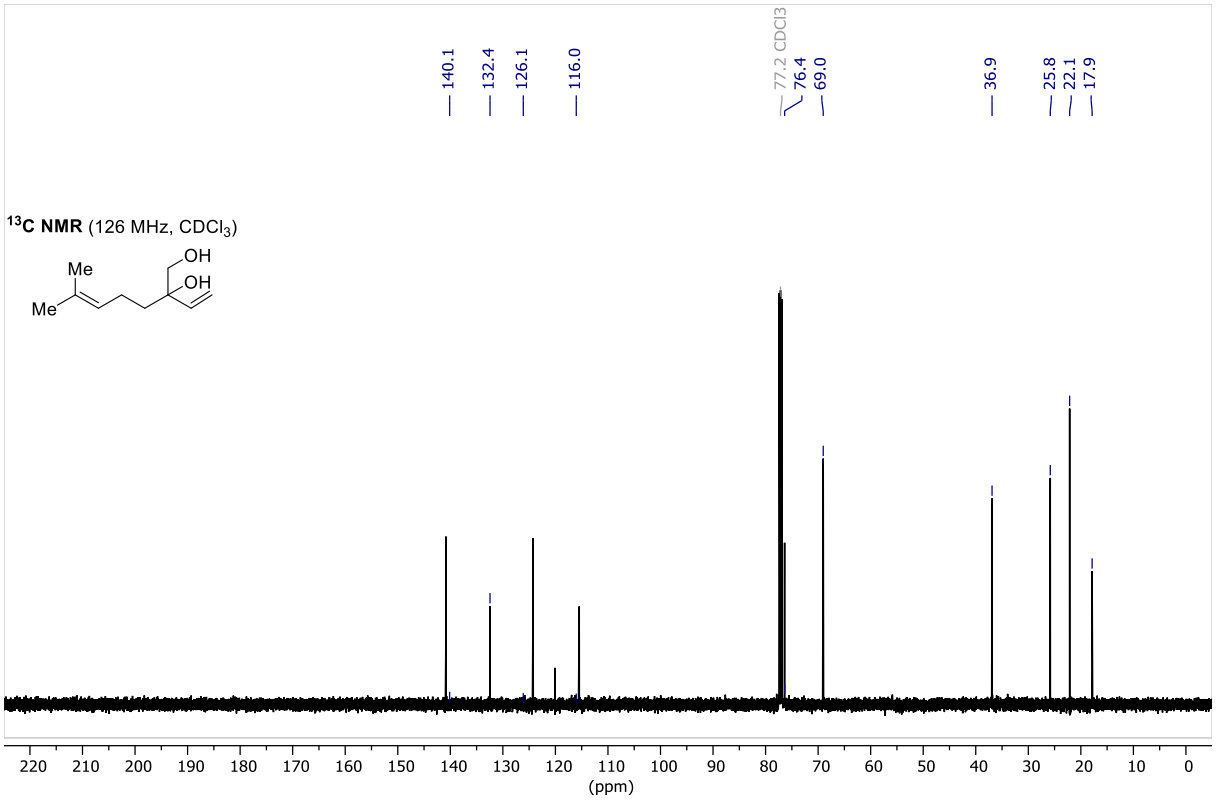

Tosylate 123

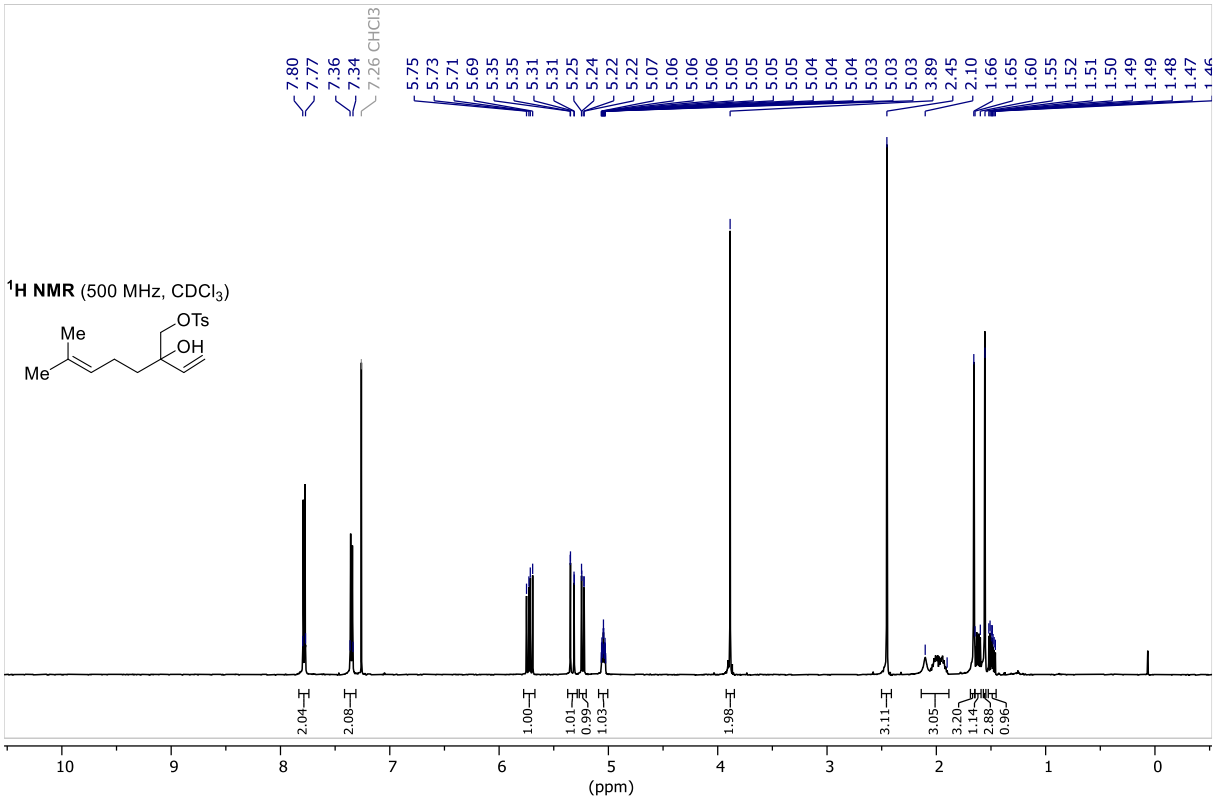

^{1}H NMR (500 MHz, $CDCl_3$)

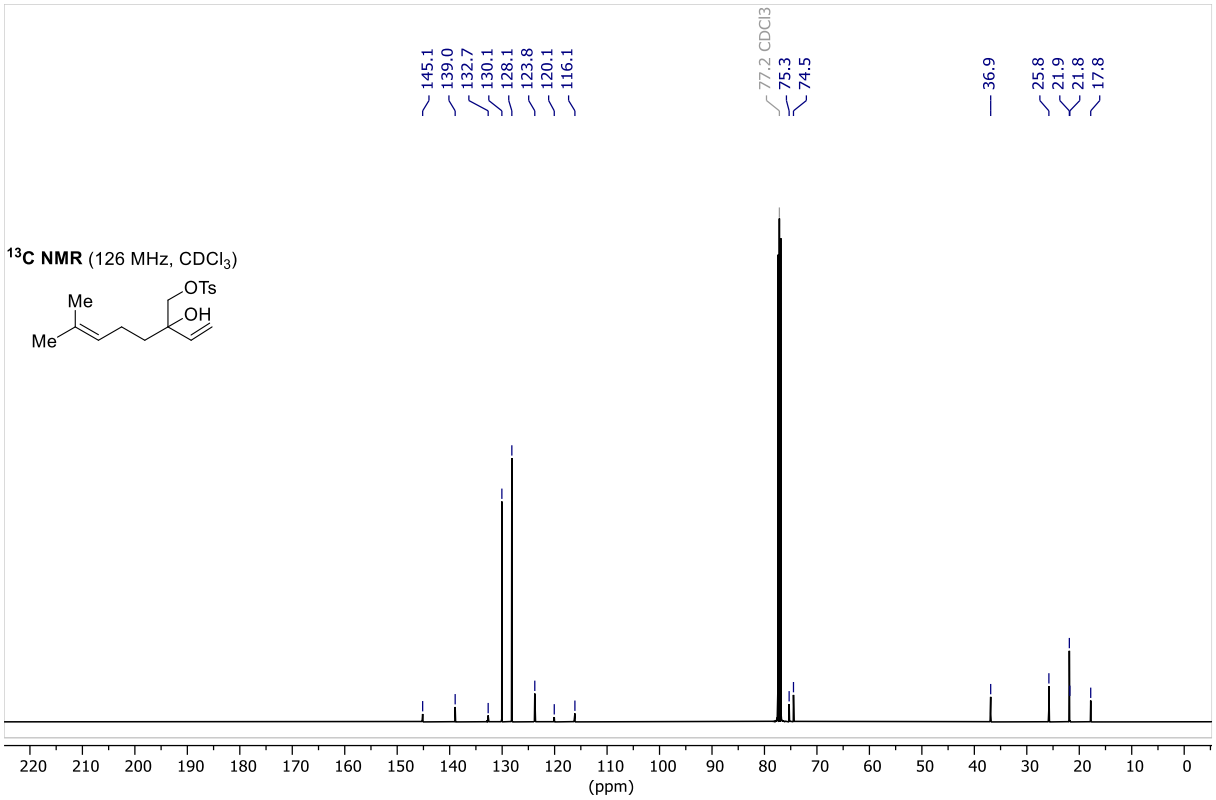

^{13}C NMR (126 MHz, $CDCl_3$)

Epoxide 124

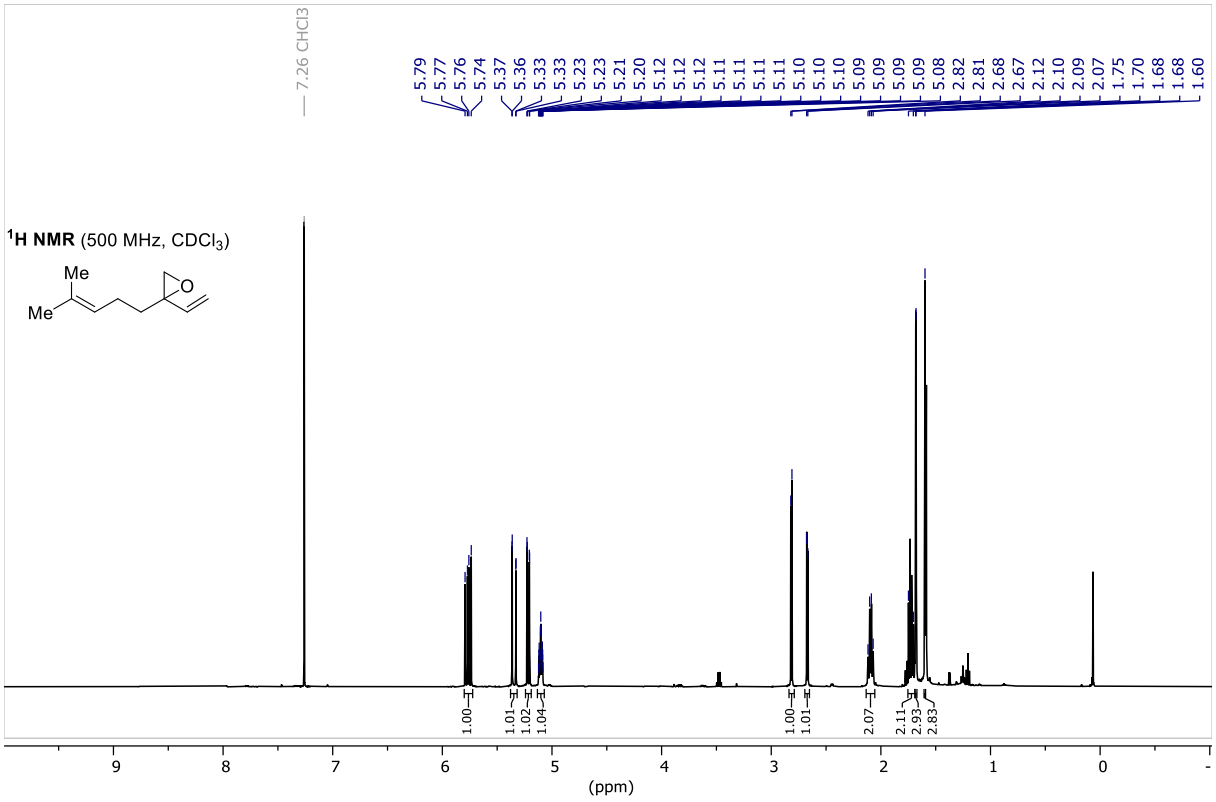
7.26 CHCl3
5.79
5.77
5.76
5.74
5.37
5.36
5.33
5.33
5.23
5.23
5.21
5.20
5.12
5.12
5.12
5.11
5.11
5.11
5.11
5.10
5.10
5.10
5.09
5.09
5.09
5.09
5.08
2.82
2.81
2.68
2.67
2.12
2.10
2.09
2.07
1.75
1.70
1.68
1.68
1.60
1H NMR (500 MHz, CDCl3)
Me
Me
O
1.00
1.01
1.02
1.04
1.00
1.01
2.07
2.11
2.93
2.83
9
8
7
6
5
4
3
2
1
0
(ppm)

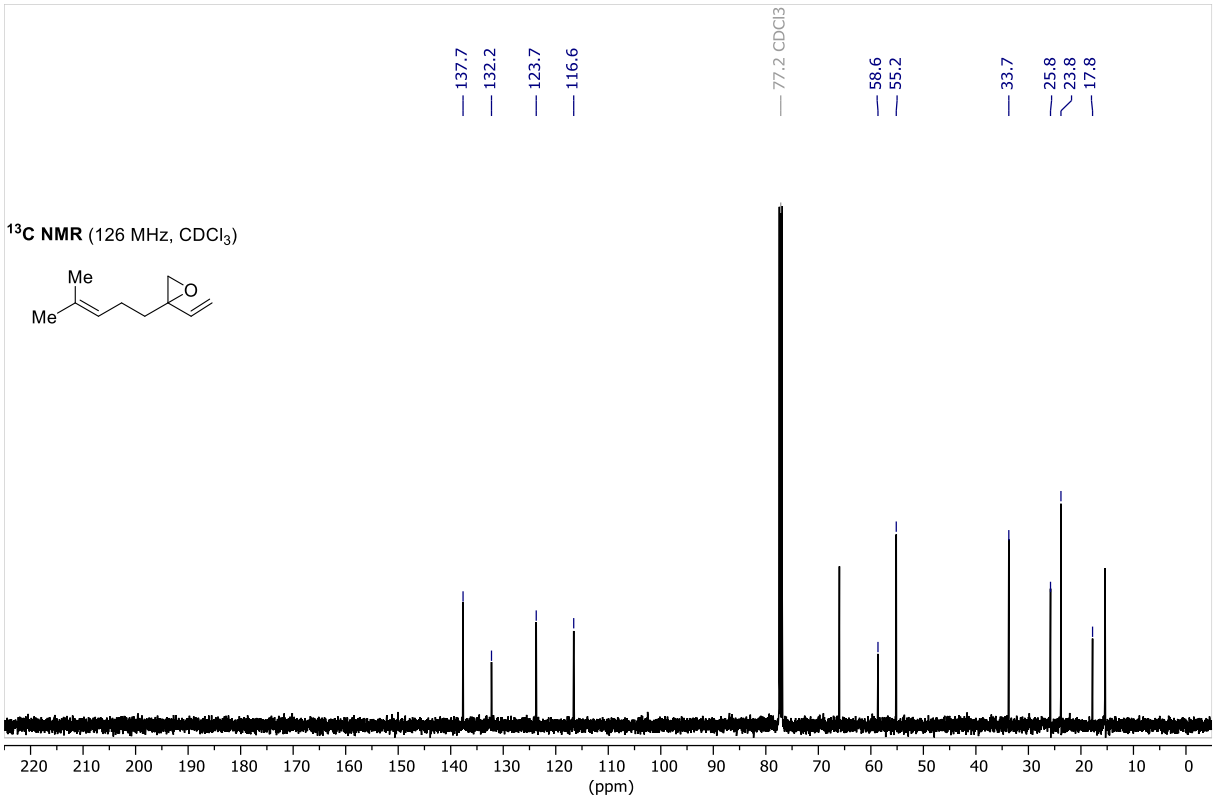
137.7
132.2
123.7
116.6
77.2 CDCl3
58.6
55.2
33.7
25.8
23.8
17.8
13C NMR (126 MHz, CDCl3)
Me
Me
O
220
210
200
190
180
170
160
150
140
130
120
110
100
90
80
70
60
50
40
30
20
10
0
(ppm)

(*E*)-Cleistocaltone B (23)

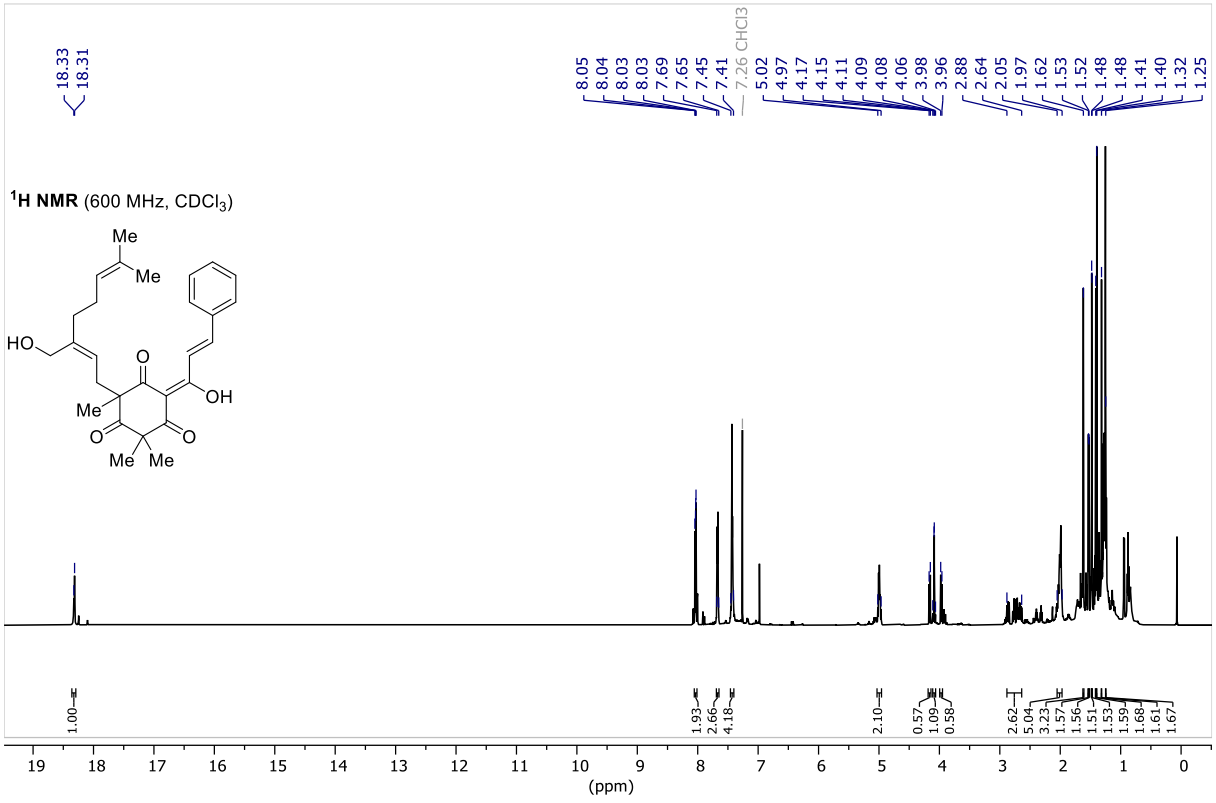

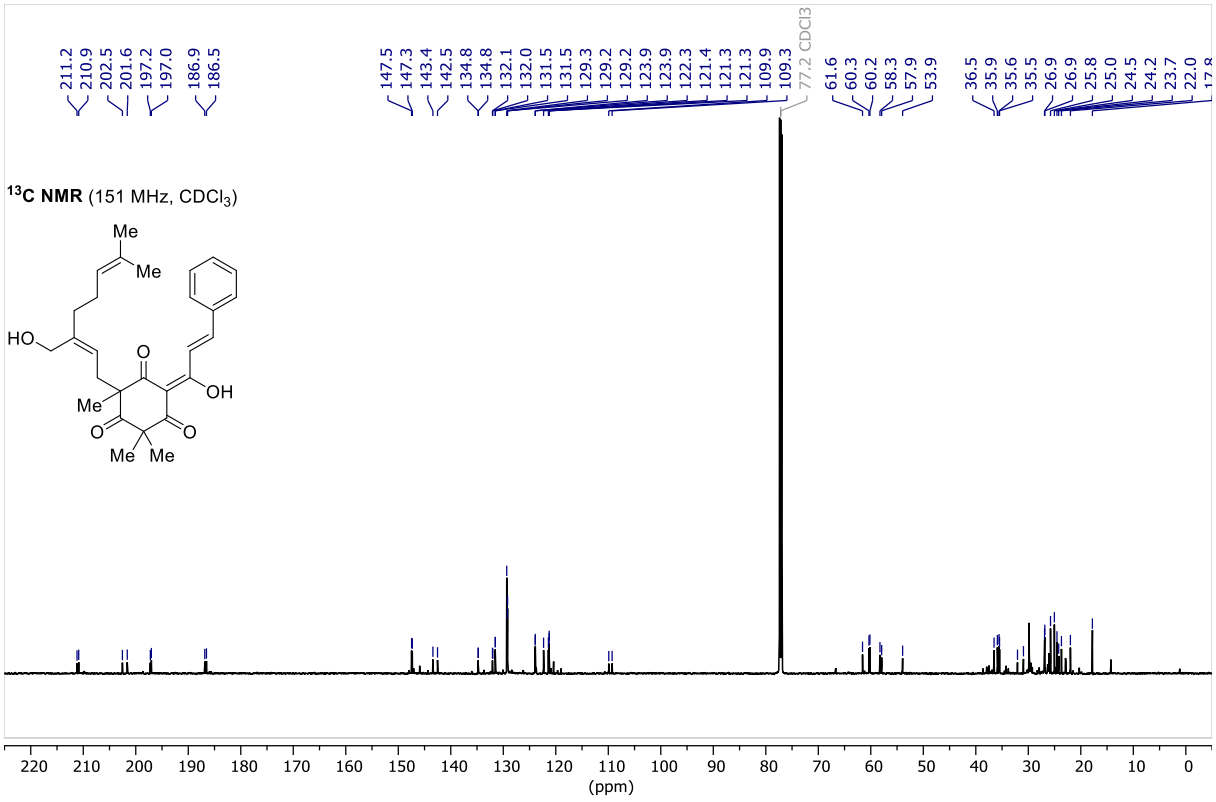

Dihydroxymyrcenol *tert*-Butyl Carbonate *tert*-Butyl Dimethyl Silyl Ether 138

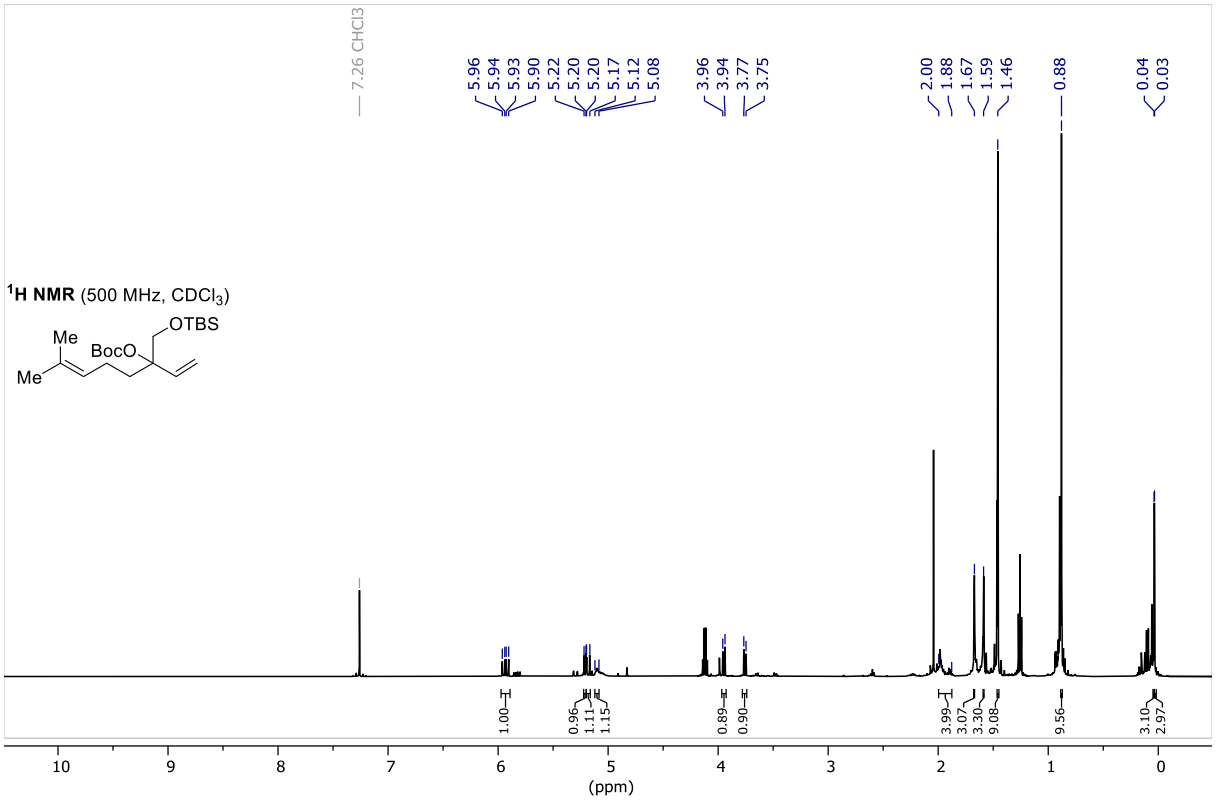

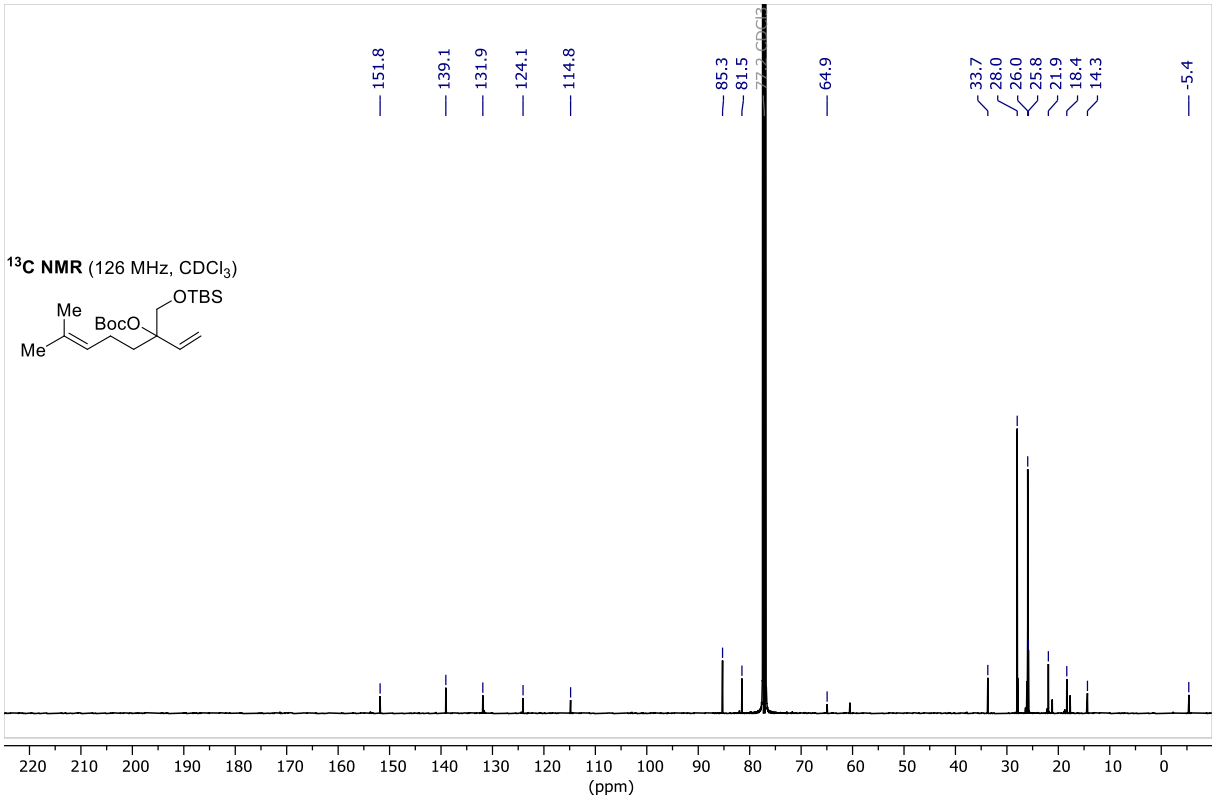

Geranial (133)

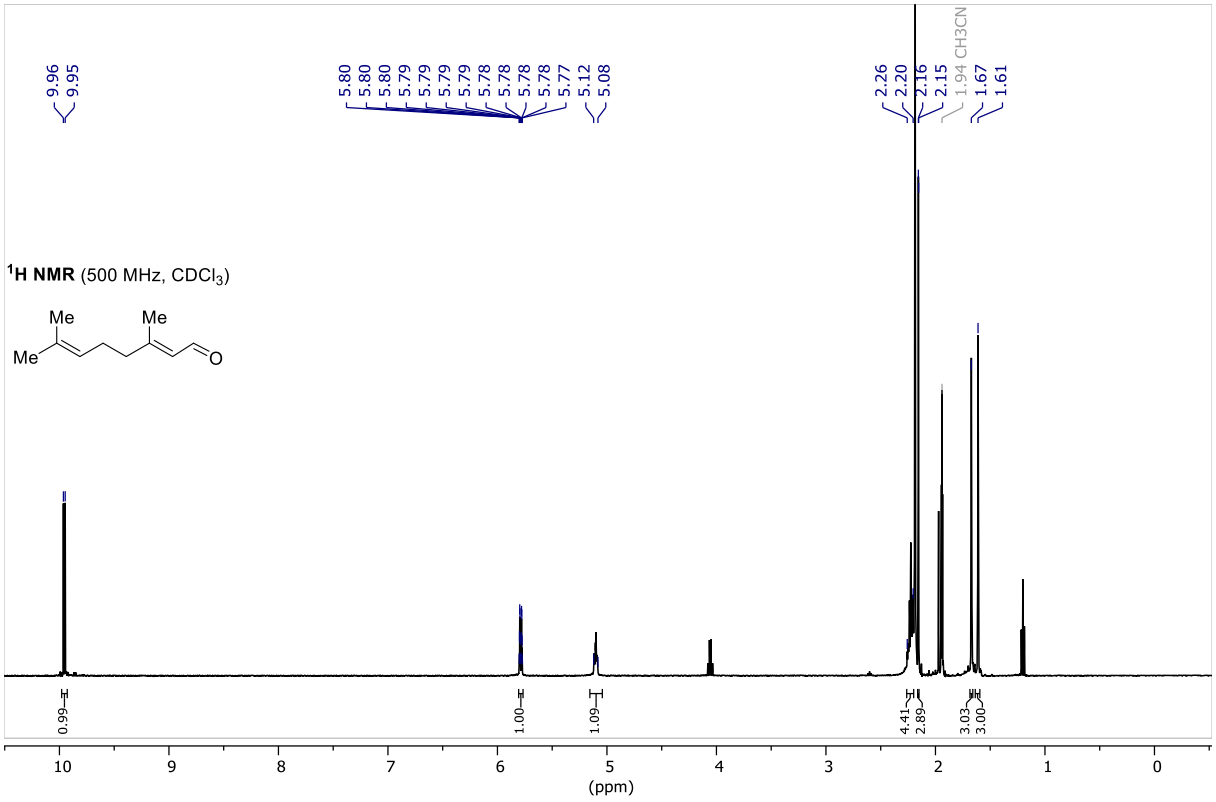

Butenolide 128